Studying the role of micro RNAs in tuber development in potato

(*Solanum tuberosum* ssp *andigena*)

A Thesis

Submitted in partial fulfilment of the requirements
of the degree of
Doctor of Philosophy

By

SNEHA BHOGALE

20093031

INDIAN INSTITUTE OF SCIENCE EDUCATION AND RESEARCH, PUNE

2015

CERTIFICATE

Certified that the work incorporated in the thesis entitled **"Studying the role of micro RNAs in tuber development in potato (*Solanum tuberosum* ssp *andigena*)"** submitted by Ms. Sneha Bhogale was carried out by the candidate, under my supervision. The work presented here or any part of it has not been included in any other thesis submitted previously for the award of any degree or diploma from any other university or institution.

Dr. Anjan K. Banerjee
Supervisor

Date: 31st March 2015

DECLARATION

I declare that this written submission represents my ideas in my own words and where other's ideas have been included; I have adequately cited and referenced the original sources. I also declare that I have adhered to all principles of academic honesty and integrity and have not misrepresented or fabricated or falsified any idea/data/fact/source in my submission. I understand that violation of the above will be cause for disciplinary action by the Institute and can also evoke penal action from the sources which have thus not been properly cited or from whom proper permission has not been taken when needed.

Sneha Bhogale

20093031

Date: 31st March 2015

Acknowledgements

First of all, and most importantly, I thank my advisor, Dr. Anjan K. Banerjee, for all his wonderful ideas, encouragement and great support. I very much enjoyed my time in AKB lab and hope that it keeps its unique spirit. I thank IISER, Pune and Prof. L.S. Shashidhara for providing me the opportunity to work at IISER, Pune with all the required facilities and for giving me financial support when required.

I greatly acknowledge Council of Scientific and Industrial Research (CSIR), India for my fellowship and travel grant. Also Department of Science and technology (DST), India, for the Indo-Argentine bilateral grant.

I also want to thank the members of my advisory committee, Prof. Sujata Bhargava (Pune University) and Dr. Aurnab Ghose (IISER, Pune) for their helpful comments and discussions.

I acknowledge our collaborator Prof. Rita Ulloa (INGEBI, Argentina) for her help and support in the *miR390-StCDPK1* project. I thank Rita, Franco and Elisa for making my stay in Argentina a memorable experience.

I greatly acknowledge Prof. David Hannapel (Iowa State University) and Prof. Julia Kehr (University of Hamburg) for the critical reading of our manuscript.

I also thank Prof. Galande (IISER, Pune) and Dr. Thulasiram (NCL, Pune) for their help in carrying out EMSA and HR-MS experiments respectively.

I thank all the AKB lab members for their help and support throughout my PhD. A special thanks to Ameya, Bhavani, Mohit and Boominathan for all the scientific and non-scientific discussions and for a lot of help in the lab. I also thank Dr. Jana and Nitish for their help in growing and maintaining plants, one of the most important parts of my work! Mrinalini, Piyush, Shabnam and Kalpesh have been very helpful with respect to our lab requirements. I thank them for the same.

Many thanks to all my friends at IISER for the fun times on campus and for our absurd discussions especially during ‘chai’ time.

Lastly, I thank my family for all their love, encouragement and support. They have been an active part of my PhD right from the start. They have made it all easy for me. Thank you for everything!

Sneha Bhogale

Synopsis

Title: Studying the role of micro RNAs in tuber development in potato

(*Solanum tuberosum* ssp *andigena*)

Name: Sneha Bhogale

Roll Number: 20093031

Name of Supervisor: Dr. Anjan K. Banerjee

Department: Biology

Date of Registration: 19th January, 2009

Indian Institute of Science Education and Research (IISER), Pune, India.

Introduction:

Tuber development in potato (tuberization) is a complex developmental pathway which results from the interplay of many exogenous and endogenous signals (Sarkar, 2008). It involves the formation of a specialized underground stem (stolon), which further develops into a mature tuber. Tuberization and flowering are two different reproductive strategies of the plant which share many similar environmental cues and molecular players (Rodríguez-Falcón et al., 2006; Abelenda et al., 2014). Environmental signals like photoperiod & temperature and hormonal signals like gibberellins, cytokinins etc play important roles in both these pathways and the molecular framework that regulates flowering and tuberization appears to be conserved. The photoperiod dependent CONSTANS-FLOWERING LOCUS T (CO-FT) pathway demonstrated to regulate flowering in *Arabidopsis* (Corbesier et al., 2007) and rice (Tamaki et al., 2007) was also shown to control tuberization pathway in potato (Navarro et al., 2011; González-Schain et al., 2012). Two independent reports by Sawa et al., 2007 and Song et al., 2012 have shown CYCLING DOF FACTOR 1 (CDF1) and FLAVIN-BINDING KELCH REPEAT F-BOX 1 (FKF1) to regulate CO-FT flowering pathway. Interestingly, Kloosterman and co-workers in 2013 have demonstrated that similar module of regulation play important role in tuberization pathway. These studies confirmed the similarities between tuberization and flowering. Apart from transcription factors, signalling

proteins and hormonal signals, micro RNAs are also shown to play an important role in regulation of both these pathways. *miR172* (Aukerman and Sakai, 2003), *miR159* (Achard et al., 2004) and *miR156* (Wu et al., 2009) were demonstrated to be involved in flowering. Interestingly, Martin et al, in 2009 demonstrated the role of *miR172* as a positive signal for tuberization pathway. Recently few reports (Zhang et al., 2009; Xie et al., 2011; Zhang et al., 2013; Lakhotia et al., 2014) have profiled the miRNA population in potato. However, the functional analysis of these miRNAs in potato development has not been investigated. Considering the similarities between tuberization and flowering, we hypothesized that regulation of tuberization pathway via miRNAs may also be conserved. There could be other miRNAs that are possibly involved in regulating the tuberization pathway along with *miR172*.

We aimed to understand the miRNA mediated control of tuber development in potato using *Solanum tuberosum* ssp *andigena* and potato cultivar *Desiree* as a model system. The study is divided in following three objectives:

1. To short list, validate and predict targets of candidate miRNAs potentially involved in tuber development.
2. To characterize the role of *miR156* in potato development and tuberization pathway.
3. To understand the interaction of *miR390* and its target *StCDPK1* in tuber development.

1. To shortlist, validate and predict target genes of candidate miRNAs potentially involved in tuber development:

Based on the evolutionarily conserved nature of miRNAs, many reports predicted miRNAs from potato by using computational tools (Yang et al., 2009; Zhang et al., 2009; Xie et al., 2011). The availability of complete potato genome in 2011 [http://www.potatogenome.net (Potato Genome Sequencing Consortium., 2011)] and the advances in high throughput sequencing technologies unravelled a new platform for profiling the miRNA populations in potato. Zhang et al (2013) reported 28 conserved miRNA families as well as 120 potato specific miRNA families with their in-silico target predictions in *andigena* while Lakhotia and co-workers (2014) reported 89 conserved miRNAs and 147

potato specific miRNAs in potato cultivar *Chandramukhi*. The authors also demonstrated differential miRNA expression in tuber transition stages along with their target predictions. These two studies demonstrated a complex miRNA population in potato and suggested their potential involvement in regulating different pathways including tuberization.

Based on above reports and the similarities between flowering and tuberization, we shortlisted 15 miRNAs (conserved and potato-specific miRNAs) potentially to be involved in tuberization pathway. Of these 15 miRNAs, we validated 12 miRNAs in potato, few of which showed SD-LD dependent detection. Further, a detailed target prediction of these validated miRNAs revealed a set of miRNA candidates potentially involved in tuber formation pathway. Finally, based on our results, we selected *miR156* and *miR390* to test for their role in tuberization pathway.

2. **To characterize the role of *miR156* in potato development and tuberization pathway:**

miR156 is a well conserved miRNA present in all land plants (Axtell and Bowman, 2008). It targets Squamosa Promoter binding-Like (SPL) transcription factors (Schwab et al., 2005) and acts as a master regulator of plant development as demonstrated in *Arabidopsis* (Huijser and Schmid, 2011), rice (Xie et al., 2006), maize (Chuck et al., 2007) etc. *miR156* along with *miR172* regulated phase transitions and flowering (Wu et al., 2009). Considering the role of *miR172* in flowering and tuberization pathways (Martin et al., 2009; Wu et al., 2009), we hypothesized the involvement of *miR156* in tuber formation pathway. Also, *miR156* has been detected in phloem sap of pumpkin (Yoo et al., 2004), *Arabidopsis*, apple (Varkonyi-Gasic et al., 2010) and *Brassica napus* (Buhtz et al., 2008), however, mobility of *miR156* in plants has not yet been investigated.

In this part of work, we investigated *miR156* function with a focus on the tuberization pathway. Our results suggested that *miR156* is a graft-transmissible signal that affects plant architecture and tuber development in potato. It was present in the phloem of wild type plants and it accumulated in short-day (SD) induced stolons to facilitate tuber formation. Ectopic expression of *miR156* resulted in reduced tuber yield along with presence of aerial tubers under tuber inducing short-day photoperiod. Also, *miR156* OE lines displayed multiple morphological traits and demonstrated changes in hormone levels like cytokinins and strigolactones. Similar phenotype was also observed in *miR156* OE tobacco plants. This suggested that *miR156* acts as a master regulator of plant development. RLM-RACE analysis validated *St*SPL3, *St*SPL6, *St*SPL9, *St*SPL13 (Squamosa Promoter binding Like Proteins) and

*St*LG1 (Liguleless 1) as targets of *miR156*. Overall, our results strongly suggested that *miR156* is a phloem-mobile signal regulating potato development.

3. To understand the interaction of *miR390* and its target *St*CDPK1 in tuber development:

Calcium Dependent Protein Kinases (CDPKs) are calcium sensor proteins which play important roles in tuber formation (Nookaraju et al., 2012). Initially, only a few CDPKs were known to be present in potato, however, due to availability of complete genome, now 27 additional CDPKs are identified in potato (Ulloa Lab, INGEBI, Argentina, unpublished data). Function of *St*CDPK1 in tuber development has been well investigated earlier (Raices et al., 2001; Raíces et al., 2003; Gargantini et al., 2009). However, very little information is available on its regulation. Our bioinformatic target prediction analysis for the shortlisted miRNAs revealed *StCDPK1* to be a potential target for *miR390*. In order to understand the miRNA mediated regulation of *StCDPK1*, we investigated the *miR390-StCDPK1* interaction in potato cultivar *Desiree*.

In our study, we validated the mature and precursor form of *miR390* in *Desiree*. Tissue specific expression analysis of *miR390* and *StCDPK1* revealed an inverse expression pattern. In aerial parts of the plant (axillary meristems, petioles, stem), the levels of *miR390* were higher than those of *StCDPK1*. While in underground organs (stolons, swollen stolons and tubers), *StCDPK1* accumulated in greater amount than *miR390*. This finding possibly indicated the *miR390* mediated control of *StCDPK1* in aerial parts of the plants, while this regulation appears to be removed in stolons and swollen stolons, allowing *CDPK1* levels to accumulate and facilitate tuber formation. Further, our *Agrobacterium*-mediated co-infiltration studies showed that *miR390* potentially directs *CDPK1* transcript cleavage, thus downregulating *CDPK1* levels. Collectively, these results suggested that *miR390-StCDPK1* interaction in potato possibly plays an important role in tuberization pathway.

Summary:

In summary, we have shortlisted and validated twelve miRNAs (in a SD-LD photoperiod dependent manner) potentially involved in tuberization pathway. Our detailed *in-silico* target prediction revealed few miRNA candidates showing potential to be tested for their involvement in tuber formation pathway. Based on our preliminary results, we selected *miR156* and *miR390* for detailed characterizations. We have demonstrated that *miR156*

facilitates tuber formation under inductive SD conditions. *miR156* over expression affects multiple morphological traits in potato and tobacco and it is a graft-transmissible signal that potentially moves long distances via phloem in potato. Overall, we have shown that *miR156* is a graft-transmissible signal that modulates tuber formation and plant architecture in potato. In our studies with *miR390-StCDPK1*, we have demonstrated that *miR390-StCDPK1* interaction in potato possibly plays an important role in tuberization pathway. To our knowledge, this is the first report of miRNA mediated post-transcriptional control of CDPKs.

List of Publications:

1. **Bhogale S**, Mahajan AS, Natarajan B, Rajabhoj M, Thulasiram HV, Banerjee AK (2014) *MicroRNA156*: a potential graft-transmissible microRNA that modulates plant architecture and tuberization in *Solanum tuberosum* ssp. *andigena*. Plant Physiology, 164:1011-1027.
2. Santin F, **Bhogale S**, Fantino E, Grandellis C, Banerjee AK, Ulloa RM (2015) *StCDPK1* expression pattern and its post transcriptional regulation by *microRNA 390* in potato (Submitted to Plant Molecular Biology, under review).

References:

Abelenda J a, Navarro C, Prat S (2014) Flowering and tuberization: a tale of two nightshades. Trends in plant science **19**: 115–122

Achard P, Herr A, Baulcombe DC, Harberd NP (2004) Modulation of floral development by a gibberellin-regulated microRNA. Development **131**: 3357–3365

Aukerman MJ, Sakai H (2003) Regulation of Flowering Time and Floral Organ Identity by a MicroRNA and Its APETALA2 -Like Target Genes. The Plant Cell **15**: 2730–2741

Axtell MJ, Bowman JL (2008) Evolution of plant microRNAs and their targets. Trends in Plant Science **13**: 343–349

Buhtz A, Springer F, Chappell L, Baulcombe DC, Kehr J (2008) Identification and characterization of small RNAs from the phloem of Brassica napus. The Plant Journal **53**: 739–749

Chuck G, Cigan AM, Saeteurn K, Hake S (2007) The heterochronic maize mutant Corngrass1 results from overexpression of a tandem microRNA. Nature Genetics **39**: 544–549

Corbesier L, Vincent C, Jang S, Fornara F, Fan Q, Searle I, Giakountis A, Farrona S, Gissot L, Turnbull C, et al (2007) FT Protein Movement Contributes to Long-Distance Signaling in Floral Induction of Arabidopsis. Science **316**: 1030–1033

Gargantini PR, Giammaria V, Grandellis C, Feingold SE, Maldonado S, Ulloa RM (2009) Genomic and functional characterization of StCDPK1. Plant molecular biology **70**: 153–172

González-Schain ND, Díaz-Mendoza M, Zurczak M, Suárez-López P (2012) Potato CONSTANS is involved in photoperiodic tuberization in a graft-transmissible manner. The Plant journal **70**: 678–690

Huijser P, Schmid M (2011) The control of developmental phase transitions in plants. Development **138**: 4117–4129

Kloosterman B, Abelenda J a, Gomez MDMC, Oortwijn M, De Boer JM, Kowitwanich K, Horvath BM, Van Eck HJ, Smaczniak C, Prat S, et al (2013) Naturally occurring allele diversity allows potato cultivation in northern latitudes ´. Nature **495**: 246–250

Lakhotia N, Joshi G, Bhardwaj AR, Katiyar-Agarwal S, Agarwal M, Jagannath A, Goel S, Kumar A (2014) Identification and characterization of miRNAome in root, stem, leaf and tuber developmental stages of potato (Solanum tuberosum L.) by high-throughput sequencing. BMC plant biology **14**: 6

Martin A, Adam H, Díaz-Mendoza M, Zurczak M, González-Schain ND, Suárez-López P (2009) Graft-transmissible induction of potato tuberization by the microRNA miR172. Development **136**: 2873–2881

Navarro C, Abelenda JA, Cruz-oro E, Cuellar CA, Tamaki S, Silva J, Shimamoto K, Prat S (2011) Control of flowering and storage organ formation in potato by FLOWERING LOCUS T. Nature **478**: 119–122

Nookaraju A, Pandey SK, Upadhyaya CP, Heung JJ, Kim HS, Chun SC, Kim DH, Park SW (2012) Role of Ca 2 + -mediated signaling in potato tuberization : An overview. Botanical Studies **53**: 177–189

Potato Genome Sequencing Consortium (2011) Genome sequence and analysis of the tuber crop potato. Nature **475**:189–195

Raices M, Chico JM, Tellez-Inon MT, Ulloa RM (2001) Molecular characterization of StCDPK1 , a calcium-dependent protein kinase from Solanum tuberosum that is induced at the onset of tuber development. Plant Molecular Biology **46**: 591–601

Raíces M, Ulloa RM, MacIntosh GC, Crespi M, Téllez-Iñón MT (2003) StCDPK1 is expressed in potato stolon tips and is induced by high sucrose concentration. Journal of experimental botany **54**: 258925–91

Rodríguez-Falcón M, Bou J, Prat S (2006) Seasonal control of tuberization in potato: conserved elements with the flowering response. Annual review of plant biology **57**: 151–80

Sarkar D (2008) The signal transduction pathways controlling in planta tuberization in potato: an emerging synthesis. Plant cell reports **27**: 1–8

Sawa M, Nusinow DA, Kay SA, Imaizumi T (2007) FKF1 and GIGANTEA Complex Formation Is Required for Day-Length Measurement in Arabidopsis. Science **318**: 261–265

Schwab R, Palatnik JF, Riester M, Schommer C, Schmid M, Weigel D (2005) Specific Effects of MicroRNAs on the Plant Transcriptome. Developmental Cell **8**: 517–527

Song YH, Smith RW, To BJ, Millar AJ, Imaizumi T (2012) FKF1 Conveys Timing Information for CONSTANS Stabilization in Photoperiodic Flowering. Science **336**: 1045–1050

Tamaki S, Matsuo S, Wong HL, Yokoi S, Shimamoto K (2007) Hd3a Protein Is a Mobile Flowering Signal in Rice. Science **316**: 1033–1037

Varkonyi-Gasic E, Gould N, Sandanayaka M, Sutherland P, MacDiarmid RM (2010) Characterisation of microRNAs from apple (Malus domestica "Royal Gala") vascular tissue and phloem sap. BMC Plant Biology **10**: 159

Wu G, Park MY, Conway SR, Wang J-W, Weigel D, Poethig RS (2009) The Sequential Action of miR156 and miR172 Regulates Developmental Timing in Arabidopsis. Cell **138**: 750–759

Xie F, Frazier TP, Zhang B (2011) Identification, characterization and expression analysis of MicroRNAs and their targets in the potato (Solanum tuberosum). Gene **473**: 8–22

Xie K, Wu C, Xiong L (2006) Genomic Organization, Differential Expression, and Interaction of SQUAMOSA Promoter-Binding-Like Transcription Factors and microRNA156 in Rice. Plant Physiology **142**: 280–293

Yang W, Liu X, Zhang J, Feng J, Li C, Chen J (2009) Prediction and validation of conservative microRNAs of Solanum tuberosum L. Molecular Biology Reports **37**: 3081–3087

Yoo B, Kragler F, Varkonyi-gasic E, Haywood V, Archer-Evans S, Lee YM, Lough TJ, Lucas WJ (2004) A Systemic Small RNA Signaling System in Plants. The Plant Cell **16**: 1979–2000

Zhang R, Marshall D, Bryan GJ, Hornyik C (2013) Identification and characterization of miRNA transcriptome in potato by high-throughput sequencing. PloS one **8**: e57233

Zhang W, Luo Y, Gong X, Zeng W, Li S (2009) Computational identification of 48 potato microRNAs and their targets. Computational Biology and Chemistry **33**: 84–93

Table of Contents:

Chapter 2

Micro RNAs in potato (*Solanum tuberosum* ssp *andigena*)

Chapter 3

Role of *miRNA156* in potato development

Chapter 4

Understanding the *miR390-StCDPK1* interaction in tuberization pathway

List of Figures

Chapter 1

Introduction

Chapter 2

Micro RNAs in potato (*Solanum tuberosum* ssp *andigena*)

Chapter 3

Role of *miRNA156* in potato development

Chapter 4

Understanding the *miR390-StCDPK1* interaction in tuberization pathway

List of Tables

Chapter 1

Introduction:

Chapter 2

Micro RNAs in potato (*Solanum tuberosum* ssp *andigena*)

Chapter 3

Role of *miRNA156* in potato development

Chapter 4

Understanding the *miR390-StCDPK1* interaction in tuberization pathway

Abbreviations used:

Abscisic Acid	ABA
ADENOSINE PHOSPHATE ISOPENTENYL TRANSFERASE 2	IPT2
ADENOSINE PHOSPHATE ISOPENTENYL TRANSFERASE 5	IPT5
APETELLA 2	AP2
ARGONAUTE	AGO
AUXIN RESISTANT PROTEIN 1	AXR1
AUXIN RESISTANT PROTEIN 3	AXR3
Auxin Response Factors	ARF
Calcium Dependent Protein Kinase	CDPK
Calmodulin	CAM
CAROTENOID CLEAVAGE DIOXYGENASE 8	CCD8
CONSTANS	CO
CUP SHAPED COTYLEDON 3	CUC3
CYCLING DOF FACTOR	CDF
Cytokinin	CK
DAWDLE	DDL
DICER-like 1	DCL1
ethyleneglycol-bis4 (i-amino ethyl ether) N, N'-tetra acetic acid	EGTA
FLAVIN-BINDING KELCH REPEAT F-BOX PROTEIN 1	FKF1
FLOWERING LOCUS T	FT
G2-like TF	G2
GA related MYB	GAMYB
Gibberellic Acid	GA
GIGANTIA	GI
High Resolution Mass Spectrometry	HR-MS
HYPONASTIC LEAVES 1	HYL
Indole Acetic Acid	IAA
Jasmonic Acid	JA

Laser Microdissection Pressure Catapulting	LMPC
Leaf mass per area	LMA
Lipoxygenase	LOX
LOV KELCH PROTEIN 2	LKP2
MicroRNA Recognition Element	MRE
MORE AXILLARY BRANCHING 1	MAX1
MORE AXILLARY BRANCHING 2	MAX2
Nitrate Transporter	NT
NO APICAL MERISREM	NAM
PHOTOPERIOD-RESPONSIVE 1	PHOR1
PHYTOCHROME A	PHYA
PHYTOCHROME B	PHYB
PINHEAD 1	PIN1
PINHEAD 5	PIN5
POTATO HOMEOBOX 1	POTH1
POTATO MADS BOX 1	POTM1
PROTEIN PHOSPHATASE 2 AC	PP2Ac
Related to APETELLA2 1	RAP1
RNA Induced Silencing Complex	RISC
SERRATE	SE
Squamosa Promoter binding-Like	SPL
SUCROSE TRANSPORTER 4	SUT4
SUPERSHOOT	SPS
SUPPRESSOR OF OVEREXPRESSION OF CO1	SOC1
TERMINAL FLOWER 1	TFL1
Three Amino Loop Extension	TALE
TOMATO LONELY GUY 1	TLOG1

Trans-Acting Short Interfering RNAs	Tasi-RNAs
Transcription Factor	TF

Chapter 1

Introduction

1.1. Potato

Potato, a herbaceous perennial crop belonging to *Solanum tuberosum* L, is the third most important food crop after wheat and rice (http://faostat.fao.org/). It belongs to *Solanaceae* family, which includes many other crops like tomato, capsicum, eggplant etc. Potatoes first originated in South America where day lengths are close to 12 hours (short days, SD) with low night temperatures. Wild Andean varieties like *Solanum tuberosum* ssp *andigena* are adapted to such conditions and are unable to tuberize under long days (LD, day lengths > 12 hours). The *andigena* variety is thus, photoperiod sensitive for tuberization. However, presently cultivated varieties of potato (*Solanum tuberosum* ssp *tuberosum*), which originated in Chile after years of selective breeding, are more adaptive and can form tubers under day lengths > 12 hours, LD (as reviewed in Rodríguez-Falcón et al., 2006). Tubers form an important part of the potato plant due to its dietary contribution. They are rich in starch and proteins. They act as caloric supplementation to human dietary needs and are considered important in world food security. Tubers serve as storage organs as well as a mode of asexual reproduction for the plant. They are modified underground stems having dormant axillary meristems (eyes). After a period of dormancy, under favourable conditions, new shoots originate from these tuber eyes giving rise to a new plant.

1.2. Tuberization pathway

Tuberization pathway (tuber development) is a complex process involving formation of a specialized underground stem (stolon), which further develops into a mature tuber. Tuber induction is associated with changes in the plant as well. Axillary branching is suppressed, flower buds are frequently aborted and leaves grow larger in size which coincides with the rapid growth of underground tubers (Ewing and Struik, 1992). In general, tuberization is promoted by short days and low temperatures (inductive condition), while long days and high temperatures delay tuber formation (non-inductive condition) (Ewing and Wareing, 1978). Understanding the tuberization pathway is thus strategic in terms of world food security, besides it being a fundamental developmental question. For past many decades, tuberization has been the key question of many researchers around the world. Many aspects of the pathway are now known. Tuberization appears to be a complex process and it is shown to be governed by various environmental, hormonal and molecular factors (Hannapel et al., 2004; Rodríguez-Falcón et al., 2006; Sarkar, 2008; Sarkar, 2010; Abelenda et al., 2011).

1.3. Environmental control of tuberization

Environmental factors like photoperiod, temperature, light intensity and nitrogen levels have been shown to play important role in tuber development. The effect of these factors has been described in the following sections.

1.3.1. Role of photoperiod

Of all the environmental factors, photoperiod (day length) is the most widely studied factor as it has the most critical effect on tuberization. Photoperiod is defined as the proportion of light and dark hours in a 24 hour daily cycle (Jackson, 2009). Short days have inductive effect on tuber formation while long days have repressive effect (Ewing and Wareing, 1978). Many developmental processes like flowering, bud growth etc are under photoperiodic control (Jackson, 2009). In case of potato, to survive the harsh winters, potato plant forms underground tubers, which remain dormant throughout the winter season, while the plant above dies. Under favourable conditions, these tubers sprout and give rise to a new plant. The short days during the onset of winter season thus act as a cue for the tuberization process to initiate. Short days in general induce tuber formation in all potato varieties with considerable variation in the degree to which photoperiod is required for induction. Wild potato varieties like *Solanum tuberosum* ssp *andigena* and *Solanum demissum* are strictly dependent on short days for tuber formation (Ewing and Struik, 1992). 8 to 10 hours (SD) of light promote tuber formation. They do not form tubers under long days or short days with night break (NB) or a pulse of light during night period (SD + NB) (Figure 1.1). However, another wild-type: *Solanum tuberosum ssp tuberosum* is not sensitive to photoperiod (Rodriguez-Falcon et al., 2006). Also, the modern cultivated potato varieties have lost the photoperiod control and they tuberize under LDs as well. As photoperiod has the most critical effect on tuber formation and *andigena* being one of the photoperiod sensitive wild-type variety, maximum studies on understanding of tuberization pathway have been reported in *andigena* cultivar. *Solanum tuberosum* ssp *andigena* thus, serves a good model system to study photoperiod mediated tuber formation pathways.

Experiments by Gregory in 1950s had suggested that the photoperiod dependent signal is perceived in the leaves of potato plants grown under SD conditions (Gregory, 1956). In these experiments, scions from the plants grown in SD photoperiod were grafted onto the stocks of plants grown in LD. It was observed that the induced scions were capable of promoting tuberization under non-inducing LD conditions. These experiments were

repeated in different potato varieties showing similar effect (Chapman, 1958). Also, in *andigena* lines, this tuber inducing graft-transmissible signal was demonstrated to move acropetally as well as basipetally (Kumar and Wareing, 1974). Further studies identified the molecular players involved in this photoperiod dependent pathway as well, which are described in section 1.5 and table 1.1.

1.3.2. Effects of temperature

Temperature is another important environmental factor that affects tuberization (Bushnell, 1927; Werner, 1934; Gregory, 1956; Cao and Tibbitts, 1992). As tuber formation is the plant's strategy to survive harsh winters, cooler temperatures promote tuber formation in potato plants. In general, temperatures of 18 to 20 ˚C promote tuberization, while higher temperatures inhibit the pathway (Gregory, 1956). A study by Bushnell (1927) reported that at higher temperatures, the amount of carbohydrates utilized by potato plant for respiration is more. This in turn reduces the amount of carbohydrates available for tuber bulking. Therefore, tubers are not formed at higher temperatures. In a study conducted by Werner (1934), the author stated that, temperature and photoperiod can be viewed as similar environmental cues. Longer days can be easily associated with higher temperature and vice versa. A strong day length response is observed during high temperatures, while day length control is less prominent during low temperatures. The authors concluded that photoperiod and temperature cues converge at some point in the pathway and exert their effect on tuberization.

1.3.3. Effects of light intensity

The effect of light intensity on tuberization is not as extensively investigated as photoperiod. However, it has been established that high light intensity promotes tuber formation in potato. A study by Wheeler and Tibbitts (1986) demonstrated that high intensity light (400 umol m-2 s-') can promote tuber formation even under LD conditions. These results were consistent with the high yields observed under LD in field conditions with high levels of natural light intensity. Also, plants placed under continuous high light intensity successfully tuberized (Wheeler and Tibbitts, 1986). Another study by Bodlaender (1963) demonstrated that the LD tuber suppression can be over ruled by growing plants in high light intensity. However, all these studies were conducted with cultivars which were not strictly dependent on photoperiod. Effect of different light intensities on tuber induction of *andigena* or *demissum* plants (photoperiod dependent) has not been yet investigated.

1.3.4. Effects of Nitrogen levels

Of all the environmental factors affecting tuberization, nitrogen content is the least investigated. Low rates of nitrogen supply promote tuberization while nitrogen rich environments inhibit tuber formation (Werner, 1934). This study reported that in presence of shorter days and cold temperatures, nitrogen cannot be assimilated, thus assisting tuberization in general.

1.4. Hormonal control of tuberization

A number of hormones have also been found to have significant effect on tuberization pathway. These have been described in following sections.

1.4.1. Role of gibberellic acid

The function of gibberellic acid (GA) in regulating tuberization has been well investigated (Rodriguez-Falcon et al., 2006; Sarkar, 2010). GA_3 application delayed tuber initiation (Xu et al., 1998a) while addition of GA synthesis inhibitors enhanced tuber formation (Harvey et al., 1991; Abdala et al., 1995). Another study conducted in 2000 manipulated GA levels by overexpression or inhibition (antisense) of GA_{20} oxidase gene (*$StGA_{20}ox1$*) which resulted in delayed tuberization in plants grown in SD conditions (Carrera et al., 2000). These reports clearly established the correlation between GA levels and tuberization. A study was conducted by van der Berg and co-workers (1995) in which GA biosynthetic step was blocked (*ga1* mutant). These mutant plants formed tubers even in LD (non-inducing) conditions upon prolonged incubation. While, transfer of these mutants in SD conditions induced tuberization within 3-4 days post induction. According to the authors, these results indicated that although SD requirement was less severe in mutants as compared to wild-type plants, tuberization was still dependent on photoperiod (van Den Berg et al., 1995). This study implicated the presence of two separate pathways for tuberization: photoperiod (SD-LD) dependent pathway and GA dependent pathway. SD photoperiod being the tuber inductive pathway, while GA being the inhibitory pathway. The balance between these two pathways thus, determined the onset of tuberization.

There is ample evidence on the inhibitory effect of GA on tuberization as discussed above. However, the general idea of low levels of GA in the whole plant promote tuber formation does not hold true. There is difference in the spatial GA levels which play an important part in promoting tuberization. Microarray analysis of tuber development identified *GA_2 oxidase* (catalyses the degradation of bioactive GA molecules) mRNA to be

upregulated specifically in stolons (Kloosterman et al., 2005). The authors have found that expression of this transcript is activated very early on during SD inductions. Upregulation of this transcript ensured low levels of GA in stolons, the key event for tuber formation. Another study conducted by Bou-Torrent et al (2011) examined the role of GA_3 oxidase (*$StGA_3ox2$*: GA biosynthetic gene) in tuberization using overexpression strategy. Overexpression lines showed a taller phenotype with increased shoot GA_1 levels (Bou-Torrent et al., 2011). As per the general consideration, high levels of GA should have resulted in delayed tuber formation. However, these plants tuberized earlier in SD conditions with higher yield as compared to controls. Another study by Carrera et al (2000) showed that overexpression of another GA biosynthetic gene, *GA_{20} oxidase*, resulted in delayed tuber formation (Carrera et al., 2000). Considering these reports, it appears that increased levels of GA_{20} precursor in the aerial parts of the plant delay tuberization, while increased levels of GA1 promote tuberization. This difference in action was possibly due to differential mobility of these GAs as suggested by the authors reviewing role of GA in tuberization pathway (Rodriguez-Falcon et al., 2006). They concluded that GA_{20} is transported throughout the plant, thus inhibiting tuberization, while GA_1 is present in the cells, where it is produced resulting in taller plant phenotype and early tuberization. Therefore, as opposed to the general idea of inhibitory effect of GAs on tuberization, it was proposed that high levels of GAs in stolons inhibit tuberization, whereas high rate of GA_{20} to GA_1 conversion in the shoots favours tuber formation. How do low levels of GAs inhibit tuber formation? In a study conducted by Shibaoka (1993), it was found that increased GA in stolon tips promotes stolon elongation by inducing microtubule alignment to the long axis of growing cells (Shibaoka, 1993). On the other hand, reduced levels of GA caused reorientation of stolon microtubules initiating radial expansion of the tubers as demonstrated by Fujino et al (1995). Considering these data, the authors reviewing role of GAs in tuberization pathway (Rodriguez-Falcon et al., 2006) proposed that under LD conditions, high levels of GA in stolon tips promote shoot outgrowth. On the other hand, under SD conditions, low levels of GA in stolon tips promote tuber formation.

1.4.2. Role of auxins

Auxins also play an important role in tuber transitions. Application of auxin to a single node of *in vitro* potato plants resulted in an earlier tuberization phenotype with small, sessile tubers (Xu et al., 1998a) suggesting role of auxins in tuber formation. A micro array based study by Kloosterman and co-workers (2008) in different tuber developmental stages revealed many auxins related genes being differentially expressed (Kloosterman et al., 2008). Genes involved in auxin transport (PIN family of proteins), auxin response factors (ARFs) and Aux/IAA genes showed differential expression. For example, ARF6 was found to be highly expressed prior to stolon swelling. Also, levels of IAA (Indole Acetic Acid: type of auxin) increased in the stolons after a few days in SD conditions, which coincided with increased expression of IAA biosynthetic gene as demonstrated by Roumeliotis et al (2012). It was proposed that the role of auxins in regulating stolon outgrowth was quite similar to its role in shoot branching above ground.

1.4.3. Role of abscisic acid

Apart from GA and auxins, abscisic acid (ABA) was also found to be involved in tuberization pathway. Application of ABA resulted in early tuberization and higher number of tubers suggesting its role in tuberization (Menzel, 1980). Similar results of early tuberization were obtained when ABA was applied to *in vitro* plants in presence of high sucrose (Xu et al., 1998a). It was also found that ABA can promote tuber formation in presence of low sucrose and GA (Xu et al., 1998a). Thus, the authors concluded that ABA can surpass the inhibitory effect of low sucrose and high GA levels. However, ABA deficient mutant in *Solanum phureja* tuberized normally as compared to wild-type indicating that ABA was not required for tuberization (Quarrie, 1982). The authors concluded that, the tuber promoting effect of ABA was due to the antagonistic relationship of ABA and GA (Xu et al., 1998a).

1.4.4. Effects of cytokinin

Another phytohormone shown to play a role in tuber formation was cytokinin (CK). Direct application of cytokinins to *in vitro* cultured stolons promoted tuberization (Palmer et al, 1970). However, CK application to soil grown *andigena* leaves failed to promote tuberization under LD conditions. In another study (Mauk and Langille, 1978), CK levels increased during tuber induction in stolon tips. While the tuber inducing effect of CK was observed only in presence of high levels of sucrose in a study by Palmer and co-workers (1970). This indicated that CK is not required for tuber induction but functions in the

stages of tuber growth. However, a study by Eviatar-Ribak and co-workers (2013) demonstrated that *TLOG1* (*Tomato Lonely Guy1*) overexpressing tomato plants produced aerial tubers from first few nodes on the primary shoot. *LOG1* is a CK biosynthetic gene which converts inactive CK to active CK. Increased levels of *TLOG1* resulted in production of aerial tubers from juvenile axillary meristems of tomato plant (which naturally does not form tubers). This study demonstrated that increased CK promotes tuber formation in juvenile meristems and highlighted the importance of CK in tuberization pathway (Eviatar-Ribak et al., 2013).

1.4.5. Other hormonal signals

A study conducted by Takahashi et al (1994) showed that application of 12-OH jasmonic acid (JA) to *in vitro* potato plants induced tuber formation. Also, JA was isolated from potato plants induced for tuberization (Koda et al., 1988). These studies indicated involvement of JA in regulating tuber formation. However, studies where application of JA to non-induced andigena leaves failed to tuberize (Jackson and Willmitzer, 1994) questioning the direct role of JA in tuber induction. A study on a JA biosynthetic gene (*hydroxyjasmonate sulphotransferase*) revealed that JA signalling is not specific to tuber formation but is involved in other developmental processes as well (Gidda et al., 2003). A study in 2013, demonstrated the role of another group of hormones; strigolactones in tuber formation (Roumeliotis et al., 2012). Application of strigolactone analogue- GR24 to *in vitro* potato plants resulted in reduced tuber formation. However, detailed mechanism of how strigolactones could control tuberization needs to be investigated.

1.5. Molecular control of tuberization

Under inductive SD conditions, tuberization signal is perceived in the leaves followed by its transport to the underground stolons, which are induced to form tubers. This mobile tuberization signal is termed as tuberigen' which is similar to 'florigen', the mobile flowering signal. After tuberization signal has been transported to the stolons, tuber transition process is initiated. In this transition process of stolon to tuber formation, stolon undergoes massive changes like rapid cell expansion and cell elongation. It passes through a series of developmental stages, which finally forms a tuber (so called potatoes). While under non-inductive LD conditions, the stolons continue to form vegetative shoots (reviewed in Rodriquez-Falcon et al., 2006; Sarkar, 2008; Sarkar, 2010). A number of molecular factors involved in all these stages have been elucidated mostly using *andigena* potato plants.

1.5.1. Signal perception

Andigena lines tuberized under SD conditions, while do not form tubers under LD, LD+NB or SD+NB as discussed earlier. It has been observed that red light was most effective for interrupting long nights while a pulse of far red light given after red pulse reversed the inhibitory effect of the red light night break (Batutis and Ewing, 1982). This indicated that length of the night is sensed by phytochromes (PHYs). Two phytochrome genes have been characterized in potato, PHYA and PHYB (Heyer and Gatz, 1992a; Heyer and Gatz, 1992b). A detailed study by Jackson and co-workers (1998) on PHYB demonstrated its role in tuberization pathway. The authors showed that PHYB antisense lines in *andigena* background were non-responsive to photoperiod and they tuberized under LD and SD+NB conditions along with early tuberization SD conditions. These lines were strongly induced to tuberize and they even formed sessile tubers attached to the main stem. This clearly showed the role of PHYB in day length control. There authors also showed that grafting with *phyb* potato scions onto wild-type stocks tuberized in LDs, while tuber formation was not observed in reverse grafts (wild-type scion, *phyb* stock). Considering these data, the authors demonstrated that PHYB repressed tuberization signal under tuber non-inductive conditions (Jackson et al., 1998). Role of PHYA in day length perception has been demonstrated using PHYA antisense lines (Heyer et al., 1995). Concerted action of PHYA, PHYB and blue light receptors seemed to exert photoperiodic control of tuberization (as reviewed by Rodriguez-Falcon et al., 2006).

1.5.2. Signalling in leaves

Previous studies showed that the CONSTANS/FLOWERING LOCUS T (CO/FT) module plays a central role in photoperiod response pathways like flowering (Zeevaart, 2006; Amasino and Michaels, 2010). Role of CO in potato tuberization pathway was known in 2002, when *Arabidopsis* CO was overexpressed in potato (Martínez-García et al., 2002). Later, a study conducted in potato, demonstrated the role of *StCO* in tuber formation (González-Schain et al., 2012). The authors showed that *StCO* mRNA accumulation pattern followed a daily oscillation pattern and was under photoperiod control. Overexpression of *StCO* delayed tuberization, while antisense lines tuberized under LD conditions. However, antisense lines did not affect tuberization under SD conditions indicating that *StCO* does not play role under tuber inducing conditions. It repressed tuberization under LD conditions.

A study in 2013 investigated the upstream pathway of *StCO* in SD dependent and independent potato cultivars (Kloosterman et al., 2013). How is *StCO* regulated under different photoperiods? Authors showed that a member of the CYCLING DOF FACTOR gene family, *St*CDF1 forms a complex with GIGENTIA (GI) and FKF1, the clock gene components. This complex is then marked for proteosomal degradation. When free, *St*CDF1 binds to the promoter of *St*CO and repressed its expression, resulting in tuber induction. This study also reported the presence of *St*CDF1 variant (truncated form) which lacks the FKF1 interacting domain and is thus not marked for degradation. The truncated *St*CDF1 is stabilized and it represses *St*CO by binding to its promoter. The cultivars in which *St*CDF1 truncated variant was present showed early tuberization and were insensitive to photoperiod. Consistent with this observation, it has been reported that photoperiod insensitive cultivars (Neo tuberosum) have alleles for both, full length and truncated *St*CDF1, while *andigena*, the photoperiod sensitive variety has only full length *St*CDF1. The authors clearly showed that circadian clock and photoperiod worked in concert to control tuberization in different potato varieties. As mentioned before, *St*CO acts as an inhibitor of tuber formation. How does *StCO* inhibit the tuberization pathway in LDs? Once *St*CDF1 is bound to GI-FKF1 and marked for degradation, *St*CO positively regulates *St*SP5G, an inhibitor of *St*FT/SP6A, the mobile signal for tuberization (González-Schain et al., 2012; Kloosterman et al., 2013). Low expression of *St*FT/SP6A in turn resulted in absence of tuber formation under LD conditions. However, under tuber inductive SD conditions, GI-FKF1-*St*CDF1 complex is not formed. Free *St*CDF1 binds to *St*CO promoter leading to its repression. This in turn releases the control on *St*FT/SP6A tuberization signal.

1.5.3. Tuberigen

The search for finding out the elusive mobile signal for tuberization (tuberigen) was going on for a long time. Right from 1950s, it was known that a systemic signal produced in the leaves is transported to underground stolons via plant's vasculature that results in tuber formation under inductive conditions (Gregory, 1956). However, only recently this 'tuberigen' has been identified. This signalling factor was *St*SP6A, the potato ortholog of FLOWERING LOCUS T (FT) which is responsible for flowering; the florigen (Navarro et al., 2011). The authors have shown that expression of *StSP6A* coincides with tuberization. It is highly expressed in leaves and stolons of SD induced *andigena* plants while not detected in plants grown in LD conditions. Also, its expression analysis coincides with

early, intermediate and late tuberizing potato cultivars indicating that *StSP6A* is involved in regulation of tuberization in photoperiod insensitive cultivars as well. Over expression of *StSP6A* in *andigena* plants resulted in these plants tuberizing in LD conditions, while silencing lead to delay in tuberization under SD photoperiod. As described earlier, *St*SP6A is regulated by clock genes, GI-FKF1 and by *St*CDF-*St*CO under SD- LD photoperiod. Also, grafting experiments demonstrated that *St*SP6A is a mobile signal which is transported from leaves to stolons to induce tuber formation (Navarro et al., 2011).

1.5.4. Other mobile tuberization signals

*St*BEL5 and POTH1 are two transcription factors (TFs) belonging to the TALE (Three Amino acid Loop Extension) family of transcription factors. Studies have demonstrated their role in tuberization pathway where in, both the factors are shown to positively regulate tuber formation. Overexpression of *St*BEL5 (Banerjee et al., 2006a) and POTH1 (Rosin et al., 2003a; Mahajan et al., 2012) in *andigena* plants resulted in plants which produced tubers under LD photoperiod and also showed earliness in tuberization when incubated in SD conditions. Grafting studies have demonstrated that transcripts of these two TFs are expressed highly in SD induced leaves and are then transported to stolons to induce tuber formation. In stolons, *StBEL5* and *POTH1* transcripts are then translated into proteins, where they form heterodimers. These heterodimers bind to the promoter of *StGA-20oxidase* gene and downregulated its expression (Chen et al., 2003; Chen et al., 2004). This resulted in reduction of GA levels in stolons, which is critical for tuber formation as discussed before.

Sucrose is an important metabolic signal involved in tuber initiation and growth. *In vitro* tuber formation is highly dependent on sucrose concentration (reviewed in Gibson, 2005) suggesting its role in triggering sink storage function. Silencing of a sucrose transporter- *StSUT4* in potato resulted in increased sucrose transport and tuber formation in *andigena* plants grown in LD photoperiod. In *StSUT4* silenced plants, the effect was more pronounced when external GA was applied (Chincinska et al., 2008). While, in another study, the levels of *StCO* and *StSP6A* were found to be downregulated and upregulated in *StSUT4* silenced plants respectively (Chincinska et al., 2013). From these data, the authors proposed that there is a possible link between sucrose transport, photoperiodic pathway and circadian clock that resulted in tuber formation under inductive conditions.

1.5.5. Stolon to tuber transition

Stolon to tuber transition is a highly regulated and timely orchestrated process and serves as a good model system for studying organ development. It involves interactions of a number of molecular players as discussed below. Raíces et al., (2003a and 2003b) showed that a Calcium Dependent Protein Kinase, *St*CDPK1, is a key mediator in sucrose-signalling pathways during tuber induction and development and is transiently expressed in tuberizing stolons. Considering the importance of calcium signaling in tuber development (reviewed in Nookaraju et al., 2012), involvement of other CDPKs could be expected. In another study, during stolon to tuber transitions, auxin levels were found to be increased dramatically in the stolons and remained relatively high in developing tubers, indicating a promoting role for auxins in tuber formation (Roumeliotis et al., 2012). Also, many auxin related genes like auxin response factors (ARFs), genes involved in auxin transport (PINs) were differentially expressed during early tuber development (Kloosterman et al., 2008) as mentioned before. For example, ARF6 was highly expressed in stolons prior to swelling and down regulated as the tuber developed (Faivre-Rampant et al., 2004). Apart from auxins, GA and CK also function in tuber development, where low levels of GA and high levels of CK in stolons induced tuber formation (Rodríguez-Falcón et al., 2006). Other phytohormones like JA, ABA and LOXs (Lipoxygenases) are also reported to function in tuber transitions (Rodriguez-Falcon et al., 2006). A study in 2005 (Kloosterman et al., 2005), demonstrated expression of ~1300 transcripts during tuber transitions using cDNA microarrays, while Agrawal and co workers (2008) employed comparative proteomic approach to identify app ~100 proteins involved in different stages of tuber transitions (Agrawal et al., 2008). Such reports demonstrated the involvement of a number of genes in different stages of tuber transitions. However, majority of the genes identified functioned either in starch metabolism, protein synthesis, storage and turn over, carbon and energy metabolism, disease/defense and secondary metabolism with no information on their regulations. Considering the complexity of tuber transitions and the involvement of a variety of molecular players, regulation of tuber transitions remains as an important question for future investigations.

A list of genes involved in tuberization pathway, from signal perception to tuber formation has been listed in table 1.1.

Table 1.1: Genes controlling tuberization pathway in potato

#	Name of the gene	Function	References
1.	*PHYA (PHYTOCHROME A)*	Functions in day length perception.	Heyer et al., 1995.
2.	*PHYB (PHYTOCHROME B)*	PHYB repressed formation of tuber inducing signal under LDs.	Jackson et al., 1998.
3.	*GA20ox1 (GA 20 OXIDASE 1)*	Part of GA pathway. Responsible for photoperiodic regulation of endogenous GA levels and for controlling tuber induction in leaves.	Jackson et al., 2000; Carrera et al., 2000.
4.	*PHOR1 (PHOTOPERIOD-RESPONSIVE 1)*	GA responsive gene, showed upregulated expression in SD induced leaves, proposed to regulate tuberization.	Amador et al., 2001.
5.	*POTLX1 (Potato LOX)*	Codes for dioxygenases (LOX) and controls development of tubers	Kolomiets et al., 2001.
6.	*Stgan*	Codes for a protein homologous to steroid dehydrogenase. Suppression of *Stgan* resulted in significant stolon elongation and elongated tubers in Karnika and Binge cultivars.	Bachem et al., 2001.
7.	*POTM1 (POTATO MADS BOX 1)*	*potm1* mutants showed reduction in tuber yields. *POTM1* mediates control of axillary bud development including stolon tips.	Kang and Hannapel, 1995 ; Rosin et al., 2003b.
8.	*StCDPK1 (CALCIUM DEPENDENT PROTEIN KINASE 1)*	Acts as a key mediator in sucrose signalling pathways during tuber induction.	Raices et al,2001; Raices et al., 2003b.
9.	*ARF6 (AUXIN RESPONSE FACTOR 6)*	Key regulator of tuberization and tuber dormancy release.	Faivre-Rampant et al., 2004.
10.	*StBel5*	Forms heterodimer with *POTH1* and downregulates GA20 oxidase. Mobile positive tuberization signal.	Banerjee et al., 2006b.
11.	*GA2ox1 (GA 2 OXIDASE 1)*	Part of GA pathway. Regulates the transition from longitudinal to radial stolon growth initiating tuber formation.	Kloosterman et al., 2007.
12.	*GA3ox2 (GA 3 OXIDASE 2)*	Part of GA pathway. Its levels are reduced in stolon tip which is critical for tuber formation.	Kloosterman et al., 2007.
13.	*StSUT4 (SUCROSE TRANSPORTER 4)*	Sucrose transporter which acts as a tuberization inhibitor.	Chincinska et al., 2008.
14.	*miR172*	Negatively regulates RAP1 and promotes tuber formation.	Martin et al., 2009.
15.	*RAP1 (Related to APETELLA2 1)*	Proposed to negatively regulate *StBel5*	Martin et al., 2009.

16.	*LKP2 (LOV KELCH PROTEIN 2)*	Overexpression of *AtLKP2* in potato resulted in tuber formation under LDs. Proposed to function in tuberization pathway.	Inui et al., 2010.
17.	*PP2AC* isoforms (*PROTEIN PHOSPHATASE 2 AC)*	PP2A activity is required for the transcriptional activation of *Patatin* and *PIN2* in leaves under tuberizing conditions.	Pais et al., 2010.
18.	*StTFL1 (TERMINAL FLOWER 1)*	Highly expressed in initial stolons. Overexpression resulted in normal tuberization under LDs. Authors proposed *StTFL1* regulates tuberization.	Guo et al., 2010.
19.	*SP6A*	FT homolog which transports from leaves to stolons and promotes tuber formation. Considered to be 'tuberigen'.	Navarro et al., 2011.
20.	*StCO (CONSTANS)*	Inhibits tuberization under LD, non-inductive conditions.	Gonzalez-Schein et al., 2012.
21.	*POTH1 (POTATO HOMEOBOX 1)*	Forms heterodimer with *StBel5* and downregulates GA20 oxidase. Mobile positive tuberization signal.	Rosin et al., 2003a; Mahajan et al., 2012.
22.	*CDF1 (CYCLING DOF FACTOR 1)*	Regulates *StCO* with *StGI* and *StFKF1*. Overexpression *StCDF1* results in early tuberization phenotype.	Kloosterman et al., 2013.
23.	*StFKF1* (FLAVIN-BINDING KELCH REPEAT F-BOX PROTEIN 1)	Forms protein complex with *St*CDF1 and *St*GI to regulate *StCO*.	Kloosterman et al., 2013.
24.	*StGI (GIGANTIA)*	Forms protein complex with *St*CDF1 and *St*FKF1 to regulate *StCO*.	Kloosterman et al., 2013.
25.	*TLOG1 (Tomato LONELY GUY 1)*	Overexpression of this CK biosynthetic gene facilitated tuber formation in tomato.	Eviator-Ribak et al., 2013.
26.	*AtABF4 and AtABF2 (Arabidopsis ABRE binding factor 4 and 2)*	Transgenic potato plants expressing *AtABF4* and *AtABF2* showed increased tuber yield. *AtABF4* and *AtABF2* positively regulate tuber induction through ABA-GA crosstalk.	Muniz-Garcia et al, 2014.

* The table 1.1 contains a list of genes and their functions in tuberization pathway. Only those studies that describe the detailed analysis of the respective gene in tuberization pathway were listed in the above table. Whereas, studies involving transcriptome analysis (by micro array experiments and deep sequencing strategies) to identify potential transcripts involved in different stages of tuberization pathway have not been listed here.

1.6. Similarities between tuberization and flowering

The shift from vegetative to reproductive phase is very crucial for plant survival. Using photoperiod as a cue, plants anticipate seasonal change and favorable conditions and then reproduce (Jackson, 2009). Tuberization and flowering are two reproductive strategies of the plant that share many similar environmental cues and molecular players (Abelenda et al., 2014). The pathway (s) that control flowering, also regulated tuberization was first demonstrated in 1981 (Chailakhyan MKh et al, 1981). In this study, authors demonstrated that the flowering signal produced in tobacco leaves was similar to the tuberization signal in potato. Also, tobacco grown in different photoperiodic requirements for flowering, were grafted onto andigena potato plants and these potato stock plants were analyzed for tuber formation. It was found that only those grafts in which tobacco scions were induced to flower, their potato stocks produced tubers. The authors thus concluded that signal for flowering was the same as tuberization signal (Chailakhyan MKh et al., 1981).

Photoperiod acts as one of the most important cues for flowering and is well dissected in the model plant- *Arabidopsis* which flowers in LDs while showed delayed flowering in SD photoperiod as reviewed by Jackson (2009). Photoperiod signal is perceived in leaves by phytochromes (PHYA and PHYB). This signal or the 'florigen' is transported to the shoot apical meristem which then transforms into an inflorescence meristem leading to the development of flowers. The 'florigen' was identified as the FLOWERING LOCUS T (FT) which encodes a RAF-kinase inhibitor like protein (Corbesier et al., 2007). Under LD inductive conditions, this protein moved from leaves to the shoot apex and induced flowering acting in concert with a MADS box TF: SUPPRESSOR OF OVEREXPRESSION OF CO1 (SOC1). These authors also demonstrated that overexpression of FT resulted in extreme early flowering phenotype (Corbesier et al., 2007).

FT is positively regulated by CONSTANS (CO), a light dependent clock output gene (Kardailsky et al., 1999; Samach et al., 2000). Overexpression of CO resulted in early flowering similar to FT overexpression. Also, overexpression of CO in *gigentia (gi)* mutant plants rescued the late flowering phenotype of *gi* mutants (Suárez-López et al., 2001). GI/CO/FT signalling forms a major part of the photoperiod induced flowering pathway and it is found to be conserved in rice as well (Tamaki et al., 2007). In other reports (Sawa et al., 2007; Song et al., 2012), it was shown that CYCLING DOF FACTOR (CDF) along with FKF1 and GI regulated CO and FT by binding to their promoters leading to inhibition of flowering in *Arabidopsis*.

As described earlier (section 1.3.1 and 1.5), photoperiod has a critical effect on tuberization, wherein the potato homologs of PHYB-GI-CO-FT (*St*PHYB, *St*GI, *St*CO and *St*SP6A respectively) regulated tuber formation under inductive conditions. Also, the CDF homolog in potato (*St*CDF) with *St*FKF1 and *St*GI controlled *St*CO expression and regulated tuberization (similar to their role in flowering, as described above). In general, CO acts as an activator of flowering, however, in potato; it inhibits tuber formation (González-Schain et al., 2012). Also, hormonal cues have been reported to be common between flowering and tuberization pathways. For example, GA levels play important functions in both these pathways. All these studies clearly demonstrated that tuberization and flowering, the two reproductive strategies of the plant, share environmental cues and molecular players (Figure 1.2). Thus, knowledge from the well investigated flowering pathway could be used as a framework to study tuberization mechanism.

Apart from transcription factors, signalling proteins and hormones that are common between flowering and tuberization process, micro RNAs also shown to play an important role in regulation of both these pathways which has been described in the following sections.

1.7. Micro RNAs (miRNAs) - Biogenesis, mode of action and function in plants

1.7.1. miRNA biogenesis

Micro RNAs are small (21-24 nucleotides), endogenous, non-coding RNAs that negatively regulate gene expression. In plants, MIR genes are predominantly located in the intergenic regions and are transcribed by their gene promoters. Transcription from these MIR gene promoters by RNA polymerases II (Lee et al., 2004) results in primary transcripts (pri-miRNAs) which are polyadenylated. These primary transcripts (pri-miRNAs) are stabilized by a RNA binding protein called DAWDLE (DDL). They are then processed into hairpin looped secondary structures called the precursor miRNAs (pre-miRNAs) by the concerted action of zinc finger protein SERRATE (SE), double stranded RNA binding protein HYPONASTIC LEAVES1 (HYL1), DICER-like1 (DCL1) and a nuclear cap binding complex. Precursor miRNAs (pre-miRNAs) are further processed by DICER-like 1 (DCL1) to form mature miRNA duplexes. These duplexes are methylated by HEN1 to avoid their degradation by small RNA degrading nucleases. They are then transported from nucleus to cytoplasm possibly by plant exportin 5 ortholog HASTY and other unknown factors. The guide miRNA strand is incorporated into the ARGONAUTE (AGO) proteins to form the RNA induced silencing complex: RISC

(Figure 1.3). Based on the complementarity, the guide strand leads the RISC to its target mRNAs (miRNA biogenesis reviewed in Zhu, 2008; Jung et al., 2009; Voinnet, 2009).

1.7.2. Mode of action

miRNAs downregulate expression of their target genes by target cleavage and/or translational inhibition. Plant miRNAs share near perfect complementarity with their target mRNAs. This complementarity is required for effective target cleavage by AGO proteins (Mallory et al., 2004). Various studies have experimentally reported a number of sliced targets in plants by conducting cleavage assays (Achard et al., 2004; Mica et al., 2006; Martin et al., 2009; Nair et al., 2010). While, sequencing of mRNA degradomes have indicated that a large number of miRNA targets are indeed cleaved (Addo-Quaye et al., 2008; Li et al., 2010b; Xu et al., 2012). Another mode of action of miRNAs is translation inhibition. Initially it was considered that translation inhibition is less dominant in plants unlike in animals. However, detailed studies on miRNA action indicated that plant miRNAs inhibit their target by not only transcript cleavage but also concurrent translation inhibition (Schwab et al., 2005; Brodersen et al., 2008). It is now suggested that target cleavage and translational inhibition are distinct processes and are quite widespread in plants than considered previously. However, the mechanism of translation inhibition in plants is now being investigated (Iwakawa and Tomari, 2013).

1.7.3. miRNA functions in plants

Mutations in key miRNA pathway components results in drastic developmental defects in plants (Mallory and Vaucheret, 2006). Micro RNAs regulate different plant development pathways like leaf development (Palatnik et al., 2003), floral development (Aukerman and Sakai, 2003; Chen, 2004), root development etc. Some classic examples are of *miR165/166* involved in regulation of leaf polarity, specifying the abaxial and adaxial surface of leaves by interaction with their target transcripts (Juarez et al., 2004). Various micro RNAs (*miR156*, *miR157*, *miR159*, *miR172*) have been demonstrated to be involved in the phase transitions and flowering pathway (discussed in section 1.9). *miR172* was also shown to function in potato, where it positively regulated tuberization pathway (discussed in section 1.10). miRNAs also regulate abiotic as well as biotic stress response pathways in plants. For example, *miR395* (targeting APT sulfurylase) regulated sulphur response pathways and is expressed only under stressed conditions (Kawashima et al., 2009; Buhtz et al., 2010). While, *miR399* was found to be expressed under low phosphate environment and it regulated phosphate homeostasis (Pant et al., 2008). A study in 2010

by Li and co-workers, demonstrated that *miR160* regulates PAMP (Pathogen Associated Molecular Patterns) - induced callose deposition at the cell wall indicating the role of this miRNA in regulation of plant innate immune responses to bacterial infections (Li et al., 2010a). Micro RNAs also regulate their own biosynthesis. As described before, DCL1 and AGO1 are major components of the miRNA biogenesis pathway. Studies have shown that *miR162* targets DCL1 while AGO1 is targeted by *miR168* (reviewed in Mallory and Vaucheret, 2006). Thus, the spectrum of miRNA function seems to be quite wide, including different aspects of plant development, stress response pathways and regulation of the miRNA pathway itself.

1.8. Micro RNA mediated control of flowering

miRNAs are important gene regulators that function in various different aspects of plant development and growth as described before. Flowering, a complex mechanism dependent on different environmental and endogenous stimuli has also been shown to be regulated by miRNAs. Role of miRNAs in flowering has been discussed below.

1.8.1. *miR156/miR157*

miR156 is a highly conserved miRNA present in all land plants (Axtell and Bowman, 2008). Over expression of *miR156* in *Arabidopsis* results in increased juvenile phase with delayed flowering while mimicry lines of *miR156* (reduced *miR156* levels) lead to early flowering phenotype. This clearly demonstrated the role of *miR156* in flowering pathway (Wu et al., 2009). Schwab and co-workers (2005) have shown that *miR156* targets Squamosa Promoter binding-Like Proteins (SPLs) TFs. The prolonged juvenile phase phenotype of *miR156* overexpression is reported in many plant species like maize (Chuck et al., 2007), rice (Xie et al., 2006), switchgrass (Fu et al., 2012), tomato (Zhang et al., 2011b) etc highlighting the conserved function of this micro RNA.

miR157 is found to be similar to *miR156* in sequence and targets the same SPL TFs. Hence, they are predicted to function like *miR156*. Experimental evidence regarding *miR157* function is not available. Nevertheless, presence of *miR157* is validated in a few plant species by deep sequencing studies (Xie et al., 2005; Zhang et al., 2013; Jiang et al., 2014).

1.8.2. *miR172*

In contrast to *miR156*, *miR172* promoted flowering and was found to be associated with adult epidermal traits in *Arabidopsis* leaves. Also, overexpression of *miR172* resulted in early flowering phenotype (Aukerman and Sakai, 2003). It was shown to target APETELLA (AP2) TFs which are juvenile identity genes and downregulation of AP2 activated the flowering pathway. Thus, *miR156* and *miR172* have important opposing effects on the flowering pathway (Figure 1.4). The link between *miR156* and *miR172* in regulating phase transitions and flowering is discussed in detail in section 3.1.2.

1.8.3. *miR159*

GA is one of the important factors required for floral induction in *Arabidopsis* under LD condition as mentioned before. GA is found to up-regulate the expression of GA related MYB TFs (GAMYBs) (Gubler et al., 1995). A GAMYB, *MYB33* in turn activated *LEAFY*, a floral meristem identity gene which resulted in flowering (Blazquez and Weigel, 2000; Gocal et al., 2001). Achard et al (2004) demonstrated that *miR159* targets the transcript of MYB33 and affects the flowering pathway. Overexpression of *miR159* results in delayed flowering in LDs. The authors also showed that *miR159* was positively regulated by GA levels via DELLA proteins. Therefore, a model was proposed in which *miR159* acted as a homeostatic regulator of GAMYB function in GA regulated flowering pathway (Figure 1.5).

1.9. Micro RNA mediated control of tuberization

In addition to the role of *miR172* in flowering pathway, its function in tuberization pathway was reported by Martin and co-workers in (2009). It was shown that *miR172* acts as a positive signal for tuberization (Martin et al., 2009). *miR172* overexpressing *andigena* lines tuberized under LD (non-inductive conditions) while in SDs they tuberized earlier than wild-type. This clearly demonstrated their positive effect on tuberization pathway. Also, authors demonstrated that *miR172* exhibited SD-LD photoperiod dependent expression pattern having high expression in SD induced leaves and stolons as compared to LDs. Target analysis of *miR172* revealed RAP1 (RELATIVE TO APETELLA2 1), an APETELLA 1 TF to be its target which inhibited activity of *St*BEL5, another positive regulator of tuberization. Therefore, under SD inductive conditions, high levels of *miR172* positively affect *StBEL5* expression by cleaving its target RAP1 transcripts (Martin et al., 2009). As mentioned before, *StBEL5* then moved from leaves to stolons and induced tuberization (Banerjee et al., 2006a). However, under LD conditions, levels of *miR172*

were detected to be low. RAP1 inhibited *St*BEL5 expression by possibly binding to its promoter as it was no more under *miR172* regulation (Figure 1.6). Grafting studies in *andigena* potato plants showed that *miR172* possibly transports from leaves to stolons, similar to the movement of *StBEL5* (Banerjee et al., 2006a) and *POTH1* transcripts (Mahajan et al., 2012). Another independent experiment conducted in tobacco confirmed the *miR172* mobility from source to sink (Kasai et al., 2010). It is quite clear that *miR172* is involved in regulation of flowering and tuberization pathways. *miR172* expression was observed to be photoperiod dependent in both the pathways, it acted downstream of PHYB, targeted AP2 like TFs and promoted tuberization in potato and flowering in *Arabidopsis* respectively. Recent report from our investigation (Bhogale et al., 2014) demonstrated the role of another miRNA, *miR156* in regulation of tuberization pathway which is discussed in detail in chapter 3.

1.10. Possible role of other miRNAs in potato

Although many plant miRNAs and their targets have been identified using computational and experimental approaches, majority of studies were conducted in model species like *Arabidopsis*, rice and maize. However, due to availability of other plant genomes, miRNAs and their targets are now predicted from various other plant species like apple (Varkonyi-Gasic et al., 2010), wheat (Kantar et al., 2011), soyabean (Wong et al., 2011), tobacco (Lang et al., 2010), sugarcane (Zanca et al., 2010) etc. In 2009 and 2010, few studies predicted miRNAs and their targets in potato as well (Yang et al., 2009; Zhang et al., 2009; Xie et al., 2011). Using previously known miRNAs from *Arabidopsis* and rice against potato ESTs (Expressed Sequence Tags), GSS (Genome Survey Sequences) and nucleotide sequences, Zhang and co-workers (2009) reported 48 miRNAs from potato. Using similar approach, Yang and co-workers (2009) reported 71 miRNAs in potato. Both these reports also predicted miRNA targets using bioinformatics. Xie et al (2011) using newly modified comparative genome strategy identified 202 potential miRNAs in potato belonging to 78 families along with their target prediction. The authors demonstrated experimental validation of few representative miRNAs using qRT-PCRs. Such reports only provided a general outline of potato miRNAs and by their target predictions provided an idea of different pathways possibly regulated by them. Above studies predicted potato miRNAs using miRNAs from other plant species which limited the identification of novel and/or potato specific miRNAs if any. However, a study in 2013 (Zhang et al., 2013) utilized the newly published potato genome information (2011)

and characterized miRNA population in leaves and stolons of photoperiod dependent *andigena* plants. They identified 28 conserved miRNA families and 120 potato specific miRNA families. Also a study in 2014 (Lakhotia et al., 2014) characterized the miRNA population in different vegetative tissues and developmental stages of tuber transitions in potato and reported 89 conserved miRNAs and 147 potato specific miRNAs. Target prediction was also performed for these targets. However, this study was restricted to photoperiod non-responsive potato cultivar- *Chandramukhi*. These two separate studies indicated the existence of a complex miRNA population in potato and suggested their possible involvement in regulation of different pathways including tuberization. However, no further studies reported the functional role of miRNAs in potato development except for *miR172* (Martin et al., 2009).

1.11. Hypothesis

Literature survey suggested that flowering and tuberization are two different reproductive strategies, both of which require photoperiod sensing as one of the cues. There is evidence that some of the molecular components involved in the photoperiodic control of flowering are also involved in photoperiodic control of tuberization (Jackson, 2009) (also discussed in section 1.6). A number of micro RNAs such as *miR156, miR157, miR172, miR159* have been demonstrated to regulate flowering pathway. In addition, *miR172* was also shown to positively regulate the tuberization. Availability of potato genome sequence and new miRNA prediction tools led to the identification of a number of miRNAs in potato (section 1.10). However, what function do these miRNAs perform in potato development is not yet investigated. Before the present study, only role of *miR172* as a positive regulator of tuberization was demonstrated (Martin et al., 2009). Our review of literature indicate that the function of other micro other miRNAs in potato are not explored. Do they function in regulating this complex pathway of tuberization? Considering the similarities between tuberization and flowering, regulation of tuberization pathway via miRNAs may also be conserved. We hypothesize that other miRNAs are possibly involved in regulating the tuberization pathway along with *miR172*.

1.12. Model system

To investigate the involvement of miRNAs in regulation of tuberization, *Solanum tuberosum* ssp *andigena* was used as a model system. *Solanum tuberosum* ssp *andigena* is a diploid wild potato variety which is strictly dependent on photoperiod for tuberization. It tuberizes under short days (~8 hours of light) and does not form tubers under long days

(~16 hours of light) (Figure 1.7). Along with *andigena*, potato cultivar *Desiree* was also used in the later part of the study. *Desiree* is a photoperiod insensitive potato cultivar which forms tubers even under LD conditions. To test the involvement of miRNAs in regulation of tuberization, following objectives were undertaken-

1.13. Objectives

1. To short list, validate and predict target genes of candidate miRNAs potentially involved in tuber development.
2. To characterize the role of *miR156* in potato development and tuberization pathway.
3. To study the interaction of *miR390* and its target *StCDPK1* in tuber development.

Chapter 1

Figures

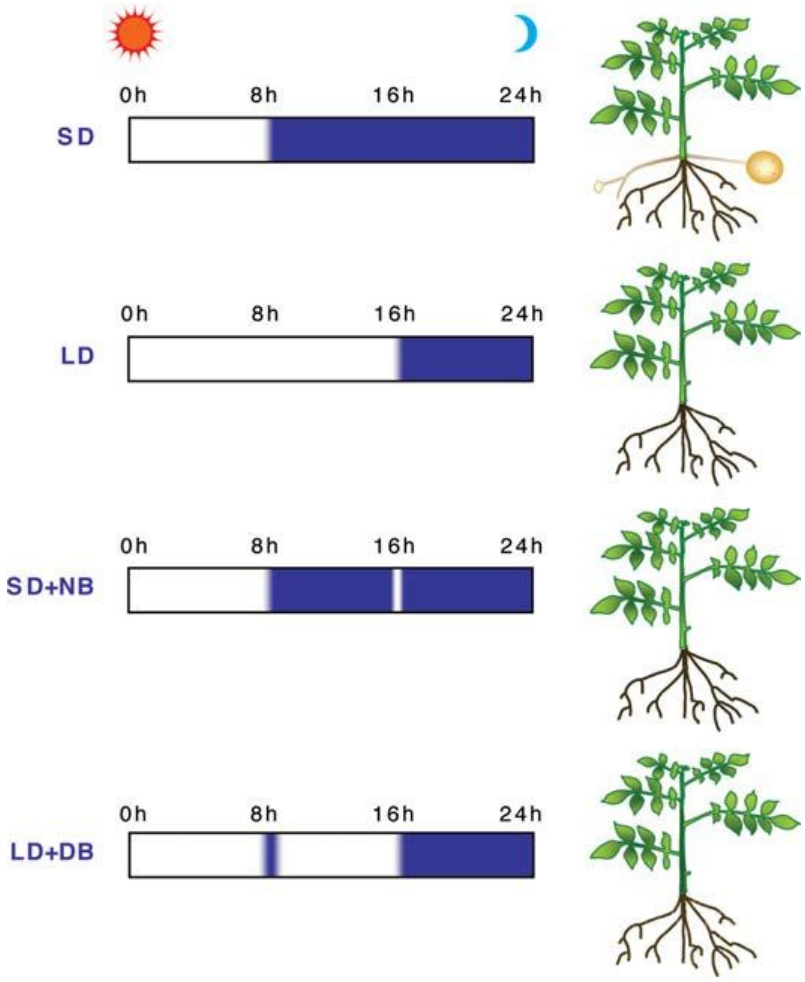

Figure 1.1: Control of tuberization by photoperiod in *Solanum tuberosum* ssp *andigena*. SD: short day, LD: long day, SD+NB: short day with night break, LD+DB: long day with day break. (Figure adapted from Rodriguez-Falcon et al., 2006).

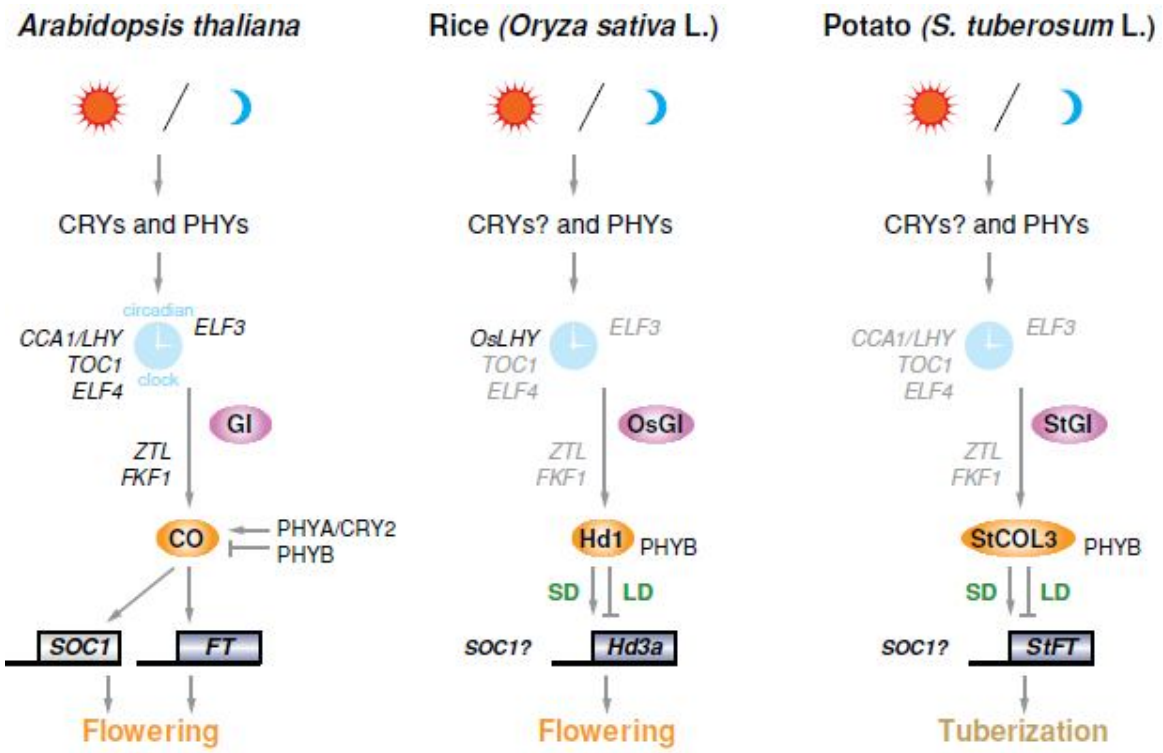

Figure 1.2: Similarities between flowering and tuberization: Short day induced tuberization pathway in potato has similarities with the flowering pathway investigated in *Arabidopsis* and rice (adapted from Rodriguez-Falcon et al., 2006).

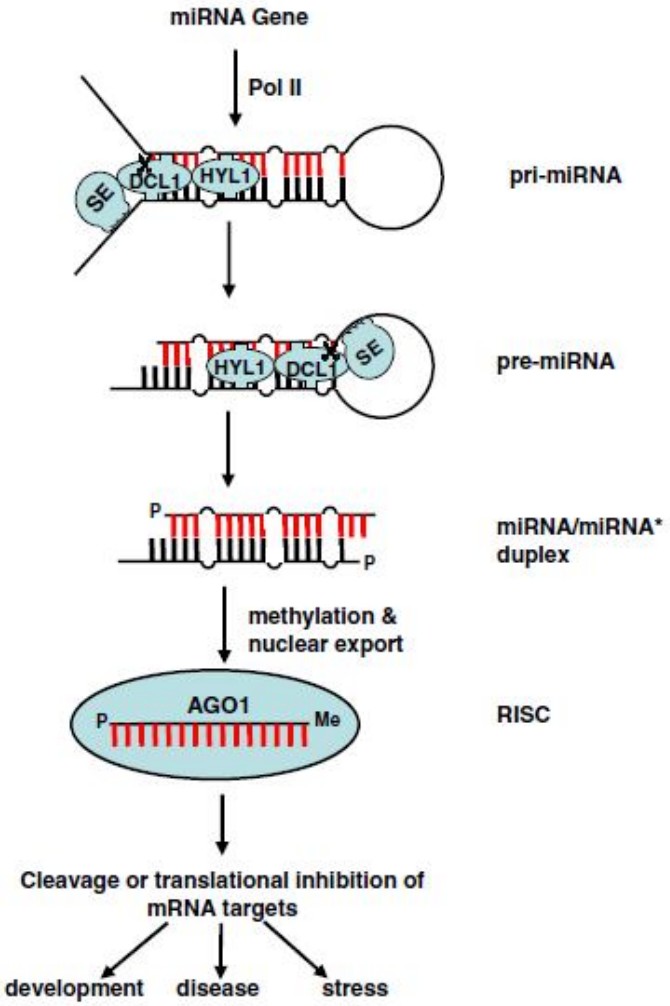

Figure 1.3: Micro RNA biogenesis: miRNAs are transcribed from their respective MIR genes by RNA polymerase II. The primary transcripts are sequentially processed to form miRNA/miRNA* duplex. Based on complementarity the guide strand is then incorporated in RISC and target cleavage and/or translational inhibition is achieved. (adapted from Zhu, 2008).

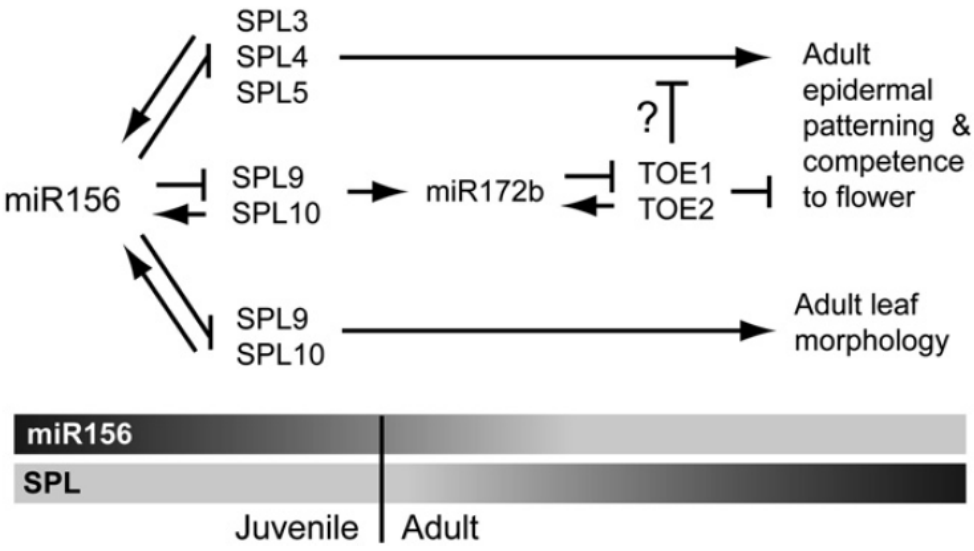

Figure 1.4: Sequential function of *miR156-miR172* in phase transitions and flowering: *miR156* promotes plant juvenile stage while *miR172* promotes adult stage and flowering. Their levels differ with the plant age along with their target transcript levels. *miR156* targets SPL TFs while, *miR172* targets AP2 TFs (adapted from Wu et al., 2009).

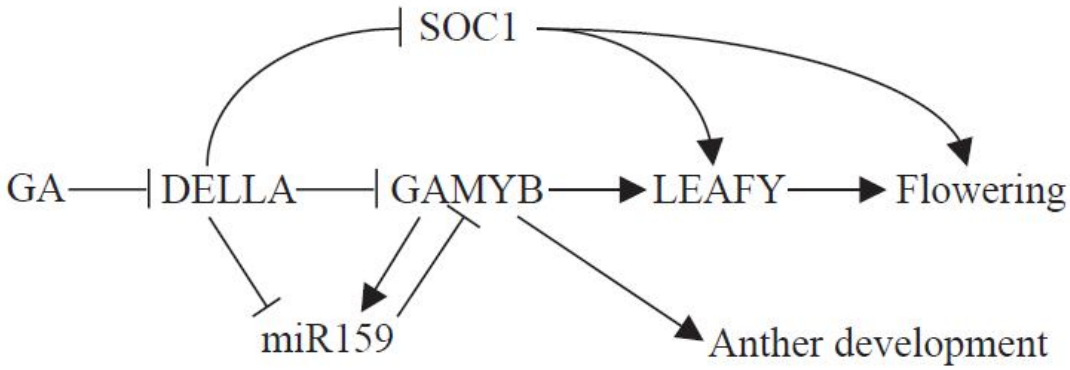

Figure 1.5: Role of *miR159* in the flowering pathway: *miR159* regulates GAMYB TFs and modulates the GA-DELLA signaling pathway of flowering. (adapted from Achard et al., 2004).

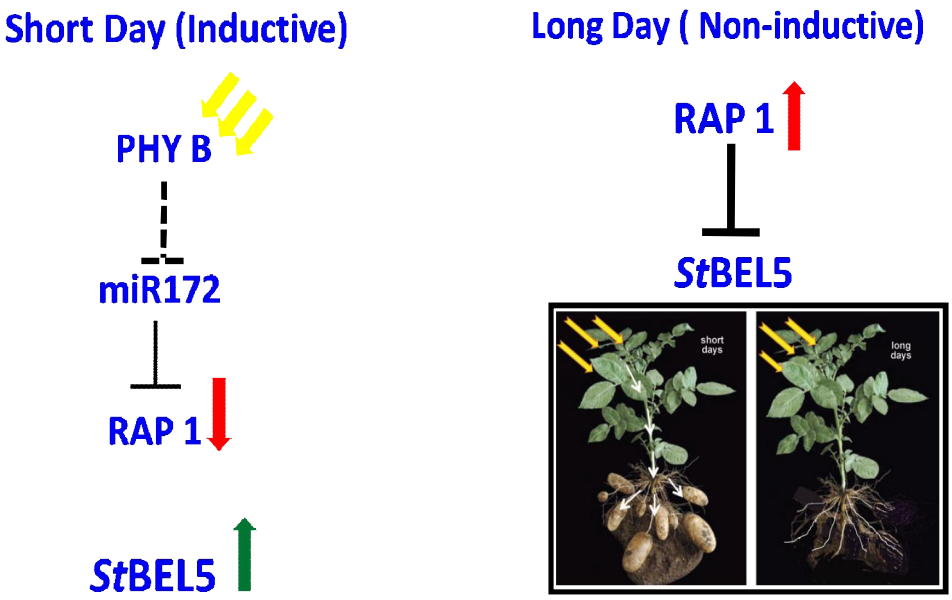

Figure 1.6: *miR172* acts as a positive signal for potato tuberization: Under SD conditions, *miR172* downregulates its target, *RAP1* TF resulting in *St*Bel5 accumulation (signal for tuberization). However, under LD conditions, due to unknown mechanism, levels of *miR172* are low resulting in *RAP1* downregulating *St*Bel5. Tuberization signal is thus not produced in LD conditions.

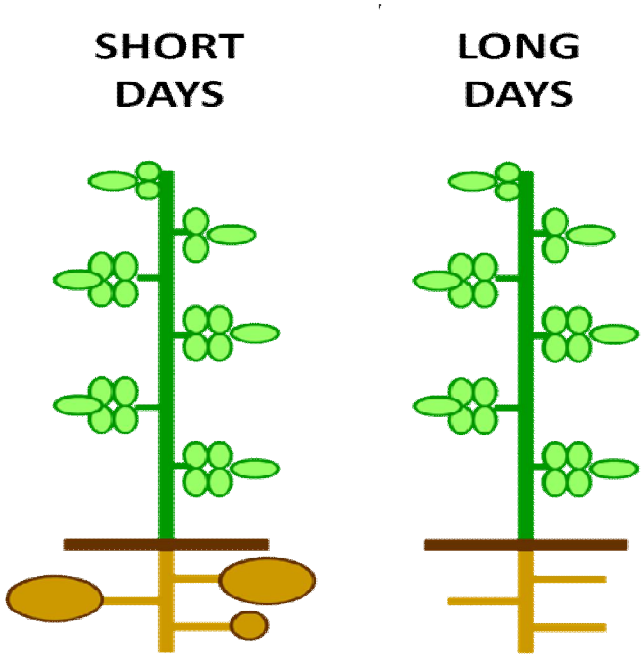

Figure 1.7: Model system: *Solanum tuberosum* ssp *andigena* as one of the model systems used in this study. It forms tubers only under SD conditions.

Chapter 2

Micro RNAs in potato (*Solanum tuberosum* ssp *andigena*)

2.1. Introduction

Micro RNAs are present in animals, plants and viruses (Yang et al., 2007). Since their discovery in *Caenorhabditis elegans*, micro RNA research has grown over the years highlighting their importance as key gene expression regulators (reviewed in Yang et al., 2007; Comai and Zhang, 2012). Both bioinformatic and experimental data have provided significant evidence for the presence and function of miRNAs in plants. Such studies have identified many plant micro RNA candidates in various different plant species. miRBase (http://www.mirbase.org/) is an online miRNA registry which hosts miRNAs from all species. Currently, it has ~7000 miRNA entries from different plant species including potato. Potato is an important food crop with its tubers serving a significant role in world food security. Studying the process of tuberization is of great interest to researchers all over the world due to its nutritional value as well as tuberization process being an important model system to study plant development. Tuberization is governed by different environmental cues and is the result of interplay between many molecular players (Sarkar, 2008; Sarkar, 2010). It is a complex pathway and therefore understanding the regulation of such a pathway is imperative. Numerous reports have shown that micro RNAs play crucial role in regulation of various developmental processes. For example, role of *miR172* as a positive regulator of potato tuberization has already been well defined (Martin et al., 2009). Additionally, during last 6-8 years, few studies (Zhang et al., 2009; Xie et al., 2011; Lakhotia et al., 2014) have identified the miRNA population in potato.

2.1.1. Bioinformatic prediction of potato micro RNAs

With the availability of complete plant genomes and computer algorithms to predict miRNA (precursors and mature) sequences, many miRNA candidates were predicted in model species like *Arabidopsis*, rice in last decade (Sunkar and Zhu, 2004; Li et al., 2010b) . It was later validated that majority of known miRNAs are evolutionarily conserved from mosses to angiosperms (Jones-Rhoades, 2012). Thus, miRNA genes present in one species may also be present as homologs or orthologs in other species. Using this strategy, miRNA candidates were predicted from potato exploring computational tools. Zhang and co-workers in 2009 predicted 48 micro RNA sequences (mature and precursor) with their predicted targets in potato. They also validated ten of the predicted miRNAs by RT-PCR using miRNA specific primers. Another study in 2009 (Yang et al., 2009) reported 71 potential potato miRNAs using similar strategy. They validated seven miRNAs by qRT-PCR in different tissues like leaf, stem, roots and SAM.

Xie et al (2011) using newly modified comparative genome strategy identified 202 potential miRNAs in potato belonging to 78 families along with their target prediction. Authors have also provided experimental validation of few representative miRNAs using qRT-PCRs. As these reports relied on evolutionarily conserved nature of miRNAs, novel or potato specific miRNAs were not identified and it was one of the limitations of these studies. Nevertheless, these reports, for the first time, provided insights of miRNAs present in potato.

2.1.2. Deep sequencing studies of potato micro RNAs

The availability of complete potato genome in 2011 [http://www.potatogenome.net (Potato Genome Sequencing Consortium., 2011)] and the advances in high throughput sequencing technologies unraveled a new platform for profiling the miRNA populations in potato. A study in 2013 by Zhang and co-workers utilized the newly published potato genome sequence information and characterized miRNA population in leaves and stolons of photoperiod dependent *andigena* plants. They reported 28 conserved miRNA families as well as 120 potato specific miRNA families. The authors also validated the presence of a few potato specific miRNAs by northern blots and predicted their target genes. This was the first report of potato miRNA population at a genome wide level using high throughput sequencing technology. However, this investigation dealt with only two tissue types, leaves and stolons. Another recent report in 2014 (Lakhotia et al., 2014) characterized the miRNA population in different vegetative tissues and developmental stages of tuber transitions in potato cultivar *Chandramukhi*, a photoperiod independent cultivar. This study identified 89 conserved miRNAs and 147 potato specific miRNAs in cultivar *Chandramukhi*. Authors have also performed target prediction for these miRNAs along with in-planta target validations for some miRNA-target gene pairs. In this study, differential abundance of miRNAs was analyzed in different tissues and stages of tuber transitions with some miRNAs expressing specifically in tuber transition stages. These two studies demonstrated a complex miRNA population in potato and suggested their potential involvement in regulating different pathways including tuberization.

All the above studies reported the miRNA population in potato with their predicted target genes. However, no further studies reported the functional role of miRNAs in potato development except for *miR172* (Martin et al., 2009), as described before. Based on the published bioinformatic and deep sequencing data in potato, we have shortlisted a number of miRNAs potentially involved in tuberization pathway. Also, considering the similarities

between tuberization and flowering, we have selected a few miRNAs known to be involved in flowering as potential candidates for their role in tuber development.

In this chapter, we present the list of shortlisted miRNAs, their in-planta validation in *S. tuberosum* ssp. *andigena* plants grown under SD-LD conditions and detailed *in-silico* analysis of their putative target genes.

2.2. Materials and Methods

2.2.1. Plant material and growth conditions

In this study, *Solanum tuberosum* ssp *andigena* 7540 was used. This is a photoperiod responsive potato plant which tuberizes under Short Days (SD, 8 hours light) and does not produce tubers under Long Day conditions (LD, 16 hours of light). *In vitro* plants were grown under LD at 25˚C in a growth incubator (Percival Scientific). Soil plants were grown at 22˚C under LD photoperiod in environmental chambers (Percival Scientific).

2.2.2. Validation of shortlisted miRNAs

Mature miRNAs were validated in leaves and stems of 2 month old soil grown *andigena* plants induced in SD and LD photoperiodic conditions for 15 days (15dpi, days post induction). They were detected by stem-loop RT-PCR as described earlier (Varkonyi-Gasic et al., 2007). In short, total RNA was isolated by TRIzol reagent (Invitrogen) as per manufacturer's instructions. Reverse transcription was carried out using specific stem-loop primers for each miRNA (STP) (details of all the primers used in this chapter are provided in Table 2.1). Pulsed reverse transcription program was used. The program details were: 16˚C for 30 mins followed by 60 cycles of 30˚C for 30 secs, 42˚C for 30 secs and 50˚C for 1 sec. This was followed by inactivation step at 85˚C for 5 mins. End-point PCR was performed using miRNA specific forward primer (FP) and universal reverse primer (univRP). cDNA reaction was used as the template for PCR. The end-point PCR reactions were incubated at 95˚C for 2 mins followed by 40 cycles of 95˚C for 15 secs, 60˚C for 1 min. The 61-bp amplicon containing the mature miRNA was cloned in a sub cloning vector pGEM-T Easy (Promega) and was confirmed by sequencing.

The secondary structure of miRNA precursors were predicted using Mfold software (Zuker, 2003). The predicted structure with lowest free energy was considered. These sequences were then further screened for having the characteristic stem-loop

secondary structure with the mature miRNA sequence in the arm region of the stem-loop. Few of the miRNA precursors were then validated in *andigena* by RT-PCR analysis. Total RNA was harvested from mature leaves and stem tissue of potato by TRIzol reagent (Invitrogen) as per manufacturer's instructions. miRNA precursors were amplified by RT-PCR using miRNA specific FP and RP (*miR156*: *miR156*preFP-*miR156*preRP, miR159: miR159FP-miR159preRP, *miR390*: *miR390*preFP-*miR390*preRP). The amplicons were then sequence confirmed.

2.2.3. Prediction of *miRNA* targets

Targets of the shortlisted miRNAs were predicted using bioinformatic tools. To increase efficiency of target prediction, psRNATarget [*plantgrn.noble.org/psRNATarget/*, (Dai and Zhao, 2011)*]* and TargetAlign [leonxie.com/targetAlign.php,(Xie and Zhang, 2010)], two online tools were used. Default parameters were used for both the softwares. For psRNATarget software, sequences showing a score up to 2.5 were considered except for miR414 where a score of 0 was considered. Targets with low score are considered to be highly potential targets for respective miRNAs. To reduce false positive hits, sequences showing *miRNA* binding site with both the softwares were considered as putative miRNA targets.

2.2.4. Primer sequences

The sequences of primers used in this chapter are in table 2.1

Table 2.1: List of primers

Primer Name	Primer Sequence
*miR156*STP	GTCGTATCCAGTGCAGGGTCCGAGGTATTCGCACTGGATACGACGTGCTC
miR156 FP	GCGGCGGTGACAGAAGAGAGT
*miR156*preFP	CGATCTAGAGTTTGTGTGAAGCAAAGAGA
*miR156*preRP	CCTGAGCTCGA GGAAGTAGTAGCTATG
miR157STP	GTCGTATCCAGTGCAGGGTCCGAGGTATTCGCACTGGATACGACGTGCTCTCTA
miR157FP	GCGGCGGTTGACAGAAGATAGA
miR159STP	GTCGTATCCAGTGCAGGGTCCGAGGTATTCGCACTGGATACGACTAGAGC
miR159FP	CGGCGGTTTGGATTGAAGGGA
miR159preFP	GACTCTAGAGGATTGAAGGGAGCTCTAC
miR159preRP	ACTGGTACCCAAATCCAAATCCAACATTTC
miR164STP	GTCGTATCCAGTGCAGGGTCCGAGGTATTCGCACTGGATACGACTGCACG
miR164FP	CGGCGTGGAGAAGCAGGGCA
*miR172*_10STP	GTCGTATCCAGTGCAGGGTCCGAGGTATTCGCACTGGATACGACTTTGATTG
*miR172*_10FP	CGCGGCGTGTTGGAATGGCT
*miR172*STP	GTCGTATCCAGTGCAGGGTCCGAGGTATTCGCACTGGATACGACTCTTAG
*miR172*FP	CGGCGGTACGTCGTAGTAGTT
*miR390*STP	GTCGTATCCAGTGCAGGGTCCGAGGTATTCGCACTGGATACGACGGTGCTAT
*miR390*FP	CGCGCCAAGCTCAGGAGGG
*miR390*preFP	ATAGGATCCTTCTTTCTCCTTTTGCCATTC

*miR390*preRP	GATCTCGAGCAAAAAAATAGATAATTAATGCTAAGG
miR398STP	GTCGTATCCAGTGCAGGGTCCGAGGTATTCGCACTGGATACGACCAGGGG
miR398FP	GCGGCGTATGTTCTCAGGTCG
miR399STP	GTCGTATCCAGTGCAGGGTCCGAGGTATTCGCACTGGATACGACCGGGGC
miR399FP	GCGGCGTGCCAAAGAAGATTT
miR414STP	GTCGTATCCAGTGCAGGGTCCGAGGTATTCGCACTGGATACGACTGACGATG
miR414FP	CGCGCGCCTCATCTAGATCA
miR34STP	GTCGTATCCAGTGCAGGGTCCGAGGTATTCGCACTGGATACGACCTTCCA
miR34FP	GCGGCGTCTGTGACAGGATAA
miR53STP	GTCGTATCCAGTGCAGGGTCCGAGGTATTCGCACTGGATACGACACCCAA
miR53FP	GCGGCGTTCCATGAGACTGTTT
miR72STP	GTCGTATCCAGTGCAGGGTCCGAGGTATTCGCACTGGATACGACCTTAGA
miR72FP	GCGGCGTTGGTTGAGTGAGCA
miR111STP	GTCGTATCCAGTGCAGGGTCCGAGGTATTCGCACTGGATACGACTCAAAT
miR111FP	GCGGCGAACATCTCCAGCCAT
miR152STP	GTCGTATCCAGTGCAGGGTCCGAGGTATTCGCACTGGATACGACAATTCC
miR152FP	GCGGCGTATCTGAGTAGCATAG
miR193STP	GTCGTATCCAGTGCAGGGTCCGAGGTATTCGCACTGGATACGACGTCCAA
miR193FP	GCGGCGTATATGCTCTAGATT
UnivRP	GTGCAGGGTCCGAGGT

2.3. Results

2.3.1. Shortlisted miRNAs

The deep sequencing data reported some miRNAs showing high abundance in stolons, swollen stolons (the organ that develops into a tuber) and leaves (site of signal perception). Few had interesting putative target genes, whose role in tuberization has been demonstrated earlier. We have considered such miRNAs as putative miRNAs to explore their role in tuberization pathway. Also, miRNAs like *miR156, miR157, miR159* have been shown to regulate flowering pathway as described before. Considering the similarities between these two pathways and the assumption that regulation of these pathways via micro RNAs may also be conserved, we have selected those miRNAs that are involved in flowering pathway as putative candidates for tuberization mechanism.

Following are the shortlisted miRNAs (Table 2.2) with their selection criteria as obtained from our literature survey:

Table 2.2: Shortlisted miRNAs potentially involved in tuberization pathway

#	miRNA	Conserved/ potato-specific	Criteria for selection
1	*miR156* *UGACAGAAGAGAGUGAGCAC*	Conserved	Regulates phase transitions and flowering with *miR172* (Wu et al., 2009)
2	*miR157* *UUGACAGAAGAUAGAGAGCAC*	Conserved	Similar to *miR156* Proposed to function in phase transitions and flowering
3	*miR159* *UUUGGAUUGAAGGGAGCUCUA*	Conserved	Targets GAMYB TFs and is involved in GA signaling pathway (Achard et al., 2004) GA signalling plays an important role in tuberization (section 1.4.1)
4	*miR164* *UGGAGAAGCAGGGCACGUGCA*	Conserved	Low abundance in all tuber transition stages (Lakhotia et al., 2014)
5	*miR172_10* *UGUUGGAAUGGCUCAAUCAAA*	Conserved	High abundance in roots but low abundance in all tuber transition stages (Lakhotia et al., 2014)
6	*miR390* *AAGCUCAGGAGGGAUAGCACC*	Conserved	Targets CDPKs which play important role in tuberization (Raices et al., 2003a and b)
7	*miR398* *UAUGUUCUCAGGUCGCCCCUG*	Conserved	Not expressed in all tuber transition stages (Lakhotia et al., 2014)
8	*miR399* *UGCCAAAGAAGAUUUGCCCCG*	Conserved	Low abundance in all tuber transition stages (Lakhotia et al., 2014) Long distance mobile miRNA (Pant et al., 2008)
9	*miR414* *UCAUCUUCAUCAUCAUCGUCA*	Lack of conservation in genomes other than *Arabidopsis* and rice.	Targets factors important in light signaling. Light is an important cue for flowering and tuberization.

10	*miR34* *UCUGUGACAGGAUAAUGGAAG*	Potato-specific	Targets protein phosphatase 2C (Lakhotia et al., 2014) Protein phosphatases positively modulate tuberization pathway (Pais et al., 2010)
11	*miR53* *UUCCAUGAGACUGUUUUUGGGU*	Potato-specific	Low abundance in all tuber transition stages (Lakhotia et al., 2014)
12	*miR72* *UUGGUUGAGUGAGCAUCUAAG*	Potato-specific	Expressed differentially in all tuber transition stages (Lakhotia et al., 2014)
13	*miR111* *AACAUCUCCAGCCAUAUUUGA*	Potato-specific	Expressed differentially in all tuber transition stages (Lakhotia et al., 2014) Targets protein phosphatase 2C (Lakhotia et al., 2014)
14	*miR152* *UAUCUGAGUAGCAUAGGGAAUU*	Potato-specific	High abundance in swollen stolons (Lakhotia et al., 2014)
15	*miR193* *UAUAUGCUCUAGAUUUUGGAC*	Potato-specific	High abundance in all tuber transition stages (Lakhotia et al., 2014)

2.3.2 Validation of shortlisted miRNAs in SD-LD grown potato plants

To validate the presence of shortlisted miRNAs in our model system, *Solanum tuberosum* ssp *andigena*, we performed stem-loop RT-PCR with miRNA specific primers as per a previously described protocol (Varkonyi-Gasic et al., 2007). This technique specifically amplifies mature miRNAs (21-24 nucleotides) and not their precursor forms. Out of the 15 miRNAs shortlisted as above, we could validate 12 miRNAs in potato. *miR172* was used as a positive control, which is already validated in *Solanum tuberosum* ssp *andigena* (Martin et al., 2009). Our analysis indicated that all 12 miRNAs were present in leaves and stem tissue of *andigena* grown under SD and LD conditions. Only *miR398* showed differential detection in SD and not in LD tissue (Figure 2.1). As part of our on going work, *miR156*, *miR157*, *miR159*, *miR414* and *miR390* were cloned in pGEMT vector and sequence confirmed as well. The secondary structures of *miR156* (BI432985.1), *miR159* (BI431534.1) and *miR390* (CK247568.1) were predicted using Mfold software

(Zuker, 2003). All of them had typical hairpin loop structures. Mature sequences of all miRNAs were in the stem region of the hairpin loop structure, a characteristic of miRNA precursors (Figure 2.2 A to C). We also validated the presence of precursors of *miR156* (~300bp), *miR159* (~300bp) and *miR390* (~900bp) in potato by RT-PCR using gene specific primers (Figure 2.2 D and E).

2.3.3. Prediction of miRNA targets

To gain further insights into the miRNA functions in potato, *in silico* target prediction was carried out for the validated miRNAs (Table 2.3). Except for *miR398* and *miR34*, all miRNAs showed more than one putative target genes. The mode of action was transcript cleavage for majority of targets; however, translation inhibition was also predicted as a mode of action for few miRNAs like for *miR399* and its target gene PHO2, *miR159* and its target gene cation transporting ATPase etc (Table 2.3). For all the miRNAs, their target genes had a score of ≤ 2.5 except for *miR414*. *miR414* showed more than 100 targets with a score up to 2.5 in psRNATarget software. Also, as per miRBase, the presence and conservation of *miR414* is unclear. Thus, we considered a score up to 0 in psRNATarget software for *miR414* followed by its testing in TargetAlign software. Use of two different target prediction softwares showed the inconsistency of this analysis and the importance of in-planta target validation experiments to confirm a particular miRNA-target interaction. For example, *miR152*, a potato specific miRNA showed three putative targets as per psRNATarget software but they were not confirmed in TargetAlign software. miRNAs like *miR390*, *miR53*, *miR159* also had a few targets which showed such inconsistency in their results. Overall, our detailed target prediction analysis (Table 2.3) for validated miRNAs gave a preliminary idea of the putative miRNA function in potato development.

Table 2.3: Detailed *in silico* target prediction of validated miRNAs in potato:

#	miRNA	Predicted targets (PGSC accession number)	Score	Mode of Action	Target -Align Results
1.	*miR156*	Gene of unknown function PGSC0003DMT400074958	1	cleavage	+
		Squamosa promoter-binding protein PGSC0003DMT400056372	1	cleavage	+
		Squamosa Promoter-binding Like Protein 13 (SPL13) PGSC0003DMT400056373	1	cleavage	+
		Squamosa Promoter-binding Like Protein 13 (SPL13) PGSC0003DMT400056374	1	cleavage	+
		LIGULELESS1 protein PGSC0003DMT400068752	1	cleavage	+
		Squamosa Promoter binding-Like Protein 9 (SPL9) PGSC0003DMT400029751	1	cleavage	+
		Squamosa Promoter binding-Like Protein 6 (SPL6) PGSC0003DMT400059813	1	cleavage	+
		Squamosa promoter-binding protein PGSC0003DMT400029749	1	cleavage	NA
		LIGULELESS1 protein (LG1) PGSC0003DMT400084734	1	cleavage	+
		Squamosa promoter-binding protein PGSC0003DMT400029750	1	cleavage	NA
		LIGULELESS1 protein PGSC0003DMT400072746	1	cleavage	+
		Squamosa promoter-binding protein PGSC0003DMT400029748	1	cleavage	+
		Unknown PGSC0003DMT400072745	1	cleavage	NA
		Unknown PGSC0003DMT400084733	1	cleavage	NA

		Squamosa promoter-binding protein PGSC0003DMT400082790	2	cleavage	NA
		Squamosa promoter-binding protein PGSC0003DMT400082789	2	cleavage	+
		LIGULELESS1 protein PGSC0003DMT400063045	2	cleavage	+
		LIGULELESS1 protein PGSC0003DMT400063046	2	cleavage	+
		Squamosa Promoter binding-Like Protein 3 (SPL3) PGSC0003DMT400058753	2	cleavage	+
2.	*miR157*	Squamosa promoter-binding protein PGSC0003DMT400076399	0	cleavage	+
		LIGULELESS1 protein PGSC0003DMT400068752	1	cleavage	+
		Squamosa Promoter binding-Like Protein 9 (SPL9) PGSC0003DMT400029751	1	cleavage	+
		Squamosa promoter-binding protein PGSC0003DMT400029749	1	cleavage	NA
		LIGULELESS1 protein (LG1) PGSC0003DMT400084734	1	cleavage	+
		Squamosa promoter-binding protein PGSC0003DMT400029750	1	cleavage	NA
		Squamosa promoter-binding protein PGSC0003DMT400029748	1	cleavage	+
		Unknown PGSC0003DMT400084733	1	cleavage	NA
		LIGULELESS1 protein PGSC0003DMT400072746	1.5	cleavage	+
		Unknown PGSC0003DMT400072745	1.5	cleavage	+
		Squamosa promoter-binding protein PGSC0003DMT400056372	2	cleavage	NA
		Squamosa Promoter-binding Like Protein 13 (SPL13)	2	cleavage	+

		PGSC0003DMT400056373			
		Squamosa Promoter-binding Like Protein 13 (SPL13) PGSC0003DMT400056374	2	cleavage	+
		Squamosa Promoter binding-Like Protein 6 (SPL6) PGSC0003DMT400059813	2	cleavage	+
		Squamosa promoter-binding protein PGSC0003DMT400082790	2	cleavage	NA
		Squamosa promoter-binding protein PGSC0003DMT400082789	2	cleavage	+
		LIGULELESS1 protein PGSC0003DMT400063045	2	cleavage	+
		LIGULELESS1 protein PGSC0003DMT400063046	2	cleavage	+
		Nitrate transporter PGSC0003DMT400043794	2.5	cleavage	+
		CONSTANS interacting protein 2b PGSC0003DMT400023211	2.5	cleavage	+
		Pyruvate kinase PGSC0003DMT400066112	2.5	cleavage	+
3.	*miR159*	GAMyb-like1 PGSC0003DMT400058427	2	cleavage	+
		GAMyb-like2 PGSC0003DMT400070549	2	cleavage	+
		GAMyb-like1 PGSC0003DMT400058426	2	cleavage	+
		GAMyb-like1 PGSC0003DMT400058425	2	cleavage	+
		Duo pollen 1 PGSC0003DMT400066066	2	cleavage	+
		Unknown PGSC0003DMT400065569	2.5	cleavage	NA
		Glycine-rich cell wall structural protein 1.8 PGSC0003DMT400045205	2.5	translation	−
		Casein kinase PGSC0003DMT400065568	2.5	cleavage	+
		GAMYB-like2 PGSC0003DMT400015156	2.5	cleavage	+

		GAMYB-like2 PGSC0003DMT400015155	2.5	cleavage	+
		Gene of unknown function PGSC0003DMT400094520	2.5	cleavage	+
		Cation transporting ATPase PGSC0003DMT400089589	2.5	translation	−
		Disease resistance protein (TIR class) PGSC0003DMT400057620	2.5	cleavage	−
		Disease resistance protein (TIR class) PGSC0003DMT400057621	2.5	cleavage	−
		Fiber expressed protein PGSC0003DMT400057734	2.5	cleavage	+
		Fiber expressed protein PGSC0003DMT400057733	2.5	cleavage	+
4.	*miR390*	Gene of unknown function PGSC0003DMT400034044	2	translation	−
		Leucine-rich repeat receptor protein kinase EXS PGSC0003DMT400045887	2	cleavage	+
		Protein phosphatase PGSC0003DMT400020699	2	cleavage	NA
		Protein phosphatase PGSC0003DMT400020698	2	cleavage	−
		Leucine-rich repeat receptor kinase PGSC0003DMT400066895	2.5	cleavage	+
5.	*miR398*	L-ascorbate oxidase PGSC0003DMT400082388	2.5	cleavage	+
6.	*miR399*	Disease resistance protein PGSC0003DMT400020354	1.5	cleavage	+
		Disease resistance protein PGSC0003DMT400020353	1.5	cleavage	+
		PHO2 PGSC0003DMT400076435	2	translation	+
		Gag-pol polyprotein PGSC0003DMT400059225	2.5	cleavage	+
7.	*miR414*	syringolide-induced protein 14-1-1 PGSC0003DMT400075641	0	cleavage	+
		Unknown	0	cleavage	NA

		PGSC0003DMT400075640			
8.	*miR34*	Gene of unknown function PGSC0003DMT400041233	2.5	cleavage	+
9.	*miR53*	Resistance protein PGSC0003DMT400030581	0.5	cleavage	+
		Resistance protein PGSC0003DMT400030580	0.5	cleavage	+
		CM0545.410.nc protein PGSC0003DMT400007477	0.5	cleavage	+
		conserved gene of unknown function PGSC0003DMT400007478	0.5	cleavage	NA
		serine-threonine protein kinase PGSC0003DMT400007479	0.5	cleavage	−
		CF-2-2 PGSC0003DMT400083857	2	translation	−
		Aceyl CoA Synthase PGSC0003DMT400064817	2	cleavage	−
		conserved gene of unknown function PGSC0003DMT400055358	2	cleavage	+
		HCR9-OR2 PGSC0003DMT400054259	2.5	translation	−
		Tyrosine-rich hydrooxyproline rich glycoprotein PGSC0003DMT400006086	2.5	cleavage	−
		RNA binding protein PGSC0003DMT400069589	2.5	cleavage	+
		poly(ADP-ribose) polymerase PGSC0003DMT400012725	2.5	cleavage	+
		serine/arginine rich splicing factor PGSC0003DMT400045694	2.5	cleavage	+
10.	*miR72*	polcalcin Jun O PGSC0003DMT400052233	2.5	cleavage	+
		Cryptochrome 1b PGSC0003DMT400022041	2.5	cleavage	NA
		Cryptochrome 1b PGSC0003DMT400022039	2.5	cleavage	+
		glycoprotein PGSC0003DMT400049507	2.5	cleavage	+
		glycoprotein	2.5	cleavage	+

		PGSC0003DMT400049506			
11.	*miR111*	ATP binding protein PGSC0003DMT400074356	1.5	cleavage	+
		ATP binding protein PGSC0003DMT400074357	1.5	cleavage	+
		Zinc finger family protein PGSC0003DMT400064005	2	translation	−
		conserved gene of unknown function PGSC0003DMT400066558	2.5	translation	+
		Vps51/Vps67 PGSC0003DMT400026847	2.5	translation	−
		tubulin β-1 chain PGSC0003DMT400037094	2.5	cleavage	+
		tubulin β-1 chain PGSC0003DMT400037093	2.5	cleavage	+
12.	*miR152*	Actin binding protein PGSC0003DMT400036332	2.5	cleavage	−
		Nitrate transporter PGSC0003DMT400043794	2.5	cleavage	−
		conserved gene of unknown function PGSC0003DMT400021449	2.5	cleavage	−

Table 2.3 legends: (+): positive result in TargetAlign software, (−): negative result in TargetAlign software, (NA): not applicable as the software gave in-conclusive result.

2.4. Discussion

2.4.1. Potential role of other miRNAs in regulation of tuberization

Role of *miR172* in regulation of tuberization pathway as demonstrated by Martin et al., 2009 opened the possibilities of probable role of other miRNAs in regulation of this complex process. A few studies have already reported the miRNA population in potato (Zhang et al., 2013; Lakhotia et al., 2014) however; no direct investigations regarding the role of miRNAs in tuberization pathway were reported. Our study was an attempt to identify miRNAs potentially involved in tuber formation pathway. The deep sequencing data published by Zhang et al., 2013 and Lakhotia et al., 2014 reported few miRNAs exhibiting differential abundance in stolons, swollen stolons (the organ that develops into a tuber) and leaves (site of signal perception). For example, *miR193*, *miR152* and *miR34*

showed differential expression pattern in tuber transition stages. Some of the micro RNAs had putative target genes, whose function in tuberization has already been demonstrated. We shortlisted such miRNAs as putative micro RNAs involved in tuberization pathway. For example, our model system potato (*Solanum tuberosum* ssp *andigena*) is strictly dependent on SD photoperiod for tuberization and therefore, light signalling plays an important role in signal perception. *miR414* was predicted to target transcription factors involved in light signalling as reported by Zhang et al., 2009. Also, *miR34* was shown to potentially target protein phosphatases which play an important role in tuberization (Pais et al., 2010), while *miR390* potentially targets Calcium Dependent Protein Kinases (CDPK), another important regulator of tuber formation pathway as demonstrated by (Raices et al., 2003a and b). As described before, miRNAs like *miR156*, *miR157*, *miR159* function in flowering pathway. Considering the similarities between flowering and tuberization pathways (described in section 1.6) and assuming that regulation of these pathways via micro RNAs may also be conserved, we have shortlisted those miRNAs involved in flowering pathway as putative candidates for studying their role in tuberization. Using this approach, we shortlisted 15 miRNAs that could potentially regulate tuberization pathway.

Since, we shortlisted the micro RNAs based on previously published data as obtained from different potato cultivars and growth conditions, at the beginning we wanted to validate the presence of these shortlisted miRNAs in our model system *Solanum tuberosum* ssp *andigena* under SD-LD photoperiod conditions. Out of 15 shortlisted miRNAs, we were able to validate the presence of only 12 miRNAs in *andigena*. In our study, *miR193* (potato-specific miRNA), *miR164* and *miR171* (conserved miRNAs) were not detected may be due to their differential spatio-temporal expression pattern.

2.4.2. miRNA-target gene prediction

Previous studies on potato miRNAs have reported their predicted target genes, however, in the present investigation, we have undertaken a detailed *in silico* target prediction of validated miRNAs. Use of two target prediction softwares with their own set of default parameters reduced the chances of false positive results and yielded consistency in the target gene analysis. Some of the target genes which showed strong complementarity with the miRNAs in psRNATarget software, failed to show alignment in TargetAlign software. For example, *miR152*-nitrate transporter, *miR390*-protein phosphatase, *miR111*-zinc finger protein etc. Such results indicated that plant miRNA

target prediction is not solely dependent on complementarity. Also, in-planta validation of the putative targets appears to be necessary. Our findings were consistent with the previous report (Didiano and Hobert, 2006). It was considered that plant miRNAs downregulated their targets by transcript cleavage while, animal miRNAs downregulated their target genes by translation inhibition (Millar and Waterhouse, 2005). However, recent studies have shown that plant miRNAs downregulate their targets by both transcript cleavage and translational repression as demonstrated by Schwab et al., 2005 and Brodersen et al., 2008. In our analysis, there were quite a few miRNAs (*miR53, miR111, miR399* etc) which showed translation inhibition as their mode of action. Previous studies have reported that a single miRNA can target more than one target while a single target gene can be regulated by multiple miRNAs as reviewed in Yang et al., 2007. In our analysis, all miRNAs except *miR398* and *miR34* (at the score of 2.5) yielded multiple putative target genes. Also, targets like protein phosphatases were potentially regulated by more than one miRNAs, *miR390* and *miR111*.

Overall, our study resulted in a list of miRNAs (Table 2.2) potentially involved in regulation of tuberization pathway along with their validation and detailed target gene predictions (Table 2.3). Of the 12 miRNAs that we analyzed, we have further selected two miRNAs, *miR156* and *miR390* to understand their role in tuberization pathway. Reason for selecting these two miRNAs for further study has been described in respective chapters. Role of *miR156* in potato development has been characterized in detail in chapter 3, whereas *miR390-StCDPK1* interaction has been described in chapter 4. Together, our study would provide more insights into the miRNA-mediated control of potato tuberization.

Chapter 2

Figures

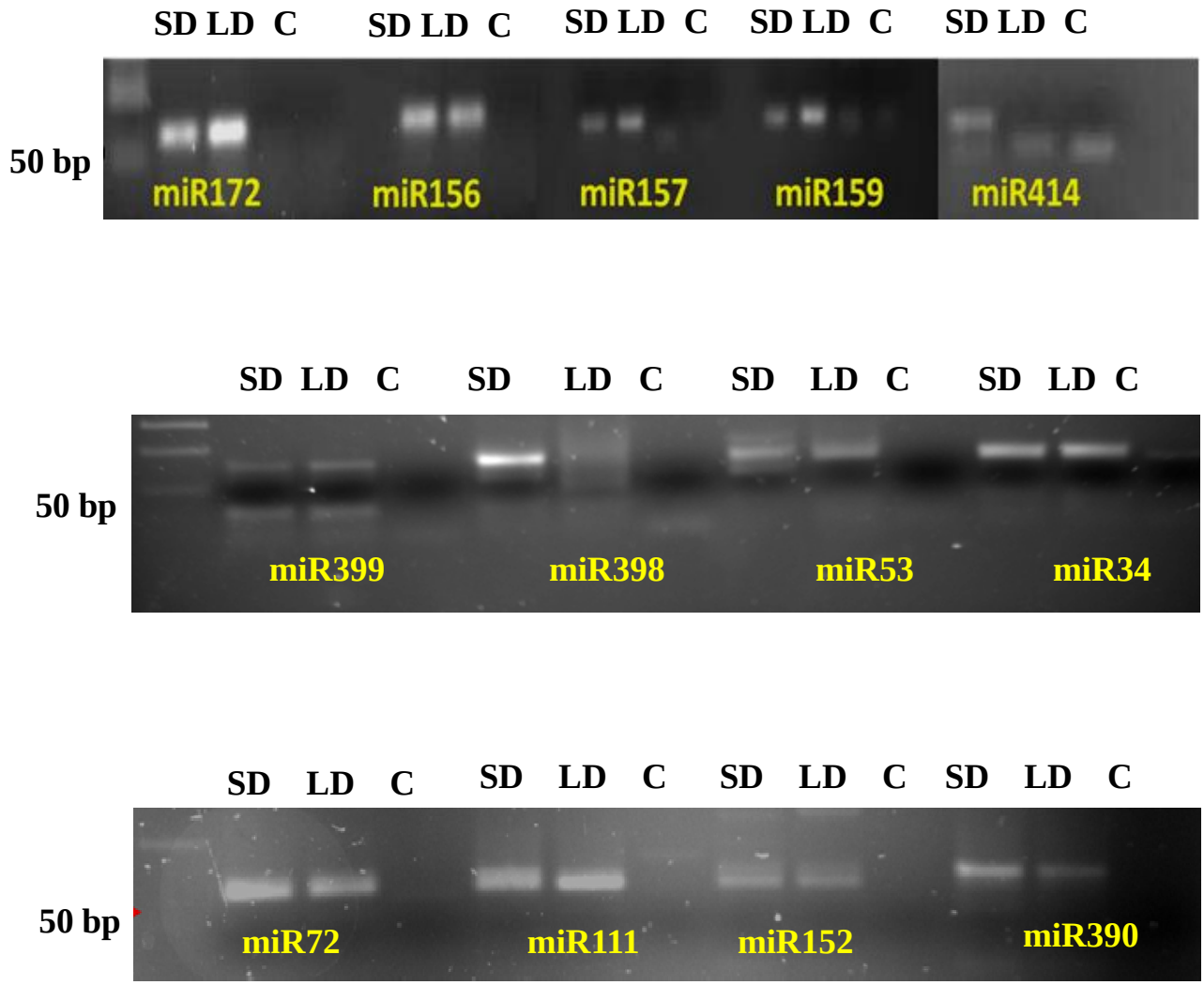

Figure 2.1: Validation of miRNAs in potato: Detection of mature miRNAs in stem and leaves tissues of SD-LD (15 days post induction, 15 dpi) grown *Solanum tuberosum* ssp *andigena* by stem-loop RT-PCR. *miR172* is a positive control. SD- short day, LD- long day and C- negative control. 50 bp ladder is on extreme left as marked.

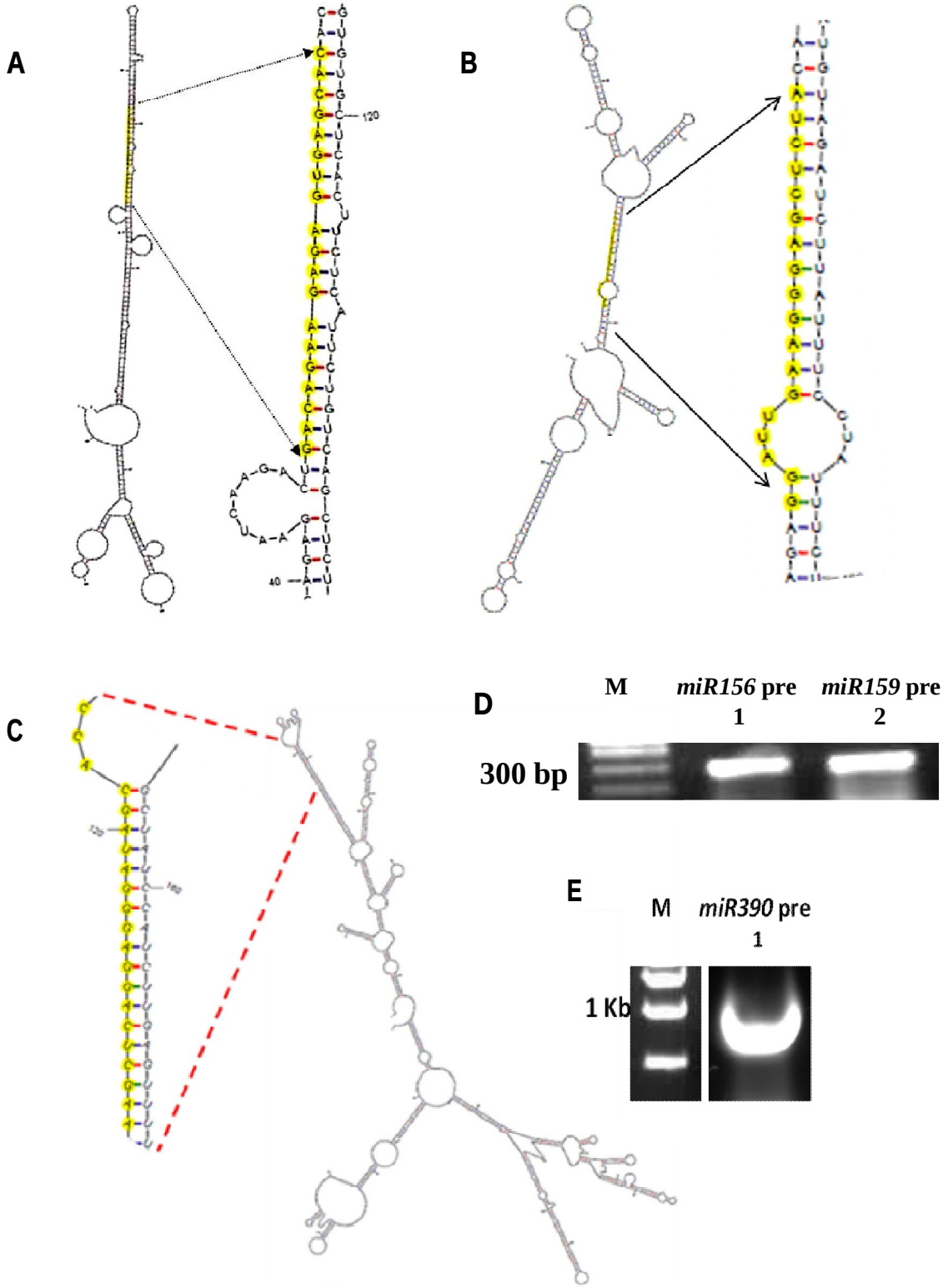

Figure 2.2: Validation of miRNA precursors in potato: A-C, Secondary structures of *miR156* (A), *miR159* (B) and *miR390* (C) precursors as predicted by MFold (Zuker, 2003). Mature *miR156, miR157* and *miR390* sequences are highlighted in yellow respectively. D and E, RT-PCR of *miR156, miR159 and miR390* precursors from leaves and stem tissues of LD grown *andigena.* (M) represents DNA marker.

Chapter 3

Role of *miR156* in potato development

3.1. Introduction

3.1.1. Role of *miR156* in plant development

miR156 is a well conserved miRNA present in all land plants (Axtell and Bowman, 2008). It targets the transcripts of Squamosa Promoter binding-Like (SPL) transcription factors (Schwab et al., 2005) and acts as a master regulator of plant development. In *Arabidopsis*, *miR156* over expression results in a prolonged juvenile phase and a delay in flowering with increased branching and production of a large number of leaves (Huijser and Schmid, 2011). Similar phenotypes of *miR156* over expression were also observed in rice (Xie et al., 2006), maize (Chuck et al., 2007), switchgrass (Fu et al., 2012) and tomato (Zhang et al., 2011b). In addition to these functions, *miR156* and its targets, SPL TFs, have also been shown to regulate embryonic patterning (Nodine and Bartel, 2010), anthocyanin biosynthesis (Gou et al., 2011) and male fertility (Xing et al., 2010). *miR156* is also reported to be present in potato (Zhang et al., 2013; Lakhotia et al., 2014), however, nothing was known about its role in potato development.

3.1.2. *miR156-miR172* cascade in phase transitions and flowering

Phase transitions and flowering is regulated by the sequential action of *miR156* and *miR172* (Wu et al., 2009; Zhu and Helliwell, 2010). In juvenile phase of the plant, *miR156* accumulated at a high level and downregulated its target genes, the SPL TFs. SPLs are positive regulators of flowering and adult epidermal leaf traits (Chen et al., 2010). High levels of *miR156* thus promoted juvenile phase of the plant. As the plant age increased, due to some unknown mechanism, levels of *miR156* decreased. This resulted in high expression of SPL TFs. Wu and co-workers demonstrated that one of the SPLs, *At*SPL9 binds to the promoter of *miR172* and positively regulated its expression, thus increasing *miR172* levels as the plant ages. High levels of *miR172* in turn downregulated AP2 TFs, the juvenile identity genes and promoted flowering. This sequential action of *miR156-miR172* has been well characterized in *Arabidopsis* (Figure 3.1). However, it has also been reported to be functional in maize and rice (Huijser and Schmid, 2011) highlighting its conserved nature. Thus, *miR156* and *miR172* have important opposing effects on the flowering pathway.

Considering the above, it can be stated that,

i) *miR156-miR172* regulate phase transitions and flowering

ii) *miR172* also plays a role in tuberization pathway

iii) There are similarities between flowering and tuberization pathways

iv) *miR156* is present in potato

The questions that we asked, is *miR156* involved in regulation of tuberization pathway like its partner *miR172*? And what are the functions it could perform in potato development?

In the current study, we have addressed *miR156* function in potato with a focus on the tuberization pathway. Interestingly, *miR156* has also been detected in phloem sap of pumpkin (Yoo et al., 2004), *Arabidopsis*, apple (Varkonyi-Gasic et al., 2010) and *Brassica napus* (Buhtz et al., 2008) earlier. Despite of its presence in phloem, *miR156* mobility in plants was not investigated. In this regard, we have validated the presence of mature and precursor form of *miR156a* in our model species *Solanum tuberosum* ssp *andigena* (section 2.3.2). To understand the role of *miR156* and its target genes in potato development, we have employed a number of strategies including target gene validations, transgenic analysis, assays of *miR156* abundance; HR-MS based hormone quantification, phloem sap analysis and grafting. Our results suggested that *miR156* is a graft-transmissible signal that affects plant architecture and tuber development in potato. It is present in the phloem of wild-type plants and it accumulated in SD induced stolons to facilitate tuber formation. In addition, *miR156* over expression lines (OE lines) show multiple morphological changes and produced aerial tubers under inductive conditions. Based on its accumulation in phloem sap of wild-type plants and its graft-transmissible effect, our results suggest that *miR156* moves through the phloem and regulates development in potato.

3.2. Materials and methods

3.2.1 Plant material and growth conditions

In this study, *Solanum tuberosum* ssp *andigena* 7540 was used. This is a photoperiod responsive plant that tuberizes under short days (SD, 8 hours light) and does not produce tubers under long day conditions (LD, 16 hours of light). *In vitro* plants were

grown under LD at 25˚C in a growth incubator (Percival Scientific). Soil plants were grown at 22˚C under LD photoperiod in environmental chambers (Percival Scientific).

For age specific expression studies of *miR156,* tissue culture raised plants were transferred to soil and incubated up to 14 weeks. Tissues (fully expanded mature leaves and stem) were collected after specific time intervals (2, 7, 12, 13 and 14 weeks) and were stored at -80˚ C until further use.

For photoperiod dependent expression studies, plants were induced under both SD and LD conditions in environmental chambers for 15 days. Different tissues (leaf, stem, stolon and swollen stolon) were harvested after 15th day post induction (dpi).

For quantifying *miR156* levels in 0 day, 15 day and 30 day old tubers stored post-harvest (tuber dormancy), tuber eyes were isolated and stored at -80˚ C.

In case of tobacco (*Nicotiana tabacum* var. Petit Havana), plants were grown under LD conditions in environmental chambers.

3.2.2. Analysis of miRNA levels

In the entire study, levels of miRNAs (*miR156* and *miR172*) were determined by stem-loop qRT-PCR. One µg of total RNA was used for all reverse transcription reactions except for quantification of miRNAs from phloem sap where 100 ng RNA were used. Stem-loop reverse primer *miR156*STP and *miR172*STP were used for *miR156* and *miR172* respectively. The primer details are provided in Table 3.1. Reverse transcription was carried out as per a previous protocol (Varkonyi-Gasic et al., 2007). Reverse transcription reaction details are also described in section 2.2.2. qPCR reactions for *miR156* (*miR156*FP and univRP) and *miR172* (*miR172*FP and univRP) were performed in a Mastercycler ep *realplex* (Eppendorf). For normalization, 5S rRNA was reverse transcribed by stem-loop primer 5s rRNASTP and amplified by 5S rRNAFP and univRP. All the PCR reactions were incubated at 95˚C for 5 min followed by 40 cycles of 95˚C for 5 s, 60˚C for 10 s and 68˚C for 8 s. PCR specificity was checked by melting curve analysis and data was analyzed using the $2^{-\Delta\Delta Ct}$ method (Livak and Schmittgen, 2001).

3.2.3. Construct design and plant transformation

To generate *miR156* OE lines of potato, the precursor sequence (*StmiR156a*; BI432985.1) of *miR156* was amplified from total RNA harvested from leaves using the primers *miR156*preFP and *miR156*preRP. The PCR product was digested with *Xba I-Sac I* and cloned into the binary vector pBI121 under the CaMV 35*S* promoter. This construct was then mobilized into *Agrobacterium tumefaciens* strain GV2260. Transgenic plants

were generated following the protocol by (Banerjee et al., 2006b). *miR156* OE lines of tobacco were raised as described by Horsch et al (1985). Kanamycin resistant transgenic plants were selected for further analysis and were maintained in MS basal medium (Murashige and Skoog, 1962) until further use. Whereas *miR156* resistant SPL9 (rSPL9) transgenic lines were generated by introducing silent mutations in the MicroRNA Recognition Element (MRE). Mutations were incorporated by site-directed mutagenesis using Turbo DNA polymerase (Stratagene). The primers used for site directed mutagenesis in MRE were rSPL9FP and rSPL9RP. Amplification of rSPL9 was carried out by using primer pairs SPL9FP and SPL9RP3 and was cloned in a binary vector pBI121 downstream of CaMV 35*S* promoter. Transgenic plants of rSPL9 were generated and maintained as described above.

3.2.4. Leaf and stem histology

For histology, a modified protocol of Cai and Lashbrook (2006) was followed. Briefly, leaves and stems of eight week old plants (wild-type: WT, *miR156* OE line 5.1 and 6.2) grown under LD conditions were fixed in chilled ethanol: acetic acid (3:1) (Merck). The tissues were vacuum infiltrated (400mm Hg) for 30 min and then stored at 4˚C overnight. Fixed tissues were then dehydrated at room temperature in a graded series of ethanol (75%, 95% and in 100% ethanol) followed by washes of a combination of ethanol: xylene series. Tissue blocks were prepared with molten Paraplast (Leica). Ten µm sections were cut by microtome (Leica) and placed on glass slides. Dried slides were deparaffinized by washing twice in 100% Xylene and were observed under microscope.

3.2.5. eSEM of leaves

Leaves of eight week old plants (WT, *miR156* OE line 5.1 and 6.2) grown under LD conditions were used for Scanning Electron Microscopy - Quanta 200 3D (FEI) SEM (environmental mode) and leaf morphology was documented.

3.2.6. Leaf Mass Area (LMA) analysis

Leaf 4 and leaf 5 from eight week old WT and *miR156* OE 5.1 plants were harvested. Leaf area was measured by using Image J software. The dry weight of leaves was calculated by first drying them in the oven at 65˚C for 24 hours followed by measuring their weight on a weighing balance. Leaf Mass Area (LMA) was calculated by obtaining the ratio of dry weight by leaf area.

3.2.7. Analysis of tuberization

Both WT and *miR156* OE lines were grown in soil at 22˚C under LD in environmental chambers for three weeks. Thereafter, ten plants each were shifted to SD and LD and were incubated further for 4 weeks. To analyze *St*SP6A (PGSC0003DMG400023365) and *miR172* levels in these plants, leaf tissues were harvested 8 days post induction from both these lines. *miR172* levels were also quantified in 15 days post SD induced stolons of WT and *miR156* OE plants (line 5.1). The tuberization phenotype was scored after four weeks of induction.

3.2.8. Analysis of genes involved in branching

For analysis of genes involved in branching, total RNA was isolated from stem and leaf tissues of 12 week old wild-type and *miR156* OE line by TRIzol reagent (Invitrogen). One µg total RNA was used for cDNA synthesis by Superscript III reverse transcriptase enzyme (Invitrogen) by gene specific reverse primer (GSP). qPCR reactions were performed on Mastercycler ep *realplex* with forward GSPs and same reverse GSPs. The reactions were carried out using KAPA SYBR green master mixture (Kapa Biosystems) and incubated at 95˚C for 2 min followed by 40 cycles of 95˚C for 15 s; 60˚C for 30 s. GAPDH was used for normalization. PCR specificity was checked by melting curve analysis and data was analysed using $2^{-\Delta\Delta Ct}$ method (Livak and Schmittgen, 2001). The genes analysed were:

AXR1	PGSC0003DMT400070486
AXR3	PGSC0003DMT400015610
SPS	PGSC0003DMT400078178
MAX1	PGSC0003DMT400021231
MAX2	PGSC0003DMT400085749
CCD8	PGSC0003DMT400005706
PIN1	PGSC0003DMT400014752
PIN5	PGSC0003DMT400017301
IPT2	PGSC0003DMT400015411
IPT5	PGSC0003DMT400068271

3.2.9. Analysis of zeatin riboside and orobanchyl acetate by HR-MS

Axillary meristems were harvested from WT and *miR156* OE 5.1 plants induced for 15 days in LD and SD conditions and ground in liquid nitrogen. For HR-MS analysis, a modified protocol of Forcat et al (2008) was followed. One hundred mg of tissue was used for extraction in 400µl of 10% methanol and 1% glacial acetic acid. This mixture was vigorously vortexed and stored on ice for 2 hours followed by centrifugation to obtain the supernatant. This was repeated three times and the volume of the supernatant was adjusted

to 2 ml in a volumetric flask. Samples were resolved through a Thermo Scientific Hypersil Gold column of particle size 5 µm with a flow rate of 0.5 mL/min and a gradient solvent program of 25 min (0.0 min, 10 % methanol/water; 0.5 min, 10.0 % methanol/water; 3.0 min, 45 % methanol/water; 20 min, 50 % methanol/water; 22.0 min, 90 % methanol/water; 23.0 min, 10 % methanol/water; 25.0 min, 10 % methanol/water). Formic acid (0.1 % LC-MS grade) was also added to methanol and water. MS and MS/MS experiments were performed in ESI-positive ion mode using the tune method as followed: sheath gas flow rate 45, auxiliary gas flow rate 10, sweep gas flow rate 2, spray voltage (|KV|) 3.60, spray current (µA) 3.70, capillary temperature (ºC) 320, s-lens RF level 50, heater temperature (ºC) 350. ESI-MS data were recorded in full scan mode within the mass range *m/z* 100 to 1000. A standard curve for quantification was prepared using zeatin riboside (Sigma). Orobanchyl acetate was identified based on MS analysis and quantification was performed considering the peak areas.

3.2.10. Analysis of *StSP6A*, *StLOG1* and *StCyclin D3.1*

One µg of total RNA was used for *StSP6A* (PGSC0003DMG400023365) analysis from 8 day old SD induced leaves of WT and *miR156* OE lines. 18*S* rRNA (50 ng) was used for normalization. For RT-PCR, Superscript III one step RT-PCR system with platinum Taq DNA polymerase (Invitrogen) was used as per manufacturer's instructions. Semi-quantitative RT-PCR for *StSP6A* was performed using the following primers: SP6AFP and SP6ARP. RT-PCR conditions were as follows: 50˚C for 30 min, 94˚C for 2 min, followed by 25 cycles of 94˚C 15 s, 55˚C for 15 s and 68˚C for 1 min. Cycle number for 18S RNA was restricted to ten, while the program remained the same as for *StSP6A*. For analysis of *StLOG1* (PGSC0003DMT400009551) and *StCyclin D3.1*(PGSC0003DMT400064307), total RNA was isolated from axillary meristems of WT and *miR156* OE 5.1 plants grown in SD photoperiod for 15 days by TRIzol reagent. One µg of total RNA was used for cDNA synthesis by Superscript III reverse transcriptase (Invitrogen) using an oligo dT primer. qPCR reactions were performed on a Mastercycler ep *realplex* with LOG1FP-LOG1RP and CyclinFP-CyclinRP. The reactions were carried out using KAPA SYBR green master mixture (Kapa Biosystems) and incubated at 95˚C for 2 min followed by 40 cycles of 95˚C for 15 s; 60˚C for 30 s. GAPDH was used for normalization for all the reactions. PCR specificity was checked by melting curve analysis and data was analyzed using $2^{-\Delta\Delta Ct}$ method (Livak and Schmittgen, 2001).

3.2.11. Analysis of *StCUC3* and *StYABBY*

One µg of total RNA was used for *StCUC3* (FJ435159.1) and *StYABBY* (AY495968.1) analysis from LD induced leaves of WT and *miR156* OE lines. 18*S* rRNA (50 ng) was used for normalization. For RT-PCR, Superscript III one step RT-PCR system with platinum Taq DNA polymerase (Invitrogen) was used as per manufacturer's instructions. Semi-quantitative RT-PCR for *StCUC3* and *StYABBY* was performed using the following primers: CUCFP-CUCRP and YABBYFP-YABBYRP. RT-PCR conditions were as follows: 50˚C for 30 min, 94˚C for 2 min, followed by 25 cycles of 94˚C 15 s, 55˚C for 15 s and 68˚C for 1 min. Cycle number for 18S RNA was restricted to ten, while the program remained the same.

3.2.12. Prediction of *miR156* target genes

miR156 target genes in potato were predicted using bioinformatic tools as mentioned in section 2.2.3. For further studies, five target gene sequences were short listed as potential *miR156* targets. These targets showed homology (40-80 %) with *At*SPL3, *At*SPL6, *At*SPL9, *At*SPL13 and *Rco*Liguleless1 and were termed as *St*SPL3 (TC217180), *St*SPL6 (TC200961), *St*SPL9 (TC218470), *St*SPL13 (TC197452) and *St*Liguleless1 (*St*LG1, PGSC0003DMT400084734) respectively. Their coding sequences were retrieved from the Online Resource for Community Annotation of Eukaryotes (ORCAE) [http://bioinformatics.psb.ugent.be/orcae/ (Sterck et al., 2012)] and Database of Plant Transcription Factors [http://planttfdb.cbi.edu.cn/ (Zhang et al., 2011a)].

3.2.13. Cleavage site mapping

To validate the candidate targets of *miR156 in planta*, modified RNA Ligase Mediated 5' RACE was performed, using the First Choice RLM-RACE kit (Ambion). Total RNA was extracted from WT potato leaves by TRIzol reagent and was directly ligated to RNA adaptor without any enzymatic pre-treatments. cDNA synthesis was performed using respective gene specific reverse primers. Two rounds of PCRs were conducted with adaptor specific forward primers and gene specific reverse primers (SPL3: SPL3RP1-SPL3RP2, SPL6: SPL6RP1-SPL6RP2, SPL9: SPL9RP1-SPL9RP2, SPL13: SPL13RP1-SPL13RP2, LG1: LG1RP1-LG1RP2). Amplicons were then cloned into a sub cloning vector pGEMT Easy and were sequenced to identify the miRNA cleavage sites.

3.2.14. Analysis of *StSPLs*

Total RNA from WT and *miR156* OE plants was isolated by TRIzol reagent as per manufacturer's instructions. One µg of total RNA was reverse transcribed using gene specific primers by M-MLV reverse transcriptase (Promega). For normalization, *GAPDH* was reverse transcribed. The primers used for reverse transcription were SPL3RP2, SPL6RP2, SPL9RP2, SPL13RP2, LG1RP2 and GAPDHRP. qPCR reactions were performed on a Mastercycler ep *realplex* with the same reverse primers mentioned above. Forward primers were SPL3qFP, SPL6qFP, SPL9qFP, SPL13qFP, LG1qFP and GAPDHFP. The reactions were carried out using the KAPA SYBR green master mix and incubated at 95˚C for 2 min followed by 40 cycles of 95˚C for 15 s, 52˚C for 15 s and 60˚C for 20 s. For *GAPDH*, all conditions were similar but the annealing temperature was 55˚C. For *St*LG1, all conditions were similar except extension time was 10 s. PCR specificity was checked by melting curve analysis and data was analyzed using $2^{-\Delta\Delta Ct}$ method (Livak and Schmittgen, 2001).

3.2.15. Gel retardation assay

A 6X His tagged fusion construct was generated by introducing the 1152 bp coding sequence of *St*SPL9 in frame into the pET28a expression vector and transformed into BL21 (DE3) *E. coli* cells. Cells were grown at 37°C until the OD_{600} reached 0.6, induced with 1.0 mM isopropyl-β-d-thiogalactopyranoside and cultured for 3h at 37°C. The cells were lysed by sonication. The tagged protein was purified using Ni-NTA beads. Purified *St*SPL9 protein aliquots were frozen in liquid N_2 and stored at −80°C. Four overlapping fragments of the MIR172b promoter (AC237992) were used for gel mobility shift assays. Promoter fragments were PCR amplified from potato genomic DNA and were purified on columns. The respective primer sequences are provided in Table S3. The 5' ends of the fragments were then labeled with gamma-P^{32} using KinaseMax kit (Ambion). The DNA-binding reactions were set up at 24^{o}C in 20 µl containing 10 mM Tris–HCl (pH 7.5), 5% glycerol, 0.5 mM EDTA, 0.5 mM DTT, 0.05% NP-40, 50 mM NaCl, 50 mg/l poly(dG-dC), 250 ng protein, and 1 fmol labeled DNA. After incubation at 24^{o}C for 60 min, the reactions were resolved on a 6% native polyacrylamide gel in 1× Tris-Borate-EDTA (TBE) buffer. The gel was dried and exposed to X-ray film. In the cold competition assays, 100 fold more unlabeled double-stranded DNA fragment (P1) was added to the reaction and loaded onto the gel every 15 min.

3.2.16. Detection of *miR156* in the phloem

Stem sections of twelve week old WT plants were fixed as described above in the histology section. Laser Microdissection Pressure Catapulting (LMPC) mediated harvest of phloem cells (Carl Zeiss PALM laser micro beam) and RNA extraction from these cells was done as per Yu et al (2007). Total RNA was extracted using TRIzol reagent. Mature *miR156* and *miR156** was detected by stem-loop RT-PCR as described earlier. Primer sequences for *miR156** are provided in Table S3.

For the analysis of differential accumulation of *miR156* in phloem sap of SD-LD grown wild-type plants, sap extraction and RNA isolation was done as per Campbell et al (2008) with a minor modification (the phloem exudate was harvested at 18^{o}C). Sap collection was performed at 8, 15 and 30 dpi. To assess purity of phloem sap, RT-PCR was performed for Nitrate Transporter (NT: root specific transcript, CK267169.1) and G2-like transcription factor (G2: phloem specific transcript, CK853924.1) using 150 ng of RNA as mentioned before (Banerjee et al., 2006a). Superscript III one step RT-PCR system with platinum Taq DNA polymerase was used as per manufacturer's instructions. For NT, RT-PCR conditions were as follows: 55˚C for 30 min, 94˚C for 2 min, followed by 40 cycles of 94˚C 15 s, 50˚C for 30 s and 68˚C for 1 min with final extension at 68˚C for 5 min. For G2, all conditions were similar except annealing was at 56˚C and extension was for 30 s. To quantify *miR156* levels in phloem sap, 100 ng of total RNA was used for *miR156* specific stem-loop qRT-PCR reactions as described above (Analysis of miRNA levels) except the cycle number was increased to 50. qRT-PCR Ct value differences were calculated for *miR156* accumulation and plotted as previously described (Pant et al., 2008).

3.2.17. Soil grown heterografts

WT and *miR156* OE lines were maintained in an environmental chamber until grafting was performed. Grafts were made with WT and *miR156*OE transgenic potato plants as per our previous protocol (Mahajan et al., 2012). *miR156* OE lines were used as scions and WT plants as stock (heterografts), while for reverse grafting, *miR156* OEs served as stock and WT as scion (reverse grafts). Homografts (WT on WT) were used as controls in both cases. Equal number (ten each) of heterografts, reverse grafts and homografts were made and maintained in environmental chamber for hardening for four weeks. Hardened grafts were further incubated in SD for four weeks. Scion and stock

samples (devoid of graft union) were harvested and phenotypes such as leaf number, trichomes and axillary branches were scored. qRT-PCR was performed for *miR156* accumulation in both heterograft stock samples and reverse graft scion samples with respective tissues from homograft as controls. Tuberization phenotypes were scored for all grafts.

For *miR156a* precursor transgene detection, RT-PCR was performed by Superscript III one step RT-PCR system with platinum Taq DNA polymerase using 250 ng of total RNA. The primers used were *miR156*pre FP and transgene specific NOST RP. The RT-PCR conditions were as follows: 50˚C for 30 min, 94˚C for 2 min, followed by 35 cycles of 94˚C 15 s, 50˚C for 15 s and 68˚C for 1 min with final extension of 68˚C for 5 min.

For comparative analysis of *miR156* (mature) and *miR156a* precursor levels in wild-type and grafted plants, 500 ng of RNA was used. Stem-loop qRT-PCR of *miR156* (mature) was performed as described above (Analysis of miRNA levels). For *miR156a* precursor quantification, cDNA synthesis was performed using oligo dT and Superscript III reverse transcriptase enzyme. qPCR reactions were performed on a Mastercycler ep *realplex* with *miR156*preFP and *miR156*preRP primers. The reactions were carried out using KAPA SYBR green master mixture and incubated at 95˚C for 2 min followed by 40 cycles of 95˚C for 15 s, 50˚C for 10 s, 72˚C for 18s. GAPDH was used for normalization. PCR specificity was checked by melting curve analysis and data was analyzed using $2^{-\Delta\Delta Ct}$ method (Livak and Schmittgen, 2001).

3.2.18 Primer sequences-

The sequences of primers used in this chapter are in Table 3.1

Table 3.1: List of primers

Primer Name	Primer Sequence
*miR156*preFP	CGATCTAGAGTTTGTGTGAAGCAAAGAGA
*miR156*preRP	CCTGAGCTCGA GGAAGTAGTAGCTATG
miR156 STP	GTCGTATCCAGTGCAGGGTCCGAGGTATTCGCACTGGATACGAC GTGCTC
miR156 FP	GCGGCGGTGACAGAAGAGAGT
*miR156** STP	GTCGTATCCAGTGCAGGGTCCGAGGTATTCGCACTGGATACGA CTGACAG
*miR156** FP	GGCGGTGTGCTCACTTCTCATT

*miR172*STP	GTCGTATCCAGTGCAGGGTCCGAGGTATTCGCACTGGATACGACATGAG
*miR172*FP	CGGCGGTAGAATCTTGATGATG
5srRNASTP	GTCGTATCCAGTGCAGGGTCCGAGGTATTCGCACTGGATACGACCA CTCT
5srRNAFP	GGATGCGATCAT ACCAGCACT
UnivRP	GTGCAGGGTCCGAGGT
SPL3RP1	CGGTCTACAAACTATCGAAG
SPL3RP2	GCATACCTGAAGATAACATTTT
SPL3qFP	CTCCAGGAGAAGGGTCAAG
SPL6RP1	TGATGAAGCTGCGACGACAA
SPL6RP2	GGTGAGCACTAGGAGGAAC
SPL6qFP	TTGTTTCCCGCTCTCTGTTC
SPL9RP1	GGTCCAGTTCCATGTATTGT
SPL9RP2	TGCACCATGAGAACCTGAAG
SPL9qFP	GACCAGTTATCCTAGTGTTC
SPL9FP	GACTCTAGAACCTATAATGGAACTGGGTTCA
SPL9RP3	GACGAGCTCTCAAAGAGTCCAGTGCACATT
SPL13RP1	GAGCCACCACTTGTAGATGA
SPL13RP2	ACCATGTGACTCAAACCAATC
SPL13qFP	ACCATGTGACTCAAACCAATC
LG1 RP1	TTGATTTGCATGGTTGAGTG
LG1RP2	CGAATGGAGCTTTGAACACT
LG1 qFP	GTTCAATATGGTTACAGGAC
rSPL9FP	ATTCAAGTGGTTCTAAGCCTATTTTGCCAAATCGG
rSPL9RP	CCGATTTGGCAAAATAGGCTTAGAACCACTTGAAT
GAPDHFP	GAAGGACTGGAGAGGTGGA
GAPDHRP	GACAACAGAAACATCAGCAGT
SP6AFP	CCATTGATAGTTGGTCGTGTG
SP6ARP	ACAGCTGCAACAGGCAATCC
172proP1F	TTGTAGAGTAAGTCGTGCATA
172proP1R	GAAGAAGAATACAGGCAATGA
172proP2F	TCTCTTTTCCCTTCTCAACTC
172proP2R	AACACAAGAACATGAATCGGT
172proP3F	TTGATTATCTTCTCCCGTTGA
172proP3R	GCAGACAAAAAGGACAAAAAAA
172proP4F	ATGTGTAGATTTCTCATTTAG
172proP4R	CAAAATTCCTTCTCAGAAGT
AXR1 FP	GGTTGGAAGCATCACTGTTGTT
AXR1 RP	CTCAATCAGTTCCTCAGGGCAAT

AXR3 FP	GAGGATTTTCTGAGACTGTTGAT
AXR3RP	CTTTTGAGCCATTACATTCTTCC
SPS FP	GCCGACGTTGCGAAAGAGATC
SPS RP	TTTGACAAGGTTAGTGCCAATGCAC
MAX 1 FP	AGATAGTGGCAAAGAGGATGGAGGA
MAX 1 RP	ATCGAGGTACGGGAATTTCTGCTGAA
MAX2 FP	CTGCTGGACGGATGATATTCCTGTC
MAX2 RP	CCCTAGCGTTTGACAAAGCTGAAGTA
CCD8 FP	GCTTATGCTTGTGGTGCTAAGAGGC
CCD8 RP	CCAACAACCATGTAGCCCATAGGG
PIN1 FP	AGTCATCAAGAAATCCAACACCA
PIN1 RP	ACTTCCCACTTTCTTCCTCATAA
PIN5 FP	GCTATGGTTCAGTAAAATGGTGG
PIN5 RP	TAGCCCATAAGACGAGGATCAG
IPT2 FP	TCGTGATAATGGGTGCTACTGGT
IPT2 RP	CCGAGAAGATGATGGTGGATAC
IPT5 FP	GTAGTAATAATGGGAGCAACAGG
IPT5 RP	TACCAAGAAGATGATGAGGCACT
LOG1 FP	GTGTTGATTCATTTTTGTCCA
LOG1 RP	TACCAAACAATCATATACAGACAG
Cyclin FP	CTTGGATGATGATTTAGGTG
Cyclin RP	TCAACATCCAATCCAAAGCC
NT FP	TGGTGTTACTGGTAGAGAA
NT RP	TCTGTAAAGAAGCGAGGT
G2 FP	ACAACCGCACAAAGAATTTAATG
G2 RP	TGTTCTCCACATATGTTCAAAT
NOST RP	GCAACAGGATTCAATCTTAAG
CUC FP	TCATCATCATCAGCGGCAGT
CUC RP	TCCTCTTGTTTGTTGTCTTTG
YABBY FP	CTTCCACTAATCATCATCATCA
YABBY RP	GCTTCTCTGTGGCTAATATCA
18S FP	GTAGTTGGACTTTGGGATGGCAC
18S RP	GGGCATTCGTATTTCATAGTCAGAG

3.3. Results

3.3.1. Expression analysis of *miR156* in potato

The presence of *miR156* (mature and precursor form) was validated in our model species *Solanum tuberosum* ssp *andigena* (section 2.3.2). To study the age dependent accumulation pattern of *miR156*, relative levels were analyzed by stem-loop qRT-PCR in potato plants of different age groups. Two-week old plants showed higher accumulation of *miR156* in stem and their levels decreased as the plant aged. However, *miR156* levels varied in mature leaves of plants of different ages (Figure 3.2 A). To determine whether *miR156* expression is regulated by the photoperiod, plants were grown under LD and SD conditions. Stem-loop qRT-PCR analysis demonstrated a higher accumulation of *miR156* in leaves and stem under LD as compared with the plants under the SD photoperiod (Figure 3.3 A and B). However, in stolons, *miR156* levels were found to be ~8-fold higher under SD as compared to LD photoperiod (Figure. 3.3 C). Our analysis showed a range of *miR156* abundance in swollen stolons, tubers stored post-harvest for different time periods (0, 15 and 30 days) and two-week old sprouts. Zero day old tubers (post-harvest) showed a ~2.5-folds higher accumulation than in stolons harvested from SD induced plants. Whereas, *miR156* levels in juvenile tuber sprouts were almost half the level in stolons (Figure 3.3 D). Overall, our expression analysis suggested that *miR156* shows tissue-specific accumulation with respect to age of the plant and photoperiod.

3.3.2. Over expression of *miR156* in potato

miR156 precursor was cloned under a strong constitutive 35S CaMV promoter in a binary vector pBI121 (Figure 3.4 A). It was mobilized into *Agrobacterium tumefaciens* GV2260 strain and transformed to *andigena* as described in section 3.2.3. The explants started callusing on callus inducing media within a week post transformation. Following this, they were transferred to shoot inducing media. Shoots were observed 8-10 weeks post transformation. Shoots were then transferred to rooting media and the clones were confirmed to be transgenics by selection marker PCR (Kanamycin resistance). Out of 20 clones, two clones (clone 5.1 and clone 6.2) showing highest *miR156* expression were then selected for further experiments (Figure 3.4 B).

3.3.3. *miR156* over expression affects leaf architecture in potato

The leaf architecture of *miR156* OE lines was dramatically affected. Two-week old OE lines exhibited a drastic change in leaf phenotype (Figure 3.5 A and B). *miR156* OE

plants produced smaller leaves with reduced leaflet number (Figure 3.5 C and D). The venation pattern was found to be altered in which the side veins of transgenic leaves were less prominent (Figure 3.5 E and F). Transverse sections (T.S) of leaves showed disoriented cell arrangement as well as the presence of large epidermal cells in *miR156* OE 5.1 line (Figure 3.5 G and H). We have also observed a reduction in stomatal density in both OE lines as opposed to WT (Figure 3.6 A to D). In addition, trichome number was reduced with an increase in trichome length in OE lines (Figure 3.7 A to E).

A study in 2008 (Blein et al., 2008) demonstrated the conserved function of two transcription factors NAM (FJ435166.1) (NO APICAL MERISREM) and CUC3 (FJ435159.1) (CUP-SHAPED COTYLEDON3) in determining boundary domain that delimits leaflets. Silencing of these genes resulted in a fewer leaflet phenotype in four distantly related species. *miR156* over expression lines too exhibited smaller leaves with reduced leaflet number. To understand the molecular basis of this phenotype, we quantified *StNAM* and *StCUC3* levels in *miR156* OE lines along with another gene involved in leaf polarity development, *St*YABBY (AY495968.1). In *miR156* OE lines, levels of *StCUC3* and *StYABBY* were not significantly different as compared to wild-type indicating that these genes were not involved in the drastic leaf phenotype of *miR156* over expression lines (Figure 3.8 A to C). In case of *StNAM*, we were unable to specifically amplify *StNAM* from potato.

3.3.4. *miR156* over expression affects branching phenotype

miR156 OE plants also exhibited enhanced branching from axillary buds resulting in a bushy appearance (Figure 3.9 A to C). Despite of several reports of *miR156* over expression and associated branching phenotype in plants, the molecular mechanism is yet unknown. We hypothesized that key genes from different hormone regulatory pathways could be involved in branching phenotypes of *miR156* OE lines. To understand the branching phenotype of OE lines, we analyzed the transcript levels of following genes (shoot architecture- SUPERSHOOT, strigolactone synthesis – MORE AXILLARY BRANCHING 1, 2, CAROTENOID CLEAVAGE DIOXYGENASE 8; auxin transport and response- PINHEAD 1 & 5, AUXIN RESISTANT PROTEIN 1 & 3 and cytokine biosynthesis- ADENOSINE PHOSPHATE ISOPENTENYL TRANSFERASE 2 & 5) known to be involved in shoot branching (Tantikanjana et al., 2001; Domagalska and Leyser, 2011). Of the ten different genes analyzed, SUPERSHOOT (SPS), PINHEAD 1 (PIN1) and AUXIN RESISTANT PROTEIN 3 (AXR3) levels were found to be

significantly changed as compared to WT in both LD and SD plants (Figure 3.10 and 3.11). SPS mutants in *Arabidopsis* resulted in profused branching as reported earlier (Tantikanjana et al., 2001). An increased accumulation of SUPERSHOOT transcripts in our study was not expected in both SD/LD plants. Overall this analysis did not lead to a possible conclusion for the branching phenotype of *miR156* OE lines.

3.3.5. *miR156* over expression affects tuberization in potato

To examine whether an increase in *miR156* levels in OE lines could have any impact on tuber development, we examined the tuberization phenotype of *miR156* OE 5.1 and 6.2 lines. OE line 5.1 produced aerial and underground tubers after four weeks of SD induction, whereas WT plants grown under a SD photoperiod only produced underground tubers (Figure 3.12 A to C). Line 6.2 produced underground tubers and showed a delayed formation of aerial tubers. None of the plants produced tubers under LD photoperiod.

Overall, *miR156* OE lines (5.1 and 6.2) developed fewer underground tubers and showed reduced tuber yields (Figure 3.12 D). Previous reports have shown *miR172* and *StSP6A* to act as positive regulators of tuberization (Martin et al., 2009; Navarro et al., 2011). Since, *miR156* OE lines exhibited reduced tuber yield, we investigated the levels of *StSP6A* and *miR172* (tuberization markers) in leaves of OE plants. Also *miR172* levels were quantified in SD induced stolons. Our results showed a reduction in the levels of tuberization markers *miR172* and *StSP6A* in *miR156* OE lines. *miR172* levels were reduced by ~80% in leaves and stolons, while *StSP6A* levels were reduced to ~60% in leaves (Figure 3.13 A to C).

3.3.6. *miR156* over expression affects hormone levels

miR156 over expression in potato resulted in a drastic phenotype of increased branching, a higher number of leaves with reduced leaflets and formation of aerial tubers under SD. A recent paper demonstrated the effect of over expression of a single gene (TLOG1) in tomato which resulted in formation of tomato tubers and increased axillary branching in plants (Eviator-Ribak et al., 2013). LOG1 is a cytokinin biosynthetic gene that converts CK ribosides to biologically active CK (Kurakawa et al., 2007). Considering the role of cytokinins in branching (Domagalska and Leyser, 2011) and the recent report of LOG1, we investigated the effect of *miR156* on cytokinin pathway. *miR156* OE plants showed ~ 1.8 fold increased expression of *StLOG1* in the axillary meristems as compared to WT plants (Figure 3.14 A). Also, the levels of *StCyclin D3.1*, a cytokinin responsive gene, were increased up to ~8 fold as compared to WT plants (Figure 3.14 B). To

determine the amount of cytokinin (zeatin riboside- ZR), High Resolution Mass Spectrometry (HR-MS) analysis demonstrated increased levels (> 2 fold) in *miR156* OE plants as compared to WT in both SD and LD conditions (Figure 3.15 A, 3.16 and 3.17). As strigolactones are also considered to be branching hormones (Domagalska and Leyser**,** 2011), we investigated the levels of one such strigolactone - orobanchyl acetate. HR-MS analysis demonstrated reduced levels of orobanchyl acetate (~20% under LD conditions and ~60% under SD conditions) in *miR156* OE plants as compared to WT (Figure 3.15 B, 3.18 and 3.19). The changes in these hormone amounts correlated with the branching phenotype observed in *miR156* OE lines.

3.3.7. *miR156* over expression affects multiple morphological traits in potato

Other than leaf, branching and tuberization phenotype, *miR156* overexpressing lines did not form an inflorescence as compared to WT plant (Figure 3.20 D and E). These plants did not flower even after eighteen weeks of growth, whereas WT plants produced inflorescence in twelve weeks. Also, *miR156* OE lines produced more number of nodes as compared to wild-type (Figure 3.20 A). The fresh weight of roots in OE lines was also significantly reduced (Figure 3.20 B). Leaf mass per area (LMA) analysis of *miR156* OE leaves demonstrated that they have a significantly reduced LMA as compared to wild-type leaves (Figure 3.20 C).

3.3.8. *miR156* over expression in tobacco

Tobacco belongs to the same family of *Solanaceae* as potato. To understand *miR156* function in tobacco, *miR156* over expression tobacco lines were also generated and selected as described in sections 3.2.3 and 3.3.2. *miR156* over expressing tobacco plants showed similar phenotype as *miR156* overexpressing potato plants (Figure 3.21 and 3.22). They had bushy appearance with more number of leaves but reduced size (Figure 3.21 A to F; 3.22 A to C). Also, wild-type tobacco plants produced flowers (Figure 3.21 G) as opposed to OE line which continued to produce leaves (Figure 3.21 H). The fresh weight of roots in OE tobacco plants was also significantly reduced (Figure 3.22 D). This clearly indicated the conserved nature of *miR156* as previously observed.

3.3.9. *miR156* targets *StSPL* transcription factors in potato

Our *in silico* analysis with psRNATarget software (*plantgrn.noble.org/psRNATarget,* Dai et al., 2011*)* predicted nineteen potential target genes for *miR156* in potato. We short listed five *miR156* target genes *StSPL3, StSPL6,*

StSPL9, StSPL13 and StLiguleless1 (*StLG1*) for further analysis. To determine if these genes are the targets of *miR156* in potato, modified RNA Ligase Mediated 5' RACE (RLM-RACE) was performed. RNA sequences with 5' termini corresponding to the $10^{th}/11^{th}$ nucleotide of *miR156* were consistently detected demonstrating that *StSPL6, StSPL9, StSPL13* and *StLG1* are targeted by *miR156 in vivo* (Figure 3.23 A to F). However, *StSPL3* was cleaved at sites other than $10^{th}/11^{th}$ nucleotide of *miR156* (Figure 3.23 B), which is not a common observation in plant microRNAs. Levels of these targets were also quantified in *miR156* over expressing plants. As expected, transcript levels of these targets showed different degree of reduction (*StSPL3*: ~80%, *StLG1*: 70%, *StSPL*13: 60%, *StSPL9*: 40% and *StSPL6*:30% in *miR156* OE 5.1 plants (Figure 3.24 A). Our results are consistent with previous studies on *miR156*-SPLs interaction (Schwab et al., 2005).

3.3.10. Regulation of *miR172* by *miR156*-SPL module

Over expression of *miR156* in potato resulted in lower tuber yields and reduced levels of *miR172* and *SPLs* as mentioned above. Our bioinformatic analysis of the *St*MIR172b (AC237992) promoter showed the presence of multiple GTAC motifs, characteristic of SPL binding (Birkenbihl et al., 2005). We chose to continue our investigation with *St*SPL9, since *miR156*-SPL9 interaction has previously been demonstrated in *Arabidopsis* (Wu et al., 2009) and rice (Jiao et al., 2010), suggesting that a similar interaction module might also be conserved in potato. To examine if *St*SPL9 binds to the *St*MIR172b promoter, gel retardation assays were performed. The *St*MIR172b promoter was analyzed in four fragments (P1, P2, P3 and P4) (Figure 3.25 A) having two binding motifs in the P1 fragment and a single motif each in the P2 and P3, while P4 served as negative control. Recombinant *St*SPL9 protein (42 kD) retarded the mobility of P1 promoter sequence, whereas the other three promoter fragments (P2, P3 and P4) remained unaffected (Figure 3.25 B). Competition gel retardation assays were performed with P^{32} labeled and unlabeled P1 fragment. With increased unlabeled P1, the P1-SPL9 complex was diminished over time (Figure 3.25 C). Our analysis demonstrated *St*SPL9-MIR172 promoter interactions *in vitro* with *St*SPL9 binding to a promoter region with two binding sites.

To further validate the *miR156-St*SPL9 interaction, we generated *miR156* resistant *StSPL9* over-expressing potato plants (rSPL9 OE lines) driven by the CaMV 35*S* promoter (Figure 3.26 A and B). *miR156* resistant SPL9 (rSPL9) transgenics were generated by introducing silent mutations in the MicroRNA Recognition Element (MRE), so that the

mutated transcript is no longer recognized by *miR156*. Stem-loop qRT-PCR analysis revealed a ~ 5-fold increase in levels of *miR172* under SD compared to WT (Figure 3.26 C). This increase in *miR172* levels under SD conditions, however, was not reflected by the tuberization phenotype of rSPL9 OE line (Figure 3.26 D).

3.3.11. Detection of *miR156* in phloem of wild-type potato plants

Interestingly, *miR156* has been detected in phloem sap of pumpkin, *Arabidopsis*, apple and *Brassica napus* as mentioned previously. MicroRNAs present in phloem exudates are proposed to be mobile with a putative role as long-distance regulators of development and stress pathways by acting on target genes (Marín-González and Suárez-López, 2012). Although *miR156* is known to interact with the transcripts of SPL TFs (also, now shown in potato, section 3.3.9), mobility of *miR156* in plants has not yet been investigated. In order to investigate the presence of *miR156* in phloem of potato plants, we harvested phloem cells by the Laser Microdissection Pressure Catapulting (LMPC) and tested for the presence of *miR156* (mature form) in phloem cells of WT potato (Figure 3.27 A to C). While *miR156* was detected in phloem cells, we did not detect the *miR156*a precursor in phloem sap harvested from WT plants (Figure 3.27 D). *miR156** strand however, was detected in phloem sap exudates of WT plants by stem-loop qRT-PCR (Figure 3.27 E). The purity of phloem sap (phloem-enriched exudate) was confirmed by detecting the phloem specific transcript-G2 and absence of root specific transcript-NT (Figure 3.28 A). To understand if photoperiod has any role on *miR156* accumulation in the phloem, we also carried out a stem-loop qRT-PCR analysis of phloem sap harvested from WT plants incubated for 8, 15 and 30 dpi under both SD and LD conditions. Higher accumulation of *miR156* was observed in phloem sap harvested from 8 and 15 dpi SD induced plants indicating that *miR156* accumulation increased under SD conditions in phloem sap of potato. This pattern changed in plants incubated for longer time (30 dpi) (Figure 3.28 B).

3.3.12. *miR156* is potentially a graft-transmissible signal in potato

In our study, we have detected *miR156* in LMPC harvested phloem cells and it exhibited a SD-induced accumulation pattern in phloem sap. Considering this observation, we tested whether *miR156* is a phloem mobile signal in potato. Grafting experiments (homografts, heterografts and reverse grafts) were performed to demonstrate the mobility of *miR156* (Figure 3.29 A). After 4 weeks of SD induction, analysis of morphological changes in grafts as well as the quantitative analysis of *miR156* was performed. Overall,

the leaf shape and trichome morphology of stocks from the heterografts (*miR156* OEs as scion and WT as stocks) were affected. The newly emerging leaves from the axillary shoots on the stock of heterografts had more prominent but fewer trichomes (Figure 3.29 B) and exhibited small and thick lamina along with reduced number of leaflets (Figure 3.29 C). On the other hand, newly emerging leaves from WT scions of reverse grafts did not show any phenotype similar to *miR156* OE plants (Figure 3.29 D). All the heterografts had less tuber yield as compared to homografts, while reverse grafts did not form any tubers (Figure 3.29 E).

The morphological changes in the stock stems of heterografts could be due to (i) the transport of mature *miR156* itself, (ii) transport of the over expressed *miR156a* precursor transgene, or (iii) by a *miR156* mediated up-regulated mobile factor activating *miR156* transcription in stock stems. To analyze if mature *miR156* is transported, we carried out a quantitative analysis by stem-loop qRT-PCR. In stock stems of all four heterografts, a higher accumulation of mature *miR156* was observed as opposed to homografts (Figure 3.30 A). On the other hand, absence of the *miR156a* precursor transgene in heterograft stock stems confirmed that the over expressed transgene is not moving from scion to stock (Figure 3.30 B). Also, a comparative analysis of mature *miR156* and *miR156a* precursor levels in both WT and grafted plants clearly demonstrated that mature *miR156* had a higher accumulation than its precursor form (Figure 3.31 and 3.32). These findings make the possibility of *miR156a* precursor transgene movement as well as activated localized transcription of *miR156* in stock stems of heterografts unlikely. Instead, the higher accumulation of mature *miR156* in heterograft stock stems supports preferential transport of mature *miR156* itself, from scion to stock in grafted plants. Overall, our results suggest that *miR156* is a graft-transmissible phloem mobile signal that affects tuberization and plant architecture in potato.

3.3.13. Regulation of *miR156*- Upstream sequence analysis

To understand how *miR156* itself is regulated; we retrieved the upstream regulatory sequence of *miR156*. The upstream sequence (>chr07:1782100..1784700) was obtained from PGSC database [http://www.potatogenome.net (Potato Genome Sequencing Consortium., 2011)]. We performed bioinformatic analysis [PLACE software, (Higo et al., 1999)] for light regulatory motifs present in the upstream sequence as *miR156* shows photoperiod dependent accumulation pattern (section 3.3.1). The *miR156* upstream

sequence showed presence of characteristic light regulatory elements like GATA box, GT1 consensus etc indicating that *miR156* is under photoperiod regulation (Figure 3.33).

3.4. Discussion

3.4.1. *miR156* facilitates tuber formation under inductive conditions

miR156 function has been well documented in *Arabidopsis*, rice and maize with *miR156* over expression phenotypes studied in plants like tomato, switchgrass, poplar etc as mentioned before. *miR156* was reported to be present in potato, however, its function was not known. Based on its role in flowering pathway with another miRNA, *miR172*, we proposed that *miR156* might function in regulation of tuberization pathway. We observed that *miR156* accumulates at a higher level in SD induced stolons and *miR156* over expression gives rise to aerial tubers clearly indicating its role in tuberization pathway. Even though *miR156* over expression resulted in aerial tubers, the overall tuber yield decreased with reduced *miR172* and *StSP6A* levels (tuberization markers). Considering these observations, should *miR156* be termed as an activator or a repressor of tuberization? If *miR156* would act as an activator, *miR156* OE lines would have produced tubers under LD (non-inductive conditions) as previously observed for *St*BEL5 (Banerjee et al., 2006a), *miR172* (Martin et al., 2009) and *St*SP6A (Navarro et al., 2011) over expression lines. In our study, *miR156* OE lines produced aerial tubers in SD conditions (Figure. 3.12 B). This rules out the possibility of *miR156* functioning as a repressor. The reduced levels of tuberization markers in *miR156* OE lines can possibly be due to the prolonged juvenile phase of these plants, which in turn reduced the overall tuber yield. In potato, all axillary meristems have the capacity to form tubers, and under permissive conditions any meristem can produce aerial tubers. However, this potential is suppressed except in stolons (Xu et al., 1998b). We proposed that under tuber inductive conditions, a threshold level of *miR156* facilitates tuber formation from a meristem. Over expression of *miR156* in potato results in levels above threshold in all the axillary meristems and hence, the plant produces aerial tubers under SD conditions. When *miR156* is over expressed, the OE plants produced aerial tubers only under SD conditions, whereas in LD conditions, the axillary meristems produced only branches. This observation clearly established that increased levels of *miR156* in OE plants alone are not sufficient for tuber formation but that tuber inductive conditions are required for aerial tuber formation. *miR156*-SPL-*miR172* module which plays a role in phase transitions in flowering in *Arabidopsis*, rice and maize also appeared to function in tuber formation as demonstrated by EMSA and

rSPL9 studies. This regulatory module is likely to be active in leaves induced under LD, as there are high levels of *miR156* but reduced levels of *SPL9* and *miR172*. Whereas, an increased accumulation of *miR156* and *miR172* in SD induced stolons reflects lack of regulation of *miR172* by *miR156*, possibly due to tissue specific action of *miR156* or spatial exclusion.

3.4.2. *miR156* over expression affects multiple morphological traits

Other than tuberization pathway, *miR156* over expression affected many developmental processes like leaf architecture and development, flowering, root phenotype, branching etc, which was also observed in tobacco plants highlighting that *miR156* acts as a master regulator of plant development. How does *miR156* affect all these changes in the plant? Target prediction studies revealed that *miR156* targets Squamosa Promoter binding Like Transcription factors (SPLs). We validated five of the predicted SPLs to be true *miR156* targets in planta (Figure 3.23 and 3.24). The altered leaf morphology in OE plants can possibly be a result of reduced levels of *SPLs*. A number of previous reports (Wu and Poethig, 2006; Shikata et al., 2009; Usami et al., 2009; Chen et al., 2010) have described the role of SPLs in leaf development in *Arabidopsis*, suggesting *StSPLs* might control leaf size and shape, altered venation and reduced leaflet number in potato as well. LG1 is a well characterized SPL Protein, whose function in leaf development has previously been reported in maize (Harper and Freeling, 1996) and rice (Lee et al., 2007). It was shown to be involved in controlling ligule and auricle development and the formation of a laminar joint between leaf blade and leaf sheath. In our study, reduced *StLG1* expression in *miR156* OE plants could possibly explain the aberrant leaf morphology (reduced leaf lamina, curled leaf margins). To understand the cause of the profuse branching phenotype of *miR156* OE plants in potato, we quantified the amounts of cytokinin and strigolactone, hormones that are known to play an important role in branching (Domagalska and Leyser**,** 2011). Reduced cytokinin leaves possibly resulted in profuse branching phenotype. On the other hand, in *Arabidopsis*, strigolactone mutants show increased branching (Gomez-Roldan et al., 2008). In our study as well, *miR156* OE plants contained reduced amounts of orobanchyl acetate (Figure. 3.15 B). The absence of flowering in both potato and tobacco OE plants supports the role of *miR156* in controlling phase transitions. In *Arabidopsis*, *At*SPL2, *At*SPL3, *At*SPL9, *At*SPL10 & *At*SPL11 are shown to act as positive regulators in promoting floral meristem identity by directly regulating genes like LEAFY, FRUITFUL, APETALA 1 (Chen et al., 2010). A

similar mechanism might also be conserved in potato, since *StSPL3* and *StSPL9* are found to be reduced in *miR156*OE plants (Figure. 3.24 A). *miR156* expression analysis demonstrated its age dependent accumulation pattern (as reported before in *Arabidopsis* and rice) but we demonstrated that *miR156* also shows a photoperiod dependent pattern. This was consistent with the LREs found in the *miR156* upstream sequence (Figure 3.33).

3.4.3. *miR156* is potentially a mobile signal in potato

Presence of *miR156* in phloem of different plant species like pumpkin, *Arabidopsis,* apple and *Brassica napus* prompted us to investigate *miR156* mobility in potato. Detection of *miR156* in LMPC harvested phloem cells of potato and an increased accumulation in phloem exudates under SD photoperiod suggests that *miR156* could possibly act as a long distance signal in potato development. Our grafting studies supports this hypothesis with further molecular analysis that mature *miR156* is a graft-transmissible tuberization signal. Although a handful of microRNAs have now been detected in phloem of several plant species such as pumpkin (Yoo et al., 2004), *Arabidopsis* (Varkonyi-Gasic et al., 2010), Brassica (Buhtz et al., 2008) etc., only three miRNAs-*miR399, miR395* and *miR172* (Pant et al., 2008; Buhtz et al., 2010; Kasai et al., 2010) were demonstrated to act as long-distance mobile signals. We show that *miR156* is involved in the regulation of plant architecture and tuberization and might be another microRNA to be transported via the phloem over long distances. Availability of techniques to differentiate between mature endogenous miRNA from transgenic miRNAs would perhaps provide the final evidence for miRNA mobility.

Based on our results, we propose a model for the regulation of tuberization by *miR156* (Figure 3.34). We hypothesize that under tuber inductive (SD) conditions, *miR156* is transported to stolons through the phloem, accumulates in underground stolons (which in turn reduces the *miR156* accumulation in leaves and stems), and facilitates underground tuber formation. Reduced *miR156* accumulation in aerial organs inhibits the formation of aerial tubers. Whereas in LD conditions, increased levels of *miR156* in leaves and stems assist the vegetative growth of the plant. *miR156* exerts this effect presumably through a *miR156* - SPL9 - *miR172* regulatory module and possibly arrests tuberization under LD conditions. It appears that *miR156* has a different function in SD and LD photoperiods. We also cannot rule out the possibility that the high accumulation of *miR156* in SD induced stolons is associated with controlling tuber transitions, maintenance of the

juvenile phase, or even tuber dormancy. Future research work will help to elucidate the additional functions of *miR156* in potato.

In summary, the results of the current study led us to conclude that

(i) *miR156* expression is dependent on plant age and SD-LD photoperiod.

(ii) *miR156* over expression affects multiple phenotypic traits in potato by targeting SPL TFs. It acts as a master regulator of various developmental pathways in potato.

(iii) *miR156* facilitates tuber formation under SD tuber inductive conditions.

(iv) EMSA analysis confirmed that *miR156-St*SPL9-*miR172* module is conserved in potato.

(v) *miR156* acts as a potential phloem-mobile long distance signal affecting plant architecture.

Collectively, these results suggest that *miR156* is a graft-transmissible signal that affects plant architecture and tuber formation in potato.

This work was published in Plant Physiology (2014), Vol 164: 1011-1027.

Bhogale S, Mahajan AS, Natarajan B, Rajabhoj M, Thulasiram HV, Banerjee AK (2014) ***MicroRNA156*: a potential graft-transmissible microRNA that modulates plant architecture and tuberization in *Solanum tuberosum* ssp. *andigena*.** *Plant Physiology*, 164:1011-1027.

Chapter 3

Figures

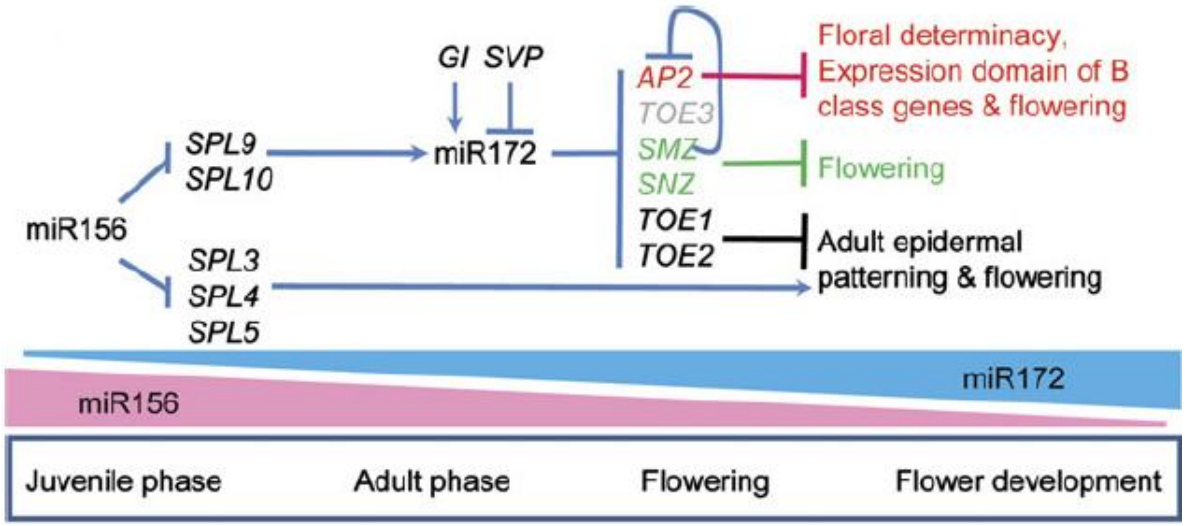

Figure 3.1. Model for regulation of vegetative to adult phase change by sequential action of *miR156* and *miR172*. Temporal changes in the levels of *miR156* and *miR172* (time increases from left to right). *miR156* is required for maintaining the juvenile phase of the plant while high levels of *miR172* are required for adult phase and flowering. *miR172* is in turn regulated by *miR156* via SPL9/10. (adapted from Zhu and Helliwell, 2010)

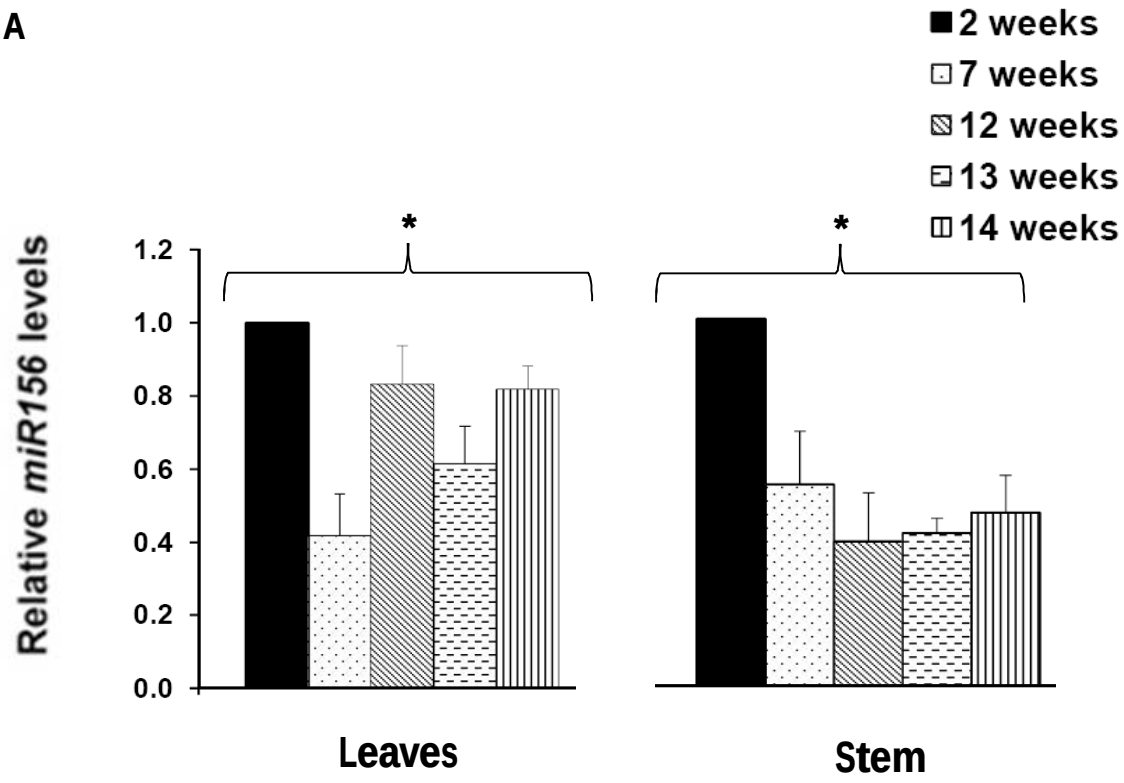

Figure 3.2. Age dependent expression analysis of *miR156* in *Solanum tuberosum* ssp *andigena*. A, Age specific *miR156* abundance in leaves and stem of WT potato grown under LD photoperiod. Error bars indicate (±) SD of two biological replicates each with three technical replicates. Asterisk indicates one factor ANOVA (* as $P<0.05$).

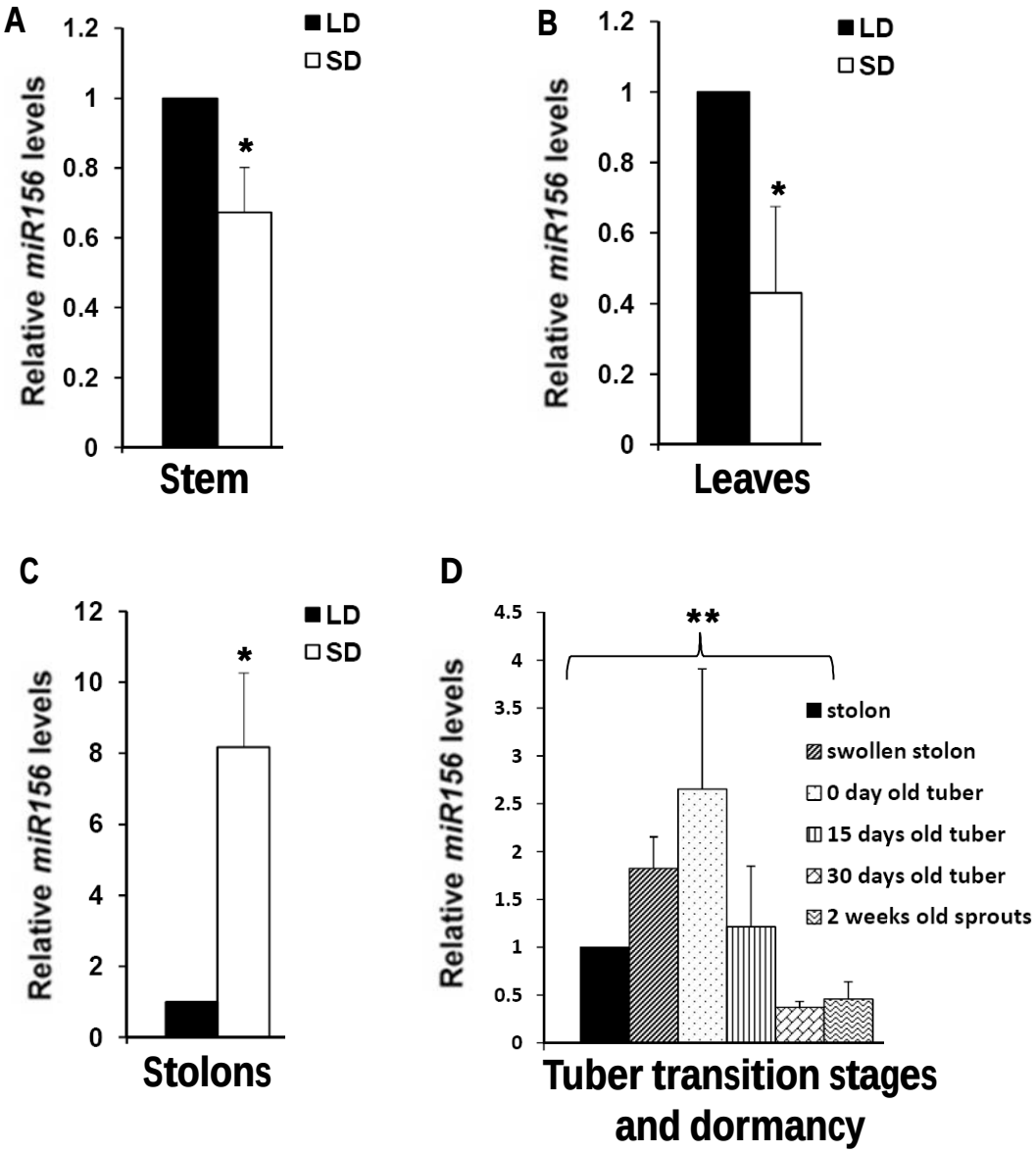

Figure 3.3. Expression analysis of *miR156* in *Solanum tuberosum* ssp *andigena*. A to C, *miR156* abundance in stem **(A)**, leaves **(B)** and stolons **(C)** of WT potato grown under LD and SD photoperiods for 15 days post induction (dpi). Error bars indicate (±) SD of three biological replicates each with three technical replicates. Asterisk indicates Student's t test (* as P<0.05). **D,** Relative abundance of *miR156* in different developmental stages of tuber formation and dormancy. Error bars indicate (±) SD of three biological replicates each with three technical replicates. Asterisks indicate one factor ANOVA (** as P<0.01).

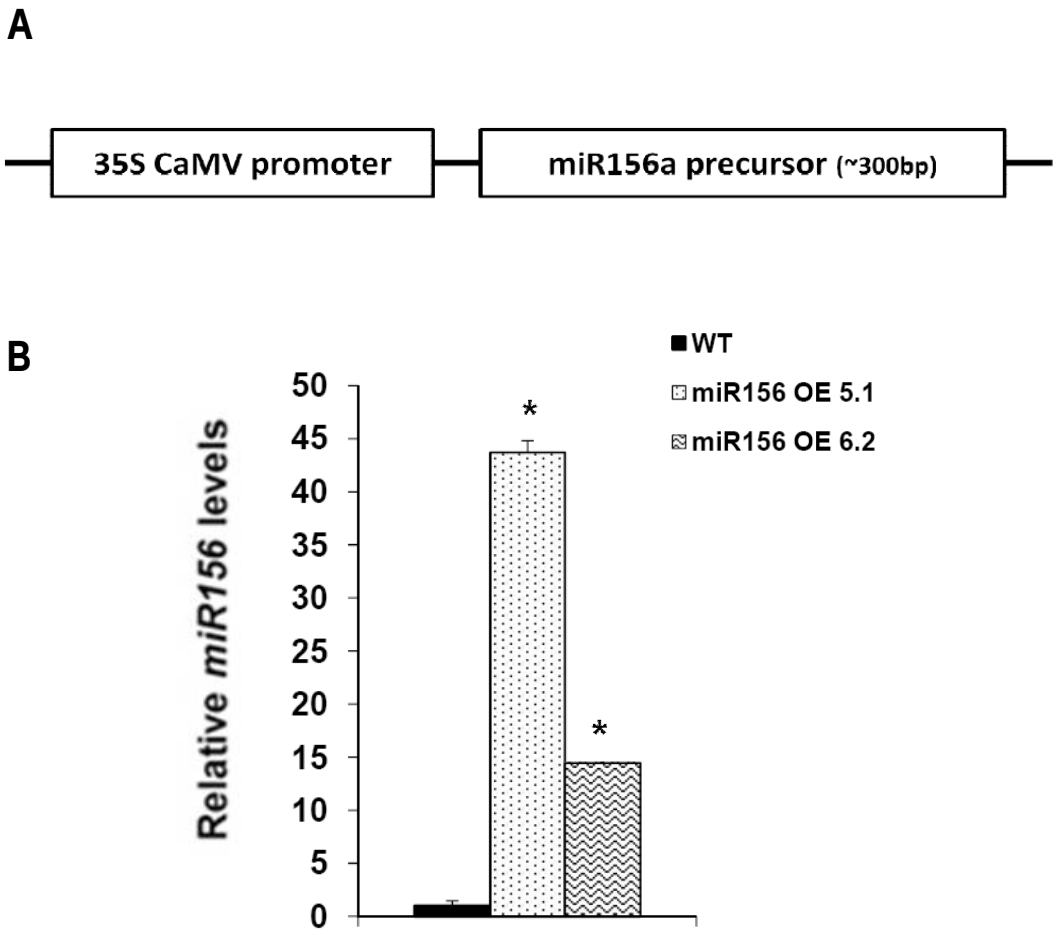

Figure 3.4. *miR156* over expression in potato. A, Diagrammatic representation of *miR156* over expression construct. **B,** Relative levels of *miR156* in WT, *miR156* OE 5.1 and *miR156* OE 6.2. Error bar indicates (±) SD of one biological replicate with three technical replicates. Asterisk indicates statistical difference as determined using Student's t test (* as $P<0.05$)

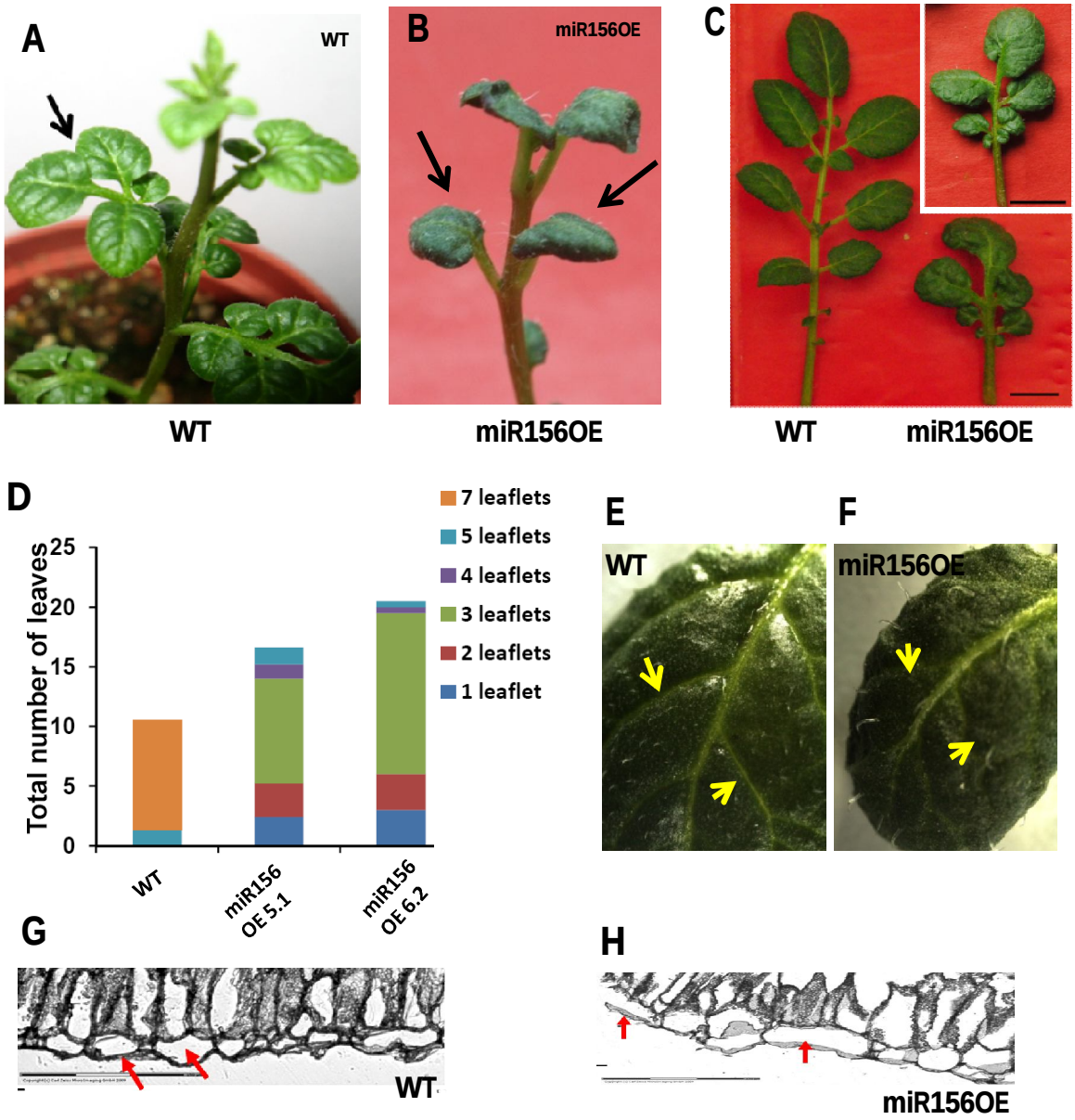

Figure 3.5. Effect of *miR156* over expression on leaf development of *Solanum tuberosum* ssp *andigena*. A and B, Two week old plants of WT (A) and *miR156* OE 5.1 (B). **C,** Leaf of eight week old plants of WT and *miR156* OE 5.1 and 6.2 (inset) (scale= 1 cm). **D,** Distribution of number of leaflets per leaf in eight week old plants of WT and *miR156* OE 5.1 and 6.2. **E and F,** Venation pattern of WT leaf (E) and *miR156* OE 5.1 leaf (F). **G and H,** Transverse sections of leaves (20X) of WT (G) and *miR156* OE 5.1 (H) showing difference in leaf architecture. The epidermal cells are marked by arrows.

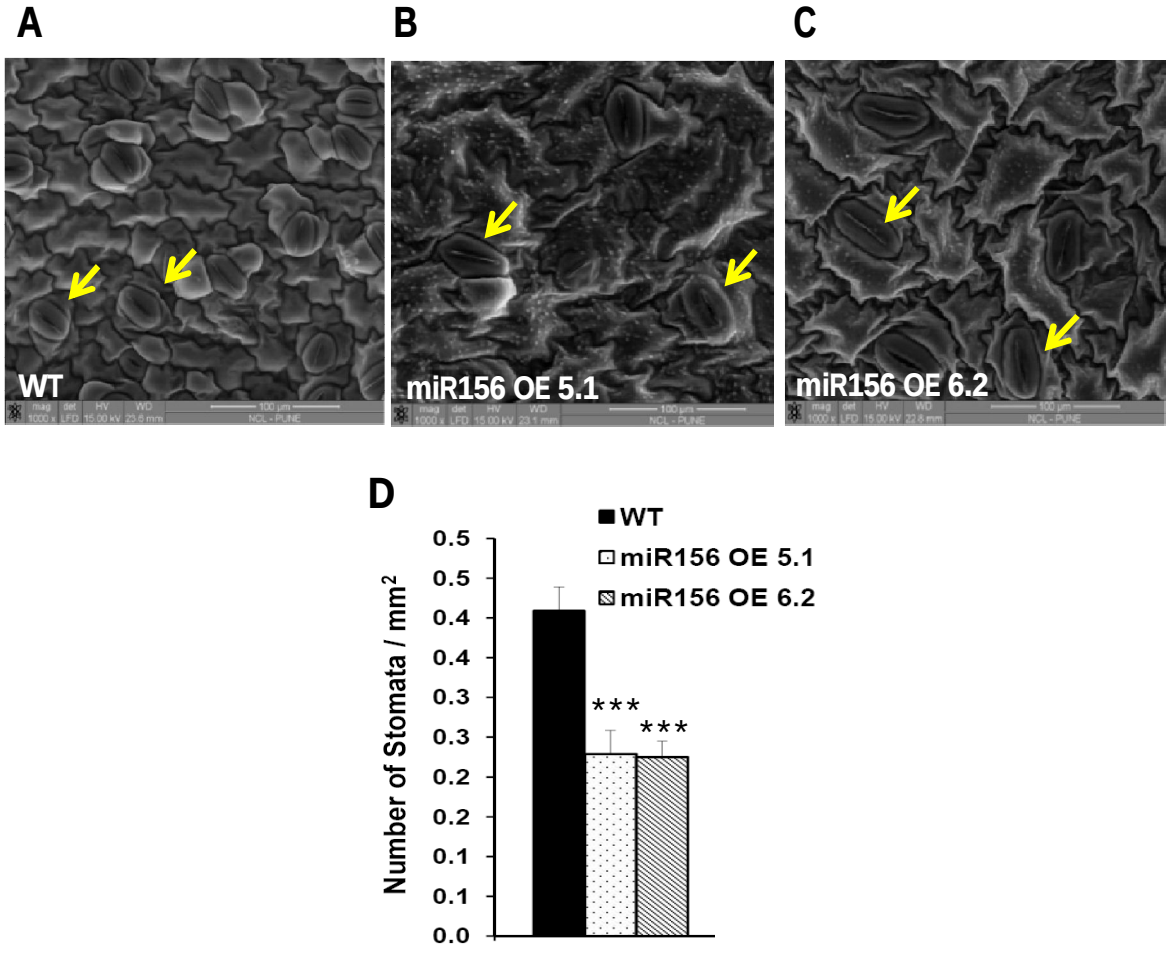

Figure 3.6. Effect of *miR156* over expression on stomatal development of *Solanum tuberosum* ssp *andigena*. A to C, eSEM images of leaf surface showing difference in the size of epidermal cells and stomata (marked by arrows) for WT (A) and *miR156* OE 5.1 (B) and *miR156* OE 6.2 (C) (scale= 100 µm). **D,** Stomatal density of WT and *miR156* OE 5.1 and 6.2 (n= 5). Error bars indicate SD. Asterisks indicate statistical differences as determined using Student's t test (*** as P<0.001).

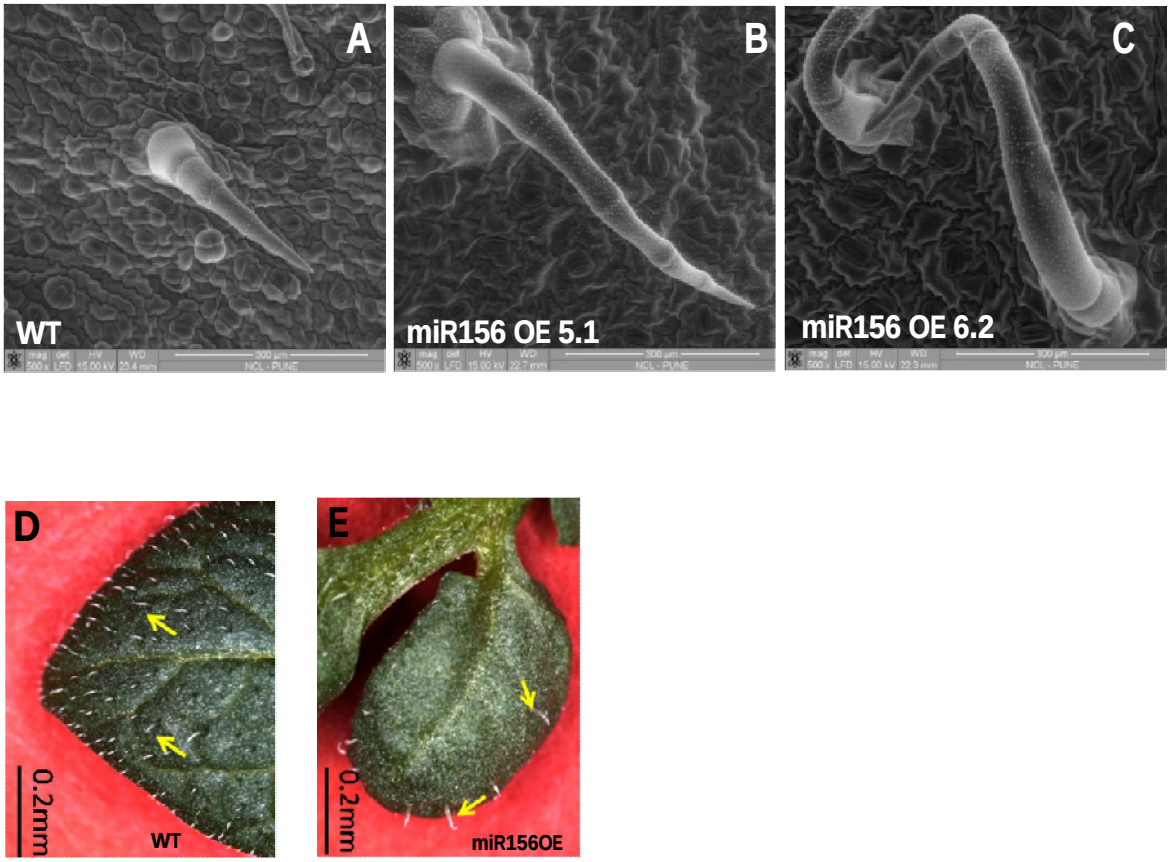

Figure 3.7. Effect of *miR156* over expression on trichome development of *Solanum tuberosum* ssp *andigena*. A to C, eSEM images of trichomes for WT (A) and *miR156* OE 5.1 (B) and *miR156* OE 6.2 (C) (scale= 300µm). **D and E,** Trichome phenotype of WT leaf (D) and *miR156* OE 5.1 leaf (E) (scale= 0.2 mm).

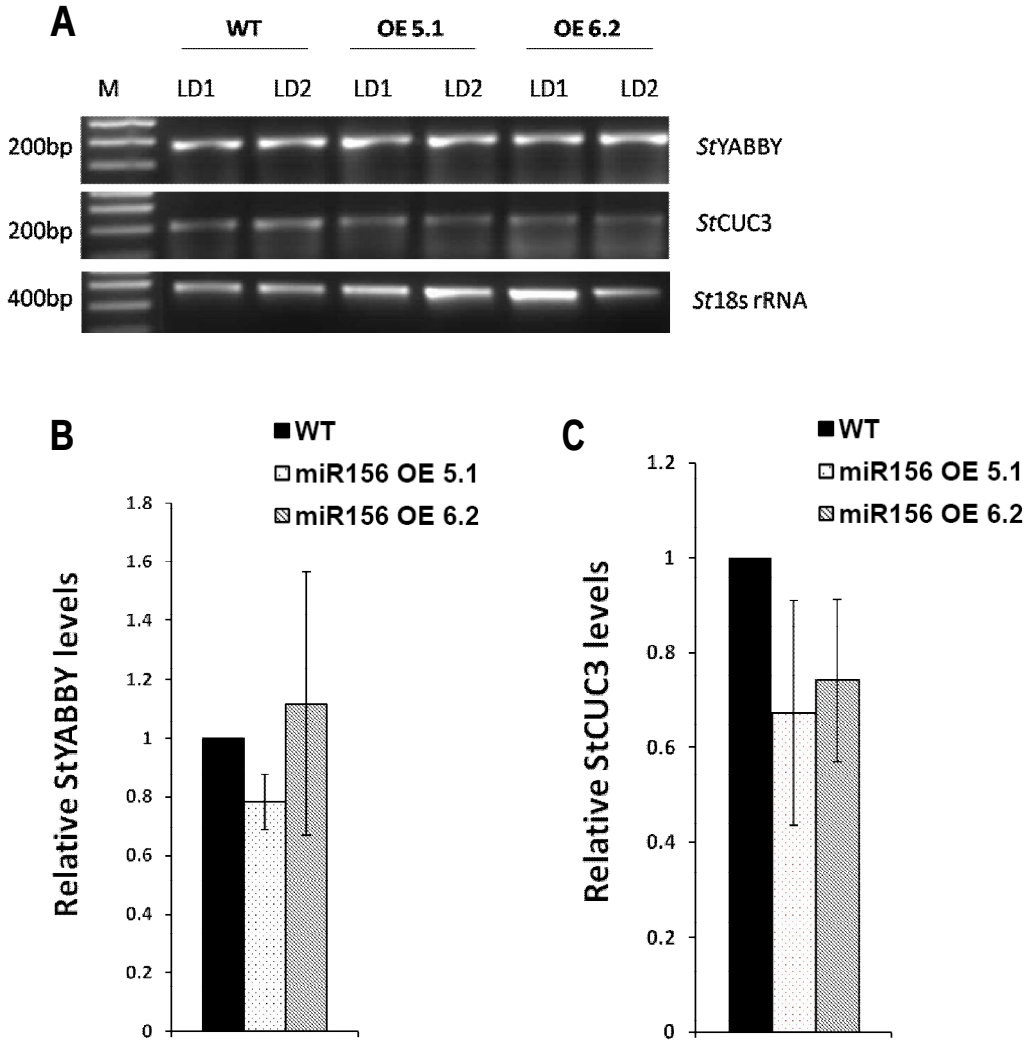

Figure 3.8. Effect of *miR156* over expression on *StCUC3* and *StYABBY* levels of *Solanum tuberosum* ssp *andigena*. A to C, Levels of leaf development markers, *StYABBY* and *StCUC3* levels in LD induced leaves of WT and *miR156* OE lines 5.1 and 6.2. Analysis was performed by semi-quantitative PCR with gel picture (A) and relative levels (B and C). Semi quantitative analysis was performed with two independent replicates. Error bars indicate (±) SD of two replicates.

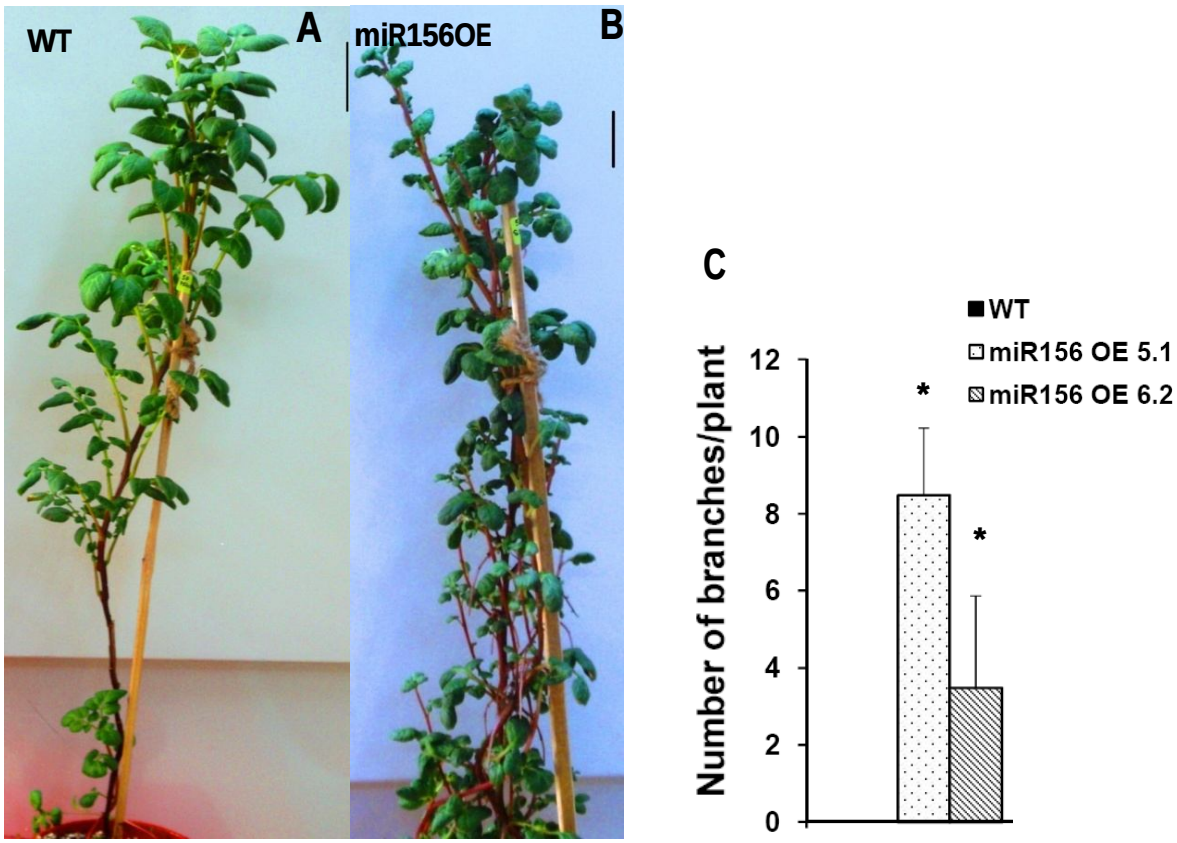

Figure 3.9. Over expression of *miR156* affects branching in *Solanum tuberosum* ssp *andigena*. A and B, Twelve week old plants of WT (A) and *miR156* OE 5.1 (B) lines of potato (scale= 5 cm). *miR156* OE plant shows bushy phenotype. **C,** Number of axillary branches (n=4) Error bars indicate SD. Asterisks indicate statistical difference as determined using Student's t test (*** as P<0.001, ** as P<0.01, * as P<0.05).

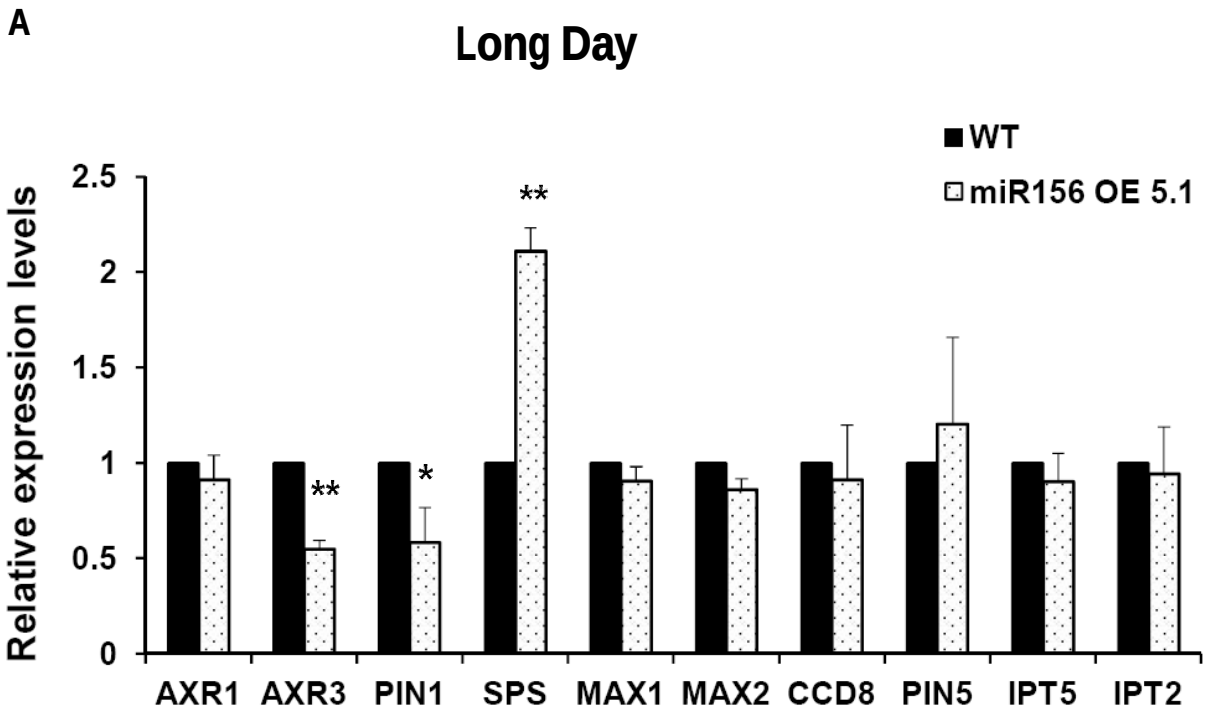

Figure 3.10. Analysis of genes involved in branching pathway (under LD conditions). **A** Relative levels of genes in WT and *miR156* OE 5.1 under LD photoperiodic conditions. Error bars indicate (±) SD of three biological replicates with three technical replicates. Asterisks indicate statistical difference as determined using Student's t test (* as P<0.05, ** as P<0.01, *** as P<0.001).
AXR1: AUXIN RESISTANT PROTEIN 1, AXR3: AUXIN RESISTANT PROTEIN 3, PIN1: PINHEAD 1, SPS: SUPERSHOOT, MAX1: MORE AXILLARY GROWTH 1, MAX2: MORE AXILLARY GROWTH 2
CCD8: CAROTENOID CLEAVAGE DIOXYGENASE, PIN5: PINHEAD 5, IPT5: ADENOSINE PHOSPHATE ISOPENTENYL TRANSFERASE 5, IPT3: ADENOSINE PHOSPHATE ISOPENTENYL TRANSFERASE 2.

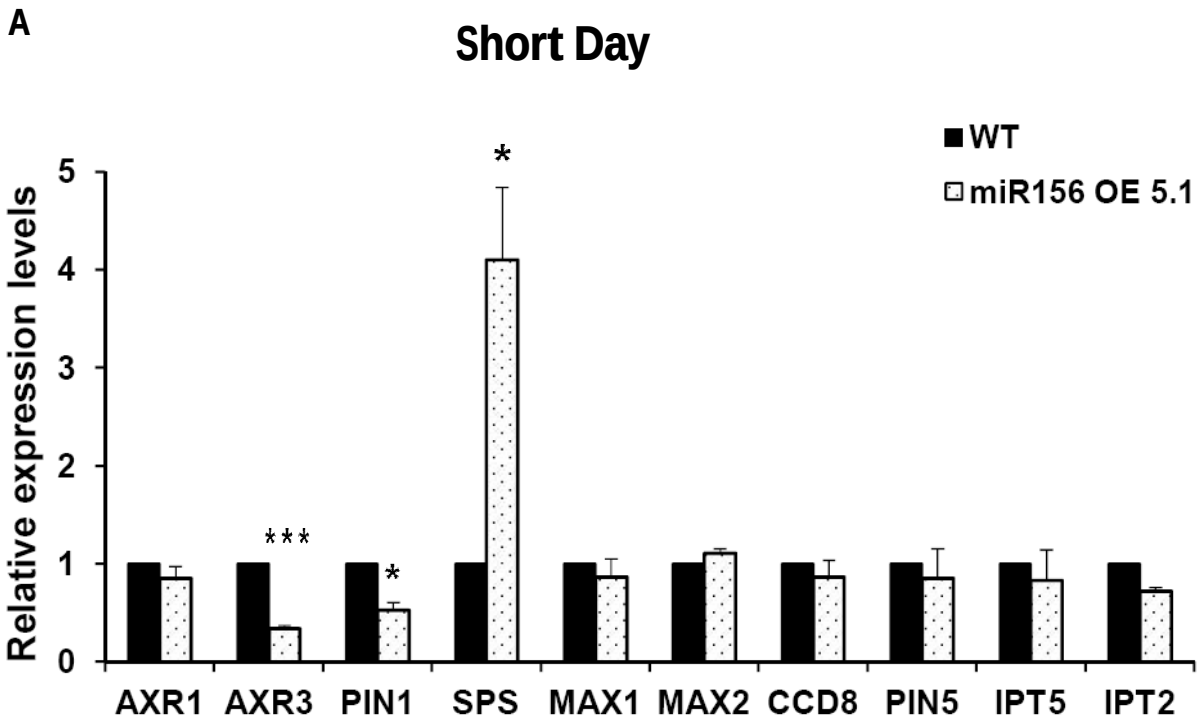

Figure 3.11. Analysis of genes involved in branching pathway (under SD conditions). **A** Relative levels of genes in WT and *miR156* OE 5.1 under SD photoperiodic conditions. Error bars indicate (±) SD of three biological replicates with three technical replicates. Asterisks indicate statistical difference as determined using Student's t test (* as P<0.05, ** as P<0.01, *** as P<0.001).
AXR1: AUXIN RESISTANT PROTEIN 1, AXR3: AUXIN RESISTANT PROTEIN 3, PIN1: PINHEAD 1, SPS: SUPERSHOOT, MAX1: MORE AXILLARY GROWTH 1, MAX2: MORE AXILLARY GROWTH 2
CCD8: CAROTENOID CLEAVAGE DIOXYGENASE, PIN5: PINHEAD 5, IPT5: ADENOSINE PHOSPHATE ISOPENTENYL TRANSFERASE 5, IPT3: ADENOSINE PHOSPHATE ISOPENTENYL TRANSFERASE 2.

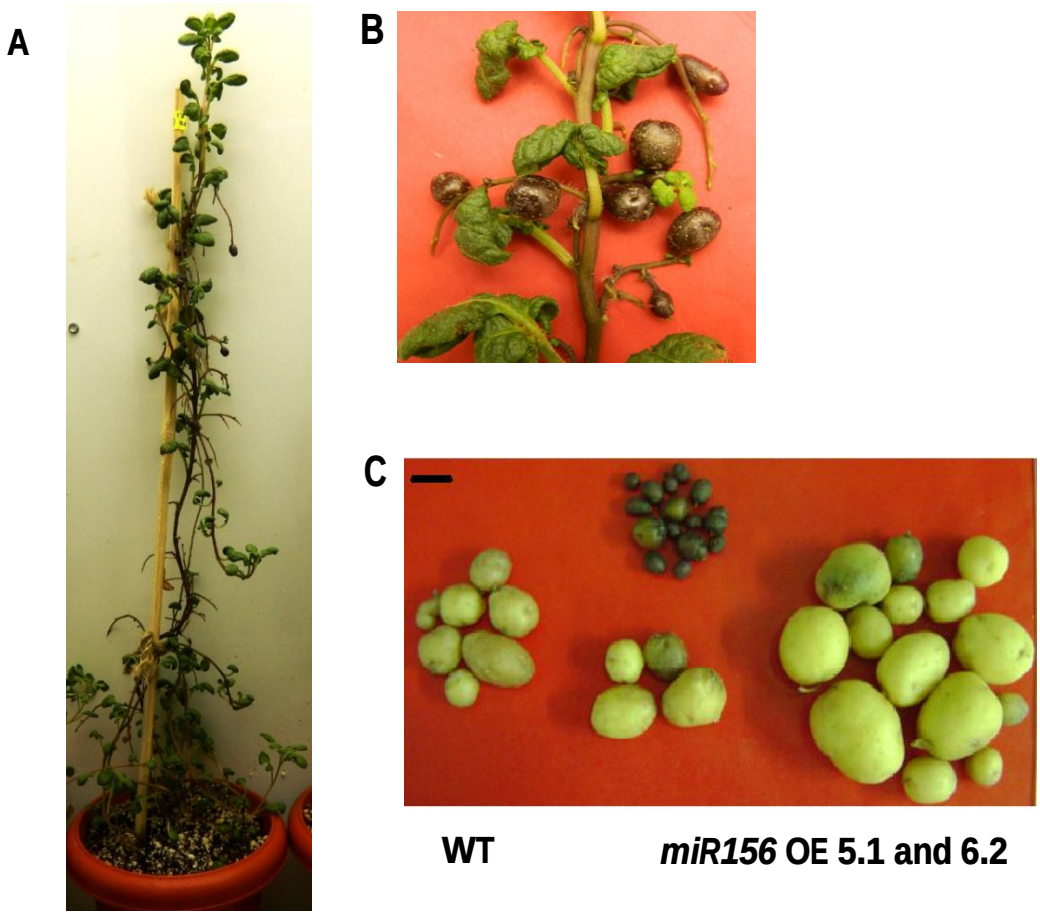

D

	Number of Tubers	Weight of tubers (g)
WT	13.0 ± 1.73	37.7 ± 2.75
miR156 OE 5.1	4.66 ± 1.15	5.83 ± 0.75
miR156 OE 6.2	7 ± 1.0	6.52 ± 2.55

Figure 3.12. *miR156* regulates potato tuberization in *Solanum tuberosum* ssp *andigena*. A, *miR156* OE 5.1 plant incubated for 30 days under SD conditions. **B,** Aerial tubers developed on the *miR156* OE 5.1. **C,** Tubers of a representative plant of WT and miR156 OE lines 5.1 and 6.2 (scale= 1 cm). **D,** For tuber yields (tuber number and weight), WT and miR156 OE 5.1 and 6.2 plants were incubated under SD for 30 days and mean of three plants each was calculated.

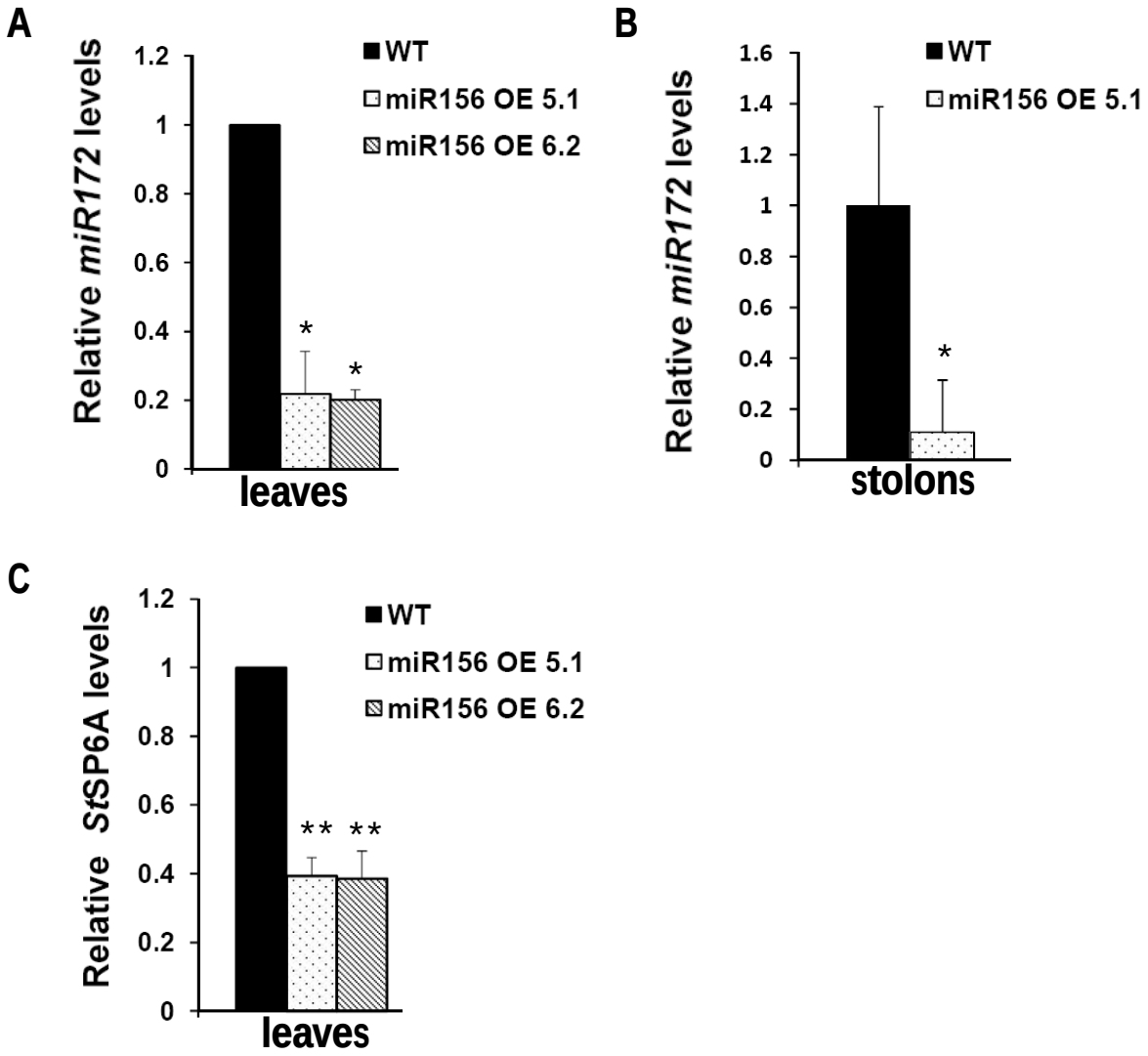

Figure 3.13. *miR156* regulates levels of *StSP6A* and *miR172* in *Solanum tuberosum*, miR172 in 8 days post SD induced leaves of WT and miR156 OE lines 5.1 & 6.2 (A); miR172 in 15 days post SD induced stolons of WT and miR156 OE lines 5.1 (B) and *St*SP6A in 8 days post SD induced leaves of WT and *miR156* OE lines 5.1 & 6.2 (C). For *miR172* in leaves (A), error bars indicate (±) SD of two biological replicates each with three technical replicates. For *miR172* in stolons (B) (15dpi in SD conditions), error bars indicate (±) SD of one biological replicate with three technical replicates. For *St*SP6A (C), semi quantitative analysis was performed with three independent replicates. Error bars indicate (±) SD of three replicates. Asterisks indicate statistical difference as determined using Student's t test (* as $P<0.05$, ** as $P<0.01$).

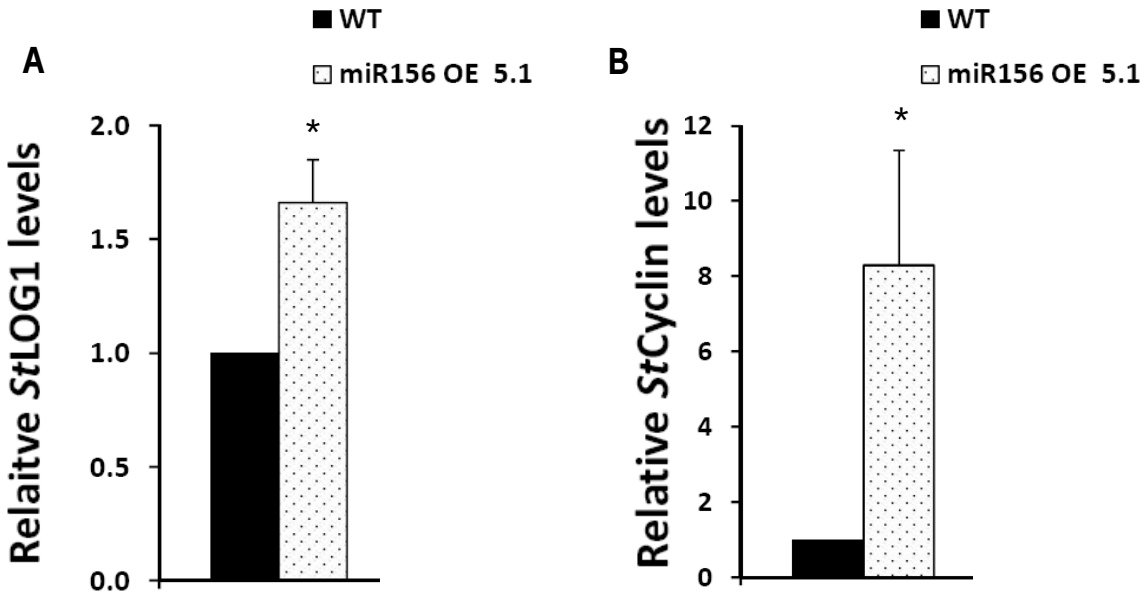

Figure 3.14. CK biosynthetic gene- *StLOG1* and responsive gene- *StCyclin D3.1* expression affected by *miR156* over expression. A and B, qRT-PCR analysis of *StLOG1* (A) and *StCyclin D3.1* (B) in axillary meristems of WT and miR156 OE 5.1 plants incubated for 15 days under SD conditions. Error bars indicate (±) SD of three biological replicates each with three technical replicates. Asterisks indicate statistical difference as determined using Student's t test (* as $P<0.05$).

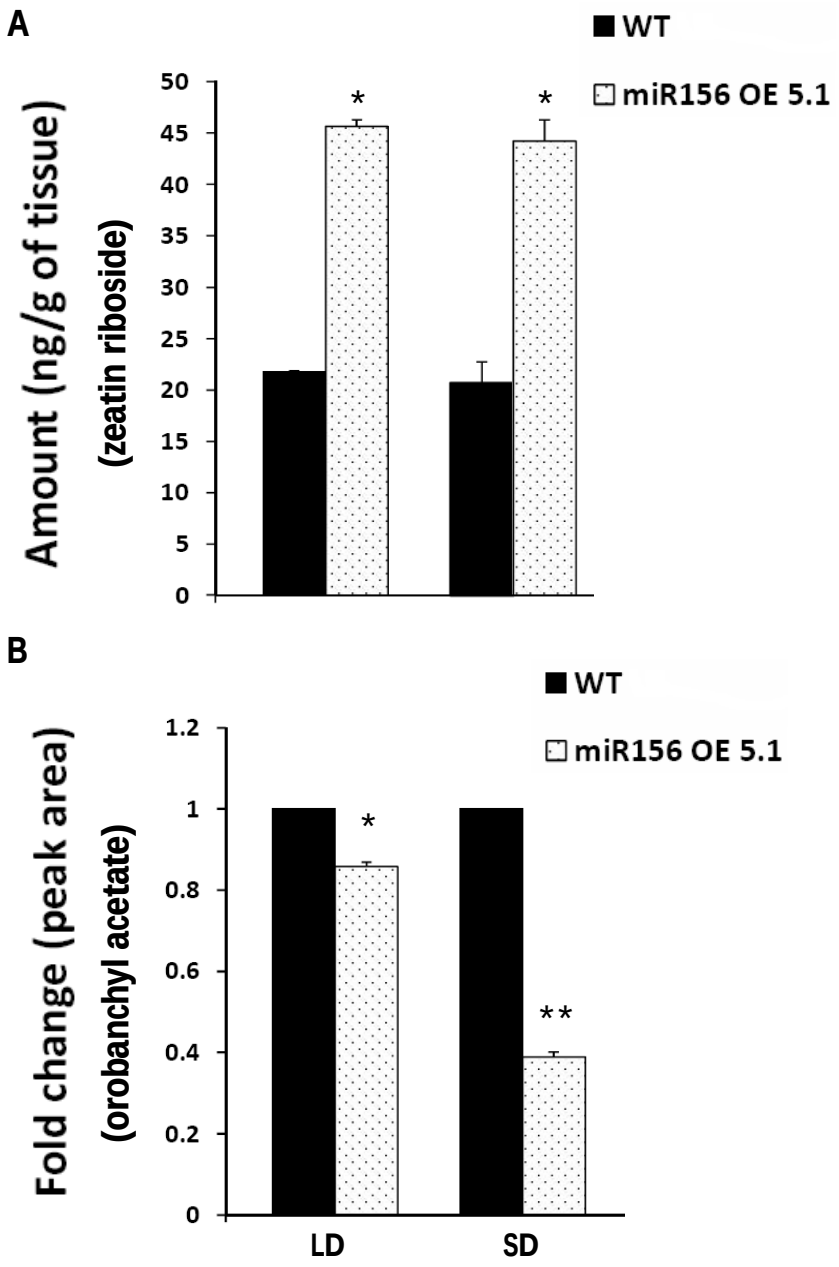

Figure 3.15. Zeatin riboside and orobanchyl acetate levels are affected by *miR156* over expression. A and B, HR-MS analysis of WT and *miR156* OE 5.1 plants for zeatin riboside (A) and orobanchyl acetate (B). Error bars indicate (±) SD of two biological replicates. Asterisks indicate statistical difference as determined using Student's t test (* as $P<0.05$, ** as $P<0.01$).

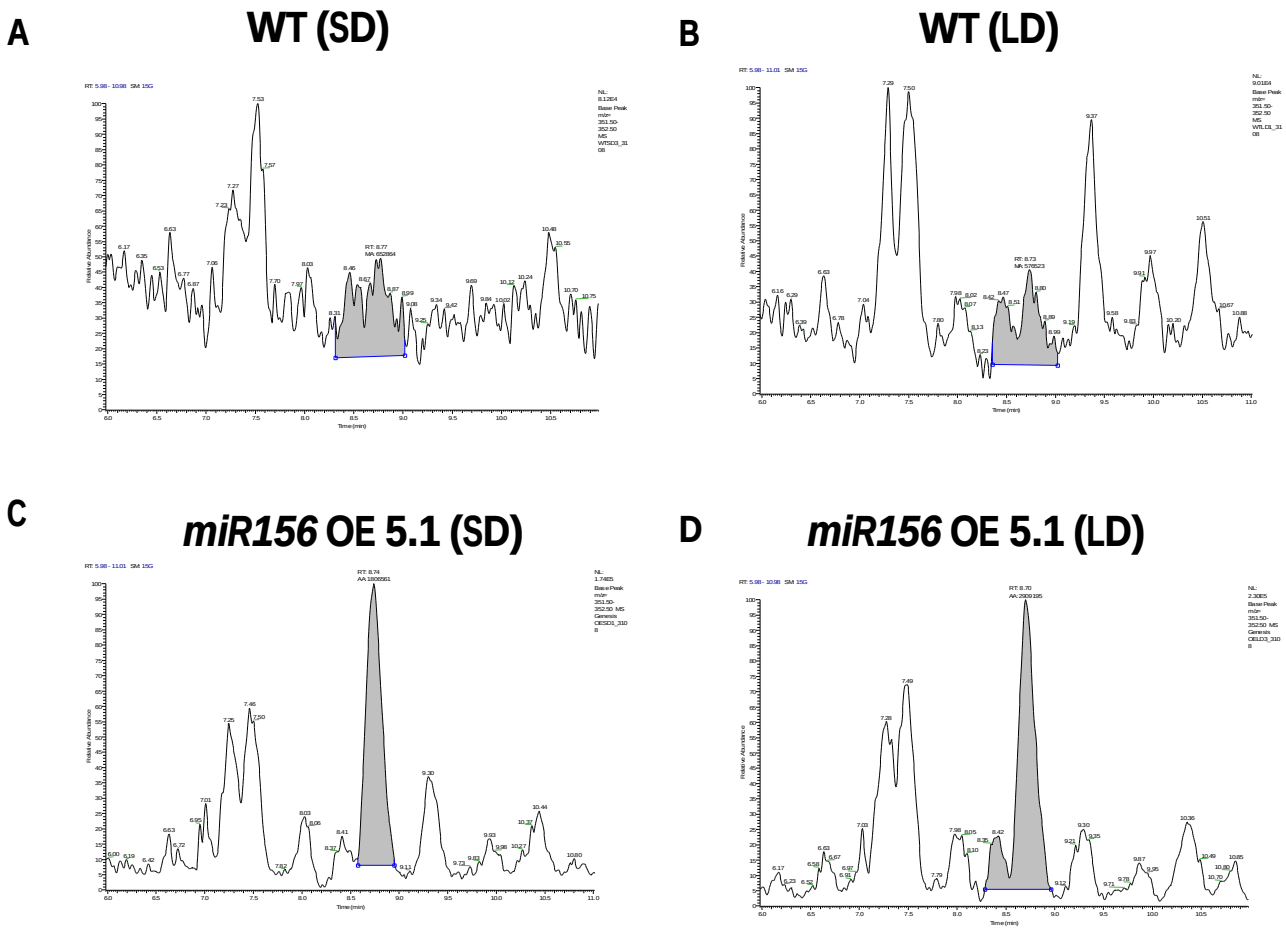

Figure 3.16. HR-MS of zeatin riboside. **A to D,** HR-MS chromatogram for zeatin riboside of WT and *miR156* OE 5.1 plants incubated under SD and LD conditions for 15 days. Axillary meristems of these plants were used for analysis. Chromatograms of representative samples are shown.

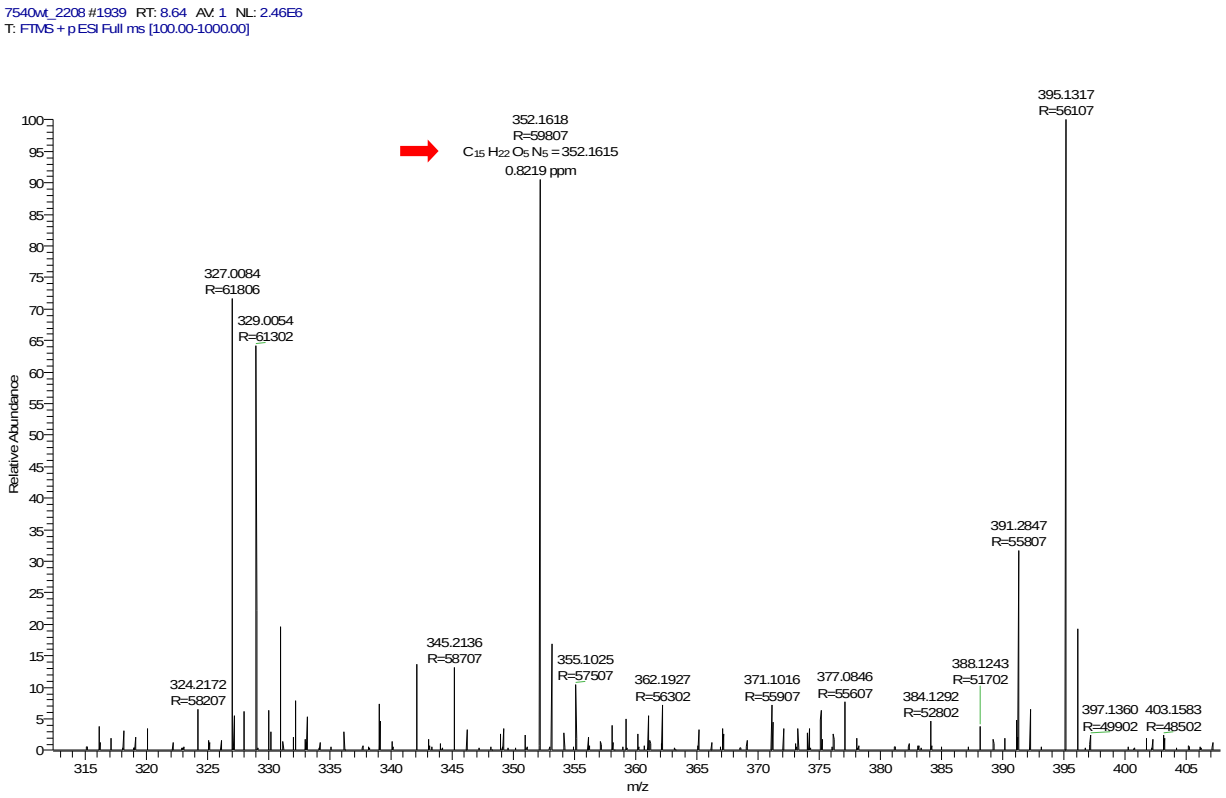

Figure 3.17. Mass spectrum of zeatin riboside ($C_{15}H_{22}O_5N_5$)

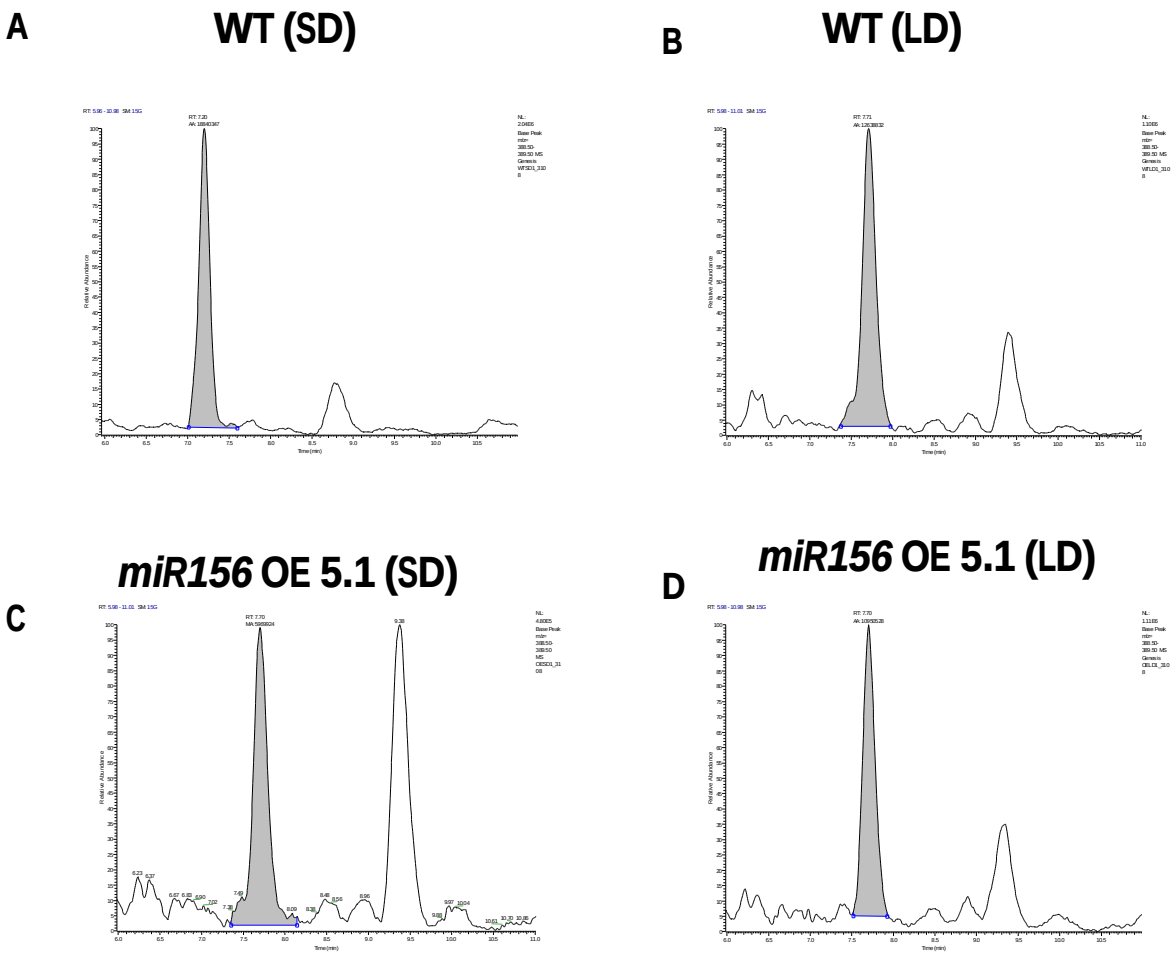

Figure 3.18. HR-MS of orobanchyl acetate. A to D, HR-MS chromatogram for orobanchyl acetate of WT and *miR156* OE 5.1 plants incubated in SD and LD conditions for 15 days. Axillary meristems of these plants were sampled. Chromatograms of representative samples are shown.

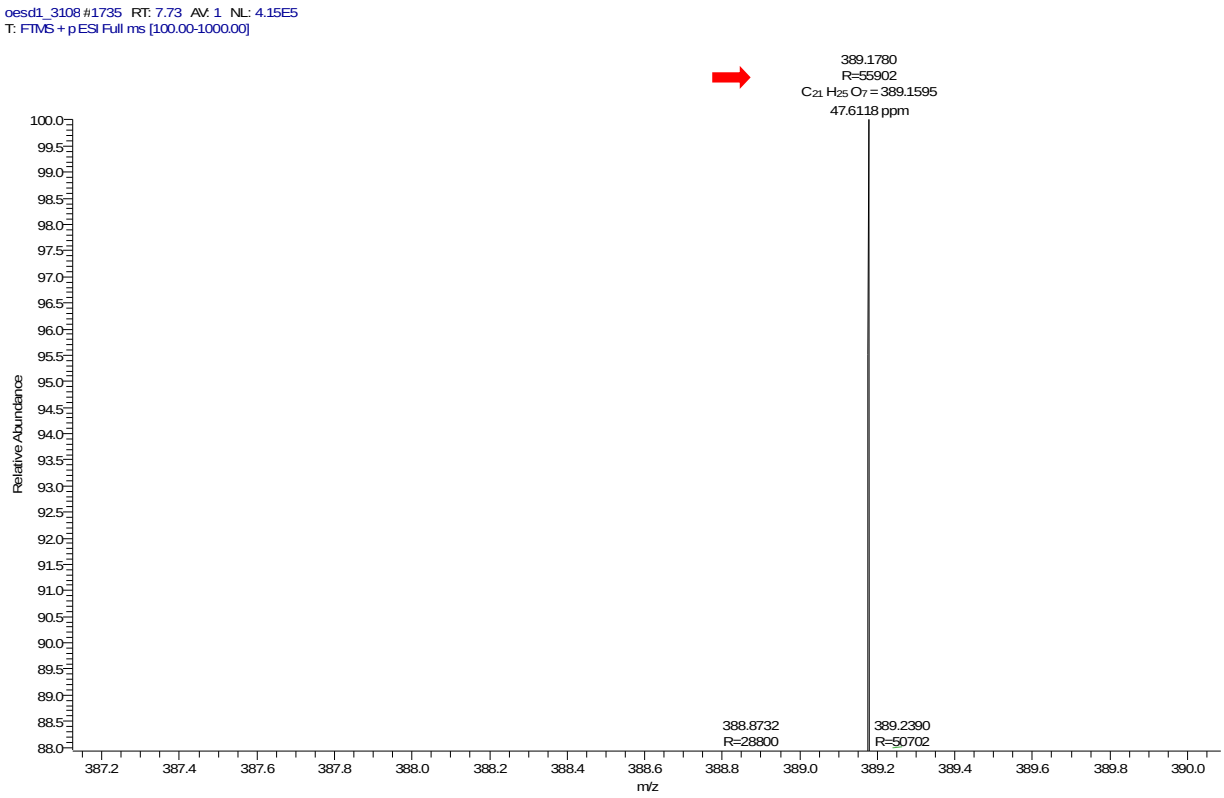

Figure 3.19. Mass spectrum of orobanchyl acetate ($C_{21}H_{25}O_7$)

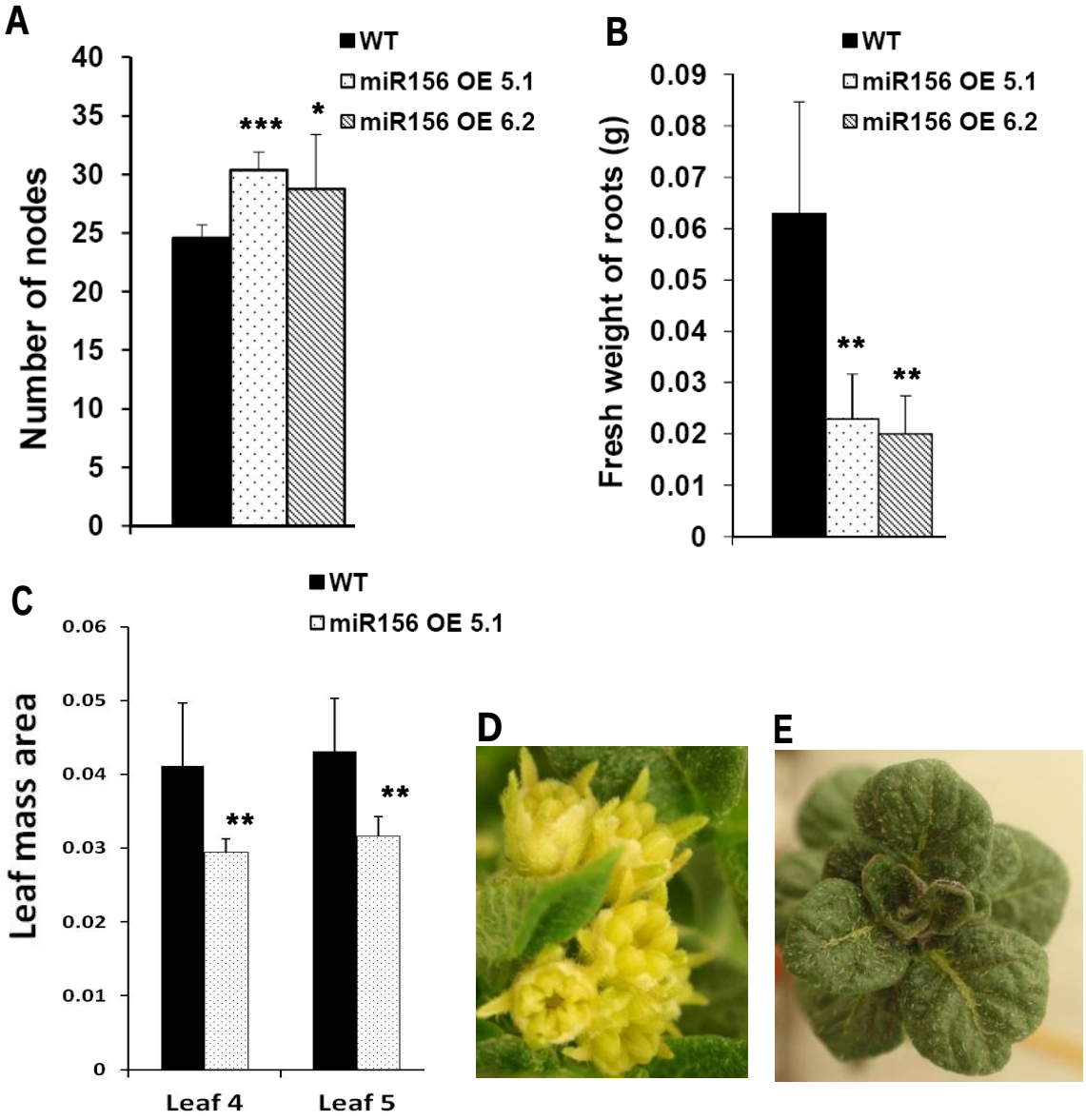

Figure 3.20. *miR156* over expression affects other traits in potato. A, Number of nodes (n= 5); **B,** Fresh weight of roots of WT and *miR156* OE lines (n=6). Error bars indicate SD. Asterisks indicate statistical difference as determined using Student's t test. **C,** Leaf mass area (LMA) analysis of leaf 4 and leaf 5 of WT and miR156 OE 5.1 (n=6). Error bars indicate SD. Asterisks indicate statistical difference as determined using Student's t test (*** as P<0.001, ** as P<0.01, * as P<0.05). **D and E,** Inflorescence produced at the apical tip of the twelve week old WT potato plants (A) while *miR156* OE 5.1 plants of same age produced leaves (B).

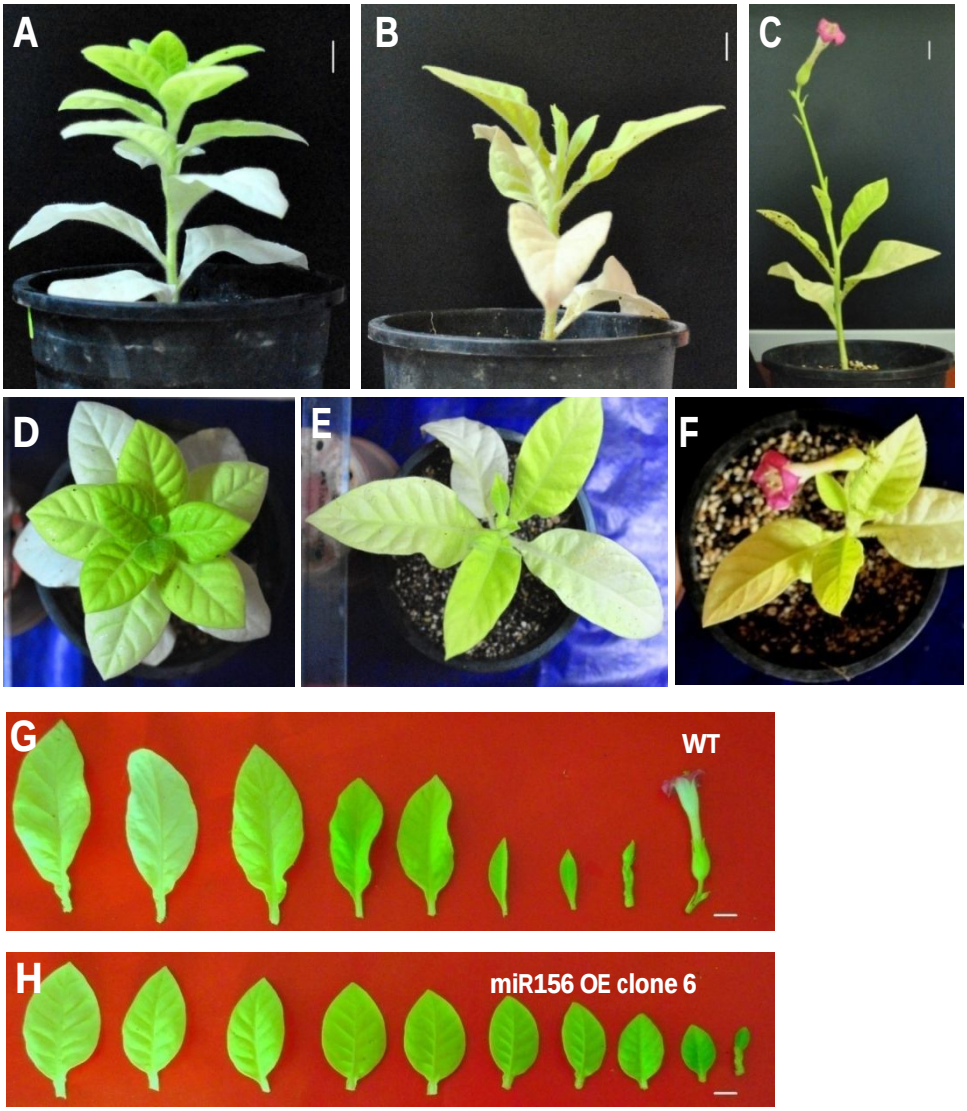

Figure 3.21. Over expression of *miR156* in tobacco. A-F, Twelve week old plants of WT (A-C) and *miR156* OE clone 6 (D-F). **G and H,** Changes in leaf morphology of WT (G) and *miR156* OE clone 6 (H). Also, the WT plant produces flowers (G) as opposed to OE line which continues to produce leaves (H).

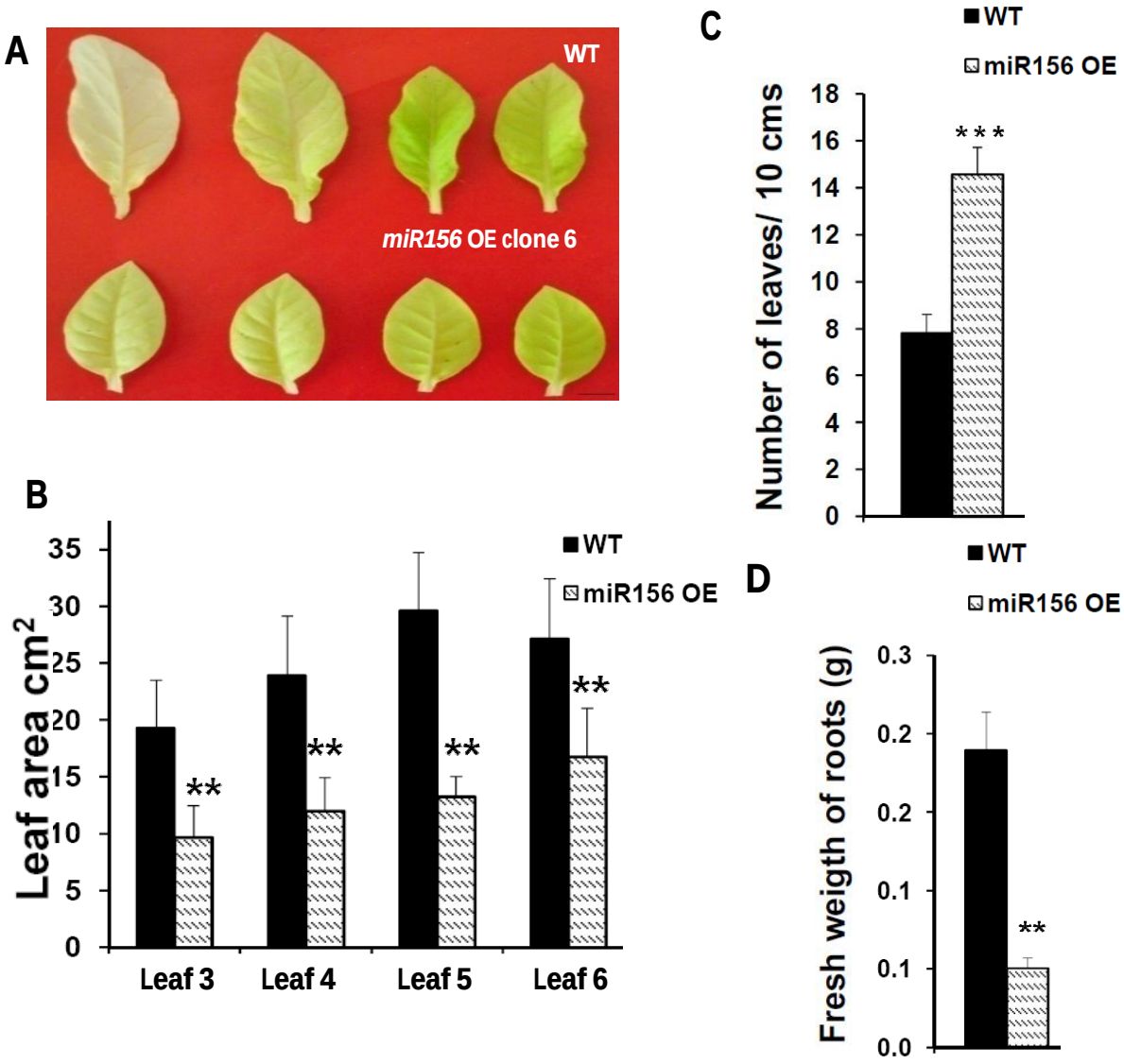

Figure 3.22. Over expression of *miR156* in tobacco (contd.) . A to C, *miR156* OE clone 6 produces more number of leaves (C) with reduced size (A and B) as compared to WT. **D,** Fresh weight of roots of WT and *miR156* OE line 6 (n=3). Asterisks indicate statistical difference as determined using Student's t test (** as P<0.01, *** as P<0.001).

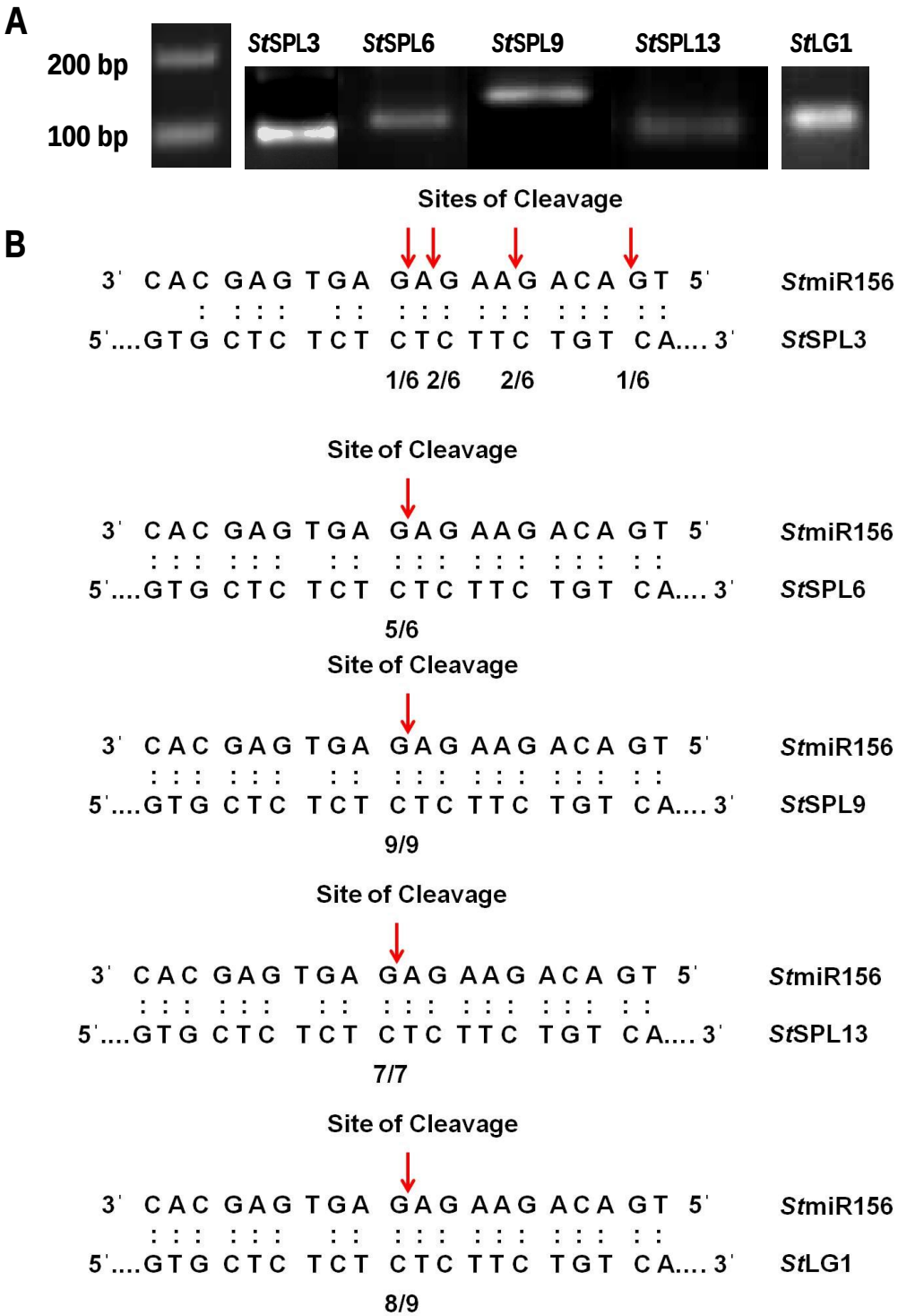

Figure 3.23. *miR156* targets SPL TFs. A to F, *miR156* cleavage site mapping in *miR156* targets as determined by modified RLM RACE. (A). Frequency of 5' RACE clones showing cleavage site (arrows) and fractions indicating proportions of clones showing these cleavage sites. *St*SPL3 (B), *St*SPL6 (C), *St*SPL9 (D), *St*SPL13 (E) and *St*LG1 (F).

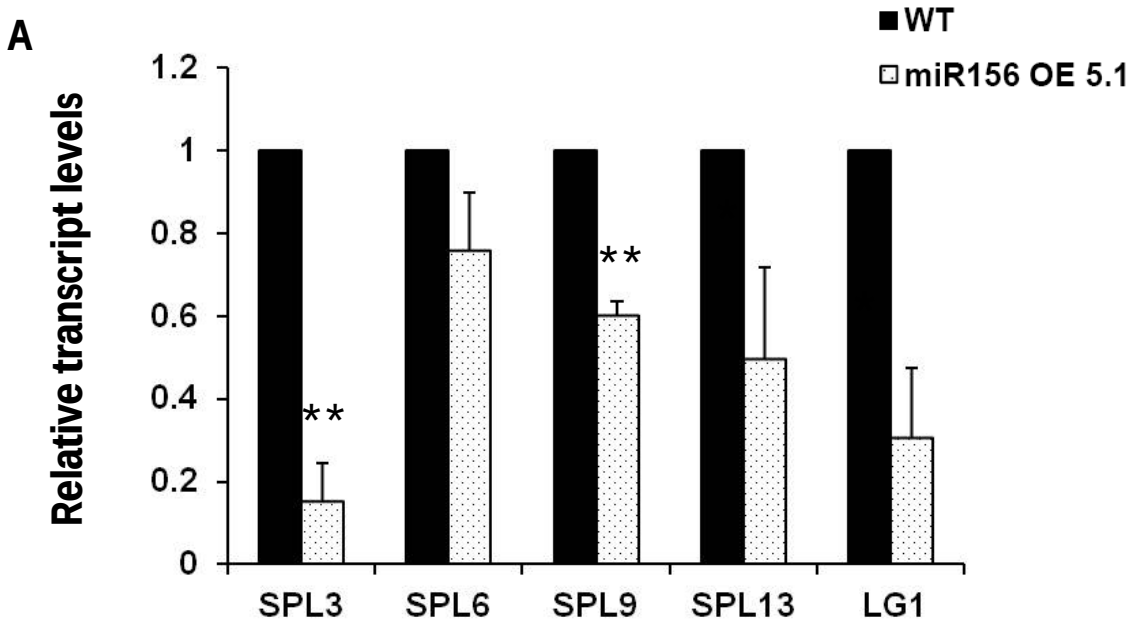

Figure 3.24. *miR156 overexpression* reduces target genes levels in *Solanum tuberosum* ssp *andigena*. A, Expression pattern of *StSPL3*, *StSPL6*, *StSPL9*, *StSPL13* and *StLG1* in WT and *miR156* OE 5.1 by qRT-PCR. Error bars indicate (±) SD of three biological replicates each with three technical replicates. Asterisks indicate statistical difference as determined using Student's t test (* as $P<0.05$, ** as $P<0.01$).

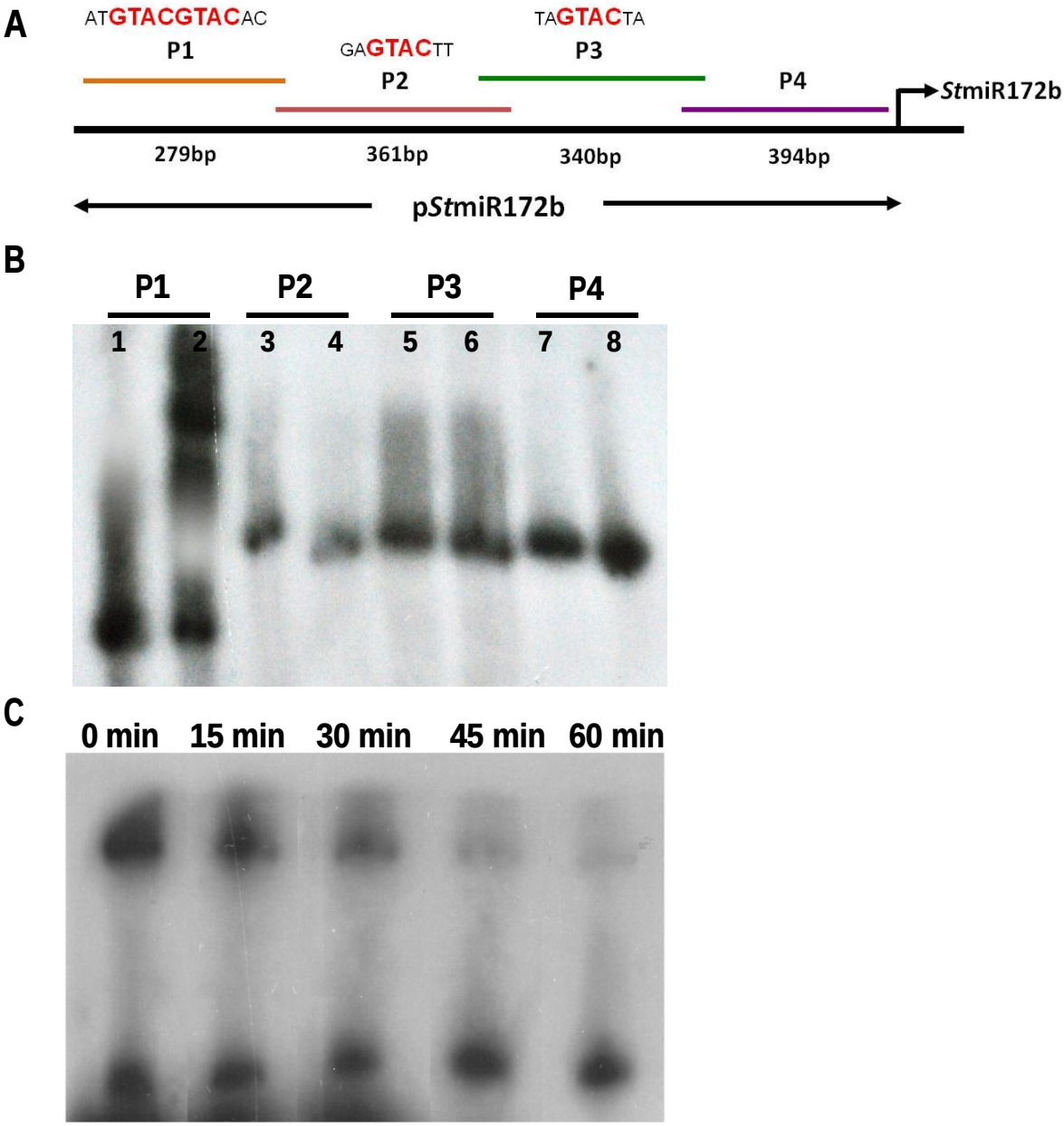

Figure 3.25. ***St*SPL9 binds to *St*MIR172b promoter. A,** The schematic representation of *St*MIR172b promoter sequence showing SPL binding motifs and lengths of four fragments. **B,** Gel retardation assay of *St*MIR172b promoter fragments P1 to P4 with *St*SPL9. The lanes are alternate for free probe and probe + protein. **C,** Cold competition retardation assay of P1 with *St*SPL9. Labeled P1 was incubated with *St*SPL9 for 30 min at 25^{o} C and then 500 fold molar excess of unlabeled P1 was added and aliquots were analyzed after indicated time (0-60 min).

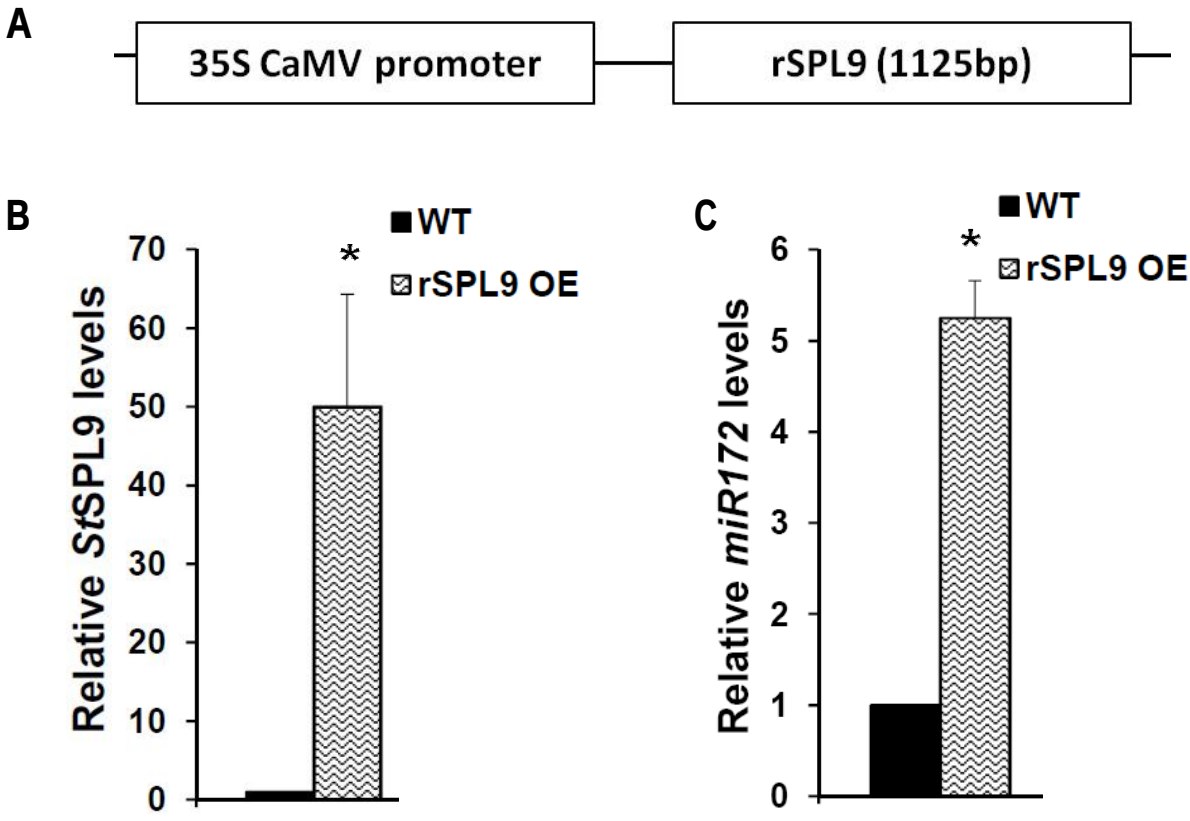

D

	Tuber number	Tuber yield (g)
WT	5.66 ±3.51	6.13 ± 5.51
rSPL9 OE	5.66 ±3.05	6.56 ±5.97

Figure 3.26. Over expression of *miR156* resistant SPL9 (rSPL9) in potato. A, Diagrammatic representation of rSPL9 over expression construct. **B,** Relative levels of *StSPL9* in leaves of WT and rSPL9 OE line. **C,** Relative levels of *miR172* in 15 days post SD induced leaves of WT and rSPL9 OE plants. Error bars indicate (±) SD of two biological replicates each with three technical replicates. Asterisk indicates statistical difference as determined using Student's t test (* as P<0.05). **D,** Tuber yield of WT and rSPL9 OE plants (n=3).

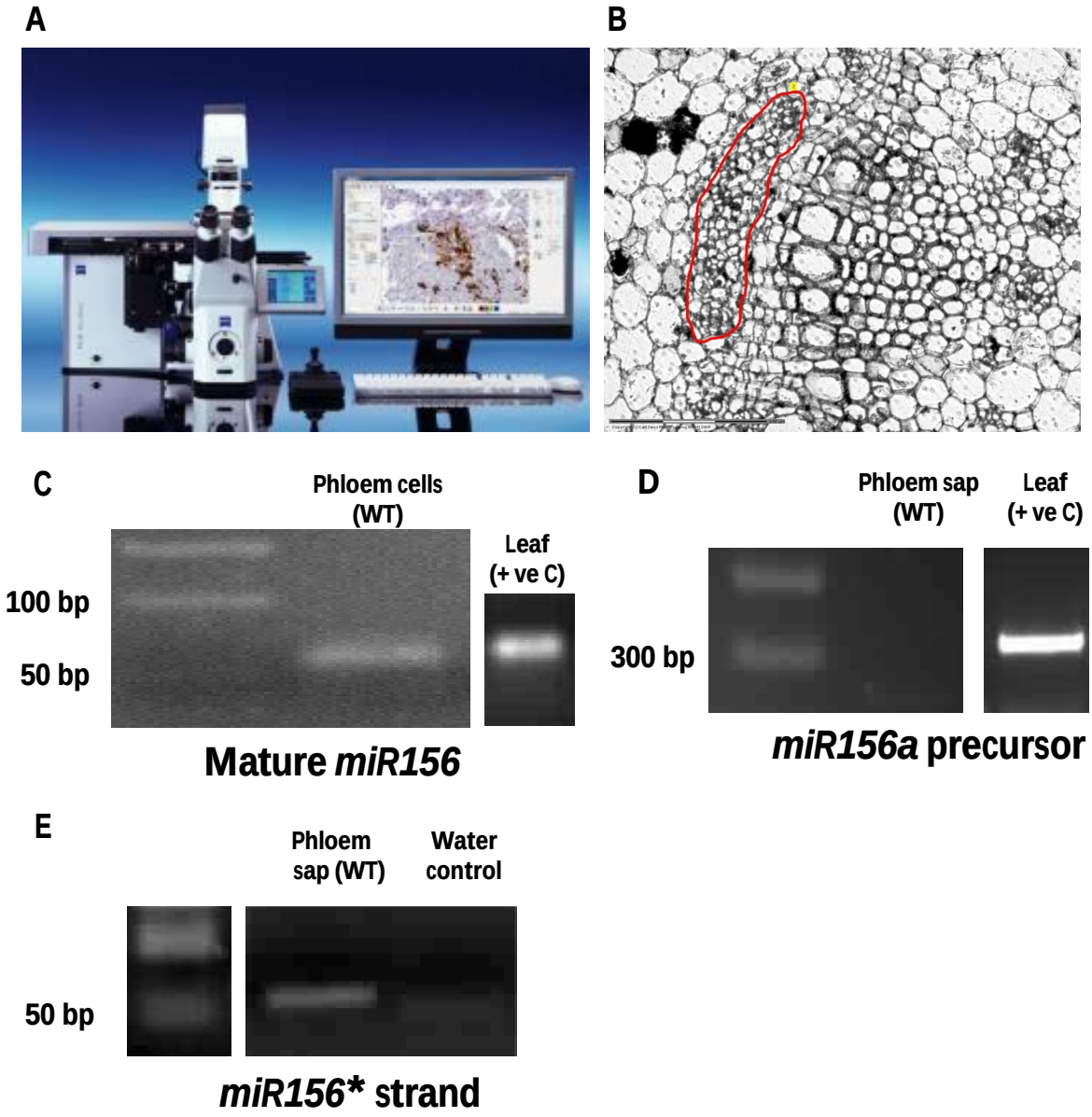

Figure 3.27. Detection of *miR156* in phloem. **A,** Picture of Laser Capture Microdissection (LCM) system. **B,** Phloem tissue in WT stem section (marked in red). This tissue was harvested by LCM. **C,** Detection of *miR156* (mature) in phloem and leaf tissue of WT (+ve Control) by stem-loop RT-PCR. **D,** Absence of *miR156a* precursor (300bp) in phloem sap (WT) and its presence in leaf (WT), acting as + ve control by RT-PCR analysis. **E,** Detection of *miR156** strand in phloem sap of WT by stem-loop RT-PCR.

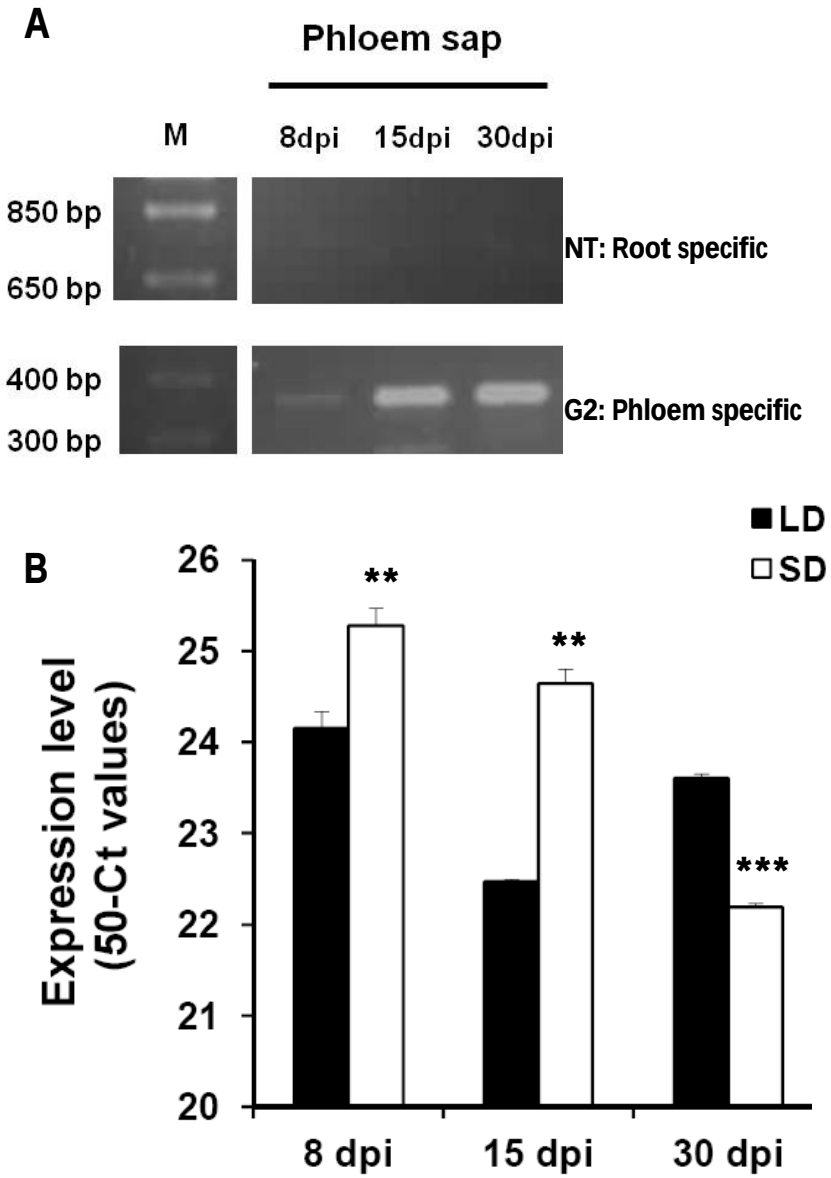

Figure 3.28. Detection of *miR156* in phloem (contd.). A, RT-PCR analysis of NT (root specific transcript) and G2 (phloem specific transcript) of potato phloem sap of WT (phloem-enriched exudate) to assess its purity (Banerjee et al., 2006a). **B,** Differential accumulation of *miR156* (mature) under SD-LD photoperiod in phloem sap of WT plants harvested after 8, 15 and 30 dpi (days post induction). *miR156* accumulation is plotted as 50-Ct values as previously described (Pant et al., 2008). Error bars indicate (±) SD of one biological replicate with three technical replicates. Asterisks indicate statistical difference as determined using Student's t test (** as P<0.01, *** as P<0.001).

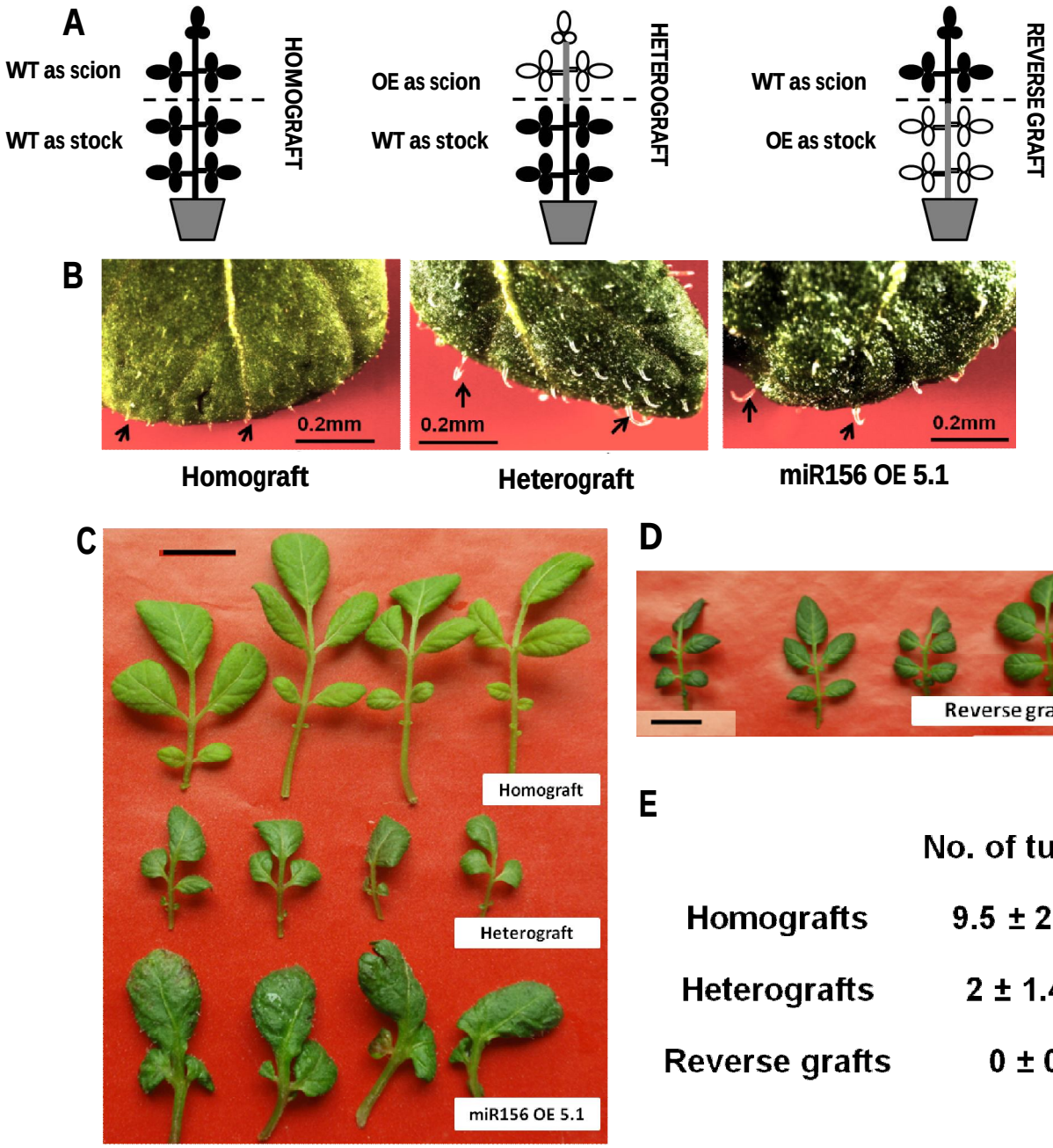

Figure 3.29. *miR156* is graft-transmissible. A, Pictorial representation of the grafts. **B,** Trichomes of homograft (stock leaves), heterograft (stock leaves) and leaves from *miR156* OE 5.1 plants where trichomes in heterografts (stock leaves) are less in number and more in length, same as observed for *miR156* OE 5.1 plants (scale= 0.2 mm). **C and D,** Leaves of homograft (stock), heterograft (stock), *miR156* OE 5.1 plants and reverse grafts (scion) where heterograft stock leaves mimic the phenotype of *miR156* OE 5.1 leaves (C). While, reverse graft scion leaves mimic the phenotype of homograft leaves (stock) (D) (scale= 1 cm). **E,** For tuber numbers, homografts, heterografts and reverse grafts were incubated under SD for 30 days and mean of three grafted plants was calculated.

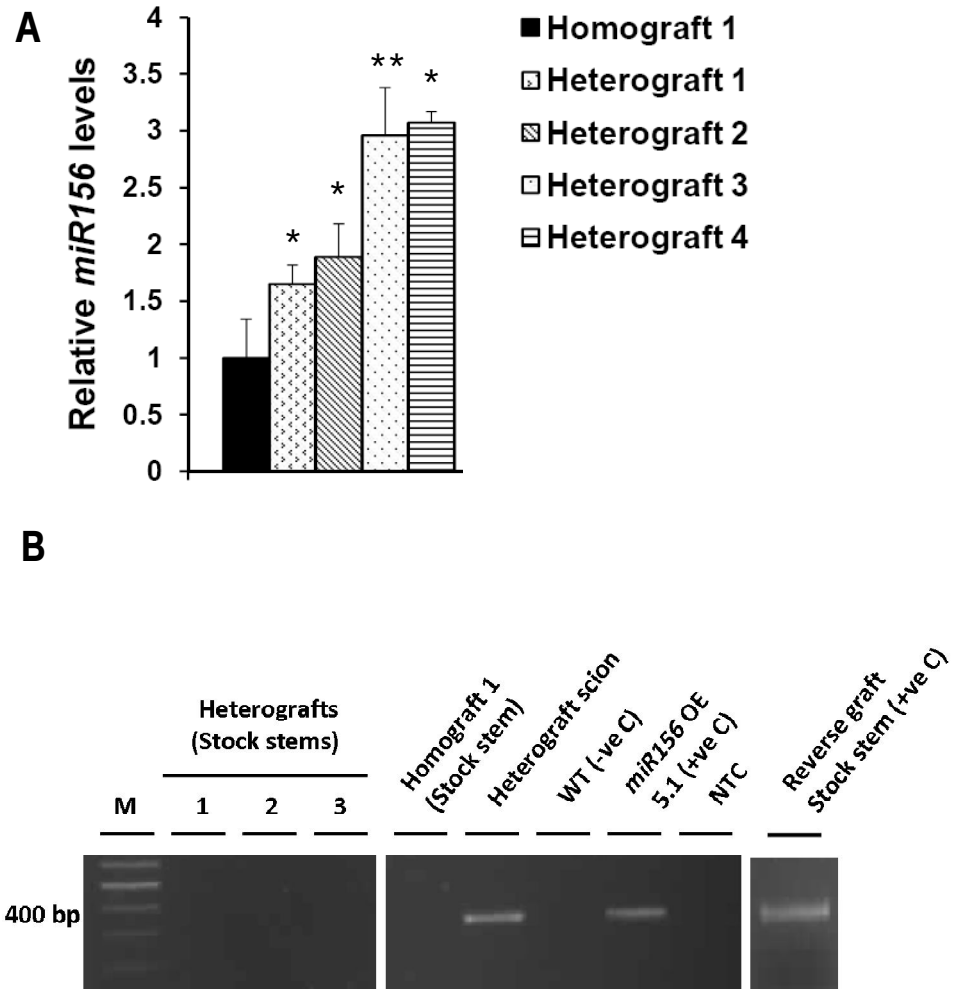

Figure 3.30. *miR156* is graft-transmissible (contd.). A, Relative levels of mature *miR156* in stock stems of four representative heterografts (1, 2, 3 and 4) and homograft incubated under SD and harvested after 30 dpi, were measured by stem-loop qRT-PCR. Error bars indicate (±) SD of one biological replicate with three technical replicates. Asterisks indicate statistical difference as determined using Student's t test (* as $P<0.05$, ** as $P<0.01$). **B,** Detection of *miR156a* precursor transgene in stock stems of homograft, three representative heterografts (1, 2 and 3) and reverse graft by RT-PCR analysis. Stem tissue of heterograft scion, reverse graft stock and *miR156* OE 5.1 plant served as positive controls, while WT as negative control. NTC is no template control.

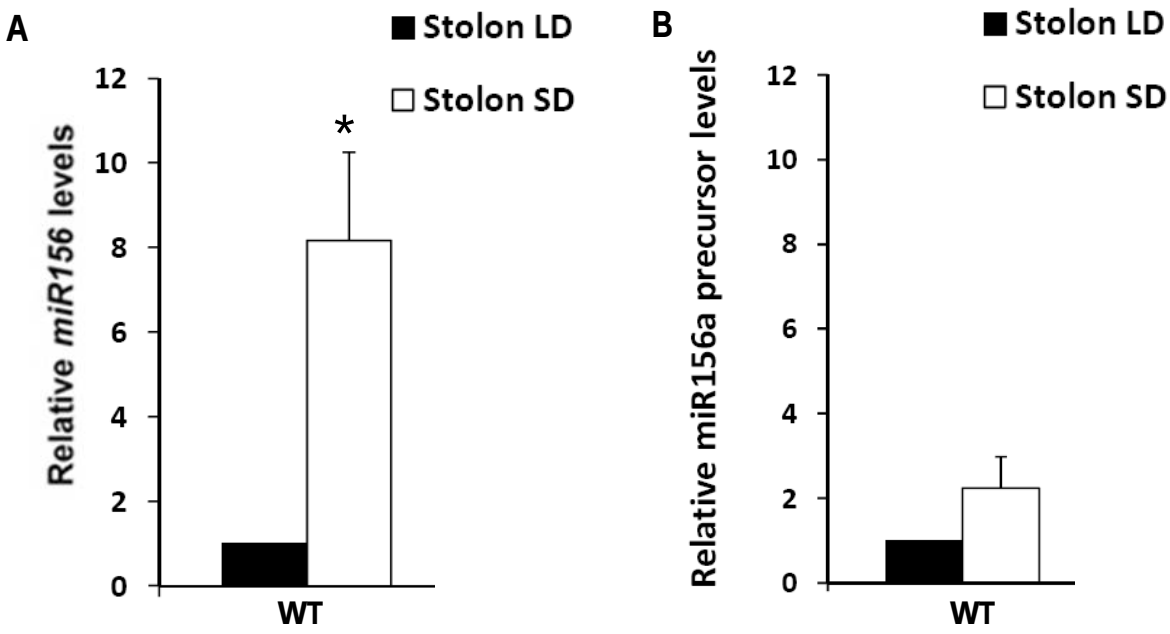

Figure 3.31. Comparative analysis of *miR156* (mature) and *miR156a* precursor levels in WT plants. A, Relative levels of mature *miR156* in 15 dpi SD & LD induced stolons of WT plants. **B,** Relative levels of *miR156a* precursor in 15 dpi SD & LD induced stolons of WT plants. Error bars indicate (±) SD of three biological replicates each with three technical replicates. Asterisk indicates Student's t test (* as $P<0.05$).

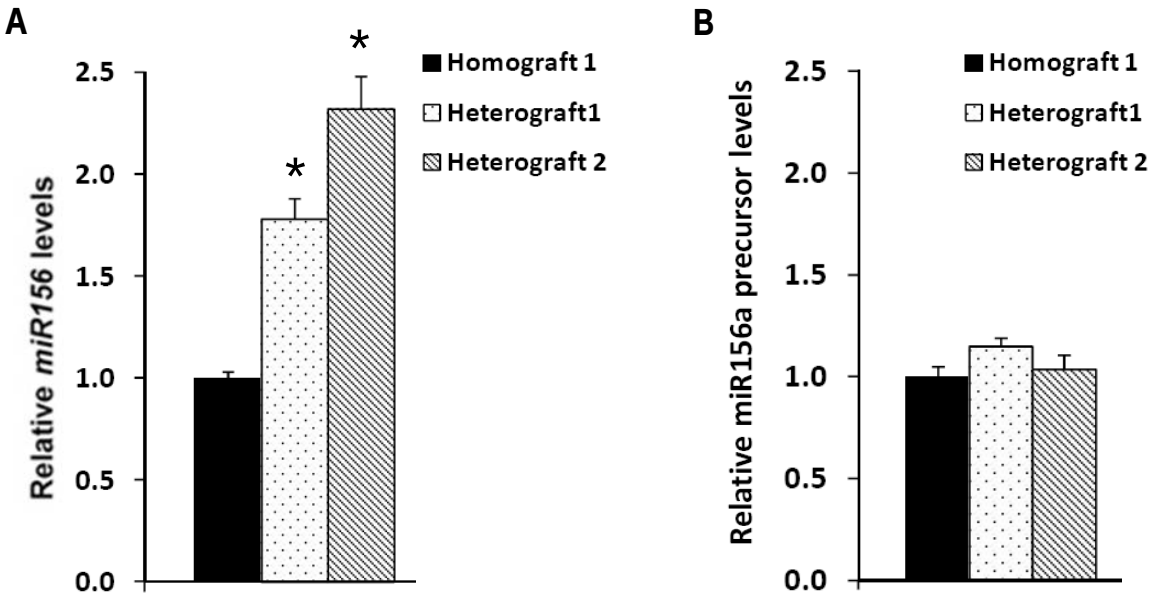

Figure 3.32. Comparative analysis of *miR156* (mature) and *miR156a* precursor levels in grafted plants. A, Relative levels of mature *miR156* in 15 dpi SD induced homograft and heterografts. Graft stock stems were used for analysis. **B,** Relative levels of *miR156a* precursor in 15 dpi SD induced homograft and heterografts. Graft stock stems were used for analysis. Error bars indicate (±) SD of one biological replicate with two technical replicates. Asterisk indicates Student's t test (* as $P<0.05$).

Light regulatory Elements of miR156 upstream sequence

Cis-acting elements	Consensus sequence	Number of motifs present	Reference
GATA box	GATA	8	Vorst et al., 1990
GT1 consensus	GRWAAW	13	Vauterin et al., 1999
I box	GATAA	4	Waksman et al., 1987

Figure 3.33. Potential Light Regulatory Elements (LREs) present in the upstream sequence of *miR156*a as per PLACE software (Higo et al., 1999). The upstream sequence (>chr07:1782100..1784700) was obtained from PGSC database [http://www.potatogenome.net (Potato Genome Sequencing Consortium., 2011)].

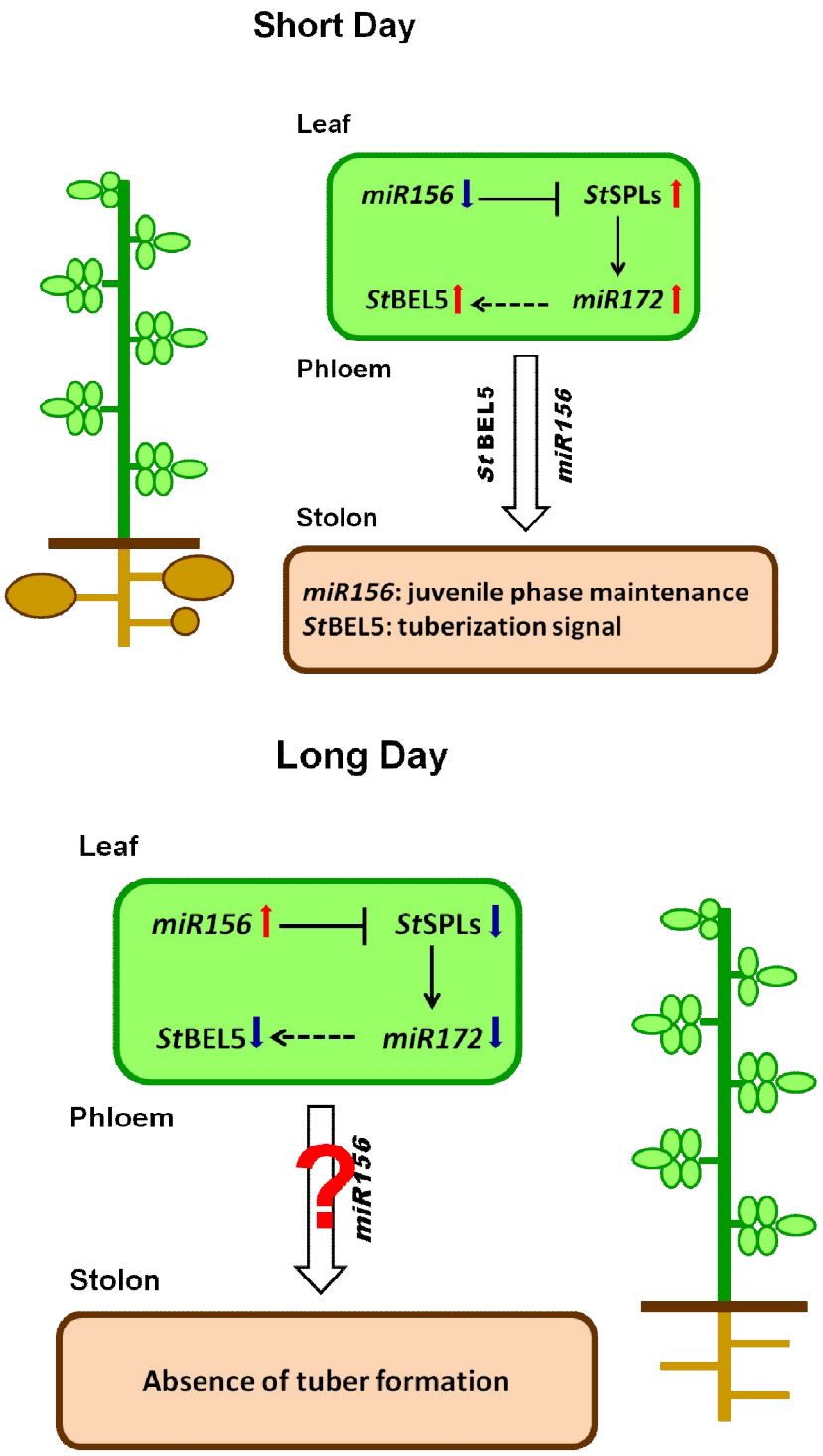

Figure 3.34. A proposed model for role of *miR156* in potato development. Dual action of *miR156* under SD and LD photoperiod. Under SD conditions, it is transported through the phloem where it facilitates tuber formation. While under LD conditions, it inhibits tuber formation by regulating *miR172* levels via *St*SPL9 in leaves.

Chapter 4

Understanding the *miR390-StCDPK1* interaction in tuberization pathway

4.1. Introduction

4.1.1 Role of Ca^{2+} in tuberization pathway

In plants, calcium ions (Ca^{2+}) are the secondary messenger molecules that couple physiological responses to developmental and environmental stimuli. It is a major nutrient required for normal growth and development of plants. As a second messenger molecule, it functions in processes like cytoplasmic streaming, cell division and differentiation, gravitropism, photo-morphogenesis, plant defence and stress related pathways (reviewed in Klimecka and Muszyńska, 2007; Valmonte et al., 2014). Ca^{2+} also functions as a signalling molecule in tuber formation in potato. A study in 1986 (Balamani et al., 1986) reported that single node cuttings of potato when treated with Ca^{2+} chelator [EGTA, ethyleneglycol-bis4 (i-amino ethyl ether) N, N'-tetra acetic acid] showed inhibition of tuberization. On the other hand, when these explants were treated with $CaCl_2$, the tuberization resumed clearly indicating the requirement of Ca^{2+} for tuberization pathway. Simmons and Kelling (1987) reported similar findings in a field study. Changes in cytosolic free calcium ions concentrations are sensed by a group of proteins called as 'the sensors'. There are two types of sensor proteins, one group is called 'sensor relays' which bind Ca^{2+} and undergo conformational changes that in turn regulate downstream target gene expressions. The other group called 'responders' have the effector domain along with Ca^{2+} binding domain (EF-hand) through which they regulate their downstream targets. Calmodulin (CaM) and Calcium dependent Protein Kinases (CDPK) belong to this category (Klimecka and Muszyńska, 2007). Calmodulin (CaM), a calcium sensor protein plays an important role during onset of tuber formation. Potato explants treated with CaM antagonistic agents showed inhibition of tuberization while addition of $CaCl_2$ resumed the tuberization pathway (Balamani et al., 1986). Jena et al (1989) demonstrated the increased accumulation of CaM transcripts in stolon tips induced for tuber formation. This clearly showed CaM function in tuberization. Multiple CaM isoforms have been reported in potato showing differential expression during plant growth and tuber formation (Takezawa et al., 1995). Importance of calcium signalling in tuberization pathway is well studied, however, its exact mechanism and regulation requires further investigations.

4.1.2. Calcium Dependent Protein Kinases (CDPKs) in potato

Calcium dependent Protein Kinases (CDPKs) are the calcium sensors which belong to 'responders' category of proteins (Klimecka and Muszyńska, 2007). CDPKs are monomeric proteins with molecular mass ranging from 40-90 kDa consisting of five domains. The five domains are namely the variable amino terminal domain, kinase domain, auto-inhibitory domain, regulatory domain and C-terminal domain of variable length (Figure. 4.1). The regulatory domain, also called the Calmodulin like (CaM-like) domain contains four EF hands, the calcium binding sites so that four moles of calcium could bind per mole of kinase. CDPKs are encoded by multigene families like in *Arabidopsis*, there are 34 CDPK genes (Cheng et al., 2002). Initially, only a few CDPKs were known to be present in potato, however, due to availability of complete genome, now in all 27 CDPKs are identified to be present in potato (Ulloa Lab, INGEBI, Argentina, unpublished data).

StCDPK1 and *StCDPK3* showed differential expression during tuber formation. *StCDPK1* expressed specifically in swollen stolons and sprouting tubers while *StCDPK3* expressed in early, thin, elongating stolons (Raíces et al., 2003a; Raíces et al., 2003b). These findings confirmed the presence of different CDPKs during specific stages of tuber formation and growth acting on different substrates. The authors suggested that activation of specific CDPKs with distinct biochemical properties and accumulation pattern could be necessary for the co-ordination of multiple calcium mediated signalling required for tuberization.

StCDPK1 which is highly expressed in swollen stolons was suggested to trigger phosphorylation events during tuber induction and thus involved in the events leading to tuber formation (MacIntosh et al., 1996). Further studies by Raices and co-workers (2003b) demonstrated that *StCDPK1* is positively regulated by sucrose application and by tuber promoting hormones like abscisic acid (ABA) and 6-benzyl adenine (Gargantini et al., 2009). These results indicated that *StCDPK1* possibly is a target of ABA action with a synergistic effect of sucrose and ABA on kinase activity (Gargantini et al., 2009). The authors also generated *StCDPK1* mutant potato lines wherein *StCDPK1* levels were reduced as compared to wild-type. These mutant lines showed early tuberization when grown in tuber inducing conditions without the presence of GA inhibitor. These mutant experiments with GA suggested that *StCDPK1* promotes stolon elongation and inhibits tuberization. Considering all the findings of *StCDPK1* with sucrose, GA and ABA, it was suggested that *StCDPK1* plays an important role in GA-signalling forming a converging point for the promoting and inhibitory signals influencing onset of tuber formation. However, regulation of *StCDPK1* is still not clear.

4.1.3. Role of *miR390* in plant development

miR390 has been experimentally identified in many plant species like *Arabidopsis*, rice, maize, soyabean, *Cucumis melo, Populas trichocarpa* etc. (miRBase: http://www.mirbase.org/). However, it has been well investigated only in *Arabidopsis* with respect to its function (Marin et al., 2010). The authors demonstrated that *miR390* is responsible for the synthesis of tasi-RNAs, the trans-acting short interfering RNAs. Tasi-RNAs are small RNA molecules which require miRNA mediated cleavage of their precursors. These cleaved products are then acted upon by RNA-dependent RNA polymerases and DICER to form short interfering RNAs which act on their target genes to downregulate their expression. Of the four tasi-RNA precursors identified in *Arabidopsis* (TAS1-4), *miR390* acts on TAS3 for tasi-RNA production which in turn target Auxin Response Factors 2, 3 and 4 (*ARF2, ARF3 and ARF4*). Also, ARFs were shown to form a feedback loop with *miR390* and responsible for *miR390* regulation. This *miR390-TAS3-ARF2/3/4* complex was demonstrated to affect leaf patterning (Adenot et al., 2006) and lateral root development (Marin et al., 2010) in *Arabidopsis*.

Recently, miR390 was identified in potato along with its predicted targets by Lakhotia et al., 2013. However, function of *miR390* in potato was not investigated. One interesting finding by Lakhotia and co-workers was that protein kinases are the potential targets of *miR390*. Considering the role of *StCDPK1* and *St*CDPK3 in potato tuberization, we conducted a bioinformatic search to identify miRNAs that could target these potato CDPKs. Out of the two *St*CDPKs, *StCDPK1* was targeted by a micro RNA, *miR390*.

In this chapter, we have presented the *miR390-StCDPK1* interaction in potato tuberization pathway. For this study, we have used a non-photoperiod responsive potato cultivar, *Desiree*. Our results suggested that *miR390* targets *StCDPK1* in planta and regulates its expression. The tissue specific expression pattern of *miR390* and *StCDPK1* in potato cultivar *Desiree* also suggested *miR390-StCDPK1* interaction during different stages of tuber transitions.

4.2. Materials and Methods

4.2.1. Plant material and growth conditions

In this study, potato *Desiree* plants were used. *In vitro* plants were grown under LD conditions, at 25˚C in a growth incubator (Percival Scientific). These plants were used for validation of *miR390*. Soil grown plants were maintained in a greenhouse under standard conditions. Two months old soil grown plants were used for quantification experiments of *miR390* and *StCDPK1*. Six weeks old *Nicotiana benthamiana* plants were used for *Agrobacterium*-co-infiltration experiments and they were maintained in the greenhouse under standard conditions.

4.2.2. Prediction of miRNA candidates targeting *StCDPK1*

miRNA candidates targeting *StCDPK1* were predicted using psRNATarget online tool [*plantgrn.noble.org/psRNATarget/,* (Dai and Zhao, 2011)]. Default parameters were used and miRNA sequences showing a score of 1 to 5 were considered. To avoid false positive result, TargetAlign software [*leonxie.com/targetAlign.php*,(Xie and Zhang, 2010)] with default parameters was also used.

4.2.3. Validation of *miR390* in potato (*Desiree*)

miR390 precursor (Accession number. CK247568.1) was amplified from total RNA harvested from *in vitro* potato plants. cDNA was prepared using oligo-dT primer followed by a PCR with *miR390* specific forward primer- *miR390*preFP and reverse primer-*miR390*preRP. Details of all the primers used in this chapter were provided in Table 4.1. The amplicon was then sequence confirmed. Mature *miR390* was detected by stem-loop RT-PCR as described earlier (Varkonyi-Gasic et al., 2007). TRIzol reagent (Invitrogen) was used to isolate total RNA following manufacturer's instructions. Reverse transcription was carried out using stem-loop primer *miR390*STP. End-point PCR was performed using *miR390*F and universal reverse primer univRP. The 61-bp amplicon was cloned in a sub cloning vector (pGEM-T Easy, Promega) and was sequence verified.

4.2.4. Analysis of *miR390* and *CDPK1* levels

Levels of *miR390* were determined by stem-loop qRT-PCR method. Different tissues were harvested from two months old Desiree plants and RNA was isolated by TRIzol (Invitrogen) as per manufacturer's instructions. One µg of total RNA was used for all reverse transcription reactions with stem-loop reverse primer *miR390STP*. Reverse transcription was carried out using *miR390* STP (stem-loop reverse primer) as described earlier (Varkonyi-Gasic et al., 2007). The reaction details are provided in section 2.2.2. qPCR was performed on Mastercycler ep *realplex* (Eppendorf) using *miR390*FP and univRP primers. PCR reactions were carried out using KAPA SYBR green master mixture (Kapa Biosystems) in

Eppendorf Light cycler and were incubated at 95˚C for 5 min followed by 40 cycles of 95˚C for 5 s, 60˚C for 10 s and 68˚C for 8 s. PCR specificity was checked by melting curve analysis.

Levels of *CDPK1* were determined by qRT-PCR. Different tissues were harvested from two months old Desiree plants and RNA was isolated by TRIzol (Invitrogen) following manufacturer's instructions. One µg of total RNA was used for cDNA synthesis using oligo dT primer and Superscript III reverse transcriptase enzyme (Invitrogen) as per manufacturer's instructions. qPCR reactions were performed on Mastercycler ep *realplex* with CDPK1 FP and CDPK1 RP. The reactions were carried out using KAPA SYBR green master mixture (Kapa Biosystems) and incubated at 95˚C for 2 min followed by 40 cycles of 95˚C for 15 s; 56˚C for 15 s and 72˚C for 20 s. GAPDH was used for normalization for both *miR390* and CDPK1. For GAPDH, oligo dT cDNA was used. qPCR was carried out with GAPDH FP and GAPDH RP with PCR conditions used earlier for CDPK1. PCR specificity was checked by melting curve analysis and data was analysed using $2^{-\Delta\Delta Ct}$ method (Livak and Schmittgen, 2001).

4.2.5. *Agrobacterium* mediated co-infiltration assays

Agrobacterium-co-infiltrations were performed in *Nicotiana benthami*ana leaves (6 weeks old plants). 35S::*miR390*precursor, 35S::CDPK1, and GWB408 (empty vector) were introduced in *Agrobacterium tumefaciens* GV3101 and the bacteria were injected into the leaves with a syringe. For co-injections with two different constructs, bacteria were grown overnight with 20µM acetosyringone. The bacteria were precipitated and the pellet was resuspended in resuspension buffer (10mM $MgCl_2$, 10mM MES-K: pH5.6, 100uM acetosyringone). The absorbance was adjusted to 0.4. Bacterial cultures were then incubated at room temperature for 2 hours and co-injections were performed. Leaves were harvested 3 days post infiltration for further analysis at the transcript levels.

4.2.6. Primer sequences

The sequences of primers used in this chapter are listed in Table 4.1

Table 4.1: List of primers

Primer Name	Primer Sequence
*miR390*STP	GTCGTATCCAGTGCAGGGTCCGAGGTATTCGCACTGGATACGACGGTGCT AT
*miR390*FP	CGCGCCAAGCTCAGGAGGG
UnivRP	GTGCAGGGTCCGAGGT
*miR390*preFP	ATAGGATCCTTCTTTCTCCTTTTGCCATTC
*miR390*preRP	GATCTCGAGCAAAAAAATAGATAATTAATGCTAAGG
CDPK1 FP	AGATCAGGTGGGAGTGATGG
CDPK1 RP	CCTCAAATGCCTTACCCAAA
GAPDHFP	GAAGGACTGGAGAGGTGGA
GAPDHRP	GACAACAGAAACATCAGCAGT

4.3. Results

4.3.1. *miR390* potentially targets *StCDPK1*

Previous reports (Raices et al., 2003a; Raices et al., 2003b; Gargantini et al., 2009) have demonstrated the role of *StCDPK1* in the tuberization pathway. However, regulation of *StCDPK1* was not investigated. As miRNA mediated regulation is one of the most widely based mechanism of gene regulation, we analyzed for miRNAs that could potentially target *StCDPK1*. To understand the post-transcriptional regulation of *StCDPK1*, we performed a bioinformatic search to identify miRNA candidates that target *StCDPK1* using psRNATarget and TargetAlign softwares. As per our bioinformatic search with both softwares, *miR390* appeared to be a regulator that potentially targets *StCDPK1* at a score of 5 at translation level (Figure 4.2 A and B).

4.3.2. Validation of *miR390* in potato (*Desiree*)

miR390 was earlier (Zhang et al., 2009) predicted to be present in potato by an *in silico* analysis. Later two additional studies confirmed its presence by deep sequencing analysis in two different potato cultivars (Zhang et al., 2013; Lakhotia et al., 2013). As our study was carried out in *Desiree* potato cultivar, we wanted to validate the presence of *miR390* in this cultivar. To confirm the presence of the *miR390* precursor (CK247568.1) in potato, RT-PCR was performed from *Desiree* leaves and the amplified fragment was sequence confirmed (Figure 4.3 B). The Mfold predicted secondary structure (Zuker, 2003) of the *miR390* precursor sequence had a hairpin loop with mature *miR390* in its stem region, a characteristic of miRNA precursors (Figure 4.3 A). A 21 bp mature *miR390* was detected by stem-loop end point PCR in tissues harvested from entire plants and stolons (Figure 4.3 C) and was verified by sequencing. This result demonstrated that *miR390* is expressed in potato cultivar *Desiree*.

4.3.3. Expression analysis of *miR390* and *StCDPK1* in potato (*Desiree*)

The relative levels of *StCDPK1* and *miR390* were analyzed in different tissues of *Desiree* by qRT-PCR. Both, *StCDPK1* and *miR390* showed differential expression pattern in leaves, axillary meristems, petioles, stem, roots, stolons, swollen stolons and tubers of two month old *Desiree* plants (Figure 4.4). Relative levels of *StCDPK1* showed that it is highly expressed in leaves followed by moderate expression in axillary meristem, stem, roots, stolons and swollen stolons. However, its levels were found to be low in tubers. This data was consistent with the *StCDPK1* promoter::GUS constructs, where high GUS expression is observed in axillary meristem, stolons and swollen stolons while in tubers, the GUS expression was seen only in tuber eyes (unpublished data from Prof. Rita Ulloa's lab). For *miR390*, highest expression was seen in tubers followed by petioles and axillary meristems. Lowest expression was observed in stolons and swollen stolons. One interesting observation from this analysis was that *miR390* and *StCDPK1* showed inverse expression pattern in aerial parts of the plants (axillary meristems, petioles, stem) and in different stages of tuber transitions (stolons, swollen stolons and tubers) (Figure 4.4).

4.3.4. In-planta validation of *StCDPK1* as *miR390* target

Bioinformatic analysis revealed *StCDPK1* to be targeted by *miR390*. *Agrobacterium*-mediated co-infiltrations were adopted to validate *miR390-StCDPK1* interaction (Figure 4.5 A and B).

Three constructs namely 35S:: *miR390* precursor, 35S:: *StCDPK1* CDS and pGWB408 (empty vector) were transformed in *Agrobacterium* and then infiltrated in *Nicotiana benthamiana* leaves. Basal levels of endogenous *miR390* were detected in un-infiltrated leaves and leaves infiltrated with only empty vector. In our *Agrobacterium* co-infiltration experiments, high levels of miR390 (~ 7 folds) were detected in leaves infiltrated with 35S:: *miR390* precursor construct (Figure 4.6 A). This indicated that overexpression and processing of transgenically derived *miR390* was successfully achieved. Similarly, high expression of CDPK1 (~22fold) was detected in leaves infiltrated with 35S:: *StCDPK1* CDS construct as compared to un-infiltrated leaves and leaves infiltrated with only empty vector (Figure 4.6 B). These results clearly indicated that *miR390* and CDPK1 were overexpressed when 35S:: *miR390* precursor, 35S:: *StCDPK1* CDS constructs were infiltrated in tobacco leaves with their appropriate controls respectively. However, when 35S:: *miR390* precursor, 35S:: *StCDPK1* CDS and pGWB408 (empty vector) were infiltrated together, expression of CDPK1 was significantly reduced (by ~20 fold), while *miR390* accumulated at increased levels (Figure 4.6 A and B). This demonstrated that *miR390* possibly regulates *StCDPK1* transcripts resulting in reduction of *CDPK1* levels even in presence of *CDPK1* OE construct. Overall, this finding indicated that *miR390* potentially directs *CDPK1* transcript cleavage, thus downregulating *CDPK1* levels. While we attempted the transcriptional regulation, the translational inhibition of *St*CDPK1 by *miR390* (evidence at protein level) was part of our collaborators work and was carried out at Prof. Rita Ulloa Lab at INGEBI, Argentina.

4.4. Discussion

Calcium Dependent Protein Kinases (CDPKs) play an important role in plant development and stress related pathways (Klimecka and Muszyńska, 2007). They have been well investigated in terms of structure and function in model plants like *Arabidopsis* and rice, however, very limited information is available on their regulation. For example, it has been reported that OsCPK1 and OsCDPK15 (CDPKs in rice) show differential expression in response to salt and draught stress (Ray et al., 2007) indicating the regulation of these proteins by some factors under abiotic stress conditions. In potato, the role of CDPKs, especially CDPK1 in tuberization pathway is well studied (Raices et al., 2003a and b; Gargantini et al., 2009). However, the regulation of CDPKs in potato development is not well investigated. *StCDPK1* promoter studies with promoter::GUS constructs have demonstrated that CDPK1 promoter is active in stolons, swollen stolons, vasculature of leaves and stolons, and in roots (unpublished data from Prof. Rita Ulloa's lab in Buenos Aires, Argentina). *In silico* analysis of *StCDPK1* promoter showed presence of many light regulatory motifs, salt stress response motifs, draught response motifs and hormones like ABA, auxin response motifs (unpublished data from Prof. Rita Ulloa's lab in Buenos Aires, Argentina). These preliminary data provide insights into the possible regulation of *StCDPK1*. We aimed to investigate *StCDPK1* regulation with a focus on miRNA mediated control.

4.4.1. *miR390* regulates *St*CDPK1 in potato

Majority of plant miRNAs share near perfect complementarity with their targets as opposed to animal miRNAs (Millar and Waterhouse, 2005). Based on this principle, many plant miRNA target prediction softwares are available. Near perfect complementarity with targets usually leads to miRNA mediated transcript cleavage, while less complementarity leads to translational arrest (Millar and Waterhouse, 2005). It was considered that plant miRNAs regulate their targets by transcript cleavage. Also, targets showing low scores in the target prediction softwares were considered to be strong targets (in-planta targets) as low score usually corresponds to good complementarity. However, a number of studies have shown that plant miRNAs could regulate their targets by both modes of action; transcript cleavage and translational arrest (Brodersen et al., 2008; Iwakawa and Tomari, 2013). For example, *miR172* targets APETELLA TFs by transcript cleavage as well as translational arrest functioning in phase transitions and flowering (Aukerman and Sakai, 2003; Chen, 2004). Thus, putative miRNA targets having high scores as per target prediction softwares (so called bad candidates for miRNA targets) can now be explored for miRNA-target interactions. In our study, *miR390* targets CDPK1 at translational arrest level at a score of 5 (Figure 4.2 A and B). Considering the above literatures, we explored *miR390-StCDPK1* interaction despite of the high score. Our *Agrobacterium*-mediated co-infiltration studies suggested that *miR390* potentially directs *CDPK1* transcript cleavage, thus downregulating *CDPK1* levels. *Agrobacterium*-mediated co-infiltrations provided an advantage to check transcript as well as protein levels of *StCDPK1* as opposed to RLM-RACE in which only miRNA mediated transcriptional cleavage is detected. Our findings as well as previous reports have highlighted the need to re-look at the target prediction data and miRNA-target validations especially for novel and/or species specific miRNAs.

4.4.2. *miR390-StCDPK1* interaction potentially facilitates tuber formation

As majority of plant miRNAs regulate their targets by transcript cleavage, it was observed that miRNA and their targets have inverse expression pattern. Our expression analysis demonstrated similar observation. In aerial parts of the plant like axillary meristems and petioles, the levels of *miR390* were more than those of *StCDPK1*. While in underground organs like stolons and swollen stolons, *StCDPK1* accumulated in higher amount than *miR390*. In tubers, however, the levels of *miR390* were much greater than *StCDPK1*. The high expression of *StCDPK1* in stolons and swollen stolons is consistent with the previous observation reported by Raices et al (2001). But the *miR390* levels in these tissues were low. This finding possibly indicated the *miR390* mediated control of *StCDPK1* in aerial parts of the plants, while this regulation appears to be removed in stolons and swollen stolons allowing CDPK1 levels to accumulate and facilitate tuber formation. Such findings support the post transcriptional regulation of *StCDPK1* by *miR390* in potato. In summary, the results of the current study led us to conclude that

(i) *miR390* is expressed in potato cultivar *Desiree*.

(ii) Tissue specific qRT-PCR analysis exhibited differential expression of *miR390* and *StCDPK1* in potato. *miR390* and its target *StCDPK1* showed inverse expression pattern in aerial tissues and in different tuber transition stages.

(iii) *miR390* targets *StCDPK1* at transcript level as demonstrated by *Agrobacterium* co-infiltration studies.

(iv) To our knowledge, this is the first report of a miRNA mediated control of CDPKs.

Collectively, these results suggest that *miR390-StCDPK1* interaction in potato possibly plays an important role in tuberization pathway. Overexpression studies with *miR390* and *StCDPK1* will provide more insights into this process.

This work was carried out in collaboration with Prof. Rita Ulloa's lab in INGEBI, Buenos Aires, Argentina as a part of the Indo-Argentine bilateral program.

The findings of this work are submitted for publication.
Santin F, Bhogale S, Fantino E, Grandellis C, Banerjee AK, Ulloa RM (2015) ***StCDPK1* expression pattern and its post transcriptional regulation by *microRNA 390* in potato** (Submitted to Plant Molecular Biology, under review).

Chapter 4

Figures

Figure 4.1. Characteristic structure of Calcium Dependent Protein Kinases (CDPKs). N-VD: N-terminal variable domain, PK-D: catalytic protein kinase domain, AJ: autoinhibitory junction domain, CBD: calcium binding domain. This domain contains EF hands (4 black boxes). CT: C-terminal variable domain. PK-D, AJ and CBD is the conserved region. (adapted from Valmonte et al., 2014)

A

miRNA Acc.	Target Acc.	Expectation (E)	Target Accessibility (UPE)	Alignment	Target Description	Inhibition	Multiplicity
stu-miR390	gi|10568115|gb|AF115406.2	5.0	15.05	miRNA 21 CCACGAUAGGGAGGACUCGAA 1 :::.::: : :: ::: ::: Target 607 GGUGUUAUGCAUCGUGAUCUU 627	| Solanum tuberosum calcium-dependent protein kinase mRNA, complete cds	Translation	1

B

miRNA Acc.	Stu-miR390
Target Acc.	gi|10568115|gb| AF115406.2
Expectation (E)	5.0
Target Accessibility (UPE)	15.05
Alignment	miRNA 21 CCACGAUAGGGAGGACUCGAA 1 :::.::: : :: ::: ::: Target 607 GGUGUUAUGCAUCGUGAUCUU 627
Target description	|Solanum tuberosum calcium-dependent protein kinase 1 mRNA cds
Inhibition	Translation
Multiplicity	1

Figure 4.2 *In silico* analysis of *StCDPK1* and *miR390*. A, *miR390* targets *StCDPK1* at the translation levels as per psRNATarget software [*plantgrn.noble.org/psRNATarget/*, (Dai and Zhao, 2011)]. **B,** *miR390* targets *StCDPK1* at the score of 5 as per TargetAlign software [*leonxie.com/targetAlign.php*,(Xie and Zhang, 2010)].

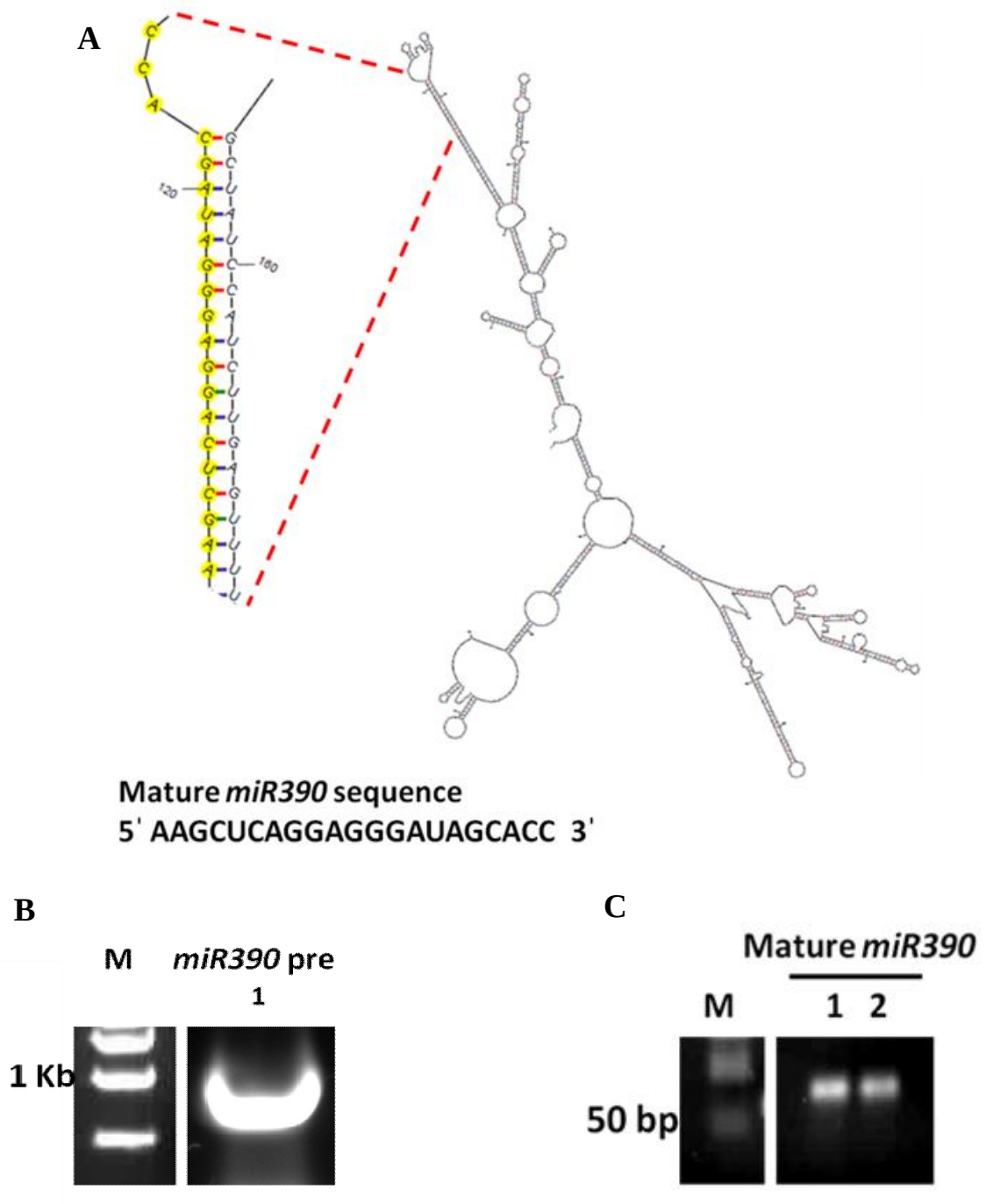

Figure 4.3 Validation of *miR390* in potato cultivar *Desiree*. A, Secondary structure of *miR390* precursor as predicted by MFold (Zuker 2003). Mature *miR390* sequence is highlighted in yellow. **B,** RT-PCR of *miR390* precursor in leaves. **C,** Stem loop RT-PCR of mature *miR390* from stolons (1) and leaves (2). M is the DNA marker.

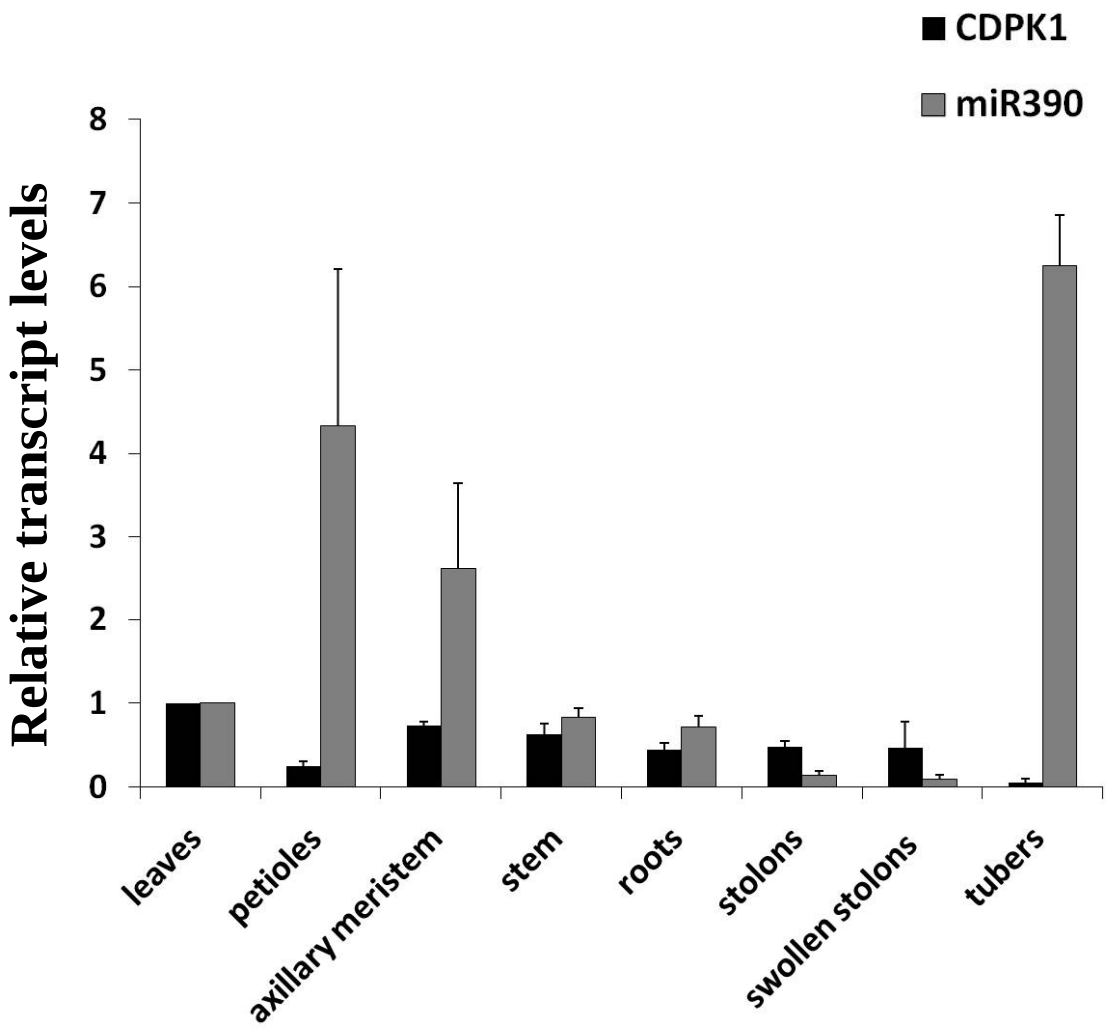

Figure 4.4 Expression analysis of *StCDPK1* and *miR390* in different tissues of potato cultivar *Desiree*. Levels of *StCDPK1* and *miR390* in petioles, axillary meristems, stems, roots, stolons, swollen stolons and mini tubers relative to leaves of desiree. Error bars indicate (±) SD of two biological replicates each with two technical replicates.

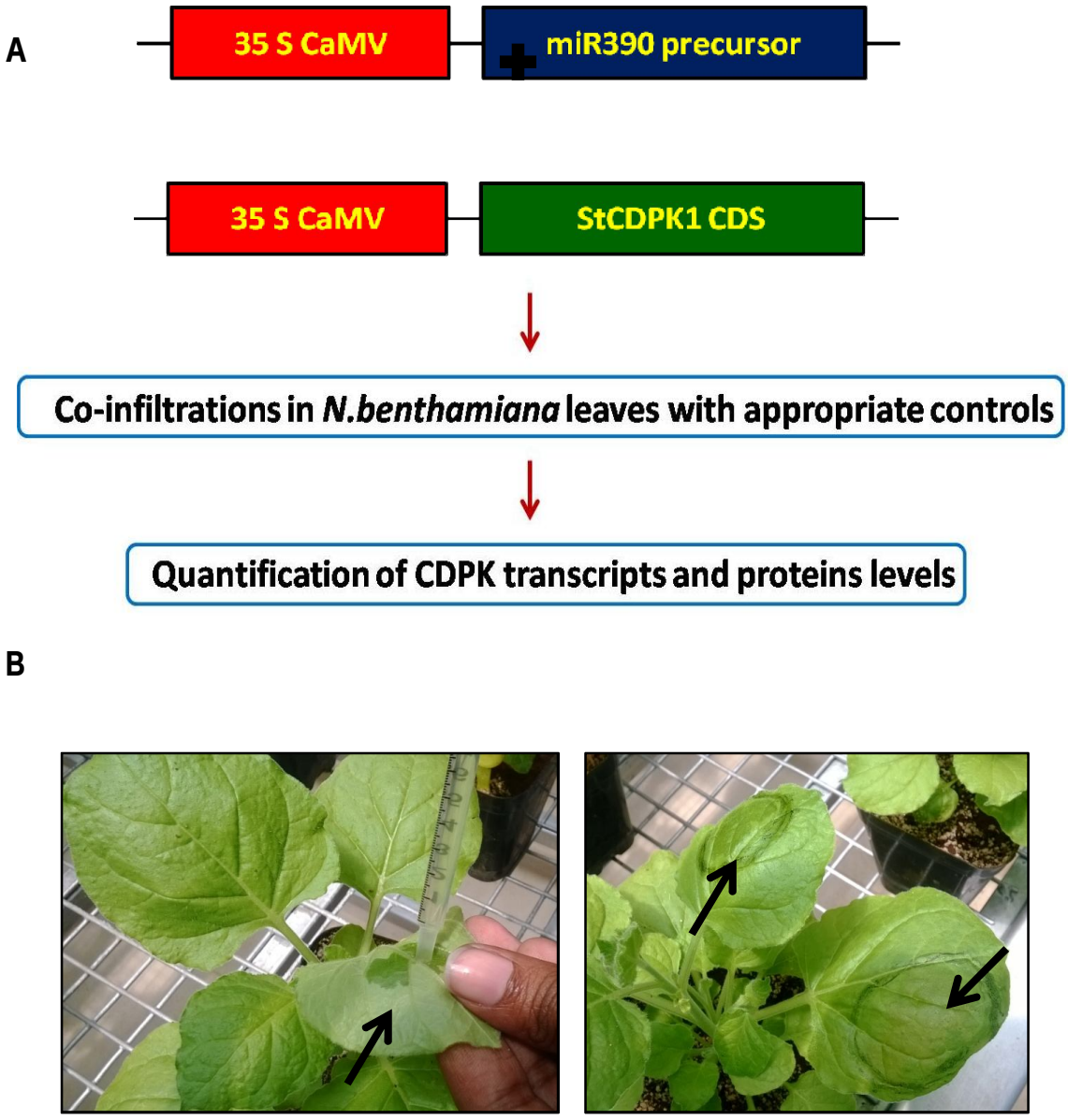

Figure 4.5 *Agrobacterium* mediated co-infiltration of *miR390* and *StCDPK1* constructs to validate their interaction in-planta. A, Flowchart of *Agrobacterium* mediated co-infiltration of *miR390* and *StCDPK1* over expression constructs. **B**, *Nicotiana benthamiana* plants used for infiltration experiments. Arrows indicate infiltration zone.

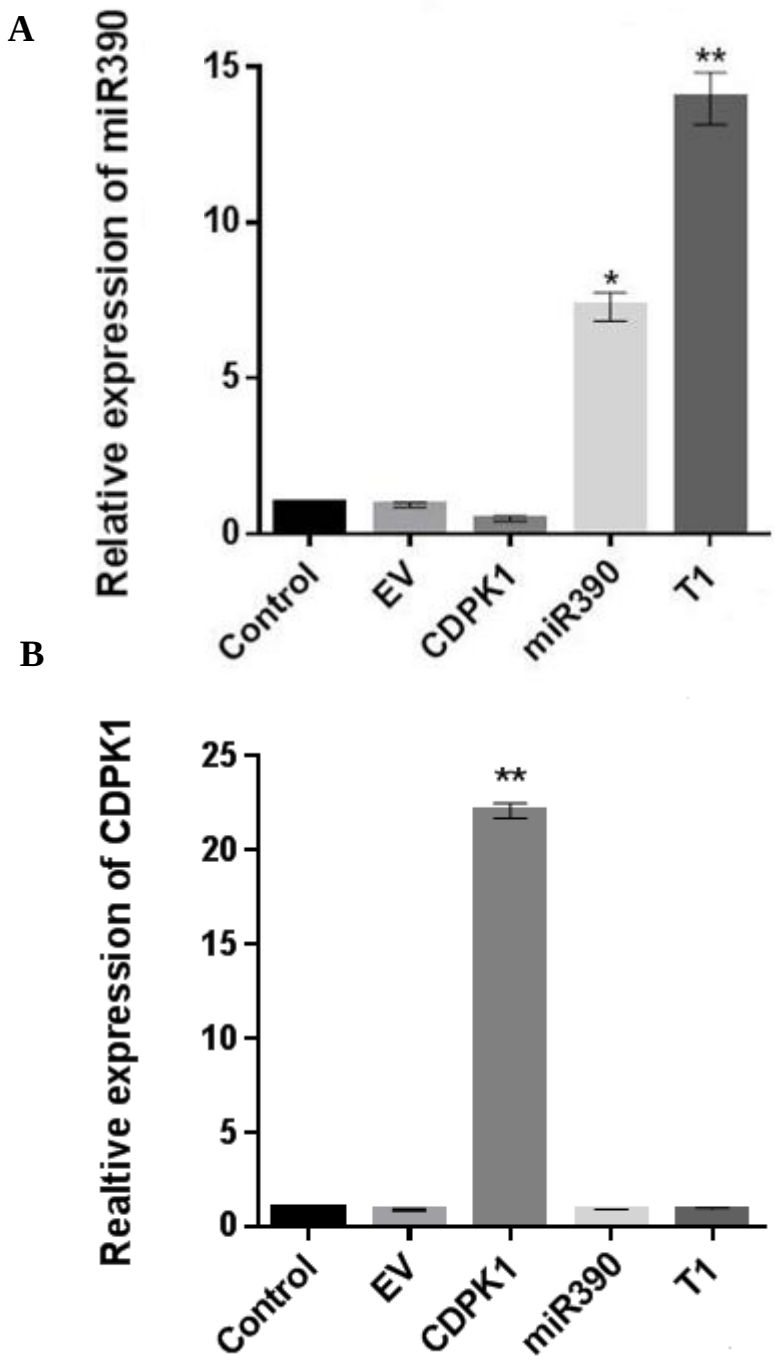

Figure 4.6 *miR390* potentially directs cleavage of *StCDPK1* and downregulates its expression. A and B, Levels of *miR390* (A) and *StCDPK1* (B) were measured in different treatments and controls by RT-qPCR. *GAPDH* was used for normalization. Control: non-infiltrated leaves, EV: leaves infiltrated with empty vector only, CDPK1: leaves infiltrated with 35S::StCDPK1 CDS (CDPK1 overexpression construct), miR390: leaves infiltrated with 35S::miR390 precursor (miR390 overexpression construct) and T1: leaves infiltrated with 35S::miR390 precursor + 35S::StCDPK1 CDS + empty vector. Means ± SEM are plotted. Data analyzed with one way ANOVA and Tukey's multiple comparison test.

Summary

Tuber development in potato (tuberization) is a complex developmental pathway that involves the formation of a specialized underground stem (stolon), which further develops into a mature tuber. It is shown to be governed by various environmental, hormonal and molecular factors (Hannapel et al., 2004; Rodríguez-Falcón et al., 2006; Sarkar, 2008; Sarkar, 2010; Abelenda et al., 2011). Tuberization and flowering are two different reproductive strategies of the plant that share many environmental cues and molecular players. For example, environmental cues like photoperiod and temperature, hormonal signals like GA and CK and molecular factors like FT, CO homologues shown to regulate flowering pathway, have similar role in tuberization pathway (Rodríguez-Falcón et al., 2006; Abelenda et al., 2014). Interestingly, *miR172* which plays an important role in flowering (Aukerman and Sakai, 2003; Chen, 2004) was also shown to act as a positive signal for tuberization by Martin and co-workers (2009). Along with *miR172*, flowering is also reported to be under the control of other miRNAs like *miR159* (Achard et al., 2004) and *miR156* (Wu et al., 2009). Considering the similarities between tuberization and flowering, regulation of tuberization pathway via miRNAs may also be conserved. A couple of reports have identified the miRNA population along with their predicted targets in different cultivars of potato (Zhang et al., 2013; Lakhotia et al., 2014). These reports indicated the existence of a complex miRNA population in potato and based on their target gene relation; possible involvement in regulation of various pathways including tuberization was proposed. However, no further reports demonstrated the functional role of miRNAs in potato development apart from *miR172*. Our aim was to identify and analyze the miRNAs potentially involved in regulation of tuberization pathway in potato. To test the involvement of miRNAs in regulation of tuberization, following objectives were undertaken-

i) To carry out a thorough literature survey on (a) potato tuberization pathway and (b) miRNAs in potato.
ii) To short list, validate and predict targets of candidate miRNAs potentially involved in tuber development.
iii) To characterize the role of *miR156* in potato development and tuberization pathway.
iv) To study the interaction of *miR390* and its target *St*CDPK1 in tuber development.

Chapter 1: Introduction

A thorough literature survey was carried out on (i) tuberization pathway and its regulators (ii) miRNAs: biogenesis, mode of action and their functions in different plant species including potato. For the purpose of present study, we have prepared a list of molecular factors that are shown to be involved in tuberization pathway (Table 1.1). Only those studies that describe the detailed analysis of the respective gene in tuberization pathway were listed in the above table. This literature survey also indicated that tuberization pathway is possibly under the control of other miRNAs apart from *miR172*.

Chapter 2: Micro RNAs in potato (*Solanum tuberosum* ssp *andigena*)

By undertaking bioinformatic and experimental approaches, previous reports have identified numerous miRNAs along with their target genes from potato (Zhang et al., 2009; Xie et al., 2011; Zhang et al., 2013; Lakhotia et al., 2014). However, no further reports have demonstrated the functional role of miRNAs in potato development apart from *miR172* (Martin et al, 2009). Based on these reports, we have shortlisted a number of miRNAs potentially to be involved in tuberization pathway. Also, considering the similarities between tuberization and flowering, we have selected a few miRNAs known to be involved in flowering, as potential candidates to test their role in tuber development. In this part of our work, we have presented the list of shortlisted miRNAs, their in-planta validation in *andigena* plants grown in SD-LD conditions and detailed *in-silico* analysis of their putative target genes.

Following are the important findings-

i) Based on our literature survey, we have shortlisted 15 miRNAs (conserved miRNAs and potato-specific miRNAs) potentially involved in tuberization pathway.
ii) Of these 15 miRNAs, we further validated 12 miRNAs in potato, few of which showed SD-LD photoperiod dependent detection.
iii) A detailed *in-silico* target prediction analysis of these miRNAs revealed few miRNA candidates that have potential to be involved in tuber formation pathway.
iv) Based on our analysis, we selected two miRNAs, *miR156* (chapter 3) and *miR390* (chapter 4), to test their functional role in tuberization pathway.

Chapter 3: Role of *miR156* in potato development

miR156 and *miR172* have been demonstrated to regulate phase transitions and flowering in *Arabidopsis* and rice (Wu et al., 2009; Huijser and Schmid, 2011). Considering the role of *miR172* in flowering and tuberization pathways (Martin et al., 2009; Wu et al., 2009), we hypothesized the involvement of *miR156* in tuber development. In this part of our work, we employed a number of strategies like target gene validations, transgenic analysis, assays of *miR156* abundance; HR-MS based hormone quantification, phloem sap analysis and grafting.

Following are the important findings-

i) *miR156* expression is dependent on plant age and SD-LD photoperiod.

ii) *miR156* over expression affects multiple phenotypic traits in potato by targeting SPL TFs. It acts as a master regulator of various developmental pathways in potato.

iii) *miR156* facilitates tuber formation under SD tuber inductive conditions.

iv) EMSA analysis confirmed that *miR156-St*SPL9-*miR172* module is conserved in potato.

v) *miR156* acts as a potential phloem-mobile long distance signal affecting plant architecture.

Part of this work has been published (Bhogale et al., 2014).

Chapter 4: Understanding the *miR390-StCDPK1* interaction in tuberization pathway

Our bioinformatic target prediction analysis for the shortlisted miRNAs revealed *StCDPK1* to be a potential target gene for *miR390*. *StCDPK1* is involved in tuberization pathway as demonstrated by Raices and co-workers (2003a and 2003b) and by Gargantini et al (2009). These reports suggested that *StCDPK1* could play an important role in GA-signalling forming a converging point for the promoting and inhibitory signals influencing onset of tuber formation. However, the regulation of *StCDPK1* is still not clearly understood. We aimed to investigate *StCDPK1* regulation with a focus on miRNA mediated control via *miR390*. In this part of our work, we have studied the *miR390-StCDPK1* interaction in potato tuberization pathway in *Desiree* potato cultivar.

Following are the important findings-

i) *miR390* is expressed in *Desiree* potato cultivar.

ii) Tissue specific RT-qPCR analysis exhibited differential expression of *miR390* and *StCDPK1* in potato. *miR390* and its target *StCDPK1* showed inverse expression pattern in aerial tissues and in different tuber transition stages.

iii) *miR390* appears to target *StCDPK1* at transcript level as demonstrated by our *Agrobacterium* co-infiltration studies.

iv) To our knowledge, this is the first report of miRNA mediated control of CDPKs.

Part of this work has been submitted for publication (Santin et al., 2015).

Future directions:

Our investigations on miRNA-mediated control of tuberization pathway has resulted several important findings as mentioned above. However, to have further insights, following directions of work could be undertaken as part of the future studies-

1. From our selected miRNA list, other miRNA candidates could be characterized in detail to test their possible role in tuberization pathway.
2. We have demonstrated that *miR156* regulates tuberization pathway. However, how *miR156* itself is regulated under SD-LD photoperiod conditions would be an interesting question to study in future.
3. Additional experiments like cleavage site mapping assay (modified RLM-RACE) and overexpression studies with *miR390* and *StCDPK1* would further provide evidence in *miR390-StCDPK1* relationship.

References

Abdala G, Guifiazti M, Tizio R, Pearce DW, Pharis R (1995) Effect of 2-chloroethyltrimethyl ammonium chloride on tuberization and endogenous GA3 in roots of potato cuttings. Plant Growth Regulation **17**: 95–100

Abelenda J a, Navarro C, Prat S (2011) From the model to the crop: genes controlling tuber formation in potato. Current opinion in biotechnology **22**: 287–92

Abelenda J a, Navarro C, Prat S (2014) Flowering and tuberization: a tale of two nightshades. Trends in plant science **19**: 115–122

Achard P, Herr A, Baulcombe DC, Harberd NP (2004) Modulation of floral development by a gibberellin-regulated microRNA. Development **131**: 3357–3365

Addo-Quaye C, Eshoo TW, Bartel DP, Axtell MJ (2008) Endogenous siRNA and miRNA targets identified by sequencing of the *Arabidopsis* degradome. Current biology **18**: 758–762

Adenot X, Elmayan T, Lauressergues D, Boutet S, Bouché N, Gasciolli V, Vaucheret H (2006) DRB4-dependent TAS3 trans-acting siRNAs control leaf morphology through AGO7. Current biology **16**: 927–932

Agrawal L, Chakraborty S, Jaiswal DK, Gupta S, Datta A, Chakraborty N (2008) Comparative proteomics of tuber induction ,development and maturation reveal the complexity of tuberization process in Potato (*Solanum tuberosum* L). Journal of Proteome Research **7**: 3803–3817

Amador V, Monte E, Garcia-Martinez JL, Prat S (2001) Gibberellins signal nuclear import of PHOR1 , a Photoperiod-Responsive Protein with homology to *Drosophila* armadillo. Cell **106**: 343–354

Amasino RM, Michaels SD (2010) The Timing of Flowering. Plant Physiology **154**: 516–520

Aukerman MJ, Sakai H (2003) Regulation of Flowering Time and Floral Organ Identity by a MicroRNA and Its APETALA2 -Like target genes. The Plant Cell **15**: 2730–2741

Axtell MJ, Bowman JL (2008) Evolution of plant microRNAs and their targets. Trends in Plant Science **13**: 343–349

Bachem CWB, Horvath B, Trindade L, Claassens M, Davelaar E, Jordi W, Visser RGF (2001) A potato tuber-expressed mRNA with homology to steroid dehydrogenases affects gibberellin levels and plant development. The Plant Journal **25**: 595–604

Balamani V, Veluthambi K, Poovaiah BW (1986) Effect of calcium on tuberization in Potato (*Solanum tuberosum* L.). Plant Physiology **80**: 856–858

Banerjee AK, Chatterjee M, Yu Y, Suh S-G, Miller WA, Hannapel DJ (2006a) Dynamics of a mobile RNA of potato involved in a long-distance signaling pathway. The Plant Cell **18**: 3443–3457

Banerjee AK, Prat S, Hannapel DJ (2006b) Efficient production of transgenic potato (*S. tuberosum* L. ssp. *andigena*) plants via *Agrobacterium tumefaciens*-mediated transformation. Plant Science **170**: 732–738

Batutis EJ, Ewing EE (1982) Far-Red reversal of Red Light effect during long-night induction of Potato (*Solanum tuberosum* L.) Tuberization. Plant Physiology **69**: 672–674

van den Berg JH, Šimko I, Davies PJ, Ewing EE, Halinska A (1995) Morphology and [14C] Gibberellin A12 metabolism in WildType and Dwarf *Solanum tuberosum* ssp. *Andigena* Grown under long and short photoperiods. Journal of Plant Physiology **146**: 467–473

Bhogale S, Mahajan A. S, Natarajan B, Rajabhoj M, Thulasiram H V., Banerjee AK (2014) MicroRNA156: A potential graft-transmissible microRNA that modulates plant architecture and tuberization in *Solanum tuberosum* ssp. *andigena*. Plant Physiology **164**: 1011–1027

Birkenbihl RP, Jach G, Saedler H, Huijser P (2005) Functional dissection of the plant-specific SBP-domain: overlap of the DNA-binding and nuclear localization domains. Journal of molecular biology **352**: 585–96

Blazquez MA, Weigel D (2000) Integration of Floral inductive signals in *Arabidopsis*. Nature **404**: 889–892

Blein T, Pulido A, Vialette-Guiraud A, Nikovics K, Morin H, Hay A, Johansen IE, Tsiantis M, Laufs P (2008) A conserved molecular framework for compound leaf development. Science **322**: 1835–1839

Bodlaender, KBA (1963) Influence of temperature, radiation, and photoperiod on development and yield, p. 199–210. In: J.D. Ivins and F.L. Milthorpe (eds.). The growth of the potato. Butterworth, London

Bou-Torrent J, Martínez-García JF, García-Martínez JL, Prat S (2011) Gibberellin A1 metabolism contributes to the control of photoperiod-mediated tuberization in potato. PloS one **6**: e24458

Brodersen P, Sakvarelidze-Achard L, Bruun-Rasmussen M, Dunoyer P, Yamamoto YY, Sieburth L, Voinnet O (2008) Widespread translational inhibition by plant miRNAs and siRNAs. Science **320**: 1185–1190

Buhtz A, Pieritz J, Springer F, Kehr J (2010) Phloem small RNAs , nutrient stress responses , and systemic mobility. BMC Plant Biology **10**: 64

Buhtz A, Springer F, Chappell L, Baulcombe DC, Kehr J (2008) Identification and characterization of small RNAs from the phloem of *Brassica napus*. The Plant Journal **53**: 739–749

Bushnell J (1927) The relation of temperature to growth and respiration in the potato plant. American Potato Journal **4:** 119

Cai S, Lashbrook CC (2006) Laser capture microdissection of plant cells from tape-transferred paraffin sections promotes recovery of structurally intact RNA for global gene profiling. The Plant Journal **48**: 628–637

Campbell BA, Hallengren J, Hannapel DJ (2008) Accumulation of BEL1-like transcripts in solanaceous species. Planta **228**: 897–906

Cao W, Tibbitts TW (1992) Temperature Cycling Periods Meet Growth and Tuberization in Potatoes under Continuous Irradiation. Hortscience **27**: 344–345

Carrera E, Bou J, Garcia-Martinez JL, Prat S (2000) Changes in GA 20-oxidase gene expression strongly affect stem length , tuber induction and tuber yield of potato plants. The Plant journal **22**: 247–256

Chailakhyan MKh, Yanina LI, Davedzhiyan AG, Lotova GN (1981) Photoperiodism and tuber formation in grafting of tobacco onto potato. Doklady Akademii Nauk SSSR **257:**1276–1280

Chapman HW (1958) Tuberization in the potato plant. Physiologia Plantarum. **11:** 215–24

Chen H, Banerjee AK, Hannapel DJ (2004) The tandem complex of BEL and KNOX partners is required for transcriptional repression of ga20ox1. The Plant journal **38**: 276–84

Chen H, Rosin FM, Prat S, Hannapel DJ (2003) Interacting transcription factors from the Three-Amino Acid Loop Extension Superclass regulate tuber formation. Plant Physiology **132**: 1391–1404

Chen X (2004) A microRNA as a translational repressor of APETALA2 in *Arabidopsis* flower development. Science **303**: 2022–2025

Chen X, Zhang Z, Liu D, Zhang K, Li A, Mao L (2010) Squamosa Promoter-Binding Protein-Like Transcription Factors : Star Players for plant growth and development. Journal of Integrative Plant Biology **52**: 946–951

Cheng S, Willmann MR, Chen H, Sheen J (2002) Update on Calcium Signaling through Protein Kinases. The *Arabidopsis* Calcium-Dependent Protein Kinase Gene Family. Plant Physiology **129**: 469–485

Chincinska I a, Liesche J, Krügel U, Michalska J, Geigenberger P, Grimm B, Kühn C (2008) Sucrose transporter StSUT4 from potato affects flowering, tuberization, and shade avoidance response. Plant physiology **146**: 515–528

Chincinska I, Gier K, Krügel U, Liesche J, He H, Grimm B, Harren FJM, Cristescu SM, Kühn C (2013) Photoperiodic regulation of the sucrose transporter StSUT4 affects the expression of circadian-regulated genes and ethylene production. Frontiers in plant science **4**: 26

Chuck G, Cigan AM, Saeteurn K, Hake S (2007) The heterochronic maize mutant Corngrass1 results from overexpression of a tandem microRNA. Nature Genetics **39**: 544–549

Comai L, Zhang B (2012) MicroRNAs: key gene regulators with versatile functions. Plant Molecular Biology **80**: 1

Corbesier L, Vincent C, Jang S, Fornara F, Fan Q, Searle I, Giakountis A, Farrona S, Gissot L, Turnbull C, et al (2007) FT Protein movement contributes to long-distance signaling in floral induction of *Arabidopsis*. Science **316**: 1030–1033

Dai X, Zhao PX (2011) psRNATarget: a plant small RNA target analysis server. Nucleic Acids Research **39**: W155–W159

Didiano D, Hobert O (2006) Perfect seed pairing is not a generally reliable predictor for miRNA-target interactions. Nature Structural and Molecular Biology **13:** 849-851

Domagalska MA, Leyser O (2011) Signal integration in the control of shoot branching. Nature Reviews Molecular Cell Biology **12**: 211–221

Eviatar-ribak T, Shalit-kaneh A, Chappell-maor L, Amsellem Z, Eshed Y, Lifschitz E (2013) A Cytokinin-Activating enzyme promotes tuber formation in tomato. Current Biology **23**: 1057–1064

Ewing EE, Struik PC (1992) Tuber formation in potato: induction, initiation, and growth. Horticultural Reviews. **14:** 89–198

Ewing EE, Wareing PF (1978) Shoot , Stolon , and Tuber Formation on Potato (*Solanum tuberosum* L.) cuttings in response to photoperiod. Plant Physiology **61**: 348–353

Faivre-Rampant O, Cardle L, Marshall D, Viola R, Taylor MA (2004) Changes in gene expression during meristem activation processes in *Solanum tuberosum* with a focus on the regulation of an auxin response factor gene. Journal of experimental botany **55**: 613–22

Fu C, Sunkar R, Zhou C, Shen H, Zhang J-Y, Matts J, Wolf J, Mann DGJ, Stewart CN, Tang Y, et al (2012) Overexpression of miR156 in switchgrass (*Panicum virgatum* L.) results in various morphological alterations and leads to improved biomass production. Plant Biotechnology Journal **10**: 443–452

Forcat S, Bennet MH, Mansfield JW, Grant MR (2008) A rapid and robust method for simultaneously measuring changes in phytohormones ABA, JA and SA in plants following biotic and abiotic stress. Plant Methods **4**: 16-23

Fujino K, Koda Y, Kikuta Y (1995) Reorientation of cortical microtubules in the sub-apical region during tuberization in single-node stem segments of potato in culture. Plant Cell Physiology **36:**891–95

Gargantini PR, Giammaria V, Grandellis C, Feingold SE, Maldonado S, Ulloa RM (2009) Genomic and functional characterization of StCDPK1. Plant molecular biology **70**: 153–72

Gibson SI (2005) Control of plant development and gene expression by sugar signaling. Current opinion in plant biology **8**: 93–102

Gidda SK, Miersch O, Levitin A, Schmidt J, Wasternack C, Varin L (2003) Biochemical and Molecular Characterization of a Hydroxyjasmonate Sulfotransferase from Arabidopsis thaliana *. The Journal of biological chemistry **278**: 17895–17900

Gocal GFW, Sheldon CC, Gubler F, Moritz T, Bagnall DJ, Macmillan CP, Li SF, Parish RW, Dennis ES, Weigel D, et al (2001) GAMYB-like Genes, flowering and gibberellin signaling in *Arabidopsis*. Plant Physiology **127**: 1682–1693

Gomez-Roldan V, Fermas S, Brewer PB, Puech-Pagès V, Dun E a, Pillot J-P, Letisse F, Matusova R, Danoun S, Portais J-C, et al (2008) Strigolactone inhibition of shoot branching. Nature **455**: 189–94

González-Schain ND, Díaz-Mendoza M, Zurczak M, Suárez-López P (2012) Potato CONSTANS is involved in photoperiodic tuberization in a graft-transmissible manner. The Plant journal **70**: 678–690

Gou J-Y, Felippes FF, Liu C-J, Weigel D, Wang J-W (2011) Negative regulation of anthocyanin biosynthesis in *Arabidopsis* by a miR156-targeted SPL transcription factor. The Plant Cell **23**: 1512–1522

Gregory LE (1956) Some factors for Tuberization in the Potato Plant. American Journal Of Botany **43**: 281–288

Gubler F, Kalla R, Roberts JK, Jacobsen J V (1995) Gibberellin-regulated expression of a myb Gene in Barley Aleurone Cells: Evidence for Myb transactivation of a high-pl alpha-amylase gene promoter. The Plant Cell **7**: 1879–1891

Guo J-L, Yu C-L, Fan C-Y, Lu Q-N, Yin J-M, Zhang Y-F, Yang Q (2010) Cloning and characterization of a potato TFL1 gene involved in tuberization regulation. Plant Cell, Tissue and Organ Culture **103**: 103–109

Hannapel DJ, Chen H, Rosin FM, Banerjee AK, Davies PJ (2004) Molecular Controls of Tuberization. American Journal of Pottao Research **81**: 263–274

Harper L and Freeling M (1996) Interactions of liguleless1 and liguleless2 function during ligule development in maize. Genetics **144**: 1871-1882

Harvey BMR, Crothers SH, I INEE, Selby C (1991) The use of growth retardants to improve microtuber formation by potato (*Solanum tuberosum*). Plant Cell, Tissue and Organ Culture **27**: 59–64

Heyer A, Gatz C (1992a) Isolation and characterization of a cDNA-clone coding for potato type A phytochrome. Plant Molecular Biology **18**: 535–544

Heyer A, Gatz C (1992b) Isolation and characterization of a eDNA-clone coding for potato type B phytochrome. Plant Molecular Biology **20**: 589–600

Heyer AC, Mozley D, Landschütze V, Thomas B, Gatz C (1995) Function of Phytochrome A in potato plants as revealed through the study of transgenic plants. Plant Physiology **109**: 53–61

Higo K, Ugawa Y, Iwamoto M, Korenaga T (1999) Plant cis-acting regulatory DNA elements (PLACE) database : 1999. Nucleic Acids Research **27**: 297–300

Horsch RB, Rogers SG, Fraley RT (1985) Transgenic plants. Cold Spring Harb Symp Quant Biol **50**: 433–437

Huijser P, Schmid M (2011) The control of developmental phase transitions in plants. Development **138**: 4117–4129

Inui H, Ogura Y, Kiyosue T (2010) Overexpression of *Arabidopsis thaliana* LOV KELCH REPEAT PROTEIN 2 promotes tuberization in potato (*Solanum tuberosum* cv. May Queen). FEBS letters **584**: 2393–2396

Iwakawa H, Tomari Y (2013) Molecular insights into microRNA-mediated translational repression in plants. Molecular cell **52**: 591–601

Jackson SD (2009) Plant responses to photoperiod. The New Phytologist **181**: 517–531

Jackson SD, James P, Prat S, Thomas B (1998) Phytochrome B affects the levels of a graft-transmissible signal involved in tuberization. Plant Physiology **117**: 29–32

Jackson SD, James PE, Carrera E, Prat S, Thomas B (2000) Regulation of transcript levels of a potato gibberellin 20-Oxidase gene by light and phytochrome B. Plant Physiology **124**: 423–430

Jackson SD, Willmitzer L (1994) Jasmonic acid spraying does not induce tuberisation in short-day-requiring potato species kept in non-inducing conditions. Planta **194**: 155–159

Jena PK, Reddy ASN, Poovaiah BW (1989) Molecular cloning and sequencing of a cDNA for plant calmodulin : Signal-induced changes in the expression of calmodulin. PNAS **86**: 3644–3648

Jiang J, Lv M, Liang Y, Ma Z, Cao J (2014) Identification of novel and conserved miRNAs involved in pollen development in *Brassica campestris* ssp. chinensis by high-throughput sequencing and degradome analysis. BMC genomics **15**: 146

Jiao Y, Wang Y, Xue D, Wang J, Yan M, Liu G, Dong G, Zeng D, Lu Z, Zhu X, et al (2010) Regulation of OsSPL14 by OsmiR156 defines ideal plant architecture in rice. Nature Genetics **42**: 541–545

Jones-Rhoades MW (2012) Conservation and divergence in plant microRNAs. Plant Molecular Biology **80**: 3–16

Juarez MT, Kui JS, Thomas J, Heller BA, Timmermans MCP (2004) microRNA-mediated repression of rolled leaf1 specifies maize leaf polarity. Nature **428**: 84–87

Jung J-H, Seo PJ, Park C-M (2009) MicroRNA biogenesis and function in higher plants. Plant Biotechnology Reports **3**: 111–126

Kang S, Hannapel DJ (1995) Nucleotide sequences of novel potato (*Solanum tuberosum* L.) MADS-box cDNAs and their expression in vegetative organs. Gene **166**: 329–330

Kantar M, Lucas SJ, Budak H (2011) miRNA expression patterns of *Triticum dicoccoides* in response to shock drought stress. Planta **233**: 471–484

Kardailsky I, Shukla VK, Ahn JH, Dagenais N, Christensen S, Nguyen JT, Chory J, Harrison M, Weigel D (1999) Activation Tagging of the Floral Inducer FT. Science **286**: 1962–1966

Kasai A, Kanehira A, Harada T (2010) miR172 can move long distances in *Nicotiana benthamiana*. The Open Plant Science Journal **4**: 1–6

Kawashima CG, Yoshimoto N, Maruyama-Nakashita A, Tsuchiya YN, Saito K, Takahashi H, Dalmay T (2009) Sulphur starvation induces the expression of microRNA-395 and one of its target genes but in different cell types. The Plant journal **57**: 313–321

Klimecka M, Muszyńska G (2007) Structure and functions of plant calcium-dependent protein kinases. Acta Biochimica Polonica **54**: 219–233

Kloosterman B, Abelenda J a, Gomez MDMC, Oortwijn M, De Boer JM, Kowitwanich K, Horvath BM, Van Eck HJ, Smaczniak C, Prat S, et al (2013) Naturally occurring allele diversity allows potato cultivation in northern latitudes. Nature **495**: 246–250

Kloosterman B, De Koeyer D, Griffiths R, Flinn B, Steuernagel B, Scholz U, Sonnewald S, Sonnewald U, Bryan GJ, Prat S, et al (2008) Genes driving potato tuber initiation and growth: identification based on transcriptional changes using the POCI array. Functional & integrative genomics **8**: 329–40

Kloosterman B, Navarro C, Bijsterbosch G, Lange T, Prat S, Visser RGF, Bachem CWB (2007) StGA2ox1 is induced prior to stolon swelling and controls GA levels during potato tuber development. The Plant journal **52**: 362–373

Kloosterman B, Vorst O, Hall RD, Visser RGF, Bachem CW (2005) Tuber on a chip: differential gene expression during potato tuber development. Plant biotechnology journal **3**: 505–519

Koda Y, Omer EA, Yoshihara T, Shibata H, Sakamura S, Okazawa Y (1988) Isolation of a specific potato tuber-inducing substance from potato leaves. Plant Cell Physiology **29**: 1047–1051

Kolomiets M V, Hannapel DJ, Chen H, Tymeson M, Gladon RJ (2001) Lipoxygenase is involved in the control of potato tuber development. The Plant Cell **13**: 613–626

Kumar D, Wareing PF (1974) Studies on Tuberization of *Solanum andigena*. New Phytologist **73**: 833–840

Kurakawa T, Ueda N, Maekawa M, Kobayashi K, Kojima M, Nagato Y, Sakakibara H and Kyozuka J (2007) Direct control of shoot meristem activity by a cytokinin-activating enzyme. Nature **445**: 652–655

Lakhotia N, Joshi G, Bhardwaj AR, Katiyar-Agarwal S, Agarwal M, Jagannath A, Goel S, Kumar A (2014) Identification and characterization of miRNAome in root, stem, leaf and tuber developmental stages of potato (*Solanum tuberosum* L.) by high-throughput sequencing. BMC plant biology **14**: 6

Lang Q, Jin C, Lai L, Feng J, Chen S, Chen J (2010) Tobacco microRNAs prediction and their expression infected with Cucumber mosaic virus and Potato virus X. Molecular biology reports **38**: 1523–1531

Lee Y, Kim M, Han J, Yeom K-H, Lee S, Baek SH, Kim VN (2004) MicroRNA genes are transcribed by RNA polymerase II. The EMBO journal **23**: 4051–4060

Li Y, Zhang Q, Zhang J, Wu L, Qi Y, Zhou JM (2010a) Identification of MicroRNAs involved in Pathogen-Associated Molecular Pattern-Triggered plant innate immunity. Plant Physiology **152**: 2222–2231

Li Y-F, Zheng Y, Addo-Quaye C, Zhang L, Saini A, Jagadeeswaran G, Axtell MJ, Zhang W, Sunkar R (2010b) Transcriptome-wide identification of microRNA targets in rice. The Plant journal **62**: 742–759

Livak KJ, Schmittgen TD (2001) Analysis of relative gene expression data using real-time quantitative PCR and the $2^{-\Delta\Delta Ct}$ Method. Methods **25**: 402–408

Lee J, Park JJ, Kim SL, Yim J, An G (2007) Mutations in the rice liguleless generesult in a complete loss of the auricle, ligule and laminar joint. Plant Mol Biol **65:** 487-499

MacIntosh GC, Ulloa RM, Raices M, Tellez-inn MT (1996) Changes in Calcium-Dependent Protein Kinase activity during in vitro tuberization in potato. Plant Physiology **112**: 1541–1550

Mahajan A, Bhogale S, Kang IH, Hannapel DJ, Banerjee AK (2012) The mRNA of a Knotted1-like transcription factor of potato is phloem mobile. Plant Molecular Biology **79**: 595–608

Mallory AC, Reinhart BJ, Jones-Rhoades MW, Tang G, Zamore PD, Barton MK, Bartel DP (2004) MicroRNA control of PHABULOSA in leaf development: importance of pairing to the microRNA 5' region. The EMBO journal **23**: 3356–3364

Mallory AC, Vaucheret H (2006) Functions of microRNAs and related small RNAs in plants. Nature genetics **38**: S31–536

Marin E, Jouannet V, Herz A, Lokerse AS, Weijers D, Vaucheret H, Nussaume L, Crespi MD, Maizel A (2010) miR390, *Arabidopsis* TAS3 tasiRNAs, and their AUXIN RESPONSE FACTOR targets define an autoregulatory network quantitatively regulating lateral root growth. The Plant cell **22**: 1104–1117

Marín-González E, Suárez-López P (2012) "And yet it moves": cell-to-cell and long-distance signaling by plant microRNAs. Plant Science **196**: 18–30

Martin A, Adam H, Díaz-Mendoza M, Zurczak M, González-Schain ND, Suárez-López P (2009) Graft-transmissible induction of potato tuberization by the microRNA miR172. Development **136**: 2873–2881

Martínez-García JF, Virgós-Soler A, Prat S (2002) Control of photoperiod-regulated tuberization in potato by the *Arabidopsis* flowering-time gene CONSTANS. PNAS **99**: 15211–15216

Mauk CS, Langille AR (1978) Physiology of Tuberization in *Solanum tuberosum* L. Plant Physiology **62**: 438–442

Menzel CM (1980) Tuberization in potato at high temperatures : Responses to Gibberellin and growth Inhibitors. Annals of Botany **46**: 259–265

Mica E, Gianfranceschi L, Pè ME (2006) Characterization of five microRNA families in maize. Journal of experimental botany **57**: 2601–2612

Millar A a, Waterhouse PM (2005) Plant and animal microRNAs: similarities and differences. Functional & integrative genomics **5**: 129–135

Muñiz García MN, **Stritzler M, Capiati AD** (2014) Heterologous expression of *Arabidopsis* ABF4 gene in potato enhances tuberization through ABA-GA crosstalk regulation. Planta **239:** 615-631

Murashige T, Skoog F (1962) A revised medium for rapid growth and bioassays with tobacco tissue cultures. Physiologia Plantaria **15**: 473–497

Nair SK, Wang N, Turuspekov Y, Pourkheirandish M, Sinsuwongwat S, Chen G, Sameri M, Tagiri A, Honda I, Watanabe Y, et al (2010) Cleistogamous flowering in barley arises from the suppression of microRNA-guided HvAP2 mRNA cleavage. PNAS **107**: 490–495

Navarro C, Abelenda JA, Cruz-oro E, Cuellar CA, Tamaki S, Silva J, Shimamoto K, Prat S (2011) Control of flowering and storage organ formation in potato by FLOWERING LOCUS T. Nature **478**: 119–122

Nodine MD, Bartel DP (2010) MicroRNAs prevent precocious gene expression and enable pattern formation during plant embryogenesis. Genes & Development **24**: 2678–2692

Nookaraju A, Pandey SK, Upadhyaya CP, Heung JJ, Kim HS, Chun SC, Kim DH, Park SW (2012) Role of Ca^{2+} -mediated signaling in potato tuberization : An overview. Botanical Studies **53**: 177–189

Pais SM, Garcia MNM, Tellez-Inon MT, Capiati DA (2010) Protein phosphatases type 2A mediate tuberization signaling in *Solanum tuberosum* L . leaves. Planta **232**: 37–49

Palatnik JF, Allen E, Wu X, Schommer C, Schwab R, Carrington JC, Weigel D (2003) Control of leaf morphogenesis by microRNAs. Nature **425**: 257–263

Palmer CE, Smith OE (1970) Effect of kinetin on tuber formation on isolated stolons of *Solanum tuberosum* L. cultured in vitro. Plant Cell Physiology **11:**303–14

Pant BD, Buhtz A, Kehr J, Scheible W-R (2008) MicroRNA399 is a long-distance signal for the regulation of plant phosphate homeostasis. The Plant Journal **53**: 731–738

Potato Genome Sequencing Consortium (2011) Genome sequence and analysis of the tuber crop potato. Nature **475**:189–195

Quarrie S (1982) Droopy : a wilty mutant of potato deficient in abscisic acid. Plant, Cell and Environment **5**: 23–26

Ray S, Agarwal P, Arora R, Kapoor S, Tyagi AK (2007) Expression analysis of calcium-dependent protein kinase gene family during reproductive development and abiotic stress conditions in rice (*Oryza sativa* L. ssp. indica). Molecular Genetics and Genomics **5**:493-505

Raices M, Chico JM, Tellez-Inon MT, Ulloa RM (2001) Molecular characterization of StCDPK1 , a calcium-dependent protein kinase from *Solanum tuberosum* that is induced at the onset of tuber development. Plant Molecular Biology **46**: 591–601

Raíces M, Gargantini PR, Chinchilla D, Crespi M, Téllez-Iñón MT, Ulloa RM (2003a) Regulation of CDPK isoforms during tuber development. Plant molecular biology **52**: 1011–24

Raíces M, Ulloa RM, MacIntosh GC, Crespi M, Téllez-Iñón MT (2003b) StCDPK1 is expressed in potato stolon tips and is induced by high sucrose concentration. Journal of experimental botany **54**: 258925–91

Rodríguez-Falcón M, Bou J, Prat S (2006) Seasonal control of tuberization in potato: conserved elements with the flowering response. Annual review of plant biology **57**: 151–80

Rosin FM, Hart JK, Horner HT, Davies PJ, Hannapel DJ (2003a) Overexpression of a Knotted-Like Homeobox Gene of Gibberellin Accumulation. Plant Physiology **132**: 106–117

Rosin FM, Hart JK, Onckelen H Van, Hannapel DJ (2003b) Suppression of a Vegetative MADS Box Gene of Potato Activates Axillary Meristem Development. Plant Physiology **131**: 1613–1622

Roumeliotis E, Kloosterman B, Oortwijn M, Kohlen W, Bouwmeester H, Visser RGF, Bachem CWB (2012) The effects of auxin and strigolactones on tuber initiation and stolon architecture in potato. Journal of experimental botany **63**: 695–709

Samach A, Onouchi H, Gold SE, Ditta GS, Schwarz-sommer Z, Yanofsky MF, Coupland G (2000) Distinct Roles of CONSTANS Target Genes in Reproductive Development of *Arabidopsis*. Science **288**: 1613–1617

Sarkar D (2008) The signal transduction pathways controlling in planta tuberization in potato: an emerging synthesis. Plant cell reports **27**: 1–8

Sarkar D (2010) Photoperiodic inhibition of potato tuberization: an update. Plant Growth Regulation **62**: 117–125

Sawa M, Nusinow DA, Kay SA, Imaizumi T (2007) FKF1 and GIGANTEA Complex Formation Is Required for Day-Length Measurement in *Arabidopsis*. Science **318**: 261–265

Schwab R, Palatnik JF, Riester M, Schommer C, Schmid M, Weigel D (2005) Specific Effects of MicroRNAs on the Plant Transcriptome. Developmental Cell **8**: 517–527

Shibaoka H (1993) Regulation by gibberellins of the orientation of cortical microtubules in plant cells. Australian Journal of Plant Physiology **20:**461–470

Shikata M, Koyama T, Mitsuda N, Ohme-takagi M (2009) *Arabidopsis* SBP-Box Genes SPL10, SPL11 and SPL2 control morphological change in association with shoot maturation in the reproductive phase. Plant and Cell Physiology **50**: 2133–2145

Simmons KE, Kelling KA (1987) Potato responses to calcium application. American Potato Journal **64**: 119–136

Song YH, Smith RW, To BJ, Millar AJ, Imaizumi T (2012) FKF1 Conveys Timing Information for CONSTANS Stabilization in Photoperiodic Flowering. Science **336**: 1045–1050

Sterck L, Billiau K, Abeel T, Rouze P, Van de Peer Y (2012) ORCAE: Online Resource for Community Annotation of Eukaryotes. Nat methods **9**: 1041

Suárez-López P, Wheatley K, Robson F, Onouchi H, Valverde F, Coupland G (2001) CONSTANS mediates between the circadian clock and the control of ¯ owering in *Arabidopsis*. Nature **410**: 1116–1120

Sunkar R, Zhu J (2004) Novel and Stress-Regulated MicroRNAs and other Small RNAs from *Arabidopsis*. The Plant Cell **16**: 2001–2019

Takahashi F, Fujino K, Kikuta Y, Koda Y (1994) Expansion of potato cells in response to jasmonic acid. Plant Science **100:**3–8

Takezawa D, ZH L, An G, Poovaiah B (1995) Calmodulin gene family in potato: developmental and touch-induced expression of the mRNA encoding a novel isoform. Plant Molecular Biology **27**: 693–703

Tamaki S, Matsuo S, Wong HL, Yokoi S, Shimamoto K (2007) Hd3a Protein Is a Mobile Flowering Signal in Rice. Science **316**: 1033–1037

Tantikanjana T, Yong JWH, Letham DS, Griffith M, Hussain M, Ljung K, Sandberg G, Sundaresan V (2001) Control of axillary bud initiation and shoot architecture in *Arabidopsis* through the SUPERSHOOT gene. Genes and Development **15**: 1577–1588

Usami T, Horiguchi G, Yano S, Tsukaya H (2009) The more and smaller cells mutants of *Arabidopsis thaliana* identify novel roles for SQUAMOSA PROMOTER BINDING PROTEIN-LIKE genes in the control of heteroblasty. Development **136**: 955–964

Valmonte GR, Arthur K, Higgins CM, MacDiarmid RM (2014) Calcium-dependent protein kinases in plants: evolution, expression and function. Plant & cell physiology **55**: 551–569

Varkonyi-Gasic E, Gould N, Sandanayaka M, Sutherland P, MacDiarmid RM (2010) Characterisation of microRNAs from apple (*Malus domestica* "Royal Gala") vascular tissue and phloem sap. BMC Plant Biology **10**: 159

Varkonyi-Gasic E, Wu R, Wood M, Walton EF, Hellens RP (2007) Protocol: a highly sensitive RT-PCR method for detection and quantification of microRNAs. Plant methods **3**: 12

Voinnet O (2009) Origin, biogenesis, and activity of plant microRNAs. Cell **136**: 669–687

Werner H (1934) The Effect of Temperature, Photoperiod and Nitrogen level upon Tuberization in the Potato. The American Potato Journal 274–280

Wheeler RM, Tibbitts TW (1986) Growth and Tuberization of Potato (*Solanum tuberosum* L.) under Continuous Light. Plant Physiology **80**: 801–804

Wong CE, Zhao Y-T, Wang X-J, Croft L, Wang Z-H, Haerizadeh F, Mattick JS, Singh MB, Carroll BJ, Bhalla PL (2011) MicroRNAs in the shoot apical meristem of soybean. Journal of experimental botany **62**: 2495–2506

Wu G, Park MY, Conway SR, Wang J-W, Weigel D, Poethig RS (2009) The Sequential Action of miR156 and miR172 Regulates Developmental Timing in *Arabidopsis*. Cell **138**: 750–759

Wu G, Poethig S (2006) Temporal Regulation of Shoot Development in *Arabidopsis* thaliana By miR156 and its target SPL3. Development **133**: 3539–3547

Xie F, Frazier TP, Zhang B (2011) Identification, characterization and expression analysis of MicroRNAs and their targets in the potato (*Solanum tuberosum*). Gene **473**: 8–22

Xie F, Zhang B (2010) Target-align : a tool for plant microRNA target identification. Bioinformatics **26**: 3002–3003

Xie K, Wu C, Xiong L (2006) Genomic Organization, Differential Expression, and Interaction of SQUAMOSA Promoter-Binding-Like Transcription Factors and microRNA156 in Rice. Plant Physiology **142**: 280–293

Xie Z, Allen E, Fahlgren N, Calamar A, Givan SA, Carrington JC (2005) Expression of *Arabidopsis* MIRNA Genes. Plant Physiology **138**: 2145–2154

Xing S, Salinas M, Höhmann S, Berndtgen R, Huijser P (2010) miR156-Targeted and Nontargeted SBP-Box Transcription Factors Act in Concert to Secure Male Fertility in *Arabidopsis*. The Plant Cell **22**: 3935–3950

Xu MY, Dong Y, Zhang QX, Zhang L, Luo YZ, Sun J, Fan YL, Wang L (2012) Identification of miRNAs and their targets from *Brassica napus* by high-throughput sequencing and degradome analysis. BMC genomics **13**: 421–435

Xu X, Lammeren AM Van, Vermeer E, Vreugdenhil D (1998a) The Role of Gibberellin , Abscisic Acid , and Sucrose in the Regulation of Potato Tuber Formation in Vitro. Plant Physiology **117**: 575–584

Xu X, Vreugdenhil D, van Lammeren, A. A. M (1998b) Cell division and cell enlargemnent during potato tuber formation. J Exp Bot **49**: 573-582

Yang T, Xue L, An L (2007) Functional diversity of miRNA in plants. Plant Science **172**: 423–432

Yang W, Liu X, Zhang J, Feng J, Li C, Chen J (2009) Prediction and validation of conservative microRNAs of *Solanum tuberosum* L. Molecular Biology Reports **37**: 3081–3087

Yoo B, Kragler F, Varkonyi-gasic E, Haywood V, Archer-Evans S, Lee YM, Lough TJ, Lucas WJ (2004) A Systemic Small RNA Signaling System in Plants. The Plant Cell **16**: 1979–2000

Yu YY, Lashbrook CC, Hannapel DJ (2007) Tissue integrity and RNA quality of laser microdissected phloem of potato. Planta **226**: 797–803

Zanca AS, Vicentini R, Ortiz-Morea F a, Del Bem LE, Da Silva MJ, Vincentz M, Nogueira FT (2010) Identification and expression analysis of microRNAs and targets in the biofuel crop sugarcane. BMC Plant Biology **10**: 260

Zeevaart JA (2006) Florigen Coming of Age after 70 Years. The Plant Cell **18**: 1783–1789

Zhang H, Jin J, Tang L, Zhao Y, Gu X, Gao G, Luo J (2011a) PlantTFDB 2.0: update and improvement of the comprehensive plant transcription factor database. Nucleic Acids Research **39**: D1114–D1117

Zhang R, Marshall D, Bryan GJ, Hornyik C (2013) Identification and characterization of miRNA transcriptome in potato by high-throughput sequencing. PloS one **8**: e57233

Zhang W, Luo Y, Gong X, Zeng W, Li S (2009) Computational identification of 48 potato microRNAs and their targets. Computational Biology and Chemistry **33**: 84–93

Zhang X, Zou Z, Zhang J, Zhang Y, Han Q, Hu T, Xu X, Liu H, Li H, Ye Z (2011b) Over-expression of sly-miR156a in tomato results in multiple vegetative and reproductive trait alterations and partial phenocopy of the sft mutant. FEBS Letters **585**: 435–439

Zhu J (2008) Reconstituting plant miRNA biogenesis. PNAS **105**: 9851–9852

Zhu Q-H, Helliwell C a (2010) Regulation of flowering time and floral patterning by miR172. Journal of experimental botany **62**: 487–495

Zuker M (2003) Mfold web server for nucleic acid folding and hybridization prediction. Nucleic Acids Research **31**: 3406–3415

Author’s publication

MicroRNA156: A Potential Graft-Transmissible MicroRNA That Modulates Plant Architecture and Tuberization in *Solanum tuberosum* ssp. *andigena*[1][C][W][OPEN]

Sneha Bhogale, Ameya S. Mahajan, Bhavani Natarajan, Mohit Rajabhoj, Hirekodathakallu V. Thulasiram, and Anjan K. Banerjee*

Indian Institute of Science Education and Research, Biology Division, Pune 411008, Maharashtra, India (S.B., A.S.M., B.N., M.R., A.K.B.); and Council of Scientific and Industrial Research-National Chemical Laboratory, Chemical Biology Unit, Division of Organic Chemistry, Pune 411008, Maharashtra, India (H.V.T.)

MicroRNA156 (*miR156*) functions in maintaining the juvenile phase in plants. However, the mobility of this microRNA has not been demonstrated. So far, only three microRNAs, *miR399*, *miR395*, and *miR172*, have been shown to be mobile. We demonstrate here that *miR156* is a potential graft-transmissible signal that affects plant architecture and tuberization in potato (*Solanum tuberosum*). Under tuber-noninductive (long-day) conditions, *miR156* shows higher abundance in leaves and stems, whereas an increase in abundance of *miR156* has been observed in stolons under tuber-inductive (short-day) conditions, indicative of a photoperiodic control. Detection of *miR156* in phloem cells of wild-type plants and mobility assays in heterografts suggest that *miR156* is a graft-transmissible signal. This movement was correlated with changes in leaf morphology and longer trichomes in leaves. Overexpression of *miR156* in potato caused a drastic phenotype resulting in altered plant architecture and reduced tuber yield. *miR156* overexpression plants also exhibited altered levels of cytokinin and strigolactone along with increased levels of LONELY GUY1 and StCyclin D3.1 transcripts as compared with wild-type plants. RNA ligase-mediated rapid amplification of complementary DNA ends analysis validated SQUAMOSA PROMOTER BINDING-LIKE3 (StSPL3), StSPL6, StSPL9, StSPL13, and StLIGULELESS1 as targets of *miR156*. Gel-shift assays indicate the regulation of *miR172* by *miR156* through StSPL9. *miR156*-resistant SPL9 overexpression lines exhibited increased *miR172* levels under a short-day photoperiod, supporting *miR172* regulation via the *miR156*-SPL9 module. Overall, our results strongly suggest that *miR156* is a phloem-mobile signal regulating potato development.

Long-distance transport of signaling molecules is known to be a major component in regulating plant growth and development as well as their adaptation to changing environmental conditions. This transport is implemented by the plant's vascular system, especially through the complex of companion cells and sieve elements present in the phloem. Recent evidence has established the movement of macromolecules like proteins, mRNAs, and microRNAs (miRNAs) through the phloem. It is now clear that these entities act as long-distance signals for development and stress response pathways (Kehr and Buhtz, 2008; Atkins et al., 2011). A well-established example is the movement of FLOWERING TIME protein from leaves to the shoot apex in Arabidopsis (*Arabidopsis thaliana*) as a long-distance signal for the regulation of flowering time (Corbesier et al., 2007). Similarly, the movement of transcripts such as *GIBBERELLIC ACID INSENSITIVE* (Haywood et al., 2005), *BELL1 LIKE TRANSCRIPTION FACTOR5* (Banerjee et al., 2006a; Lin et al., 2013), *TOMATO KNOTTED2* (Kim et al., 2001), and *POTATO HOMEOBOX1 TRANSCRIPTION FACTOR* (Mahajan et al., 2012), acting as long-distance signals for plant developmental processes such as leaf development, tuberization, and root growth, has been demonstrated. The movement of small interfering RNAs is also reported in a few cases where the induction of posttranscriptional gene silencing against viruses has been well studied (Waterhouse et al., 2001). In addition, small interfering RNAs were also demonstrated to be mobile and to exert epigenetic changes in recipient cells (Molnar et al., 2010). However, very limited information is available on the mobility of plant miRNAs, another group of small noncoding RNAs. Recent reviews have summarized the miRNAs found in phloem exudates of different plant species, but little information is available on their mobility (Kehr and Buhtz, 2008, 2013; Chuck and O'Connor, 2010).

The cellular movement of *microRNA165/166* (*miR165/166*) in root patterning, where mature *miR165/166* appears

[1] This work was supported by the Indian Institute of Science Education and Research, the Council of Scientific and Industrial Research, India, and the Department of Biotechnology, India.

* Address correspondence to akb@iiserpune.ac.in.

The author responsible for distribution of materials integral to the findings presented in this article in accordance with the policy described in the Instructions for Authors (www.plantphysiol.org) is: Anjan Kumar Banerjee (akb@iiserpune.ac.in).

[C] Some figures in this article are displayed in color online but in black and white in the print edition.

[W] The online version of this article contains Web-only data.

[OPEN] Articles can be viewed online without a subscription.

www.plantphysiol.org/cgi/doi/10.1104/pp.113.230714

to move from its site of biogenesis to adjacent cell layers, is an example of the short-distance movement of miRNA (Carlsbecker et al., 2010; Miyashima et al., 2011). Although some reports (Yoo et al., 2004; Buhtz et al., 2008; Varkonyi-Gasic et al., 2010) have demonstrated the presence of numerous miRNAs in phloem tissues, so far, only three miRNAs (*miR399*, *miR395*, and *miR172*) have been shown to move long distance in plants. *miR399* acts as a long-distance mobile signal that regulates phosphate homeostasis in Arabidopsis (Pant et al., 2008), whereas *miR395* was shown to move from wild-type scions to rootstocks of the miRNA-processing mutant *hen1-1* under sulfate stress (Buhtz et al., 2010). In another study, Martin and coworkers (2009) proposed that *miR172* functions as a long-distance mobile signal for potato (*Solanum tuberosum*) tuberization. Later, Kasai et al. (2010) showed that *miR172* molecules can move systemically from source to sink tissues in *Nicotiana benthamiana*. Earlier studies have shown that *miR172*, along with another miRNA (*miR156*), regulate phase transitions and flowering in Arabidopsis. *miR172* has been demonstrated to promote adult phase and flowering, whereas *miR156* is involved in juvenile stage development (Wu et al., 2009). Similar roles of *miR156* and *miR172* were also reported in rice (*Oryza sativa*; Xie et al., 2006) and maize (*Zea mays*; Chuck et al., 2007). Sequential action of both these miRNAs appears to be pivotal for phase transition and flowering in plant development. Flowering and tuberization are reproductive strategies that bear similar environmental cues and molecular players (Jackson, 2009). With the evidence of *miR172* being involved in both these pathways, we hypothesize that *miR156* could be involved in the potato tuberization pathway acting in concert with *miR172*.

miR156 is a well-conserved miRNA present in all land plants (Axtell and Bowman, 2008). It targets the transcripts of SQUAMOSA PROMOTER BINDING-LIKE (SPL) transcription factors and acts as a master regulator of plant development (Schwab et al., 2005). In Arabidopsis, *miR156* overexpression results in a prolonged juvenile phase and a delay in flowering, with increased branching and production of a large number of leaves (Huijser and Schmid, 2011). Similar phenotypes of *miR156* overexpression were also observed in rice (Xie et al., 2006), maize (Chuck et al., 2007), switchgrass (*Panicum virgatum*; Fu et al., 2012), and tomato (*Solanum lycopersicum*; Zhang et al., 2011b). In a recent study, Eviatar-Ribak et al. (2013) overexpressed the Arabidopsis *miR156* gene in potato (cv Desiree), where *miR156*-overexpressing lines exhibited suppressed leaf complexity and produced aerial tubers, indicating a role of *miR156* in tuberization. In addition to these functions, *miR156* and its targets, SPL transcription factors, have also been shown to regulate embryonic patterning (Nodine and Bartel, 2010), anthocyanin biosynthesis (Gou et al., 2011), and male fertility (Xing et al., 2010). Interestingly, *miR156* has also been detected in phloem sap of pumpkin (*Cucurbita maxima*; Yoo et al., 2004), Arabidopsis, apple (*Malus domestica*; Varkonyi-Gasic et al., 2010), and *Brassica napus* (Buhtz et al., 2008, 2010). miRNAs present in phloem exudates are proposed to be mobile, with a putative role as long-distance regulators of development and stress pathways by acting on target genes (Marín-González and Suárez-López, 2012). Although *miR156* is known to interact with the transcripts of SPL transcription factors, the mobility of *miR156* in plants has not yet been investigated.

In this study, we have identified and validated a *miR156a* precursor from potato. To understand the role of *miR156* and its target genes in potato development, we employed a number of strategies, including target gene validations, transgenic analysis, assays of *miR156* abundance, high-resolution mass spectrometry (HR-MS)-based hormone quantification, phloem sap analysis, and grafting. Our results suggest that *miR156* is a graft-transmissible signal that affects plant architecture and tuber development in potato. It is present in the phloem of wild-type plants, and it accumulates in short-day (SD)-induced stolons to facilitate tuber formation. In addition, *miR156* overexpression (OE) lines show multiple morphological changes and produce aerial tubers under inductive conditions. Although the formation of aerial tubers was recently demonstrated by Eviatar-Ribak et al. (2013), our study reveals additional novel functions of *miR156* in potato. Based on its accumulation in phloem sap of wild-type plants and its graft-transmissible effect, our results suggest that *miR156* moves through the phloem and regulates development in potato.

RESULTS

Identification, Validation, and Expression Analysis of *miR156* in Potato

miR156 was predicted to be present in potato by an in silico analysis reported earlier (Zhang et al., 2009). The MFold-predicted secondary structure (Zuker, 2003) of the *miR156a* precursor sequence (BI432985.1) had a hairpin loop with mature *miR156* in its stem region, a characteristic of miRNA precursors (Fig. 1A). To validate the presence of the *miR156a* precursor in potato, reverse transcription (RT)-PCR was performed, and the amplified fragment was sequence confirmed (Fig. 1B). A 20-bp mature *miR156* was detected by stem-loop end-point PCR in leaves and was verified by sequencing (Fig. 1C), demonstrating that *miR156* is expressed in potato.

The relative levels of *miR156* were analyzed by stem-loop quantitative reverse transcription (qRT)-PCR in potato plants of different age groups. Two-week-old plants showed higher accumulation of *miR156* in stem, and their levels decreased as the plant aged. However, *miR156* levels varied in mature leaves of plants of different ages (Fig. 1D). To determine whether *miR156* expression is regulated by the photoperiod, plants were grown under long-day (LD; tuber-noninductive) and SD (tuber-inductive) conditions. Stem-loop qRT-PCR analysis demonstrated a higher accumulation of *miR156* in leaves and stem under LD conditions as compared

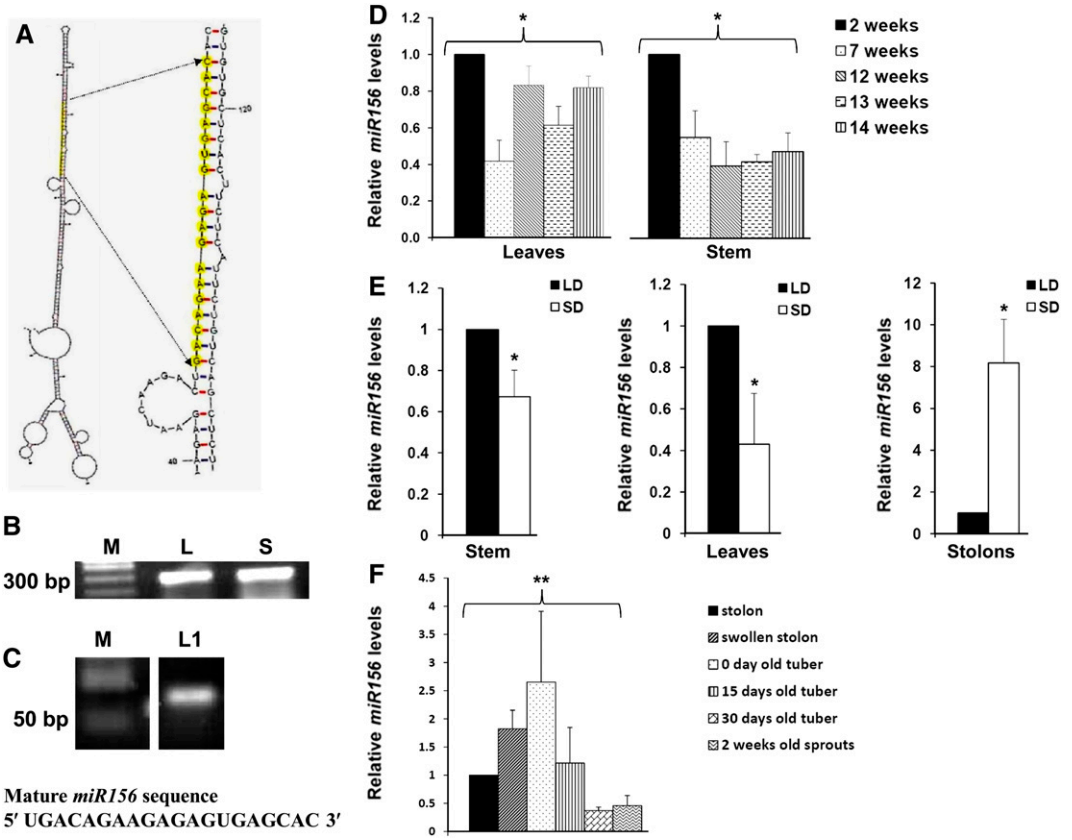

Figure 1. Identification, validation, and expression analysis of *miR156* in potato. A, Secondary structure of *miR156a* precursor as predicted by MFold (Zuker, 2003). Mature *miR156* sequence is highlighted in yellow. B, RT-PCR of *miR156a* precursor from leaf (L) and shoot (S). M represents a DNA marker. C, Stem-loop RT-PCR of mature *miR156* from leaves of LD-grown plants (L1). D, Age-specific *miR156* abundance in leaves and stem of wild-type potato grown under LD photoperiod. Error bars indicate SD of two biological replicates each with three technical replicates. Asterisks indicate one-factor ANOVA (*$P < 0.05$). E, *miR156* abundance in stem, leaves, and stolons of wild-type potato grown under LD and SD photoperiods for 15 dpi. Error bars indicate SD of three biological replicates each with three technical replicates. Asterisks indicate Student's *t* test (*$P < 0.05$). F, Relative abundance of *miR156* in different developmental stages of tuber formation and dormancy. Error bars indicate SD of three biological replicates each with three technical replicates. Asterisks indicate one-factor ANOVA (**$P < 0.01$). [See online article for color version of this figure.]

with the plants under the SD photoperiod (Fig. 1E). However, in stolons, *miR156* levels were found to be approximately 8-fold higher under SD as compared with LD photoperiod (Fig. 1E). Our analysis showed a range of *miR156* abundance in swollen stolons, tubers stored postharvest for different time periods (0, 15, and 30 d), and 2-week-old sprouts. Zero-day-old tubers (postharvest) showed an approximately 2.5-fold higher accumulation than in stolons harvested from SD-induced plants, whereas *miR156* levels in juvenile tuber sprouts were almost half the level in stolons (Fig. 1F). Overall, our expression analysis suggests that *miR156* shows tissue-specific accumulation with respect to the age of the plant and the photoperiod.

Overexpression of *miR156* Affects Multiple Morphological Traits

The level of *miR156* in *miR156* OE lines (*miR156* OE 5.1 and 6.2) was determined by stem-loop qRT-PCR (Supplemental Fig. S1, A and B). Two-week-old OE lines exhibited a drastic change in leaf phenotype (Fig. 2, A and B), and as they matured, they did not form an inflorescence compared with wild-type plants (Fig. 2, C and D). These plants did not flower even after 18 weeks of growth, whereas wild-type plants produced inflorescences in 12 weeks. *miR156* OE plants also exhibited enhanced branching from axillary buds and an increased number of nodes, resulting in a bushy appearance (Fig. 2, E–H). The fresh weight of roots in OE lines was also significantly reduced (Fig. 2I). The leaf architecture of *miR156* OE lines was dramatically affected. *miR156* OE plants produced smaller leaves with reduced leaflet number (Fig. 3, A and B). The venation pattern was found to be altered such that the side veins of transgenic leaves were less prominent (Fig. 3, C and D). Transverse sections of leaves showed disoriented cell arrangement as well as the presence of large epidermal cells in the *miR156* OE 5.1 line (Fig. 3, E and F). We also observed a reduction in stomatal

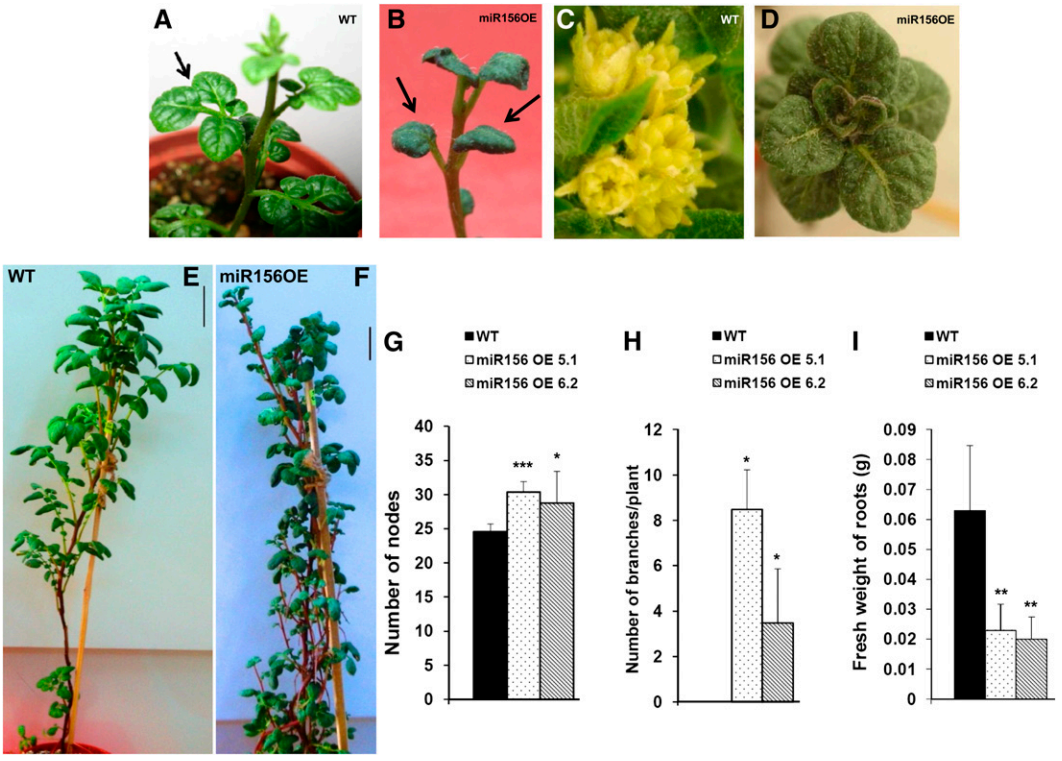

Figure 2. Overexpression of *miR156* affects multiple morphological traits in potato. A and B, Two-week-old plants of the wild type (WT; A) and *miR156* OE 5.1 (B). C and D, Inflorescence produced at the apical tip of 12-week-old wild-type potato plants (C), while *miR156* OE 5.1 plants of the same age produced leaves (D). E and F, Twelve-week-old plants of wild-type (E) and *miR156* OE 5.1 (F) lines of potato. Bars = 5 cm. G to I, Number of nodes (G; $n = 5$), number of axillary branches (H; $n = 4$), and fresh weight of roots (I; $n = 6$) of wild-type and *miR156* OE plants. Error bars indicate SD. Asterisks indicate statistical differences as determined using Student's *t* test (***$P < 0.001$, **$P < 0.01$, *$P < 0.05$). [See online article for color version of this figure.]

density in both OE lines as opposed to the wild type (Fig. 3, G–J). In addition, trichome number was reduced with an increase in trichome length in OE lines (Fig. 3, K–O). To gain more insight into the function of *miR156*, 35S::*miR156* tobacco (*Nicotiana tabacum*) plants were generated. All the tobacco OE plants showed a similar phenotype to that observed in *miR156* OE potato plants (Supplemental Fig. S2).

miR156 Regulates Potato Tuberization

To examine whether an increase in *miR156* levels in OE lines could have any impact on tuber development, we examined the tuberization phenotype of the *miR156* OE 5.1 and 6.2 lines. OE line 5.1 produced aerial and underground tubers after 4 weeks of SD induction, whereas wild-type plants grown under an SD photoperiod only produced underground tubers (Fig. 4, A–C). Line 6.2 produced underground tubers and showed a delayed formation of aerial tubers. None of the plants produced tubers under the LD photoperiod.

Overall, *miR156* OE lines (5.1 and 6.2) developed fewer underground tubers and showed reduced tuber yields (Table I). Previous reports have shown *miR172* and the *Flowering Locus T*-like paralog *StSP6A* to act as positive regulators of tuberization (Martin et al., 2009; Navarro et al., 2011). Since *miR156* OE lines exhibited reduced tuber yield, we investigated the levels of *StSP6A* and *miR172* (tuberization markers) in leaves of OE plants. Also, *miR172* levels were quantified in SD-induced stolons. Our results showed a reduction in the levels of the tuberization markers *miR172* and *StSP6A* in *miR156* OE lines. *miR172* levels were reduced by approximately 80% in leaves and stolons, while *StSP6A* levels were reduced by approximately 60% in leaves (Fig. 4, D–F).

Zeatin Riboside and Orobanchyl Acetate Levels Are Affected by *miR156* Overexpression

miR156 overexpression in potato resulted in a drastic phenotype of increased branching, a higher number of leaves with reduced leaflets, and a delay in flowering, a phenotype that was also recently described for tomato LONELY GUY1 (TLOG1) overexpression in tomato (Eviatar-Ribak et al., 2013). LONELY GUY1 (LOG1) is a cytokinin biosynthetic gene that converts cytokinin ribosides to biologically active cytokinin (Kurakawa et al., 2007). Considering the role of cytokinins in branching (Domagalska and Leyser, 2011), we investigated the effect of *miR156* on the cytokinin pathway. *miR156* OE plants

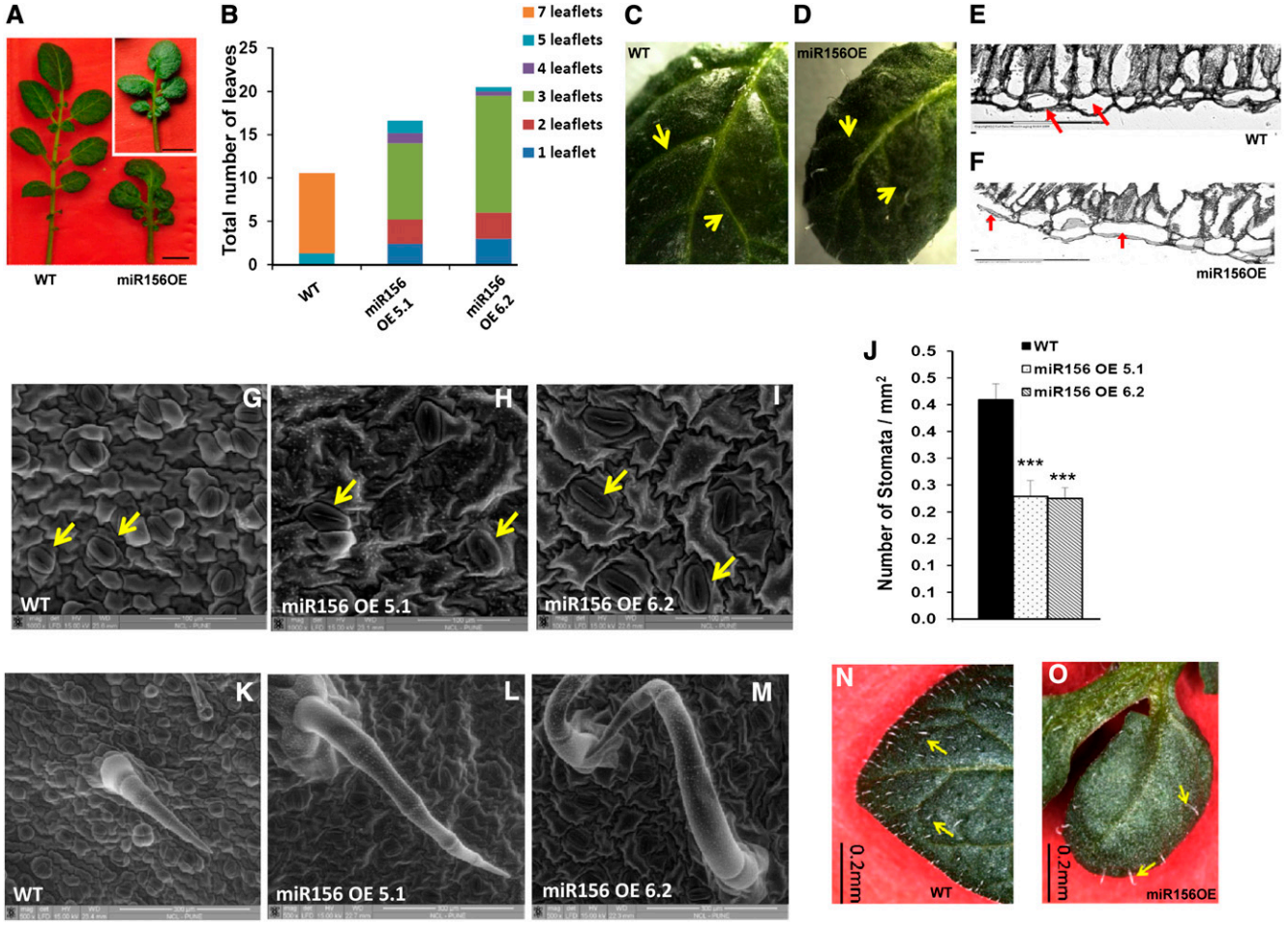

Figure 3. Effect of *miR156* overexpression on leaf development of potato. A, Leaves of 8-week-old wild-type (WT) and *miR156* OE 5.1 and 6.2 (inset) plants. Bars = 1 cm. B, Distribution of the number of leaflets per leaf in 8-week-old wild-type and *miR156* OE 5.1 and 6.2 plants. C and D, Venation pattern of wild-type leaf (C) and *miR156* OE 5.1 leaf (D). Arrows indicate veins. E and F, Transverse sections of leaves (20×) of wild-type (E) and *miR156* OE 5.1 (F) plants showing differences in leaf architecture. The epidermal cells are marked by arrows. G to I, eSEM images of the leaf surface showing differences in the size of epidermal cells and stomata (marked by arrows) for wild-type (G) and *miR156* OE 5.1 (H) and *miR156* OE 6.2 (I) plants. Bars = 100 μm. J, Stomatal density of wild-type and *miR156* OE 5.1 and 6.2 plants ($n = 5$). Error bars indicate SD. Asterisks indicate statistical differences as determined using Student's *t* test (***$P < 0.001$). K to M, eSEM images of trichomes for wild-type (K) and *miR156* OE 5.1 (L) and *miR156* OE 6.2 (M) plants. Bars = 300 μm. N and O, Trichome phenotype of wild-type leaf (N) and *miR156* OE 5.1 leaf (O). Bars = 0.2 mm. [See online article for color version of this figure.]

showed approximately 1.8-fold increased expression of *StLOG1* in the axillary meristems as compared with wild-type plants (Fig. 5A). Also, the levels of *StCyclin D3.1*, a cytokinin-responsive gene, were increased up to approximately 8-fold as compared with wild-type plants (Fig. 5B). To determine the amount of cytokinin (zeatin riboside), HR-MS analysis demonstrated increased levels (more than 2-fold) in *miR156* OE plants as compared with the wild type in both SD and LD conditions (Fig. 5C; Supplemental Figs. S3 and S4). As strigolactones are also considered to be branching hormones (Domagalska and Leyser, 2011), we investigated the levels of one such strigolactone: orobanchyl acetate. HR-MS analysis demonstrated reduced levels of orobanchyl acetate (approximately 20% under LD conditions and approximately 60% under SD conditions) in *miR156* OE plants as compared with the wild type (Fig. 5D; Supplemental Figs. S5 and S6). The changes in these hormone amounts correlated with the branching phenotype observed in *miR156* OE lines.

miR156 Targets *StSPL* Transcription Factors

Our in silico analysis with psRNATarget software (plantgrn.noble.org/psRNATarget; Dai and Zhao, 2011) predicted 12 potential target genes for *miR156* in potato (Supplemental Table S1). Further analysis of these target genes revealed that nine out of the 12 genes (including LIGULELESS1 [LG1]) belong to the SPL family of transcription factors. Two belong to the DNA topoisomerase family of proteins, while one target is of unknown function. Additionally, we have

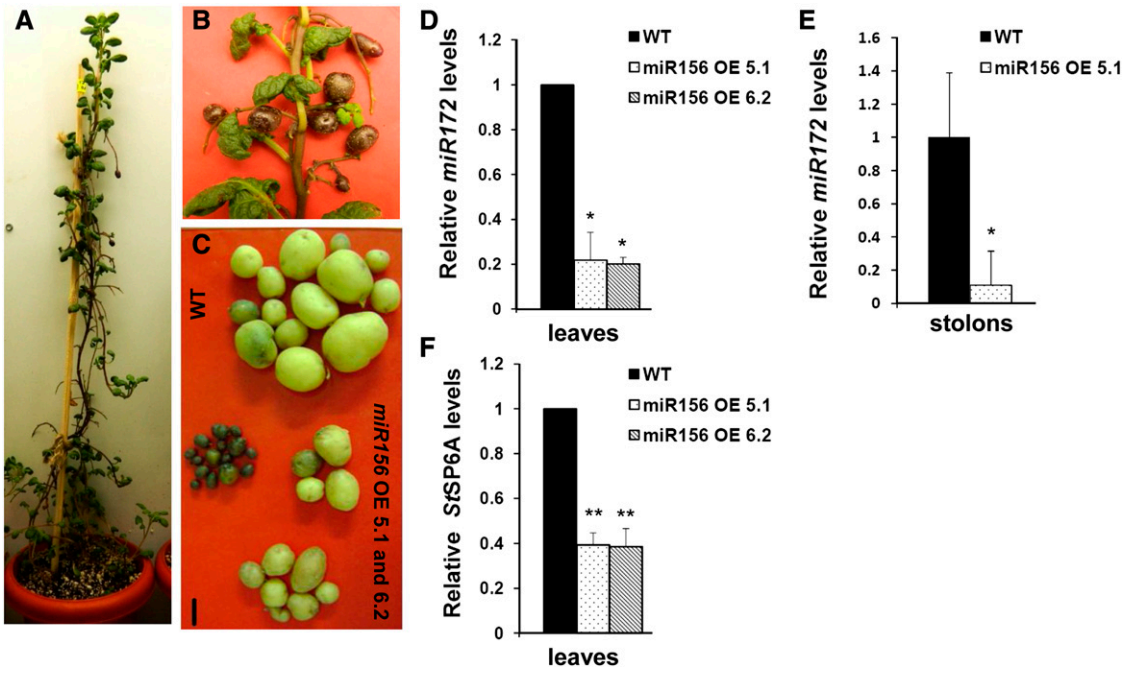

Figure 4. *miR156* regulates potato tuberization. A, *miR156* OE 5.1 plant incubated for 30 d under SD conditions. B, Aerial tubers developed on *miR156* OE 5.1. C, Tubers of representative wild-type (WT) and miR156 OE line 5.1 and 6.2 plants. Bar = 1 cm. D to F, Levels of tuberization markers: miR172 in 8-d post SD-induced leaves of wild-type and miR156 OE line 5.1 and 6.2 plants (D); *miR172* in 15-d post SD-induced stolons of wild-type and *miR156* OE line 5.1 plants (E); and *StSP6A* in 8-d post SD-induced leaves of wild-type and *miR156* OE line 5.1 and 6.2 plants (F). For *miR172* in leaves (D), error bars indicate SD of two biological replicates each with three technical replicates; for *miR172* in stolons (E; 15 dpi in SD conditions), error bars indicate SD of one biological replicate with three technical replicates; for *StSP6A* (F), semiquantitative analysis was performed with three independent replicates. Error bars indicate SD of three replicates. Asterisks indicate statistical differences as determined using Student's *t* test (*$P < 0.05$, **$P < 0.01$). [See online article for color version of this figure.]

also predicted all these target genes by TargetAlign software. Finally, based on their scores and consistency of analysis in both softwares, we short listed five *miR156* target genes, *StSPL3*, *StSPL6*, *StSPL9*, *StSPL13*, and *StLG1*, for further analysis. To determine if these genes are the targets of *miR156* in potato, modified RNA ligase-mediated (RLM) 5′ RACE was performed. RNA sequences with 5′ termini corresponding to the 10th/11th nucleotides of *miR156* were consistently detected, demonstrating that *StSPL6*, *StSPL9*, *StSPL13*, and *StLG1* are targeted by *miR156* in vivo (Fig. 6, A and B). However, *StSPL3* was cleaved at sites other than the 10th/11th nucleotides of *miR156*, which is not a common observation in plant miRNAs. Levels of these targets were also quantified in *miR156* OE plants. As expected, transcript levels of these targets showed different degrees of reduction (*StSPL3*, approximately 80%; *StLG1*, 70%; *StSPL13*, 60%; *StSPL9*, 40%; and *StSPL6*, 30% in *miR156* OE 5.1 plants [Fig. 6C]). Our results are consistent with previous studies on the *miR156*-SPL interaction (Schwab et al., 2005).

Regulation of *miR172* by the *miR156*-SPL Module

Overexpression of *miR156* in potato resulted in lower tuber yields and reduced levels of *miR172* and *SPLs* as mentioned above. Our bioinformatic analysis of the StMIR172b promoter showed the presence of multiple GTAC motifs, characteristic of SPL binding (Birkenbihl et al., 2005). We chose to continue our investigation with StSPL9, since the *miR156*-SPL9 interaction has previously been demonstrated in Arabidopsis (Wu et al., 2009) and rice (Jiao et al., 2010), suggesting that a similar interaction module might also be conserved in potato. To examine if StSPL9 binds to the StMIR172b promoter, gel retardation assays were performed. The StMIR172b promoter was analyzed in four fragments (P1–P4; Fig. 7A), having two binding motifs in the P1 fragment, a single motif each in P2 and P3, while P4 served as a negative control. Recombinant StSPL9 protein (42 kD) retarded the mobility of the P1 promoter sequence, whereas the other three promoter

Table I. *Tuber yields (tuber number and weight) of wild-type and miR156 OE 5.1 and 6.2 plants incubated under SD conditions for 30 d*

Means of three plants each were calculated.

Plant	No. of Tubers	Weight of Tubers
		g
Wild type	13.0 ± 1.73	37.7 ± 2.75
miR156 OE 5.1	4.66 ± 1.15	5.83 ± 0.75
miR156 OE 6.2	7 ± 1.0	6.52 ± 2.55

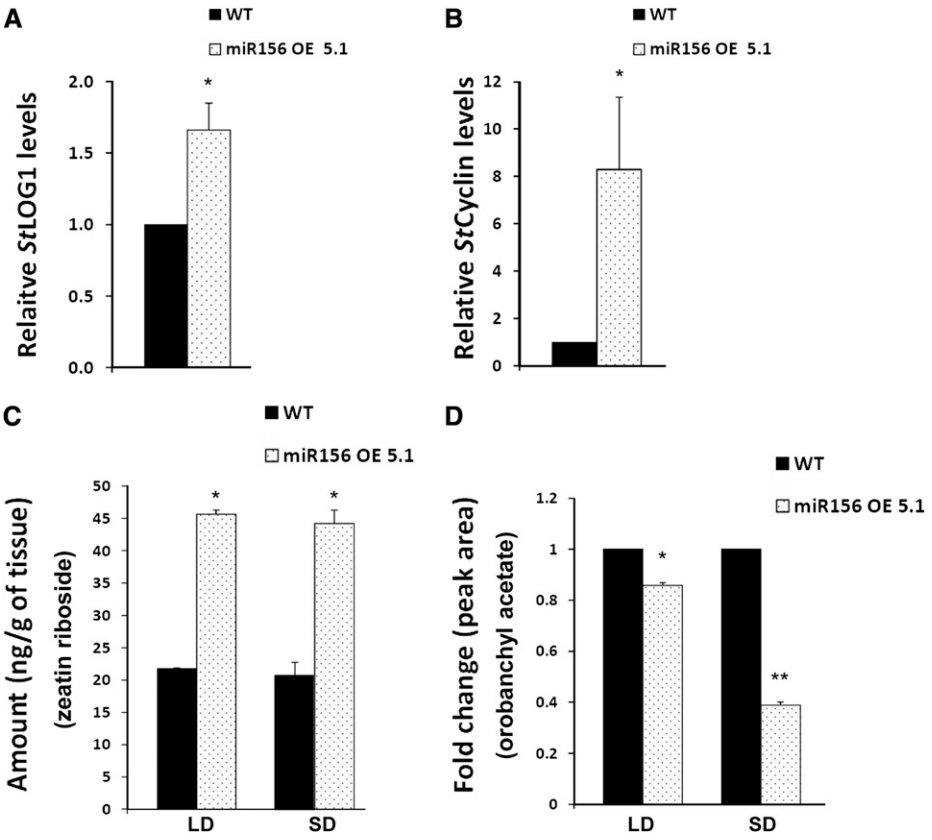

Figure 5. Zeatin riboside and orobanchyl acetate levels are affected by *miR156* overexpression. A and B, qRT-PCR analysis of *StLOG1* (A) and *StCyclin D3.1* (B) in axillary meristems of wild-type (WT) and miR156 OE 5.1 plants incubated for 15 d under SD conditions. Error bars indicate SD of three biological replicates each with three technical replicates. Asterisks indicate statistical differences as determined using Student's *t* test (*$P < 0.05$). C and D, HR-MS analysis of wild-type and *miR156* OE 5.1 plants for zeatin riboside (C) and orobanchyl acetate (D). The tissues were axillary meristems of wild-type and *miR156* OE 5.1 plants incubated for 15 d under both SD and LD conditions. Error bars indicate SD of two biological replicates. Asterisks indicate statistical differences as determined using Student's *t* test (*$P < 0.05$, **$P < 0.01$).

fragments (P2–P4) remained unaffected (Fig. 7B). Competition gel retardation assays were performed with ^{32}P-labeled and unlabeled P1 fragment. With increased unlabeled P1, the P1-SPL9 complex was diminished over time (Fig. 7C). Our analysis demonstrated StSPL9-MIR172 promoter interactions in vitro, with StSPL9 binding to a promoter region with two binding sites.

To further validate the *miR156*-StSPL9 interaction, we generated *miR156*-resistant StSPL9 OE potato plants (rSPL9 OE lines) driven by the cauliflower mosaic virus (CaMV) 35S promoter (Supplemental Fig. S7, A and B). rSPL9 transgenics were generated by introducing silent mutations in the microRNA recognition element (MRE), so that the mutated transcript is no longer recognized by *miR156*. Stem-loop qRT-PCR analysis revealed an approximately 5-fold increase in levels of *miR172* under SD conditions compared with the wild type (Fig. 7D). This increase in *miR172* levels under SD conditions, however, was not reflected by the tuberization phenotype of the rSPL9 OE line (Supplemental Fig. S7C).

Detection of *miR156* in Phloem of Wild-Type Potato

In order to investigate the presence of *miR156* in phloem of potato plants, we harvested phloem cells by laser microdissection pressure catapulting (LMPC) and tested for the presence of *miR156* in phloem cells of wild-type potato (Fig. 8, A and B). While *miR156* was detected in phloem cells, we did not detect the *miR156*a precursor in phloem sap harvested from wild-type plants (Fig. 8C). The purity of phloem sap (phloem-enriched exudate) was confirmed by detecting the phloem-specific transcript G2-like transcription factor and the absence of root-specific transcript nitrate transporter (Fig. 8D). The *miR156** strand, however, was detected in phloem sap exudates of wild-type plants by stem-loop qRT-PCR (Fig. 8E). To understand if photoperiod has any role in *miR156* accumulation in the phloem, we also carried out a stem-loop qRT-PCR analysis of phloem sap harvested from wild-type plants incubated for 8, 15, and 30 d post induction (dpi) under both SD and LD conditions. Higher accumulation of *miR156* was observed in phloem sap harvested from 8- and 15-dpi SD-induced plants, indicating that *miR156* accumulation increased under SD conditions in phloem sap of potato. This pattern changed in plants incubated for longer times (30 dpi; Fig. 8F).

miR156 Is Potentially a Graft-Transmissible Signal in Potato

In our study, we detected *miR156* in LMPC-harvested phloem cells, and it exhibited an SD-induced accumulation

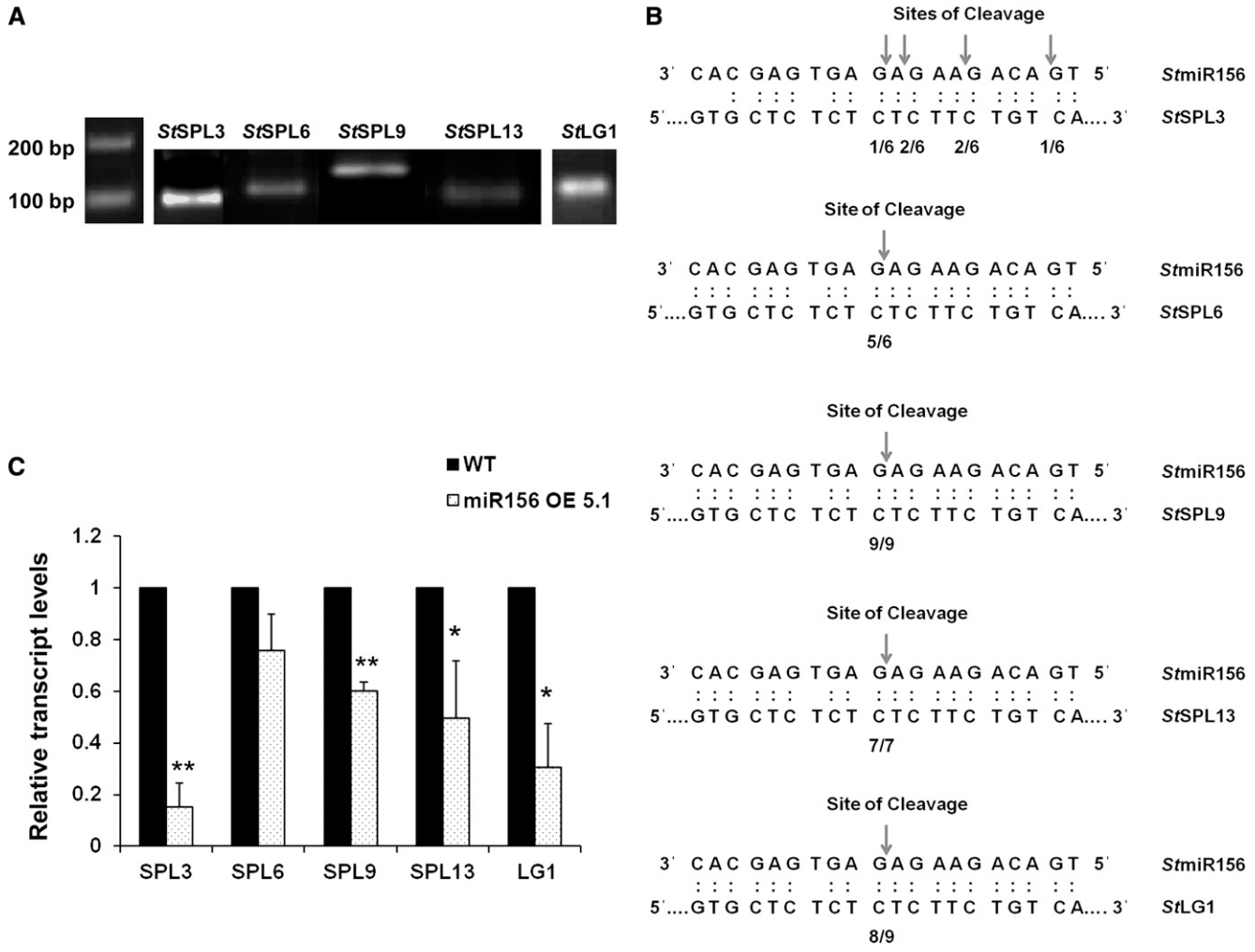

Figure 6. *miR156* targets in potato. A and B, *miR156* cleavage site mapping in *miR156* targets as determined by modified RLM-RACE. A, Nested PCR products were cloned and sequenced. B, Frequency of 5′ RACE clones showing cleavage site (arrows) and fractions indicating proportions of clones showing these cleavage sites. C, Expression pattern of *StSPL3*, *StSPL6*, *StSPL9*, *StSPL13*, and *StLG1* in wild-type (WT) and *miR156* OE 5.1 plants by qRT-PCR. Error bars indicate SD of three biological replicates each with three technical replicates. Asterisks indicate statistical differences as determined using Student's *t* test (*$P < 0.05$, **$P < 0.01$).

pattern in phloem sap. Considering this observation, we tested whether *miR156* is a phloem-mobile signal in potato. Grafting experiments (homografts, heterografts, and reverse grafts) were performed to demonstrate the mobility of *miR156* (Fig. 9A). After 4 weeks of SD induction, analysis of morphological changes in grafts as well as the quantitative analysis of *miR156* were performed. Overall, the leaf shape and trichome morphology of stocks from the heterografts (*miR156* OE plants as scion and the wild type as stock) were affected. The newly emerging leaves from the axillary shoots on the stock of heterografts had more prominent but fewer trichomes (Fig. 9B) and exhibited small and thick lamina along with reduced numbers of leaflets (Fig. 9C). On the other hand, newly emerging leaves from wild-type scions of reverse grafts did not show any phenotype similar to *miR156* OE plants (Fig. 9D). All the heterografts had less tuber yield as compared with homografts, while reverse grafts did not form any tubers (Table II).

The morphological changes in the stock stems of heterografts could be due to (1) the transport of mature *miR156* itself, (2) the transport of the overexpressed *miR156a* precursor transgene, or (3) a *miR156*-mediated up-regulated mobile factor activating *miR156* transcription in stock stems. To analyze if mature *miR156* is transported, we carried out a quantitative analysis by stem-loop qRT-PCR. In stock stems of all four heterografts, a higher accumulation of mature *miR156* was observed, as opposed to homografts (Fig. 9E). On the other hand, absence of the *miR156a* precursor transgene in heterograft stock stems confirmed that the overexpressed transgene is not moving from scion to stock (Fig. 9F). Also, a comparative analysis of mature *miR156*

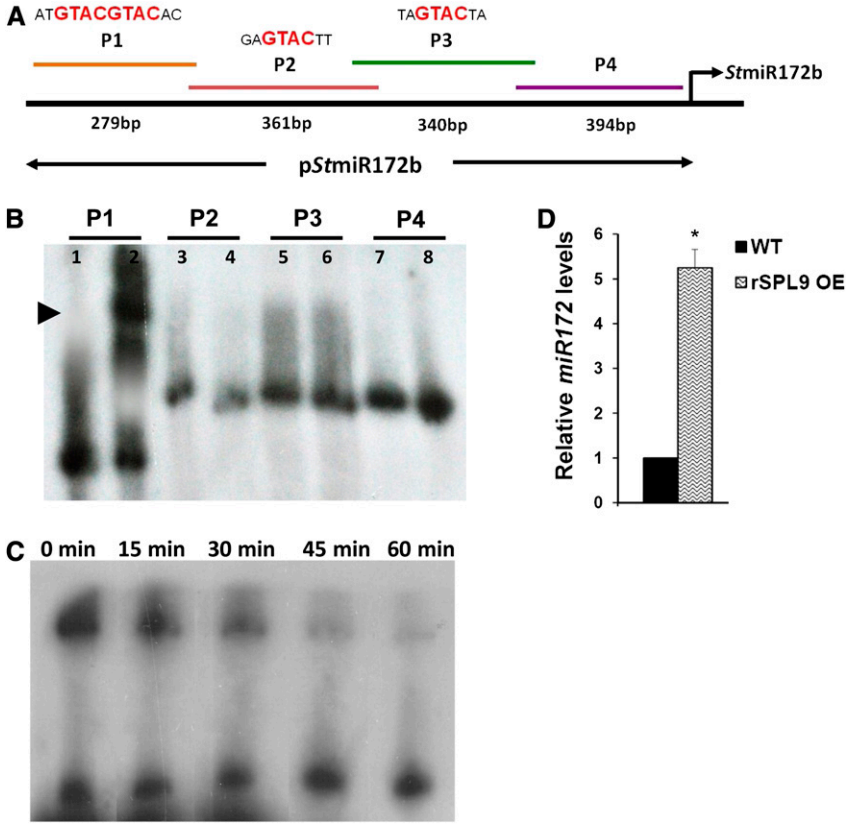

Figure 7. StSPL9 binds to the StMIR172b promoter. A, Schematic representation of StMIR172b promoter sequence showing SPL binding motifs and lengths of four fragments. B, Gel retardation assay of StMIR172b promoter fragments P1 to P4 with StSPL9. The lanes are alternate for free probe and probe + protein. C, Cold competition retardation assay of P1 with StSPL9. Labeled P1 was incubated with StSPL9 for 30 min at 25°C, and then a 100-fold molar excess of unlabeled P1 was added and aliquots were analyzed after the indicated times (0–60 min). D, Relative levels of *miR172* in 15-d post SD-induced leaves of wild-type (WT) and rSPL9 OE plants. Error bars indicate SD of two biological replicates each with three technical replicates. The asterisk indicates a statistical difference as determined using Student's *t* test ($*P < 0.05$). [See online article for color version of this figure.]

and *miR156a* precursor levels in both wild-type and grafted plants clearly demonstrated that mature *miR156* had a higher accumulation than its precursor form (Supplemental Fig. S8, A–D). These findings make the possibility of *miR156a* precursor transgene movement as well as activated localized transcription of *miR156* in stock stems of heterografts unlikely. Instead, the higher accumulation of mature *miR156* in heterograft stock stems supports the preferential transport of mature *miR156* itself, from scion to stock in grafted plants. Overall, our results suggest that *miR156* is a graft-transmissible phloem-mobile signal that affects tuberization and plant architecture in potato.

DISCUSSION

miR156 in Potato

Several reports have previously demonstrated the function of *miR156* in various plant species like maize (Chuck et al., 2007), Arabidopsis (Huijser and Schmid, 2011), switchgrass (Fu et al., 2012), rice (Xie et al., 2006), tomato (Zhang et al., 2011b), and poplar hybrid (*Populus trichocarpa*; Wang et al., 2011). Earlier studies (Zhang et al., 2009; Yang et al., 2010; Xie et al., 2011) have predicted *miR156* in potato through a bioinformatic approach. The recent study by the Tomato Genome Consortium (2012) reported 13 members of the miR156 family in potato, whereas the miR156 family has 12 members in Arabidopsis, 12 in rice, and 11 in poplar hybrid (Griffiths-Jones et al., 2008). A very recent report (Eviatar-Ribak et al., 2013) has shown that overexpression of *miR156* in the potato cv Desiree (a day-neutral cultivar) resulted in stolon-borne aerial mini tubers from almost all of the distal buds. *miR156* OE plants had exhibited late flowering, suppression of leaf complexity, and a profuse branching phenotype. We had similar observations for *miR156* overexpression in potato, but in the photoperiod-sensitive subspecies *andigena* 7540. We wanted to investigate the following. (1) Does *miR156* affect multiple morphological traits other than what was already observed in potato? (2) What could be the target genes of *miR156* and their roles in potato? (3) What is the role of *miR156* in tuberization under different photoperiods? (4) Knowing its presence in phloem of other plant species, our hypothesis was to test if *miR156* acts as a potential mobile signal in potato development.

To answer these questions, we started with validating the presence of one member of the *miR156* family, *miR156a* in potato. This is different from the approach followed in a previous report (Eviatar-Ribak et al., 2013), where the Arabidopsis *miR156a* precursor was overexpressed in potato. The sequence of mature potato *miR156* was found to be identical to that of *miR156* of Arabidopsis, rice, maize, and sorghum (*Sorghum bicolor*), suggesting its conserved nature. In our analysis,

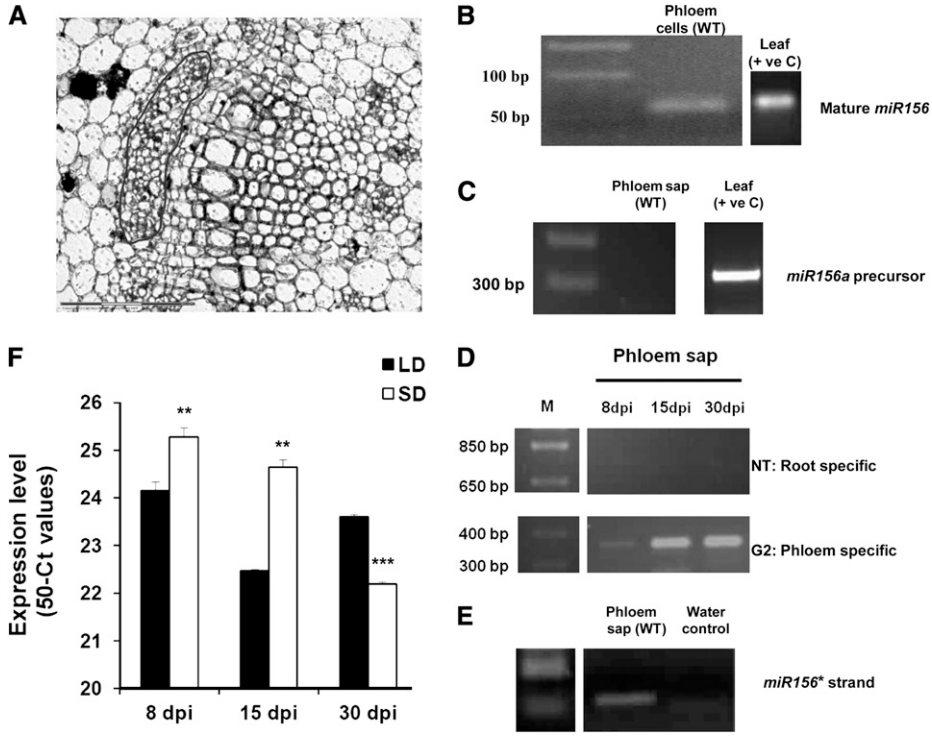

Figure 8. Detection of *miR156* in phloem. A, Phloem tissue in a wild-type stem section (marked in red). This tissue was harvested by LMPC. B, Detection of *miR156* (mature) in phloem of wild-type plants (WT) and leaf tissue of wild-type plants (positive control [+ ve C]) by stem-loop RT-PCR. C, Absence of *miR156a* precursor (300 bp) in wild-type phloem sap and its presence in wild-type leaf, acting as a positive control, by RT-PCR analysis. D, RT-PCR analysis of nitrate transporter (NT; root-specific transcript) and G2-like transcription factor (G2; phloem-specific transcript) of potato phloem sap of the wild type (phloem-enriched exudate) to assess its purity (Banerjee et al., 2006a). E, Detection of the *miR156** strand in phloem sap of the wild type by stem-loop RT-PCR. F, Differential accumulation of *miR156* (mature) under SD and LD photoperiods in phloem sap of wild-type plants harvested after 8, 15, and 30 dpi. *miR156* accumulation is plotted as 50 minus Ct (for cycle threshold; 50-Ct) values as described previously (Pant et al., 2008). Error bars indicate SD of one biological replicate with three technical replicates. Asterisks indicate statistical differences as determined using Student's *t* test (**$P < 0.01$, ***$P < 0.001$).

miR156 exhibited an age-dependent expression pattern in potato stem tissues, and its levels decreased as the plant aged (Fig. 1D). This observation was consistent with the earlier studies in Arabidopsis and rice (Wu et al., 2009; Xie et al., 2012). Both of these reports showed a gradual decrease of the expression of *miR156* in shoots as the plant aged. However, in developing leaves of rice, an opposite expression pattern of *miR156* was demonstrated. In our study, no significant pattern of *miR156* expression was observed in leaves (Fig. 1D). All of the previous reports mentioned above demonstrate decreased *miR156* expression with respect to plant age, suggesting its role in juvenile phase maintenance. However, photoperiod-mediated expression and function of *miR156* have not been documented earlier. Because tuberization in potato is a photoperiod-regulated process, we investigated the effect of the photoperiod on *miR156* expression and its function. Our analysis suggests that *miR156* is differentially expressed under SD/LD conditions in a tissue-specific manner (Fig. 1, E and F). As we have validated the *miR156a* precursor in potato, we carried out bioinformatic analysis of the upstream sequence of the MIR156a gene using the PLACE online tool (Higo et al., 1999). The MIR156a upstream sequence exhibited a number of light regulatory motifs (Supplemental Table S2; Waksman et al., 1987; Vorst et al., 1990; Vauterin et al., 1999), indicating a putative light-mediated regulation of this miRNA along with an endogenous, age-mediated regulation.

Overexpression of *miR156* Affects Plant Architecture in Potato and Tobacco

In our study, *miR156* OE lines (potato and tobacco) exhibited phenotypes like profuse axillary branching, altered leaf and trichome morphology, and delayed or no flowering, documented earlier in a number of plants such as Arabidopsis (Huijser and Schmid, 2011), rice (Xie et al., 2006), tomato (Zhang et al., 2011b), and potato (Eviatar-Ribak et al., 2013). In addition to these phenotypes, an altered venation pattern in leaves, disoriented cell organization with larger epidermal

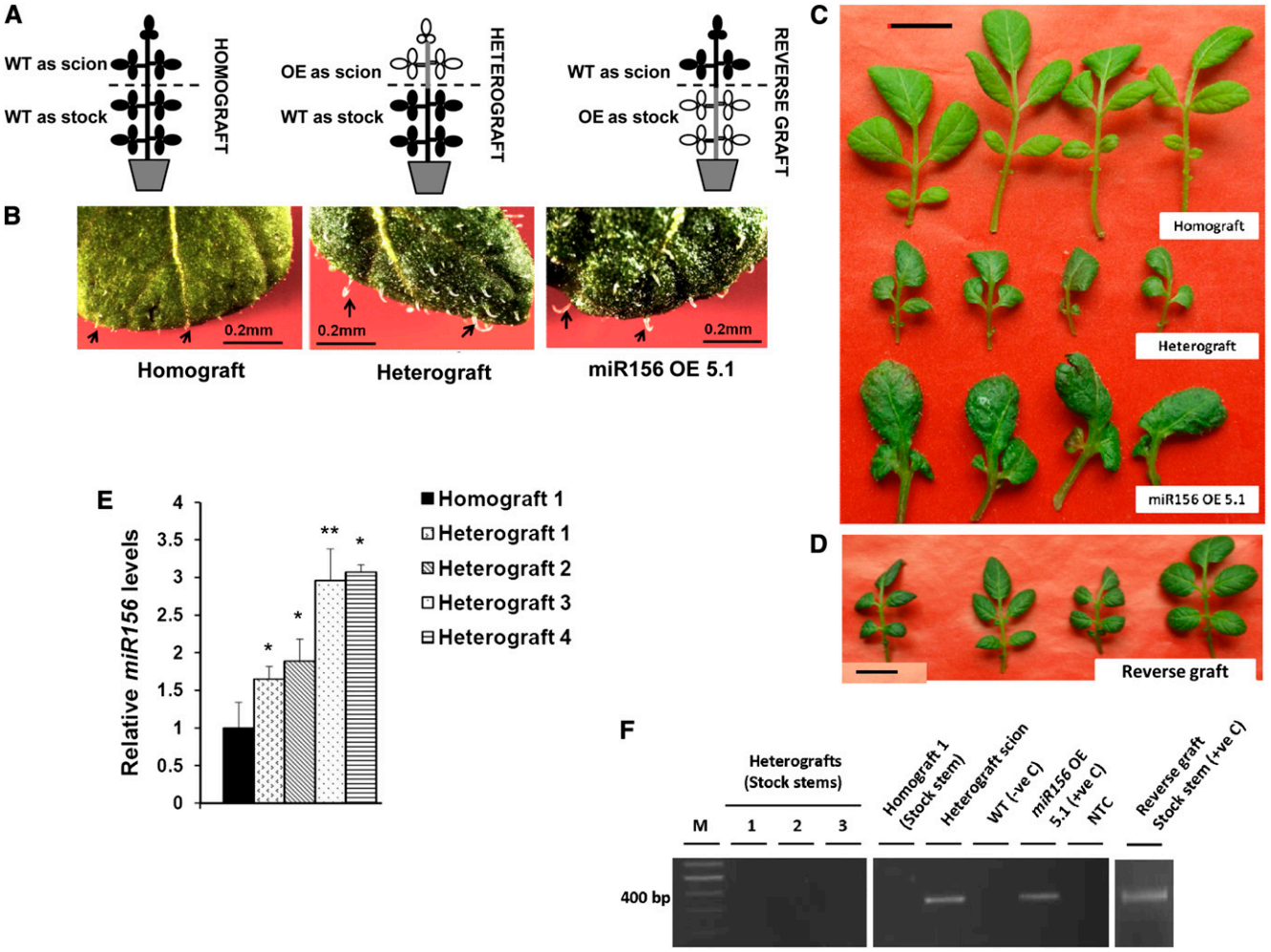

Figure 9. *miR156* is a potential graft-transmissible signal. A, Pictorial representation of the grafts. WT, Wild type. B, Trichomes of homograft (stock leaves), heterograft (stock leaves), and leaves from *miR156* OE 5.1 plants, where trichomes in heterografts (stock leaves) are less in number and more in length, as observed for *miR156* OE 5.1 plants. Bars = 0.2 mm. C and D, Leaves of homograft (stock), heterograft (stock), *miR156* OE 5.1 plants, and reverse grafts (scion), where heterograft stock leaves mimic the phenotype of *miR156* OE 5.1 leaves (C), while reverse graft scion leaves mimic the phenotype of homograft leaves (stock; D) Bars = 1 cm. E, Relative levels of mature *miR156* in stock stems of four representative heterografts (1–4) and homograft incubated under SD conditions and harvested after 30 dpi were measured by stem-loop qRT-PCR. Error bars indicate SD of one biological replicate with three technical replicates. Asterisks indicate statistical differences as determined using Student's *t* test ($*P < 0.05$, $**P < 0.01$). F, Detection of *miR156a* precursor transgene in stock stems of homograft, three representative heterografts (1–3), and reverse graft by RT-PCR analysis. Stem tissue of heterograft scion, reverse graft stock, and a *miR156* OE 5.1 plant served as positive controls (+ve C), with the wild type as a negative control (−ve C). NTC, No template control. [See online article for color version of this figure.]

cells, and reduced stomatal density and root biomass were also observed in both the OE lines (Figs. 2 and 3), indicating several new functions for *miR156* in potato. Overall, this suggests that *miR156* acts as a master regulator involved in the regulation of different plant developmental traits. The altered leaf morphology in OE plants can possibly be a result of reduced levels of *SPLs* (Fig. 6C). A number of previous reports (Wu and Poethig, 2006; Shikata et al., 2009; Usami et al., 2009; Chen et al., 2010) have described the role of SPLs in leaf development in Arabidopsis, suggesting that *StSPLs* might control leaf size and shape, altered venation, and reduced leaflet number in potato as well. LG1 is a well-characterized SPL protein whose function in leaf development has previously been reported in maize (Harper and Freeling, 1996) and rice (Lee et al., 2007). It was shown to be involved in controlling ligule and auricle development and the formation of a laminar joint between leaf blade and leaf sheath. In our study, reduced *StLG1* expression in *miR156* OE plants could possibly explain the aberrant leaf morphology (reduced leaf lamina and curled leaf margins). To understand the cause of the profuse branching phenotype of *miR156* OE plants in potato, we quantified the amounts

Table II. *Number of tubers of homografts, heterografts, and reverse grafts incubated under SD conditions for 30 d*

Means of three grafted plants were calculated.

Graft	No. of Tubers
Homografts	9.5 ± 2.12
Heterografts	2 ± 1.41
Reverse grafts	0 ± 0

of cytokinin and strigolactone, hormones that are known to play an important role in branching (Domagalska and Leyser, 2011). Cytokinins act antagonistically to auxins and promote branching from axillary meristems, leading to the loss of apical dominance (Domagalska and Leyser, 2011). *miR156* OE plants exhibited increased levels (more than 2-fold) of zeatin riboside under both SD and LD photoperiods (Fig. 5C), which is consistent with the bushy phenotype of these OE plants. Increased cytokinin amount was also accompanied by increased expression of the cytokinin biosynthesis gene *StLOG1* and the cytokinin-responsive gene *StCyclin D3.1* (Fig. 5, A and B). This increase in the activity of cytokinin might have caused the profuse branching phenotype. On the other hand, in Arabidopsis, strigolactone mutants show increased branching (Gomez-Roldan et al., 2008). In our study as well, *miR156* OE plants contained reduced amounts of orobanchyl acetate (Fig. 5D). The absence of flowering in both potato and tobacco OE plants supports the role of *miR156* in controlling phase transitions. In Arabidopsis, AtSPL2, AtSPL3, AtSPL9, AtSPL10, and AtSPL11 are shown to act as positive regulators in promoting floral meristem identity by directly regulating genes like LEAFY, FRUITFUL, and APETALA1 (Chen et al., 2010). A similar mechanism might also be conserved in potato, since *StSPL3* and *StSPL9* are found to be reduced in *miR156* OE plants (Fig. 6C).

miR156 Regulates Potato Tuberization

Flowering and tuberization are different reproductive strategies, both of which are photoperiod-mediated mechanisms (Jackson, 2009). Several molecular components like phytochrome B (Jackson et al., 1998), CONSTANS (Martinez-Garcia et al., 2002), and StSP6A (Navarro et al., 2011) have previously been shown to play roles in flowering and potato tuberization. In addition, two other miRNAs (*miR156* and *miR172*) were shown to control developmental timing and flowering in Arabidopsis (Wu et al., 2009). The positive role of *miR172* in tuberization was reported earlier (Martin et al., 2009), while a very recent report (Eviatar-Ribak et al., 2013) demonstrated the role of *miR156* in tuber formation. In Arabidopsis, *miR156* regulates *miR172* expression via AtSPL9 (Wu et al., 2009) during phase transitions. Similarly, we observed reductions of *miR172* and *StSPL9* in *miR156* OE lines (Figs. 4, D and E, and 6C) in potato. Although in our analysis, *StSPL9* was found to be reduced by 40%, there is a possibility of *miR156* acting on StSPL9 by translational arrest as well (Gandikota et al., 2007). Gel retardations assays confirmed the regulatory role of the *miR156*-SPL-*miR172* module in potato. However, control of *miR172* by SPLs other than StSPL9 cannot be ruled out. This regulatory module is likely to be active in leaves induced under LD conditions, as there are high levels of *miR156* but reduced levels of *SPL9* and *miR172*, whereas an increased accumulation of *miR156* and *miR172* in SD-induced stolons reflects a lack of regulation of *miR172* by *miR156*, possibly due to the tissue-specific action of *miR156* or spatial exclusion.

Several interesting observations regarding the effect of *miR156* on tuberization were noted in our study. In stolons (the tissue destined to form a tuber) harvested from SD-induced wild-type plants, an approximately 8-fold increase in the level of *miR156* was detected (Fig. 1E). Also, *miR156* OE lines, when incubated under SD conditions, produced aerial tubers, as reported in a recent work (Eviatar-Ribak et al., 2013). However, in our study, *miR156* OE lines exhibited a reduction in overall tuber yield and the levels of the tuberization markers *miR172* and *StSP6A* (Fig. 4, D–F). Considering these observations, should *miR156* be termed as an activator or a repressor of tuberization? If *miR156* acts as an activator, *miR156* OE lines would have produced tubers under LD (noninductive) conditions, as observed previously for StBEL5 (Banerjee et al., 2006a), *miR172* (Martin et al., 2009), and StSP6A (Navarro et al., 2011) OE lines. In our study, *miR156* OE lines produced aerial tubers in SD conditions (Fig. 4B). This rules out the possibility of *miR156* functioning as a repressor. The reduced levels of tuberization markers in *miR156* OE lines can possibly be due to the prolonged juvenile phase of these plants, which in turn reduced the overall tuber yield. In potato, all axillary meristems have the capacity to form tubers, and under permissive conditions any meristem can produce aerial tubers. However, this potential is suppressed except in stolons (Xu et al., 1998). We propose that under tuber-inductive conditions, a threshold level of *miR156* facilitates tuber formation from a meristem. Overexpression of *miR156* in potato results in levels above threshold in all the axillary meristems; hence, the plant produces aerial tubers under SD conditions. The recent work by Eviatar-Ribak and coworkers (2013) demonstrated that *TLOG1* OE tomato plants produced sessile tubers only in basal meristems, whereas *TLOG1-miR156* double OE plants produced sessile tubers from all axillary meristems. In our study, we used potato subspecies *andigena*, which is sensitive to photoperiod for tuberization. When *miR156* is overexpressed in this background, the OE plants produced aerial tubers only under SD conditions, whereas in LD conditions, the axillary meristems produced only branches. This observation clearly established that increased levels of *miR156* in OE plants alone are not sufficient for tuber formation but that tuber-inductive conditions are required for aerial tuber formation.

miR156 as a Potential Phloem-Mobile Long-Distance Signal

The detection of *miR156* in LMPC-harvested phloem cells and an increased accumulation in phloem exudates under SD photoperiod suggest that *miR156* could possibly act as a long-distance signal in potato development. Our grafting assays support this hypothesis, as increased levels of mature *miR156* could be detected in the stock stems of SD-induced heterografts (Fig. 9E). Further molecular analysis ruled out the possibility of *miR156a* precursor transgene movement (Fig. 9F; Supplemental Fig. S8, A–D). In addition, morphological changes in leaves and trichome phenotypes further support *miR156* transport. Reverse graft assays showed that the mobility of *miR156* was restricted to a shoot-to-root direction. Questions could be raised. Is *miR156* transported as a double-stranded or single-stranded form in the phloem? The presence of the *miR156** strand in potato phloem sap indicates that it is possibly transported as a *miR156*/*miR156** duplex. Similar to our results, previous studies (Buhtz et al., 2008, 2010; Pant et al., 2008; Hsieh et al., 2009) also reported the presence of a star strand along with the mature miRNA in the phloem stream. Another explanation for *miR156** in potato phloem could be its association with the RNA-induced silencing complex to target different genes. miRNA* species are reported to be associated with Argonaut proteins and to have inhibitory effects on target gene expression in *Drosophila* species (Okamura et al., 2008). A recent report by Devers and coworkers (2011) described a similar phenomenon in *Medicago truncatula* roots. Although a handful of miRNAs have now been detected in phloem of several plant species such as pumpkin (Yoo et al., 2004), Arabidopsis (Varkonyi-Gasic et al., 2010), and *Brassica* (Buhtz et al., 2008), only three miRNAs, *miR399*, *miR395*, and *miR172* (Pant et al., 2008; Buhtz et al., 2010; Kasai et al., 2010), were demonstrated to act as long-distance mobile signals. We show that *miR156* is involved in the regulation of plant architecture and tuberization and might be another miRNA to be transported via the phloem over long distances. The availability of techniques to differentiate between mature endogenous miRNAs from transgenic miRNAs would perhaps provide the final evidence for miRNA mobility.

Based on our results, we propose a model for the regulation of tuberization by *miR156*. We hypothesize that under tuber-inductive (SD) conditions, *miR156* is transported to stolons through the phloem, accumulates in underground stolons (which in turn reduces the *miR156* accumulation in leaves and stems), and facilitates underground tuber formation. Reduced *miR156* accumulation in aerial organs inhibits the formation of aerial tubers, whereas in LD conditions, increased levels of *miR156* in leaves and stems assist the vegetative growth of the plant. *miR156* exerts this effect presumably through a *miR156*-SPL9-*miR172* regulatory module and possibly arrests tuberization under LD conditions. It appears that *miR156* has a different function in SD and LD photoperiods. We also cannot rule out the possibility that the high accumulation of *miR156* in SD-induced stolons is associated with controlling tuber transitions, the maintenance of the juvenile phase, or even tuber dormancy. Future work will help to elucidate the additional functions of *miR156* in potato.

MATERIALS AND METHODS

Plant Material and Growth Conditions

In this study, potato (*Solanum tuberosum* subspecies *andigena* 7540) was used. This is a photoperiod-responsive plant that tuberizes under SD conditions (8 h of light) and does not produce tubers under LD conditions (16 h of light). In vitro plants were grown under LD conditions at 25°C in a growth incubator (Percival Scientific). Soil plants were grown at 22°C under LD photoperiod in environmental chambers (Percival Scientific). For age-specific expression studies of *miR156*, tissue culture-raised plants were transferred to soil and incubated up to 14 weeks. Tissues (fully expanded mature leaves and stem) were collected after specific time intervals (2, 7, 12, 13, and 14 weeks) and stored at −80°C until further use. For photoperiod-dependent expression studies, plants were induced under both SD and LD conditions in environmental chambers for 15 d. Different tissues (leaf, stem, stolon, and swollen stolon) were harvested after 15 dpi. For quantifying *miR156* levels in 0-, 15-, and 30-d-old tubers stored post harvest (tuber dormancy), tuber eyes were isolated and stored at −80°C. In the case of tobacco (*Nicotiana tabacum* cv Petit Havana), plants were grown under LD conditions in environmental chambers.

Validation of *miR156*

Total RNA was harvested from mature leaves and stem tissue of potato, and *StmiR156a* (BI432985.1) precursor was amplified by RT-PCR (details of all the primers and accession numbers are given in Supplemental Tables S3 and S4). The amplicon was then sequence confirmed. Mature *miR156* was detected by stem-loop RT-PCR as described earlier (Varkonyi-Gasic et al., 2007). Total RNA was isolated by TRIzol reagent (Invitrogen) following the manufacturer's instructions. RT was carried out using stem-loop primer miR156STP. End-point PCR was performed using miR156FP and universal reverse primer (univRP). The 61-bp amplicon was cloned in the subcloning vector pGEM-T Easy (Promega) and was confirmed by sequencing.

Analysis of miRNA Levels

In the entire study, levels of miRNAs (*miR156* and *miR172*) were determined by stem-loop qRT-PCR. One microgram of total RNA was used for all RT reactions except for the quantification of miRNAs from phloem sap, where 100 ng of RNA was used. Stem-loop reverse primers miR156STP and miR172STP were used for *miR156* and *miR172*, respectively. RT was carried out as per a previous protocol (Varkonyi-Gasic et al., 2007). Quantitative PCR (qPCR) for *miR156* (miR156FP and univRP) and *miR172* (miR172FP and univRP) was performed in a Mastercycler ep realplex (Eppendorf). For normalization, 5S ribosomal RNA was reverse transcribed by stem-loop primer 5S rRNASTP and amplified by 5S rRNAFP and univRP. All the PCRs were incubated at 95°C for 5 min followed by 40 cycles of 95°C for 5 s, 60°C for 10 s, and 68°C for 8 s. PCR specificity was checked by melting curve analysis, and data were analyzed using the $2^{-\Delta\Delta Ct}$ method (Livak and Schmittgen, 2001).

Construct Design and Plant Transformation

To generate *miR156* OE lines of potato, the precursor sequence (*StmiR156a*; BI432985.1) of *miR156* was amplified from total RNA harvested from leaves using the primers miR156preFP and miR156preRP. The PCR product was digested with *Xba*I-*Sac*I and cloned into the binary vector pBI121 under the control of the CaMV 35S promoter. This construct was then mobilized into *Agrobacterium tumefaciens* strain GV2260. Transgenic plants were generated following the protocol by Banerjee et al. (2006b). *miR156* OE lines of tobacco were raised as described by Horsch et al. (1985). Kanamycin-resistant transgenic plants were selected for further analysis and were maintained in Murashige and

Skoog basal medium (Murashige and Skoog, 1962) until further use, whereas rSPL9 transgenic lines were generated by introducing silent mutations in the MRE. Mutations were incorporated by site-directed mutagenesis using Turbo DNA polymerase (Stratagene). The primers used for site-directed mutagenesis in MRE were rSPL9FP and rSPL9RP. Amplification of rSPL9 was carried out by using primer pair SPL9FP and SPL9RP3, and it was cloned in binary vector pBI121 downstream of the CaMV 35S promoter. Transgenic plants of rSPL9 were generated and maintained as described above.

Leaf and Stem Histology

For histology, a modified protocol of Cai and Lashbrook (2006) was followed. Briefly, leaves and stems of 8-week-old plants (the wild type and *miR156* OE lines 5.1 and 6.2) grown under LD conditions were fixed in chilled ethanol:acetic acid (3:1; Merck). The tissues were vacuum infiltrated (400 mm of mercury) for 30 min and then stored at 4°C overnight. Fixed tissues were then dehydrated at room temperature in a graded series of ethanol (75% [v/v], 95% [v/v], and 100% [v/v] ethanol) followed by washes of a combination of ethanol and xylene series. Tissue blocks were prepared with molten Paraplast (Leica). Ten-micrometer sections were cut by a microtome (Leica) and placed on glass slides. Dried slides were deparaffinized by washing twice in 100% xylene and were observed with a microscope.

Environmental Mode Scanning Electron Microscopy of Leaves

Leaves of 8-week-old plants (the wild type and *miR156* OE lines 5.1 and 6.2) grown under LD conditions were used for scanning electron microscopy in the environmental mode (eSEM) with a Quanta 200 3D eSEM apparatus (FEI), and leaf morphology was documented.

Analysis of Tuberization

Both wild-type and *miR156* OE lines were grown in soil at 22°C under LD conditions in environmental chambers for 3 weeks. Thereafter, 10 plants each were shifted to SD and LD conditions and were incubated further for 4 weeks. To analyze *StSP6A* and *miR172* levels in these plants, leaf tissues were harvested 8 dpi from both of these lines. *miR172* levels were also quantified in 15-d post SD-induced stolons of wild-type and *miR156* OE plants (line 5.1). The tuberization phenotype was scored after 4 weeks of induction.

Analysis of Zeatin Riboside and Orobanchyl Acetate by HR-MS

Axillary meristems were harvested from wild-type and *miR156* OE 5.1 plants induced for 15 d in LD and SD conditions and ground in liquid nitrogen. For HR-MS analysis, a modified protocol of Forcat et al. (2008) was followed. One hundred milligrams of tissue was used for extraction in 400 μL of 10% (v/v) methanol and 1% (v/v) glacial acetic acid. This mixture was vigorously vortexed and stored on ice for 2 h, followed by centrifugation to obtain the supernatant. This was repeated three times, and the volume of the supernatant was adjusted to 2 mL in a volumetric flask. Samples were resolved through a Thermo Scientific Hypersil Gold column of particle size 5 μm with a flow rate of 0.5 mL min^{-1} and a gradient solvent program of 25 min (0 min, 10% methanol-water; 0.5 min, 10% methanol-water; 3 min, 45% methanol-water; 20 min, 50% methanol-water; 22 min, 90% methanol-water; 23 min, 10% methanol-water; 25 min, 10% methanol-water). Formic acid (0.1%; liquid chromatography-mass spectrometry grade) was also added to methanol and water. Mass spectrometry and tandem mass spectrometry experiments were performed in electrospray ionization-positive ion mode using the tune method as followed: sheath gas flow rate, 45 units N_2; auxiliary gas flow rate, 10 units N_2; sweep gas flow rate, 2 units N_2; spray voltage, 3.60 kV; spray current, 3.70 μA; capillary temperature, 320°C; source lens R_F level, 50; heater temperature, 350°C. Electrospray ionization-mass spectrometry data were recorded in full scan mode within the mass-to-charge ratio range 100 to 1,000. A standard curve for quantification was prepared using zeatin riboside (Sigma). Orobanchyl acetate was identified based on mass spectrometry analysis, and quantification was performed considering the peak areas.

Analysis of *StSP6A*, *StLOG1*, and *StCyclin D3.1*

One microgram of total RNA was used for *StSP6A* analysis from 8-d-old SD-induced leaves of wild-type and *miR156* OE line plants. 18S ribosomal RNA (50 ng) was used for normalization. For RT-PCR, the SuperScript III one-step RT-PCR system with platinum Taq DNA polymerase (Invitrogen) was used as per the manufacturer's instructions. Semiquantitative RT-PCR for *StSP6A* was performed using the following primers: SP6AFP and SP6ARP. RT-PCR conditions were as follows: 50°C for 30 min, 94°C for 2 min, followed by 25 cycles of 94°C 15 s, 55°C for 15 s, and 68°C for 1 min. The cycle number for 18S RNA was restricted to 10, while the program remained the same as for *StSP6A*. For analysis of *StLOG1* and *StCyclin D3.1*, total RNA was isolated from axillary meristems of wild-type and *miR156* OE 5.1 plants grown in SD photoperiod for 15 d by TRIzol reagent. One microgram of total RNA was used for complementary DNA (cDNA) synthesis by SuperScript III reverse transcriptase (Invitrogen) using an oligo(dT) primer. qPCR was performed on a Mastercycler ep realplex with LOG1FP-LOG1RP and CyclinFP-CyclinRP. The reactions were carried out using KAPA SYBR green master mix (Kapa Biosystems) and incubated at 95°C for 2 min followed by 40 cycles of 95°C for 15 s and 60°C for 30 s. Glyceraldehyde 3 phosphate dehydrogenase was used for normalization for all the reactions. PCR specificity was checked by melting curve analysis, and data were analyzed using the $2^{-\Delta\Delta Ct}$ method (Livak and Schmittgen, 2001).

Prediction of *miR156* Targets

miR156 targets in potato were predicted using bioinformatic tools. To increase the efficiency of target prediction, psRNATarget (plantgrn.noble.org/psRNATarget/; Dai and Zhao, 2011) and TargetAlign (leonxie.com/targetAlign.php; Xie and Zhang, 2010) online tools were used. Based on their score and consistency of results, five sequences were short listed as potential *miR156* targets. These targets showed homology (40%–80%) with AtSPL3, AtSPL6, AtSPL9, AtSPL13, and RcoLG1 (for *Ricinus communis* LIGULELESS1) and were termed StSPL3, StSPL6, StSPL9, StSPL13, and StLG1, respectively. Their coding sequences were retrieved from the Online Resource for Community Annotation of Eukaryotes (http://bioinformatics.psb.ugent.be/orcae/; Sterck et al., 2012) and the Database of Plant Transcription Factors (http://planttfdb.cbi.edu.cn/; Zhang et al., 2011a).

Cleavage Site Mapping

To validate the candidate targets of *miR156* in planta, modified RLM 5′ RACE was performed using the First Choice RLM-RACE kit (Ambion). Total RNA was extracted from wild-type potato leaves by TRIzol reagent and was directly ligated to RNA adaptor without any enzymatic pretreatments. cDNA synthesis was performed using the respective gene-specific reverse primers. Two rounds of PCR were conducted with adaptor-specific forward primers and gene-specific reverse primers (SPL3, SPL3RP1-SPL3RP2; SPL6, SPL6RP1-SPL6RP2; SPL9, SPL9RP1-SPL9RP2; SPL13, SPL13RP1-SPL13RP2; LG1, LG1RP1-LG1RP2). Amplicons were then cloned into the subcloning vector pGEM-T Easy and were sequenced to identify the miRNA cleavage sites.

Analysis of *StSPLs*

Total RNA from wild-type and *miR156* OE plants was isolated by TRIzol reagent as per the manufacturer's instructions. One microgram of total RNA was reverse transcribed using gene-specific primers by Moloney murine leukemia virus reverse transcriptase (Promega). For normalization, *GAPDH* was reverse transcribed. The primers used for reverse transcription were SPL3RP2, SPL6RP2, SPL9RP2, SPL13RP2, LG1RP2, and GAPDHRP. qPCR was performed on a Mastercycler ep realplex with the same reverse primers mentioned above. Forward primers were SPL3qFP, SPL6qFP, SPL9qFP, SPL13qFP, LG1qFP, and GAPDHFP. The reactions were carried out using the KAPA SYBR green master mix and incubated at 95°C for 2 min followed by 40 cycles of 95°C for 15 s, 52°C for 15 s, and 60°C for 20 s. For *GAPDH*, all conditions were similar, but the annealing temperature was 55°C. For StLG1, all conditions were similar except that the extension time was 10 s. PCR specificity was checked by melting curve analysis, and data were analyzed using the $2^{-\Delta\Delta Ct}$ method (Livak and Schmittgen, 2001).

Gel Retardation Assay

A 6× His-tagged fusion construct was generated by introducing the 1,152-bp coding sequence of StSPL9 in frame into the pET28a expression vector and transformed into *Escherichia coli* BL21 (DE3) cells. Cells were grown at 37°C until the optical density at 600 nm reached 0.6, induced with 1.0 mM isopropyl-β-D-thiogalactopyranoside, and cultured for 3 h at 37°C. The cells were lysed

by sonication. The tagged protein was purified using nickel-nitrilotriacetic acid agarose beads. Purified StSPL9 protein aliquots were frozen in liquid N_2 and stored at −80°C. Four overlapping fragments of the MIR172b promoter were used for gel mobility shift assays. Promoter fragments were PCR amplified from potato genomic DNA and were purified on columns. The respective primer sequences are provided in Supplemental Table S3. The 5′ ends of the fragments were then labeled with γ-^{32}P using the KinaseMax kit (Ambion). The DNA-binding reactions were set up at 24°C in 20 μL containing 10 mM Tris-HCl (pH 7.5), 5% glycerol, 0.5 mM EDTA, 0.5 mM dithiothreitol, 0.05% Nonidet P-40, 50 mM NaCl, 50 mg L^{-1} poly(dG-dC), 250 ng of protein, and 1 fmol of labeled DNA. After incubation at 24°C for 60 min, the reactions were resolved on a 6% native polyacrylamide gel in 1× Tris-borate-EDTA buffer. The gel was dried and exposed to x-ray film. In the cold competition assays, 100-fold more unlabeled double-stranded DNA fragment (P1) was added to the reaction and loaded onto the gel every 15 min.

Detection of *miR156* in the Phloem

Stem sections of 12-week-old wild-type plants were fixed as described above in the histology section. LMPC-mediated harvest of phloem cells (Carl Zeiss PALM laser micro beam) and RNA extraction from these cells were done as per Yu et al. (2007). Total RNA was extracted using TRIzol reagent. Mature *miR156* and *miR156** were detected by stem-loop RT-PCR as described earlier. Primer sequences for *miR156** are provided in Supplemental Table S3.

For analysis of the differential accumulation of *miR156* in phloem sap of SD- and LD-grown wild-type plants, sap extraction and RNA isolation were done as per Campbell et al. (2008) with a minor modification (the phloem exudate was harvested at 18°C). Sap collection was performed at 8, 15, and 30 dpi. To assess the purity of phloem sap, RT-PCR was performed for nitrate transporter (root-specific transcript) and G2-like transcription factor (phloem-specific transcript) using 150 ng of RNA as mentioned before (Banerjee et al., 2006a). The SuperScript III one-step RT-PCR system with platinum Taq DNA polymerase was used as per the manufacturer's instructions. For nitrate transporter, RT-PCR conditions were as follows: 55°C for 30 min, 94°C for 2 min, followed by 40 cycles of 94°C for 15 s, 50°C for 30 s, and 68°C for 1 min, with a final extension at 68°C for 5 min. For G2-like transcription factor, all conditions were similar except that annealing was at 56°C and extension was for 30 s. To quantify *miR156* levels in phloem sap, 100 ng of total RNA was used for *miR156*-specific stem-loop qRT-PCR as described above, except that the cycle number was increased to 50. qRT-PCR cycle threshold (Ct) value differences were calculated for *miR156* accumulation and plotted as described previously (Pant et al., 2008).

Soil-Grown Heterografts

Wild-type and *miR156* OE lines were maintained in an environmental chamber until grafting was performed. Grafts were made with wild-type and *miR156* OE transgenic potato plants as per our previous protocol (Mahajan et al., 2012). *miR156* OE lines were used as scions and wild-type plants as stock (heterografts), while for reverse grafting, *miR156* OE plants served as stock and wild-type plants as scion (reverse grafts). Homografts (wild type on wild type) were used as controls in both cases. Equal numbers (10 each) of heterografts, reverse grafts, and homografts were made and maintained in environmental chambers for hardening for 4 weeks. Hardened grafts were further incubated in SD conditions for 4 weeks. Scion and stock samples (devoid of graft union) were harvested, and phenotypes such as leaf number, trichomes, and axillary branches were scored. qRT-PCR was performed for *miR156* accumulation in both heterograft stock samples and reverse graft scion samples with respective tissues from homografts as controls. Tuberization phenotypes were scored for all grafts.

For *miR156a* precursor transgene detection, RT-PCR was performed by the SuperScript III one-step RT-PCR system with platinum Taq DNA polymerase using 250 ng of total RNA. The primers used were miR156pre FP and transgene-specific NOST RP. The RT-PCR conditions were as follows: 50°C for 30 min, 94°C for 2 min, followed by 35 cycles of 94°C for 15 s, 50°C for 15 s, and 68°C for 1 min, with a final extension of 68°C for 5 min.

For comparative analysis of *miR156* (mature) and *miR156a* precursor levels in wild-type and grafted plants, 500 ng of RNA was used. Stem-loop qRT-PCR of *miR156* (mature) was performed as described above. For *miR156a* precursor quantification, cDNA synthesis was performed using oligo(dT) and SuperScript III reverse transcriptase enzyme. qPCR was performed on a Mastercycler ep realplex with miR156preFP and miR156preRP primers. The reactions were carried out using KAPA SYBR green master mix and incubated at 95°C for 2 min followed by 40 cycles of 95°C for 15 s, 50°C for 10 s, and 72°C for 18s. GAPDH was used for normalization. PCR specificity was checked by melting curve analysis, and data were analyzed using the $2^{-\Delta\Delta Ct}$ method (Livak and Schmittgen, 2001).

Sequence data from this article can be found in the GenBank/EMBL data libraries under accession numbers BI432985.1 (miR156a precursor), AC237992 (MIR172b promoter), CK267169.1 (NT), CK853924.1 (G2), in the Online Resource for Community Annotation of Eukaryotes (ORCAE) under accession numbers sotub10g009340 (SPL3), sotub12g015890 (SPL6), sotub10g020210 (SPL9), sotub05g016640 (SPL13), sotub05g016440 (LG1), and in the Potato Genome Sequencing Consortium under accession numbers: PGSC0003DMG400023365 (SP6A), PGSC0003DMT400009551 (LOG1), PGSC0003DMT400064307 (Cyclin D3.1), PGSC chr07:1782100..1784700 (MIR156a promoter).

Supplemental Data

The following materials are available in the online version of this article.

Supplemental Figure S1. *miR156* overexpression in potato.

Supplemental Figure S2. Overexpression of *miR156* in tobacco.

Supplemental Figure S3. HR-MS of zeatin riboside.

Supplemental Figure S4. Mass spectrum of zeatin riboside.

Supplemental Figure S5. HR-MS of orobanchyl acetate.

Supplemental Figure S6. Mass spectrum of orobanchyl acetate.

Supplemental Figure S7. Overexpression of rSPL9 in potato.

Supplemental Figure S8. Comparative analysis of *miR156* (mature) and *miR156a* precursor levels in wild-type and grafted plants.

Supplemental Table S1. Detailed analysis of *miR156* targets in potato.

Supplemental Table S2. Potential light regulatory elements present in the upstream sequence of *miR156a*.

Supplemental Table S3. List of primers.

Supplemental Table S4. List of accession numbers.

ACKNOWLEDGMENTS

We thank David J. Hannapel (Iowa State University) and Julia Kehr (University of Hamburg) for their critical reading of the manuscript, the director, National Chemical Laboratory, for providing us the eSEM facilities, Sanjeev Galande (Indian Institute of Science Education and Research) for his help in the gel retardation assays, and Saikat Haldar (National Chemical Laboratory) for his technical help in carrying out HR-MS analysis.

Received October 18, 2013; accepted December 13, 2013; published December 18, 2013.

LITERATURE CITED

Atkins CA, Smith PMC, Rodriguez-Medina C (2011) Macromolecules in phloem exudates: a review. Protoplasma **248:** 165–172

Axtell MJ, Bowman JL (2008) Evolution of plant microRNAs and their targets. Trends Plant Sci **13:** 343–349

Banerjee AK, Chatterjee M, Yu Y, Suh SG, Miller WA, Hannapel DJ (2006a) Dynamics of a mobile RNA of potato involved in a long-distance signaling pathway. Plant Cell **18:** 3443–3457

Banerjee AK, Prat S, Hannapel DJ (2006b) Efficient production of transgenic potato (*S. tuberosum* L. ssp. *andigena*) plants via *Agrobacterium tumefaciens*-mediated transformation. Plant Sci **170:** 732–738

Birkenbihl RP, Jach G, Saedler H, Huijser P (2005) Functional dissection of the plant-specific SBP-domain: overlap of the DNA-binding and nuclear localization domains. J Mol Biol **352:** 585–596

Buhtz A, Pieritz J, Springer F, Kehr J (2010) Phloem small RNAs, nutrient stress responses, and systemic mobility. BMC Plant Biol **10:** 64

Buhtz A, Springer F, Chappell L, Baulcombe DC, Kehr J (2008) Identification and characterization of small RNAs from the phloem of *Brassica napus*. Plant J **53:** 739–749

Cai S, Lashbrook CC (2006) Laser capture microdissection of plant cells from tape-transferred paraffin sections promotes recovery of structurally intact RNA for global gene profiling. Plant J **48:** 628–637

Campbell BA, Hallengren J, Hannapel DJ (2008) Accumulation of BEL1-like transcripts in solanaceous species. Planta **228:** 897–906

Carlsbecker A, Lee JY, Roberts CJ, Dettmer J, Lehesranta S, Zhou J, Lindgren O, Moreno-Risueno MA, Vatén A, Thitamadee S, et al (2010) Cell signalling by microRNA165/6 directs gene dose-dependent root cell fate. Nature **465:** 316–321

Chen X, Zhang Z, Liu D, Zhang K, Li A, Mao L (2010) SQUAMOSA promoter-binding protein-like transcription factors: star players for plant growth and development. J Integr Plant Biol **52:** 946–951

Chuck G, Cigan AM, Saeteurn K, Hake S (2007) The heterochronic maize mutant Corngrass1 results from overexpression of a tandem microRNA. Nat Genet **39:** 544–549

Chuck G, O'Connor D (2010) Small RNAs going the distance during plant development. Curr Opin Plant Biol **13:** 40–45

Corbesier L, Vincent C, Jang S, Fornara F, Fan Q, Searle I, Giakountis A, Farrona S, Gissot L, Turnbull C, et al (2007) FT protein movement contributes to long-distance signaling in floral induction of *Arabidopsis*. Science **316:** 1030–1033

Dai X, Zhao PX (2011) psRNATarget: a plant small RNA target analysis server. Nucleic Acids Res **39:** W155–W159

Devers EA, Branscheid A, May P, Krajinski F (2011) Stars and symbiosis: microRNA- and microRNA*-mediated transcript cleavage involved in arbuscular mycorrhizal symbiosis. Plant Physiol **156:** 1990–2010

Domagalska MA, Leyser O (2011) Signal integration in the control of shoot branching. Nat Rev Mol Cell Biol **12:** 211–221

Eviatar-Ribak T, Shalit-Kaneh A, Chappell-Maor L, Amsellem Z, Eshed Y, Lifschitz E (2013) A cytokinin-activating enzyme promotes tuber formation in tomato. Curr Biol **23:** 1057–1064

Forcat S, Bennett MH, Mansfield JW, Grant MR (2008) A rapid and robust method for simultaneously measuring changes in the phytohormones ABA, JA and SA in plants following biotic and abiotic stress. Plant Methods **4:** 16–23

Fu C, Sunkar R, Zhou C, Shen H, Zhang JY, Matts J, Wolf J, Mann DGJ, Stewart CN Jr, Tang Y, et al (2012) Overexpression of miR156 in switchgrass (*Panicum virgatum L.*) results in various morphological alterations and leads to improved biomass production. Plant Biotechnol J **10:** 443–452

Gandikota M, Birkenbihl RP, Höhmann S, Cardon GH, Saedler H, Huijser P (2007) The miRNA156/157 recognition element in the 3′ UTR of the *Arabidopsis* SBP box gene SPL3 prevents early flowering by translational inhibition in seedlings. Plant J **49:** 683–693

Gomez-Roldan V, Fermas S, Brewer PB, Puech-Pagès V, Dun EA, Pillot JP, Letisse F, Matusova R, Danoun S, Portais JC, et al (2008) Strigolactone inhibition of shoot branching. Nature **455:** 189–194

Gou JY, Felippes FF, Liu CJ, Weigel D, Wang JW (2011) Negative regulation of anthocyanin biosynthesis in *Arabidopsis* by a miR156-targeted SPL transcription factor. Plant Cell **23:** 1512–1522

Griffiths-Jones S, Saini HK, van Dongen S, Enright AJ (2008) miRBase: tools for microRNA genomics. Nucleic Acids Res **36:** D154–D158

Harper L, Freeling M (1996) Interactions of liguleless1 and liguleless2 function during ligule induction in maize. Genetics **144:** 1871–1882

Haywood V, Yu TS, Huang NC, Lucas WJ (2005) Phloem long-distance trafficking of GIBBERELLIC ACID-INSENSITIVE RNA regulates leaf development. Plant J **42:** 49–68

Higo K, Ugawa Y, Iwamoto M, Korenaga T (1999) Plant cis-acting regulatory DNA elements (PLACE) database: 1999. Nucleic Acids Res **27:** 297–300

Horsch RB, Rogers SG, Fraley RT (1985) Transgenic plants. Cold Spring Harb Symp Quant Biol **50:** 433–437

Hsieh LC, Lin SI, Shih AC, Chen JW, Lin WY, Tseng CY, Li WH, Chiou TJ (2009) Uncovering small RNA-mediated responses to phosphate deficiency in Arabidopsis by deep sequencing. Plant Physiol **151:** 2120–2132

Huijser P, Schmid M (2011) The control of developmental phase transitions in plants. Development **138:** 4117–4129

Jackson SD (2009) Plant responses to photoperiod. New Phytol **181:** 517–531

Jackson SD, James P, Prat S, Thomas B (1998) Phytochrome B affects the levels of a graft-transmissible signal involved in tuberization. Plant Physiol **117:** 29–32

Jiao Y, Wang Y, Xue D, Wang J, Yan M, Liu G, Dong G, Zeng D, Lu Z, Zhu X, et al (2010) Regulation of OsSPL14 by OsmiR156 defines ideal plant architecture in rice. Nat Genet **42:** 541–544

Kasai A, Kanehira A, Harada T (2010) *miR172* can move long distance in *Nicotiana benthamiana*. The Open Plant Sci J **4:** 1–6

Kehr J, Buhtz A (2008) Long distance transport and movement of RNA through the phloem. J Exp Bot **59:** 85–92

Kehr J, Buhtz A (2013) Endogenous RNA constituents of the phloem and their possible roles in long-distance signaling. *In* GA Thompson, AJE van Bel, eds, Phloem: Molecular Cell Biology, Systemic Communication, Biotic Interactions. Wiley-Blackwell Publishing, Oxford, pp 186–208

Kim M, Canio W, Kessler S, Sinha N (2001) Developmental changes due to long-distance movement of a homeobox fusion transcript in tomato. Science **293:** 287–289

Kurakawa T, Ueda N, Maekawa M, Kobayashi K, Kojima M, Nagato Y, Sakakibara H, Kyozuka J (2007) Direct control of shoot meristem activity by a cytokinin-activating enzyme. Nature **445:** 652–655

Lee J, Park JJ, Kim SL, Yim J, An G (2007) Mutations in the rice liguleless gene result in a complete loss of the auricle, ligule, and laminar joint. Plant Mol Biol **65:** 487–499

Lin T, Sharma P, Gonzalez DH, Viola IL, Hannapel DJ (2013) The impact of the long-distance transport of a *BEL1*-like messenger RNA on development. Plant Physiol **161:** 760–772

Livak KJ, Schmittgen TD (2001) Analysis of relative gene expression data using real-time quantitative PCR and the $2^{-\Delta\Delta CT}$ method. Methods **25:** 402–408

Mahajan A, Bhogale S, Kang IH, Hannapel DJ, Banerjee AK (2012) The mRNA of a Knotted1-like transcription factor of potato is phloem mobile. Plant Mol Biol **79:** 595–608

Marín-González E, Suárez-López P (2012) "And yet it moves": cell-to-cell and long-distance signaling by plant microRNAs. Plant Sci **196:** 18–30

Martin A, Adam H, Díaz-Mendoza M, Zurczak M, González-Schain ND, Suárez-López P (2009) Graft-transmissible induction of potato tuberization by the microRNA miR172. Development **136:** 2873–2881

Martinez-Garcia JF, Virgos-Soler A, Prat S (2002) Control of photoperiodregulated tuberization in potato by the Arabidopsis flowering-time gene CONSTANS. PNAS **99:** 15211–15216

Miyashima S, Koi S, Hashimoto T, Nakajima K (2011) Non-cell-autonomous microRNA165 acts in a dose-dependent manner to regulate multiple differentiation status in the *Arabidopsis* root. Development **138:** 2303–2313

Molnar A, Melnyk CW, Bassett A, Hardcastle TJ, Dunn R, Baulcombe DC (2010) Small silencing RNAs in plants are mobile and direct epigenetic modification in recipient cells. Science **328:** 872–875

Murashige T, Skoog F (1962) A revised medium for rapid growth and bioassays with tobacco tissue cultures. Physiol Plant **15:** 473–497

Navarro C, Abelenda JA, Cruz-Oró E, Cuéllar CA, Tamaki S, Silva J, Shimamoto K, Prat S (2011) Control of flowering and storage organ formation in potato by FLOWERING LOCUS T. Nature **478:** 119–122

Nodine MD, Bartel DP (2010) MicroRNAs prevent precocious gene expression and enable pattern formation during plant embryogenesis. Genes Dev **24:** 2678–2692

Okamura K, Phillips MD, Tyler DM, Duan H, Chou YT, Lai EC (2008) The regulatory activity of microRNA* species has substantial influence on microRNA and 3′ UTR evolution. Nat Struct Mol Biol **15:** 354–363

Pant BD, Buhtz A, Kehr J, Scheible WR (2008) MicroRNA399 is a long-distance signal for the regulation of plant phosphate homeostasis. Plant J **53:** 731–738

Schwab R, Palatnik JF, Riester M, Schommer C, Schmid M, Weigel D (2005) Specific effects of microRNAs on the plant transcriptome. Dev Cell **8:** 517–527

Shikata M, Koyama T, Mitsuda N, Ohme-Takagi M (2009) *Arabidopsis* SBP-box genes SPL10, SPL11 and SPL2 control morphological change in association with shoot maturation in the reproductive phase. Plant Cell Physiol **50:** 2133–2145

Sterck L, Billiau K, Abeel T, Rouzé P, Van de Peer Y (2012) ORCAE: online resource for community annotation of eukaryotes. Nat Methods **9:** 1041

Tomato Genome Consortium (2012) The tomato genome sequence provides insights into fleshy fruit evolution. Nature **485:** 635–641

Usami T, Horiguchi G, Yano S, Tsukaya H (2009) The more and smaller cells mutants of *Arabidopsis thaliana* identify novel roles for SQUAMOSA

PROMOTER BINDING PROTEIN-LIKE genes in the control of heteroblasty. Development **136:** 955–964

Varkonyi-Gasic E, Gould N, Sandanayaka M, Sutherland P, MacDiarmid RM (2010) Characterisation of microRNAs from apple (*Malus domestica* 'Royal Gala') vascular tissue and phloem sap. BMC Plant Biol **10:** 159

Varkonyi-Gasic E, Wu R, Wood M, Walton EF, Hellens RP (2007) Protocol: a highly sensitive RT-PCR method for detection and quantification of microRNAs. Plant Methods **3:** 12

Vauterin M, Frankard V, Jacobs M (1999) The *Arabidopsis thaliana* dhdps gene encoding dihydrodipicolinate synthase, key enzyme of lysine biosynthesis, is expressed in a cell-specific manner. Plant Mol Biol **39:** 695–708

Vorst O, van Dam F, Oosterhoff-Teertstra R, Smeekens S, Weisbeek P (1990) Tissue-specific expression directed by an *Arabidopsis thaliana* preferredoxin promoter in transgenic tobacco plants. Plant Mol Biol **14:** 491–499

Waksman G, Lebrun M, Freyssinet G (1987) Nucleotide sequence of a gene encoding sunflower ribulose-1,5-bisphosphate carboxylase/oxygenase small subunit (rbcs). Nucleic Acids Res **15:** 7181

Wang JW, Park MY, Wang LJ, Koo Y, Chen XY, Weigel D, Poethig RS (2011) miRNA control of vegetative phase change in trees. PLoS Genet **7:** e1002012

Waterhouse PM, Wang MB, Lough T (2001) Gene silencing as an adaptive defence against viruses. Nature **411:** 834–842

Wu G, Park MY, Conway SR, Wang JW, Weigel D, Poethig RS (2009) The sequential action of miR156 and miR172 regulates developmental timing in *Arabidopsis*. Cell **138:** 750–759

Wu G, Poethig RS (2006) Temporal regulation of shoot development in Arabidopsis thaliana by miR156 and its target SPL3. Development **133:** 3539–3547

Xie F, Frazier TP, Zhang B (2011) Identification, characterization and expression analysis of microRNAs and their targets in the potato (*Solanum tuberosum*). Gene **473:** 8–22

Xie F, Zhang B (2010) Target-align: a tool for plant microRNA target identification. Bioinformatics **26:** 3002–3003

Xie K, Shen J, Hou X, Yao J, Li X, Xiao J, Xiong L (2012) Gradual increase of miR156 regulates temporal expression changes of numerous genes during leaf development in rice. Plant Physiol **158:** 1382–1394

Xie K, Wu C, Xiong L (2006) Genomic organization, differential expression, and interaction of SQUAMOSA promoter-binding-like transcription factors and microRNA156 in rice. Plant Physiol **142:** 280–293

Xing S, Salinas M, Höhmann S, Berndtgen R, Huijser P (2010) miR156-targeted and nontargeted SBP-box transcription factors act in concert to secure male fertility in *Arabidopsis*. Plant Cell **22:** 3935–3950

Xu X, Vreugdenhil D, van Lammeren AAM (1998) Cell division and cell enlargement during potato tuber formation. J Exp Bot **49:** 573–582

Yang W, Liu X, Zhang J, Feng J, Li C, Chen J (2010) Prediction and validation of conservative microRNAs of Solanum tuberosum L. Mol Biol Rep **37:** 3081–3087

Yoo BC, Kragler F, Varkonyi-Gasic E, Haywood V, Archer-Evans S, Lee YM, Lough TJ, Lucas WJ (2004) A systemic small RNA signaling system in plants. Plant Cell **16:** 1979–2000

Yu YY, Lashbrook CC, Hannapel DJ (2007) Tissue integrity and RNA quality of laser microdissected phloem of potato. Planta **226:** 797–803

Zhang H, Jin J, Tang L, Zhao Y, Gu X, Gao G, Luo J (2011a) PlantTFDB 2.0: update and improvement of the comprehensive plant transcription factor database. Nucleic Acids Res **39:** D1114–D1117

Zhang W, Luo Y, Gong X, Zeng W, Li S (2009) Computational identification of 48 potato microRNAs and their targets. Comput Biol Chem **33:** 84–93

Zhang X, Zou Z, Zhang J, Zhang Y, Han Q, Hu T, Xu X, Liu H, Li H, Ye Z (2011b) Over-expression of sly-miR156a in tomato results in multiple vegetative and reproductive trait alterations and partial phenocopy of the sft mutant. FEBS Lett **585:** 435–439

Zuker M (2003) MFold web server for nucleic acid folding and hybridization prediction. Nucleic Acids Res **31:** 3406–3415